UNITED STATES PATENT AND TRADEMARK OFFICE

BEFORE THE PATENT TRIAL AND APPEAL BOARD

GOOGLE LLC
Petitioner

v.

ADVANCED CODING TECHNOLOGIES, LLC,
Patent Owner.

Case No. IPR2025-XXXXX
U.S. Patent No. 8,090,025

DECLARATION OF JUNE ANN MUNFORD IN SUPPORT OF PETITION FOR *INTER PARTES* REVIEW OF U.S. PATENT NO. 8,090,025

I. Introduction

1. My name is June Ann Munford. I am over the age of 18, have personal knowledge of the facts set forth herein, and am competent to testify to the same.

2. I have been retained by Petitioner Google LLC ("Petitioner"), as an independent expert in this proceeding before the Patent Trial and Appeal Board ("PTAB" or "Board"). I understand that Petitioner is requesting that the Board institute an *inter partes* review ("IPR") proceeding of U.S. Patent No. 8,090,025 ("'025 patent") (Ex.1001), currently assigned to Advanced Coding Technologies, LLC ("Patentee").

3. I have been retained on behalf of the Petitioner to provide assistance in the above-illustrated matter in establishing the authenticity and public availability of the documents discussed in this declaration. I am not and have never been an employee of Petitioner. I am being compensated for my services in this matter at the rate of $200.00 per hour plus reasonable expenses. My statements are objective, and my compensation does not depend on the outcome of this matter.

A. Qualifications

4. I earned a Master of Library and Information Science (MLIS) from the University of Wisconsin-Milwaukee in 2009. I have over ten years of experience in the library/information science field. Beginning in 2004, I have served in various positions in the public library sector including Assistant Librarian, Youth Services

Librarian and Library Director. I have attached my Curriculum Vitae as Appendix CV.

5. During my career in the library profession, I have been responsible for materials acquisition for multiple libraries. In that position, I have cataloged, purchased and processed incoming library works. That includes purchasing materials directly from vendors, recording publishing data from the material in question, creating detailed material records for library catalogs and physically preparing that material for circulation. In addition to my experience in acquisitions, I was also responsible for analyzing large collections of library materials, tailoring library records for optimal catalog search performance and creating lending agreements between libraries during my time as a Library Director.

B. Background of Library Records

6. I am fully familiar with the catalog record creation process in the library sector. In preparing a material for public availability, a library catalog record describing that material would be created. These records are typically written in Machine Readable Catalog (herein referred to as "MARC") code and contain information such as a physical description of the material, metadata from the material's publisher, and date of library acquisition. In particular, the 008 field of the MARC record is reserved for denoting the date of creation of the library record itself. As this typically occurs during the process of preparing materials for public

access, it is my experience that an item's MARC record indicates the date of an item's public availability.

7. Typically, in creating a MARC record, a librarian would gather various bits of metadata such as book title, publisher and subject headings among others and assign each value to a relevant numerical field. For example, a book's physical description is tracked in field 300 while title/attribution is tracked in field 245. The 008 field of the MARC record is reserved for denoting the creation of the library record itself. As this is the only date reflecting the inclusion of said materials within the library's collection, it is my experience that an item's 008 field accurately indicates the date of an item's public availability.

8. With respect to periodicals, the MARC record typically indicates the date of public availability of the first issue of the periodical (e.g., a journal). It is my experience that the 008 field of the MARC record for a periodical may not be modified upon the library receiving new issues of a periodical. However, MARC records are still pertinent to whether a periodical is publicly available at a particular library. Additionally, it is my experience that, for periodical in a library's catalog, new issues are regularly received by the library and made available to interested readers very soon after the library receives those issues, as that is one of the primary purposes of libraries — to make available information to interested patrons on a timely basis.

C. Al-Mualla

9. I have reviewed Exhibit EX-1005, *Video Coding for Mobile Communications* by Mohammed E. Al-Mualla, C. Nishan Canagarajah and David R. Bull.

10. Attached hereto as Appendix ALMUALLA01 is a true and correct copy of the MARC record for *Video Coding for Mobile Communications* as held by the Penn State University library. Based on my experience, the Penn State University library public catalog would have had a similar search functionality in 2006; by that time, most universities had digitized their catalogs and made them available to electronically search over the Internet, or at the very least, electronically search within the library itself. I secured this record myself from the library's public catalog. The MARC record contained within Appendix ALMUALLA01 accurately describes the title, author, publisher, and ISBN number of *Video Coding for Mobile Communications*.

11. Attached hereto as Appendix ALMUALLA02 is a true and correct copy of Video Coding for Mobile Communications as held by the Penn State University library. I secured these scans myself from the library's collection. In comparing Exhibit EX-1005 to Appendix ALMUALLA02, it is my determination that Exhibit EX-1005 is a true and correct copy of Video Coding for Mobile Communications by Mohammed E. Al-Mualla, C. Nishan Canagarajah and David R. Bull.

12. The 008 field of the MARC record in Appendix ALMUALLA01 indicates the date of record creation. The 008 field of Appendix ALMUALLA01 indicates Penn State University library first acquired this book as of February 26, 2002. Considering this information, it is my determination that Video Coding for Mobile Communications was made available to the public shortly after its initial acquisition in February 26, 2002.

D. Shirani

13. I have reviewed Exhibit EX-1006, "A Concealment Method for Video Communications in an Error-Prone Environment" by Shahram Shirani, Faouzi Kossentini and Rabab Ward as published in IEEE Journal on Selected Areas in Communications, June 2000.

14. Attached hereto as Appendix SHIRANI01 is a true and correct copy of the MARC record for IEEE Journal on Selected Areas in Communications as held by the Penn State University library. I secured this record myself from the library's public catalog. The MARC record contained within Appendix SHIRANI01 accurately describes the title, author, publisher, and ISSN number of IEEE Journal on Selected Areas in Communications. The 'Availability' field of this record visible on page 4 indicates this collection includes the June 2000 edition of IEEE Journal on Selected Areas in Communications containing "A Concealment Method for Video Communications in an Error-Prone Environment."

15. Attached hereto as Appendix SHIRANI02 is a true and correct copy of "A Concealment Method for Video Communications in an Error-Prone Environment" as published in IEEE Journal on Selected Areas in Communications as held by the Penn State University library. I secured these scans myself from the library's collection. In comparing Exhibit EX-1006 to Appendix SHIRANI02, it is my determination that Exhibit EX-1006 is a true and correct copy of "A Concealment Method for Video Communications in an Error-Prone Environment" by Shahram Shirani, Faouzi Kossentini and Rabab Ward as published in IEEE Journal on Selected Areas in Communications June 2000.

16. The 008 field of the MARC record in Appendix SHIRANI01 indicates the date of record creation. The 008 field of Appendix SHIRANI01 indicates the Penn State University library first acquired this journal as of May 31, 1983. The Penn State University library webpage indicates that the library has the volume containing the June 2000 issue and makes that volume available to the public. Considering this information, it is my determination that IEEE Journal on Selected Areas in Communications June 2000 and therefore "A Concealment Method for Video Communications in an Error-Prone Environment" was made available to the public shortly its initial publication in June 2000.

E. Saito

17. I have reviewed Exhibit EX-1007, "The Polyharmonic Local Sine Transform: A New Tool for Local Image Analysis and Synthesis Without Edge Effect" by Naoki Saito and Jean-Francois Remy as published in *Applied and Computational Harmonic Analysis*, January 2006.

18. Attached hereto as Appendix SAITO01 is a true and correct copy of the MARC record for *Applied and Computational Harmonic Analysis* as held by the Penn State University library. I secured this record myself from the library's public catalog. The MARC record contained within Appendix SAITO01 accurately describes the title, author, publisher, and ISSN number of *Applied and Computational Harmonic Analysis.* The 'Dates of Publication' field of this record visible on page 2 indicates this collection includes the January 2006 edition of *Applied and Computational Harmonic Analysis* containing "The Polyharmonic Local Sine Transform: A New Tool for Local Image Analysis and Synthesis Without Edge Effect."

19. Attached hereto as Appendix SAITO02 is a true and correct copy of "The Polyharmonic Local Sine Transform: A New Tool for Local Image Analysis and Synthesis Without Edge Effect" as published in *Applied and Computational Harmonic Analysis* as held by the Penn State University library. I secured this file myself from the library's collection. In comparing Exhibit EX-1007 to Appendix

SAITO02, it is my determination that Exhibit EX-1007 is a true and correct copy of "The Polyharmonic Local Sine Transform: A New Tool for Local Image Analysis and Synthesis Without Edge Effect" by Naoki Saito and Jean-Francois Remy as published in *Applied and Computational Harmonic Analysis* January 2006.

20. The 008 field of the MARC record in Appendix SAITO01 indicates the date of record creation. The 008 field of Appendix SAITO01 indicates the Penn State University library first acquired this journal as of May 12, 1997. The MARC record indicates that the journal is available electronically. Considering this information, it is my determination that *Applied and Computational Harmonic Analysis* January 2006 and therefore "The Polyharmonic Local Sine Transform: A New Tool for Local Image Analysis and Synthesis Without Edge Effect" was made available to the public shortly after its initial release in January 2006.

F. Girod

21. I have reviewed Exhibit EX-1008, "Feedback-Based Error Control for Mobile Video Transmission" by Bernd Girod and Niko Farber as published in *Proceedings of the IEEE*, October 1999.

22. Attached hereto as Appendix GIROD01 is a true and correct copy of the MARC record for *Proceedings of the IEEE* as held by the Penn State University library. I secured this record myself from the library's public catalog. The MARC record contained within Appendix GIROD01 accurately describes the title, author,

publisher, and ISSN number of *Proceedings of the IEEE.* The 'Availability' field of this record visible on page 6 indicates this collection includes the October 1999 edition of *Proceedings of the IEEE* containing "Feedback-Based Error Control for Mobile Video Transmission."

23. Attached hereto as Appendix GIROD02 is a true and correct copy of "Feedback-Based Error Control for Mobile Video Transmission" as published in *Proceedings of the IEEE* as held by the Penn State University library. I secured these scans myself from the library's collection. In comparing Exhibit EX-1008 to Appendix GIROD02, it is my determination that Exhibit EX-1008 is a true and correct copy of "Feedback-Based Error Control for Mobile Video Transmission" by Bernd Girod and Niko Farber as published in *Proceedings of the IEEE* October 1999.

24. The 008 field of the MARC record in Appendix GIROD01 indicates the date of record creation. The 008 field of Appendix GIROD01 indicates the Penn State University library first acquired this journal as of November 1, 1975. Considering this information, it is my determination that *Proceedings of the IEEE* October 1999 and therefore "Feedback-Based Error Control for Mobile Video Transmission" was made available to the public shortly after its initial release in October 1999.

G. Stockhammer

25. I have reviewed Exhibit EX-1009, "H.264/AVC in Wireless Environments" by Thomas Stockhammer, Miska M. Hannuksela and Thomas Wiegand as published in *IEEE Transactions on Circuits and Systems for Video Technology*, July 2003.

26. Attached hereto as Appendix STOCKHAMMER01 is a true and correct copy of the MARC record for *IEEE Transactions on Circuits and Systems for Video Technology* as held by the Penn State University library. I secured this record myself from the library's public catalog. The MARC record contained within Appendix STOCKHAMMER01 accurately describes the title, author, publisher, and ISSN number of *IEEE Transactions on Circuits and Systems for Video Technology.* The 'Availability' field of this record visible on page 3 indicates this collection includes the July 2003 edition of *IEEE Transactions on Circuits and Systems for Video Technology* containing "H.264/AVC in Wireless Environments".

27. Attached hereto as Appendix STOCKHAMMER02 is a true and correct copy of "H.264/AVC in Wireless Environments" as published in *IEEE Transactions on Circuits and Systems for Video Technology* as held by the Penn State University library. I secured these scans myself from the library's collection. In comparing Exhibit EX-1009 to Appendix STOCKHAMMER02, it is my determination that Exhibit EX-1009 is a true and correct copy of "H.264/AVC in Wireless

Environments" by Thomas Stockhammer, Miska M. Hannuksela and Thomas Wiegand as published in *IEEE Transactions on Circuits and Systems for Video Technology* July 2003.

28. The 008 field of the MARC record in Appendix STOCKHAMMER01 indicates the date of record creation. The 008 field of Appendix STOCKHAMMER01 indicates the Penn State University library first acquired this journal as of May 15, 1991. Considering this information, it is my determination that *IEEE Transactions on Circuits and Systems for Video Technology* July 2003 and therefore "H.264/AVC in Wireless Environments" was made available to the public shortly its initial publication in July 2003.

H. Wada

29. I have reviewed Exhibit EX-1017, "Selective Recovery of Video Packet Loss Using Error Concealment" by Masahiro Wada as published in *IEEE Journal on Selected Areas in Communications*, June 1989.

30. Attached hereto as Appendix WADA01 is a true and correct copy of the MARC record for *IEEE Journal on Selected Areas in Communications* as held by the Penn State University library. I secured this record myself from the library's public catalog. The MARC record contained within Appendix WADA01 accurately describes the title, author, publisher, and ISSN number of *IEEE Journal on Selected Areas in Communications.* The 'Availability' field of this record visible on page 4

indicates this collection includes the June 1989 edition of *IEEE Journal on Selected Areas in Communications* containing "Selective Recovery of Video Packet Loss Using Error Concealment".

31. Attached hereto as Appendix WADA02 is a true and correct copy of "Selective Recovery of Video Packet Loss Using Error Concealment" as published in *IEEE Journal on Selected Areas in Communications* as held by the Penn State University library. I secured these scans myself from the library's collection. In comparing Exhibit EX-1017 to Appendix WADA02, it is my determination that Exhibit EX-1017 is a true and correct copy of "Selective Recovery of Video Packet Loss Using Error Concealment" by Masahiro Wada as published in *IEEE Journal on Selected Areas in Communications* June 1989.

32. The 008 field of the MARC record in Appendix WADA01 indicates the date of record creation. The 008 field of Appendix WADA01 indicates the Penn State University library first acquired this journal as of May 31, 1983. Considering this information, it is my determination that *IEEE Journal on Selected Areas in Communications* June 1989 and therefore "Selective Recovery of Video Packet Loss Using Error Concealment" was made available to the public shortly its initial publication in June 1989.

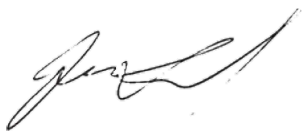
II. CONCLUSION

33. In signing this Declaration, I recognize that the Declaration will be filed as evidence in a contested case before the Patent Trial and Appeal Board of the United States Patent and Trademark Office. I also recognize that I may be subject to cross-examination. If cross-examination is required of me, I will appear for cross-examination during the time allotted for cross-examination.

34. I reserve the right to respond to any declarations that are submitted by Patentee's expert witnesses or to any testimony by Patentee's fact or expert witnesses, whether at deposition or at trial.

35. I declare under penalty of perjury that the foregoing is true and correct. I hereby declare that all statements made herein of my own knowledge are true and that all statements made on information and belief are believed to be true; and further that these statements were made the knowledge that willful false statements and the like so made are punishable by fine or imprisonment, or both, under Section 1001 of Title 18 of the United States Code.

Dated: 4/11/2025



June Ann Munford

APPENDIX CV

June A. Munford
Curriculum Vitae

Education

University of Wisconsin-Milwaukee - MS, Library & Information Science, 2009
Milwaukee, WI

- Coursework included cataloging, metadata, data analysis, library systems, management strategies and collection development.
- Specialized in library advocacy, cataloging and public administration.

Grand Valley State University - BA, English Language & Literature, 2008
Allendale, MI

- Coursework included linguistics, documentation and literary analysis.
- Minor in political science with a focus in local-level economics and government.

Professional Experience

Researcher / Expert Witness, October 2017 – present
Freelance ● Pittsburgh, Pennsylvania & Grand Rapids, Michigan

- Material authentication and public accessibility determination. Declarations of authenticity and/or public accessibility provided upon research completion. Experienced with appeals and deposition process.

- Research provided on topics of public library operations, material publication history, digital database services and legacy web resources.

- Past clients include Alston & Bird, Arnold & Porter, Baker Botts, Fish & Richardson, Erise IP, Irell & Manella, O'Melveny & Myers, Perkins-Coie, Pillsbury Winthrop Shaw Pittman and Slayden Grubert Beard.

Library Director, February 2013 - March 2015
Dowagiac District Library ● Dowagiac, Michigan

- Executive administrator of the Dowagiac District Library. Located in

Southwest Michigan, this library has a service area of 13,000, an annual operating budget of over $400,000 and total assets of approximately $1,300,000.

● Developed careful budgeting guidelines to produce a 15% surplus during the 2013-2014 & 2014-2015 fiscal years while being audited.

● Using this budget surplus, oversaw significant library investments including the purchase of property for a future building site, demolition of existing buildings and building renovation projects on the current facility.

● Led the organization and digitization of the library's archival records.

● Served as the public representative for the library, developing business relationships with local school, museum and tribal government entities.

● Developed an objective-based analysis system for measuring library services - including a full collection analysis of the library's 50,000+ circulating items and their records.

November 2010 - January 2013
Librarian & Branch Manager, Anchorage Public Library ● Anchorage, Alaska

● Headed the 2013 Anchorage Reads community reading campaign including event planning, staging public performances and creating marketing materials for mass distribution.

● Co-led the social media department of the library's marketing team, drafting social media guidelines, creating original content and instituting long-term planning via content calendars.

● Developed business relationships with The Boys & Girls Club, Anchorage School District and the US Army to establish summer reading programs for children.

June 2004 - September 2005, September 2006 - October 2013
Library Assistant, Hart Area Public Library
Hart, MI

● Responsible for verifying imported MARC records and original MARC

cataloging for the local-level collection as well as the Michigan Electronic Library.

● Handled OCLC Worldcat interlibrary loan requests & fulfillment via ongoing communication with lending libraries.

Professional Involvement

Alaska Library Association - Anchorage Chapter
- Treasurer, 2012

Library Of Michigan
- Level VII Certification, 2008
- Level II Certification, 2013

Michigan Library Association Annual Conference 2014
- New Directors Conference Panel Member

Southwest Michigan Library Cooperative
- Represented the Dowagiac District Library, 2013-2015

Professional Development

Library Of Michigan Beginning Workshop, May 2008
Petoskey, MI
- Received training in cataloging, local history, collection management, children's literacy and reference service.

Public Library Association Intensive Library Management Training, October 2011
Nashville, TN
- Attended a five-day workshop focused on strategic planning, staff management, statistical analysis, collections and cataloging theory.

Alaska Library Association Annual Conference 2012 - Fairbanks, February 2012
Fairbanks, AK
- Attended seminars on EBSCO advanced search methods, budgeting, cataloging, database usage and marketing.

Depositions

2019 ● Fish & Richardson

Apple v. Qualcomm (IPR2018-001281, 39521-00421IP, IPR2018-01282 and 39521-00421IP2)

2019 ● Erise IP

Implicit, LLC v. Netscout Systems, Inc (Civil Action No. 2:18-cv-53-JRG)

2019 ● Perkins-Coie

Adobe Inc. v. RAH Color Technologies LLC (Cases IPR2019-00627, IPR2019-00628, IPR2019-00629 and IPR2019-00646)

2020 ● O'Melveny & Myers

Maxell, Ltd. v. Apple Inc. (Case No. 5:19-cv-00036-RWS)

2021 ● Pillsbury Winthrop Shaw Pittman LLP

Intel v. SRC (IPR2020-1449)

2022 ● Perkins-Coie

Realtek v. Future Link (IPR2021-01182)

2023 ● Fish & Richardson

Neuroderm Ltd. v. Abbvie, Inc (Case No. PGR2022-00040)

2023 ● Fish & Richardson

Nearmap US Inc. v. Pictometry International Corp. (IPR2022-00735)

Limited Case History & Potential Conflicts

Alston & Bird

- Ericsson
  - v. Collision Communications (IPR2022-01233)
- Nokia
  - v. Neptune Subsea, Xtera (Case No. 1:17-cv-01876)

Arnold & Porter

- Ivantis
  - v. Glaukos (Case No. 8:18-cv-00620)
- Samsung
  - v. Jawbone (Case No. 2:21-cv-00186)

Benesch Friedlander Coplan & Aronoff

- Voyis
  - v. Cathx (Case No. 5:21-cv-00077-RWS)

Erise I.P.

- Apple
  - v. Ericsson Inc. (IPR2022-00715)
  - v. Future Link Systems (IPRs 6317804, 6622108, 6807505, and 7917680)
  - v. INVT (Case No. 20-1881)
  - v. Navblazer LLC (IPR2020-01253)
  - v. Qualcomm (IPR2018-001281, 39521-00421IP, IPR2018-01282, 39521-00421IP2)
  - v. Quest Nettech Corp (Case No. 2:19-cv-00118-JRG)
  - v. Telefonaktiebolaget LM Ericsson (IPR2022-00275)

- Fanduel
    - v. CGT (Case No. 19-1393)
- Garmin
    - v. Phillips North America LLC (Case No. 2:19-cv-6301-AB-KS)
- Netscout
    - v. Longhorn HD LLC (Case No. 2:20-cv-00349)
    - v. Implicit, LLC (Civil Action No. 2:18-cv-53-JRG)
- Sony Interactive Entertainment LLC
    - v. Bot M8 LLC (IPR2020-01288)
    - v. Infernal Technology LLC (Case No. 2:19-CV-00248-JRG)
- Unified Patents
    - v. GE Video Compression (Civil Action No. 2:19-cv-248)

Fish & Richardson

- Apple
    - v. AliveCor (3:21-cv-03958)
    - v. LBS Innovations (Case No. 2:19-cv-00119-JRG-RSP)
    - v. Koss Corporation (IPR2021-00305)
    - v. Masimo (IPR 50095-0012IP1, 50095-0012IP2, 50095-0013IP1, 50095-0013IP2, 50095-0006IP1)
    - v. Neonode (Case No. 21-cv-08872-EMC)
    - v. Qualcomm (IPR2018-001281, 39521-00421IP, IPR2018-01282, 39521-00421IP2)
- Dell
    - v. Neo Wireless (IPR2022-00616)

- Dish Network
    - v. Realtime Adaptive Streaming (Case No. 1:17-CV-02097-RBJ)
    - v. TQ Delta LLC (Case No. 18-1798)
- Evapco Dry Cooling
    - v. SPG Dry Cooling (IPR2021-00688)
- Genetec
    - v. Sensormatic Electronics (Case No. 1:20-CV-00760)
- Huawei
    - v. Bell Northern Research LLC (IPR2019-01174)
- Kianxis
    - v. Blue Yonder (Case No. 3:20-cv-03636)
- LG Electronics
    - v. Bell Northern Research LLC (Case No. 3:18-cv-2864-CAB-BLM)
- Metaswitch
    - v. Sonus Networks (IPR2018-01719)
- Microsoft
    - v. Throughputer Inc (IPR2022-00757)
- MLC Intellectual Property
    - v. MicronTech (Case No. 3:14-cv-03657-SI)
- Nearmap Inc
    - v. EagleView Technologies (IPR2022-01009)
- Neuroderm Ltd.
    - v. Abbvie, Inc (Case No. PGR2022-00040)
- Realtek Semiconductor
    - v. Future Link (IPR2021-01182)

- Quectel
    - v. Koninklijke Philips (Case No. 1:20-cv-01710)
- Samsung
    - v. Aire Technology (IPR2022-00877)
    - v. Bell Northern Research (Case No. 2:19-cv-00286-JRG)
    - v. Communication Technologies Inc (IPR2022-01221)
    - v. Jawbone Innovations (IPR2022-00865)
    - v. MemoryWeb LLC (IPR2022-00885)
    - v. Telefonaktiebolaget LM Ericsson (IPR2021-00615)
- Texas Instruments
    - v. Vantage Micro LLC (IPR2020-01261)
- Xilinx
    - v. Sentient Sensors LCC (Case No. 1:22-cv-00173)

Irell & Manella

- Curium

O'Melveny & Myers

- Apple
    - v. Maxell (Case No. 5:19-cv-00036-RWS)

Perkins-Coie

- Heru Industries
    - v. The UAB Research Foundation (IPR2022-01148)
- Realtek Semiconductor
    - v. Future Link (IPR2021-01182)

- Twitter Inc

  v. VOIP-Pal.com (Case No. 3:20-cv-02397-JD)

- TCL Industries

  v. Koninklijke Philips NV (IPR2021-00495, IPR2021-00496 and IPR2021-00497)

Pillsbury Winthrop Shaw Pittman

- Intel

  v. FG SRC LLC (Case No. 6:20-cv-00315)

- Gravel Rating Systems

  v. Costco (Case No. 4:21-cv-149)
  v. Lowe's Home Centers (Case No. 4:21-cv-150)
  v. T-Mobile USA (Case No. 4:21-cv-152)
  v. Kohl's Inc. (Case No. 4:21-cv-258)
  v. Under Armor (Case No. 4:21-cv-356)

APPENDIX ALMUALLA01

screenshot-catalog.libraries.psu.edu-2023.12.05-15_59_18
https://catalog.libraries.psu.edu/catalog/2300351
05.12.2023

MARC View

LEADER 01492nam a22003978a 4500				
001 2300351				
003 SIRSI				
005 20151215025712.0				
008 020226t20022002cau 001 0 eng				
010				a| 2001098017
015				a| GBA2-Y4214
019				a| MARS
020				a| 0120530791
035				a| (OCoLC)49238354
040				a| UKM c| UKM d| CUS d| PSt d| OCoLC d| UtOrBLW
050		4		a| TK6570.M6 b| A56 2002
082	0	4		a| 621.382 2| 21
100	1			a| Al-Mualla, Mohammed Ebrahim.
245	1	0		a| Video coding for mobile communications : b| efficiency, complexity, and resilience / c| Mohammed Ebrahim Al-Mualla, C. Nishan Canagarajah and David R. Bull.
264		1		a| San Diego, Calif. ; a| London : b| Academic Press, c| [2002]
264		4		c| ©2002
300				a| xxvi, 293 pages : b| illustrations ; c| 24 cm.
336				a| text b| txt 2| rdacontent
337				a| unmediated b| n 2| rdamedia
338				a| volume b| nc 2| rdacarrier
490	1			a| Signal processing and its applications
504				a| Includes bibliographical references (pages 267-282) and index.
650		0		a| Mobile communication systems.
650		0		a| Image transmission.
650		0		a| Multimedia systems x| Standards.
650		0		a| Video compression x| Standards.
650		0		a| Coding theory.
700	1			a| Canagarajah, C. N. q| (C. Nishan)
700	1			a| Bull, D. R. q| (David R.)
830		0		a| Signal processing and its applications.
949				a| TK6570.M6A56 2002 w| LC c| 1 i| 000048900072 d| 12/20/2006 e| 8/8/2006 l| CATO-2 m| UP-ANNEX n| 9 r| Y s| Y t| BOOK u| 5/24/2002 z| 8158

PennState

Copyright @2019 The Pennsylvania State University. All rights reserved. Except where otherwise noted, this work is subject to a Creative Commons Attribution 4.0 license. Details and exceptions.

Legal Statements | PSU Hotlines

PENN STATE UNIVERSITY LIBRARIES

Libraries Home (814) 865-6368
Libraries Intranet (Staff Only)
Accessibility Help
Website Feedback
Policies and Guidelines
Staff Directory

screenshot-catalog.libraries.psu.edu-2023.12.05-15_59_18
https://catalog.libraries.psu.edu/catalog/2300351
05.12.2023



Video coding for mobile communications : efficiency, complexity, and resilience / Mohammed Ebrahim Al-Mualla, C. Nishan Canagarajah and David R. Bull

Author:	Al-Mualla, Mohammed Ebrahim
Published:	San Diego, Calif. ; London : Academic Press, [2002]
Copyright Date:	©2002
Physical Description:	xxvi, 293 pages : illustrations ; 24 cm.
Additional Creators:	Canagarajah, C. N. (C. Nishan) and Bull, D. R. (David R.)

Availability

Browse Nearby on Shelf I Want It

Library Storage (1 item)

Call number	Material	Location
TK6570.M6A56 2002	Book	Checked out

Series:
Signal processing and its applications

Subject(s):
Mobile communication systems
Image transmission
Multimedia systems—Standards
Video compression—Standards
Coding theory

ISBN:
0120530791

Bibliography Note:
Includes bibliographical references (pages 267-282) and index.

View MARC record | catkey: 2300351

PennState

Copyright @2019 The Pennsylvania State University. All rights reserved. Except where otherwise noted, this work is subject to a Creative Commons Attribution 4.0 license. Details and exceptions.

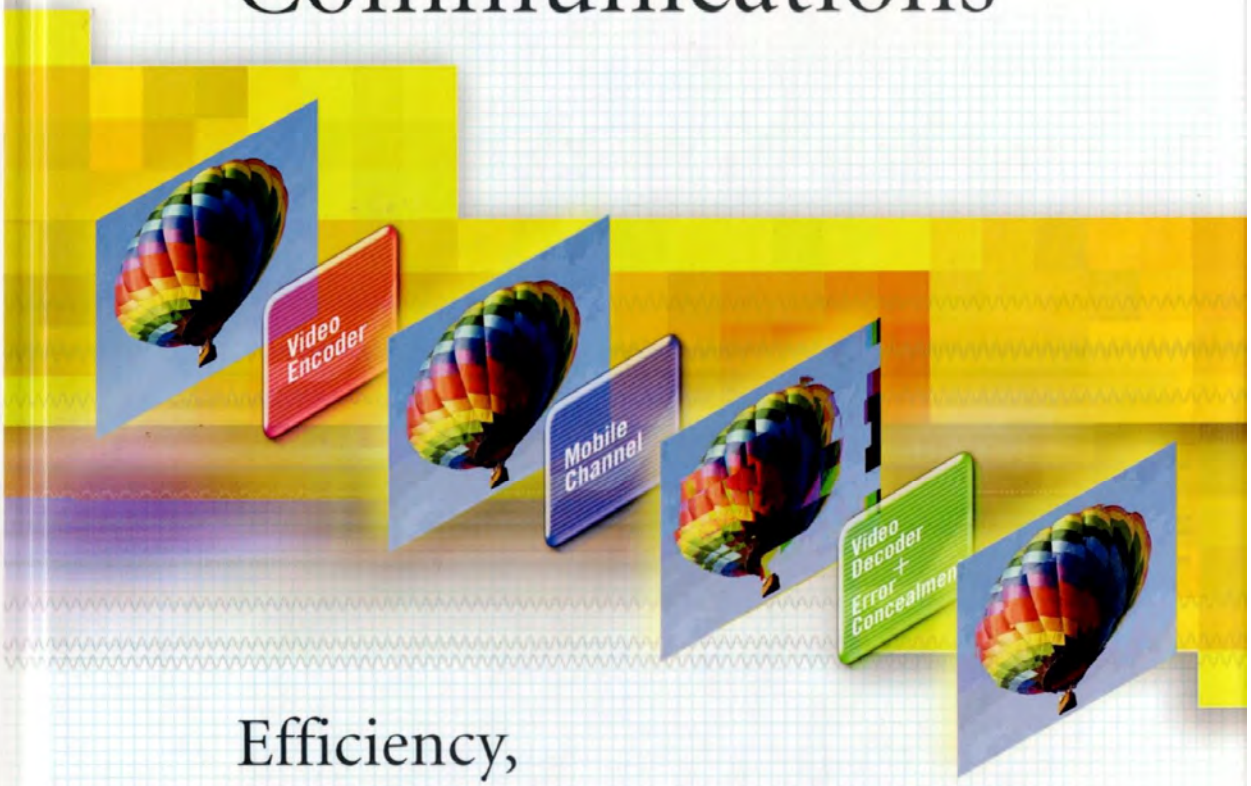
Legal Statements | PSU Hotlines

PENN STATE UNIVERSITY LIBRARIES
Libraries Home (814) 865-6368
Libraries Intranet (Staff Only)
Accessibility Help
Website Feedback
Policies and Guidelines
Staff Directory

APPENDIX ALMUALLA02

SIGNAL PROCESSING AND ITS APPLICATIONS

Video Coding for Mobile Communications



Efficiency, Complexity, and Resilience

Mohammed E. Al-Mualla
C. Nishan Canagarajah
David R. Bull

Al-Mualla
Canagarajah
Bull
Video Coding for Mobile Communications
Efficiency, Complexity, and Resilience
Engin.
TK6570
.M6
A56
2002
Press

SIGNAL PROCESSING AND ITS APPLICATIONS

a series from Academic Press

Video Coding for Mobile Communications

Efficiency, Complexity, and Resilience



Mohammed E. Al-Mualla: Etisalat College of Engineering, Emirates Telecommunications Corporation (Etisalat), Sharjah, United Arab Emirates

C. Nishan Canagarajah and David R. Bull: Image Communications Group, Centre for Communications Research, University of Bristol, Bristol, United Kingdom

Mobile multimedia communications is one of the major growth areas in engineering today. Current second-generation mobile communication systems support a number of basic multimedia communication services. However, many technologically demanding problems need to be solved before *real-time mobile video communications* can be achieved. This book focuses on *video source coding* techniques that address three important challenges: *coding efficiency, computational complexity,* and *error resilience.* The book reviews the state-of-art techniques in these three areas, with particular emphasis on those techniques adopted in the latest video coding standards. This is supported with comparative studies between techniques and investigations into the suitability of such techniques for mobile video communications. In addition, the book presents some of the authors' original contributions in this exciting field.

- A leading text addressing the problems associated with the design of mobile video communication systems
- A unique text integrating the areas of coding efficiency, reduced computational complexity, and error resilience in a single volume
- Provides a quick, easy, and practical introduction to the fundamentals of video source coding
- Presents a comprehensive overview of the latest video coding standards including H.263 (and its extensions H.263+ and H.263++) and MPEG-4
- Reviews, evaluates, and compares the state-of-art techniques in the areas of coding efficiency, reduced complexity, and error resilience
- Adopts a motion-based approach to address the problems of coding efficiency, computational complexity, and error resilience
- Acts as a repository of ideas, design examples, and novel techniques for students, instructors, researchers, engineers, and managers

PENN STATE UNIVERSITY LIBRARIES

A0000048900072

PRESS

An imprint of Elsevier Science

6 08628 30791 6

EAN 90018

9 780120 530793

ISBN 0-12-053079-1

Printed in The United States

ENGINEERING LIBRARY

Signal Processing and its Applications

SERIES EDITORS

Dr Richard Green
Department of Technology, Metropolitan Police Service, London, UK

Professor Truong Nguyen
Electrical and Computer Engineering Department,
University of Wisconsin, Wisconsin, USA

EDITORIAL BOARD

Professor Maurice G. Bellanger
CNAM, Paris, France

Professor David Bull
Department of Electrical and Electronic Engineering,
University of Bristol, UK

Professor Gerry D. Cain
School of Electronic and Manufacturing System Engineering,
University of Westminster, London, UK

Professor Colin Cowan
Department of Electronics and Electrical Engineering,
Queen's University, Belfast, Northern Ireland

Professor Roy Davies
Machine Vision Group, Department of Physics,
Royal Holloway, University of London, Surrey, UK

Dr Paola Hobson
Motorola, Basingstoke, UK

Professor Mark Sandler
Department of Electronics and Electrical Engineering,
King's College London, University of London, UK

Dr Henry Stark
Electrical and Computer Engineering Department,
Illinois Institute of Technology, Chicago, USA

Dr Maneeshi Trivedi
Horndean, Waterlooville, UK

Video Coding for Mobile Communications

Efficiency, Complexity, and Resilience

Mohammed Ebrahim Al-Mualla
Etisalat College of Engineering,
Emirates Telecommunications Corporation (ETISALAT), U.A.E.

C. Nishan Canagarajah and David R. Bull
Image Communications Group,
Center for Communications Research,
University of Bristol, U.K.



ACADEMIC PRESS

An Imprint of Elsevier Science

Amsterdam Boston London New York Oxford Paris San Diego
San Francisco Singapore Sydney Tokyo

This book is printed on acid-free paper. ♾

Copyright © 2002, Elsevier Science (USA)
All rights reserved.

No part of this publication may be reproduced or transmitted in any form or by any means, electronic or mechanical, including photocopy, recording, or any information storage and retrieval system, without permission in writing from the publisher.

Requests for permission to make copies of any part of the work should be mailed to: Permissions Department, Harcourt, Inc., 6277 Sea Harbor Drive, Orlando, Florida 32887-6777.

Explicit permission from Academic Press is not required to reproduce a maximum of two figures or tables from an Academic Press chapter in another scientific or research publication provided that the material has not been credited to another source and that full credit to the Academic Press chapter is given.

Academic Press
An Imprint of Elsevier Science
525 B Street, Suite 1900, San Diego, California 92101-4495, USA
http://www.academicpress.com

Academic Press
An Imprint of Elsevier Science
Harcourt Place, 32 Jamestown Road, London NW1 7BY, UK
http://www.academicpress.com

Library of Congress Catalog Card Number: 2001098017

International Standard Book Number: 0-12-053079-1

PRINTED IN THE UNITED STATES OF AMERICA

02 03 04 05 06 EB 9 8 7 6 5 4 3 2 1

Contents

Preface xiii

About the Authors xix

List of Acronyms xxi

1 Introduction to Mobile Video Communications **1**
1.1 Motivations and Applications 1
1.2 Main Challenges 2
1.3 Possible Solutions 4

Part I Introduction to Video Coding **7**

2 Video Coding: Fundamentals **9**
2.1 Overview 9
2.2 What Is Video? 9
2.3 Analog Video 9
2.3.1 Analog Video Signal 9
2.3.2 Color Representation 11
2.3.3 Analog Video Systems 12
2.4 Digital Video 13
2.4.1 Why Digital? 13
2.4.2 Digitization 13
2.4.3 Chroma Subsampling 14
2.4.4 Digital Video Formats 15
2.5 Video Coding Basics 17
2.5.1 The Need for Video Coding 17
2.5.2 Elements of a Video Coding System 18
2.5.3 Elements of Information Theory 19
2.5.4 Quantization 20
2.5.5 Symbol Encoding 23
2.5.6 Performance Measures 26

2.6 Intraframe Coding 28
2.6.1 Predictive Coding 28
2.6.2 Transform Coding 29
2.6.3 Subband Coding 33
2.6.4 Vector Quantization 35
2.6.5 Second-Generation Coding 37
2.6.6 Other Coding Methods 38
2.7 Interframe Coding 38
2.7.1 Three-Dimensional Coding 38
2.7.2 Motion-Compensated Coding 39
2.7.3 Model-Based Coding 41

3 Video Coding: Standards **43**
3.1 Overview 43
3.2 The Need for Video Coding Standards 43
3.3 Chronological Development 44
3.3.1 H.120 44
3.3.2 H.261 44
3.3.3 CCIR-721 45
3.3.4 CCIR-723 45
3.3.5 MPEG-1 45
3.3.6 MPEG-2 46
3.3.7 H.263 46
3.3.8 H.263+ 47
3.3.9 MPEG-4 47
3.3.10 H.263++ 48
3.3.11 H.26L 48
3.4 The H.263 Standard 49
3.4.1 Introduction 49
3.4.2 Source Format 49
3.4.3 Video Source Coding Algorithm 49
3.4.4 Decoding Process 54
3.4.5 Optional Coding Modes 55
3.4.6 H.263, Version 2 (H.263+) 57
3.4.7 H.263, Version 3 (H.263++) 70
3.5 The MPEG-4 Standard 72
3.5.1 An Object-Based Representation 72
3.5.2 Shape Coding 76
3.5.3 Motion Estimation and Compensation 79
3.5.4 Texture Coding 81
3.5.5 Still Texture Coding 84
3.5.6 Sprite Coding 84

3.5.7 Scalability 85
3.5.8 Error Resilience 86
3.5.9 Profiles and Levels 89

Part II Coding Efficiency **91**

4 Basic Motion Estimation Techniques **93**
4.1 Overview 93
4.2 Motion Estimation 93
4.2.1 Projected Motion and Apparent Motion 94
4.2.2 Problem Formulation 95
4.2.3 An Ill-Posed Problem 96
4.2.4 Deterministic and Probabilistic Models 97
4.2.5 Parametric and Nonparametric Models 97
4.2.6 Region of Support 98
4.3 Differential Methods 98
4.4 Pel-Recursive Methods 100
4.5 Frequency-Domain Methods 102
4.6 Block-Matching Methods 105
4.6.1 Matching Function 106
4.6.2 Block Size 108
4.6.3 Search Range 109
4.6.4 Search Accuracy 110
4.6.5 Unrestricted Motion Vectors 111
4.6.6 Overlapped Motion Compensation 112
4.6.7 Properties of Block Motion Fields and Error Surfaces 115
4.7 A Comparative Study 117
4.8 Efficiency of Block Matching at Very Low Bit Rates 122
4.9 Discussion 124

5 Warping-Based Motion Estimation Techniques **125**
5.1 Overview 125
5.2 Warping-Based Methods: A Review 125
5.2.1 Shape of Patches 128
5.2.2 Type of Mesh 128
5.2.3 Spatial Transformation 129
5.2.4 Continuous Versus Discontinuous Methods 129
5.2.5 Backward Versus Forward Node Tracking 130
5.2.6 Node-Tracking Algorithm 131
5.2.7 Motion Compensation Method 132
5.2.8 Transmitted Motion Overhead 133

5.3 Efficiency of Warping-Based Methods at Very Low Bit Rates 134
5.4 Discussion 139

6 Multiple-Reference Motion Estimation Techniques **141**
6.1 Overview 141
6.2 Multiple-Reference Motion Estimation: A Review 142
6.3 Long-Term Memory Motion Compensated Prediction 144
6.3.1 Properties of Long-Term Block Motion Fields 145
6.3.2 Prediction Gain 147
6.3.3 Efficiency at Very Low Bit Rates 149
6.4 Discussion 154

Part III Computational Complexity **157**

7 Reduced-Complexity Motion Estimation Techniques **159**
7.1 Overview 159
7.2 The Need for Reduced-Complexity Motion Estimation 159
7.3 Techniques Based on a Reduced Set of Motion Vector Candidates 161
7.4 Techniques Based on a Reduced-Complexity Block Distortion Measure 163
7.5 Techniques Based on a Subsampled Block Motion Field 164
7.6 Hierarchical Search Techniques 166
7.7 Fast Full-Search Techniques 168
7.8 A Comparative Study 170
7.9 Discussion 173

8 The Simplex Minimization Search **175**
8.1 Overview 175
8.2 Block Matching: An Optimization Problem 176
8.2.1 Problem Formulation 176
8.2.2 A Possible Solution 177
8.3 The Simplex Minimization (SM) Optimization Method 177
8.3.1 Basic Algorithm 177
8.3.2 SM for BMME: Why? 178
8.4 The Simplex Minimization Search (SMS) 181
8.4.1 Initialization Procedure 181
8.4.2 Constraints on the Independent Variables 182
8.4.3 Termination Criterion 182
8.4.4 Motion Vector Refinement 183

8.5 Simulation Results 183
8.5.1 Results Within an Isolated Test Environment .. 183
8.5.2 Results Within an H.263-like Codec 188
8.5.3 Results Within an MPEG-4 Codec 190
8.6 Simplex Minimization for Multiple-Reference Motion Estimation 196
8.6.1 Multiple-Reference SMS Algorithms 197
8.6.2 Simulation Results 198
8.7 Discussion 202

Part IV Error Resilience **203**

9 Error-Resilience Video Coding Techniques **205**
9.1 Overview 205
9.2 A Typical Video Communication System 205
9.3 Types of Errors 206
9.3.1 Random Bit Errors 207
9.3.2 Erasure (or Burst) Errors 207
9.4 Effects of Errors 207
9.4.1 Isolated Effects 207
9.4.2 Spatial Error Propagation 208
9.4.3 Temporal Error Propagation 208
9.5 Error Detection 209
9.6 Forward Techniques 210
9.6.1 Forward Error Correction (FEC) 211
9.6.2 Robust Waveform Coding 211
9.6.3 Robust Entropy Coding 213
9.6.4 Layered Coding with Prioritisation 217
9.6.5 Multiple Description Coding 218
9.6.6 Interleaved Coding 219
9.7 Postprocessing (or Concealment) Techniques 219
9.7.1 Spatial Error Concealment 220
9.7.2 Temporal Error Concealment 222
9.7.3 Hybrid Error Concealment 224
9.7.4 Coding-Mode Recovery 224
9.8 Interactive Techniques 224
9.8.1 Automatic Repeat Request (ARQ) 225
9.8.2 Error Tracking 225
9.8.3 Reference Picture Selection 227
9.9 Discussion 229

10 Error Concealment Using Motion Field Interpolation **231**
10.1 Overview 231

10.2 Temporal Error Concealment Using Motion Field Interpolation (MFI) 232
10.2.1 Motivation 232
10.2.2 Description of the Technique 233
10.2.3 Reduced-Complexity MFI 235
10.3 Temporal Error Concealment Using a Combined BM-MFI Technique 236
10.3.1 Motivation 236
10.3.2 Description of the Technique 236
10.4 Simulation Results 237
10.4.1 Results Within an Isolated Error Environment 237
10.4.2 Results Within an H.263 Decoder 243
10.5 Temporal Error Concealment for Multiple-Reference Motion- Compensated Prediction 246
10.5.1 Temporal-Component Recovery 248
10.5.2 Spatial-Components Recovery 250
10.5.3 Spatial-Temporal-Components Recovery 251
10.5.4 Multi-hypothesis Temporal Error Concealment 252
10.6 Discussion 255

Appendix A Fast Block-Matching Algorithms **259**

A.1 Notation and Assumptions 259
A.2 The Two-Dimensional Logarithmic Search (TDL) 260
A.3 The *N*-Steps Search (NSS) 261
A.4 The One-at-a-Time Search (OTS) 262
A.5 The Cross Search Algorithm (CSA) 263
A.6 The Diamond Search (DS) 265

Bibliography **267**

Index **283**

ENGINEERING LIBRARY

RECEIVED
JUL 12 2002
ENGINEERING LIBRARY

APPENDIX GIROD01

screenshot-catalog.libraries.psu.edu-2023.12.05-15_55_35
https://catalog.libraries.psu.edu/catalog/37409831/marc_view
05.12.2023

MARC View

LEADER 16605cas a2201945 a 4500			
001 37409831			
003 SIRSI			
005 20220602164238.0			
008 751101c19639999nyumr p 0 a0eng c			
010			a| 86645263 z| sn 80000610
016	7		a| 01120981X 2| DE-101
016	7		a| 209133-1 2| DE-600
016	7		a| 9879073 2| DNLM
016	7		a| P35165000 2| DNLM
016	7		a| 000265689 2| IsJJNL
016	7		a| 007872017 2| Uk
019			a| 5312825 a| 185062853 a| 222869421 a| 241310267 a| 316300188 a| 985143064 a| 1009011111 a| 1011949541 a| 1043961400 a| 1049731890 a| 1054218746 a| 1056258641 a| 1064299508 a| 1065062061 a| 1079938701 a| 1100904990 a| 1178636188 a| 1192413672 a| 1196165787 a| 1200069400 a| 1202991903 a| 1205392388 a| 1205513450 a| 1236051671 a| 1242785572 a| 1246524520 a| 1264050557 a| 1264645911
019			a| MARS
022	0		a| 0018-9219 l| 0018-9219 2| 1
030			a| IEEPAD
035			a| (OCoLC)1753228
037			b| IEEE Operations Center, 445 Hoes Lane, P.O. Box 1331, Piscataway, NJ 08855-1331
040			a| MUL b| eng c| MUL d| NSD d| IUL d| SER d| NSD d| AIP d| OCL d| DLC d| NSD d| DLC d| NST d| OCL d| NST d| DLC d| IUL d| MYG d| CUS d| MYG d| SYS d| OCLCQ d| HUL d| IEEEX d| NLM d| OCLCQ d| ORE d| NSD d| NLGGC d| LVB d| EEM d| OCLCQ d| HEBIS d| GBVCP d| DLC d| IUL d| OCLCQ d| AU@ d| J9U d| OCLCO d| IUL d| OCLCF d| OCLCO d| TPA d| OCLCA d| AVA d| UKMGB d| OCLCQ d| CASUM d| OCLCO d| OCLCA d| UtOrBLW
042			a| pcc a| nsdp
050	0	0	a| TK5700 b| .I6
082	0	0	a| 621.381/05 2| 19
110	2		a| Institute of Electrical and Electronics Engineers. 0| http://id.loc.gov/authorities/names/n79053217
210	0		a| Proc. I.E.E.E.
222		0	a| Proceedings of the IEEE
245	1	0	a| Proceedings of the IEEE.
246	3		a| Proceedings of the Institute of Electrical and Electronics Engineers
264		1	a| [New York, N.Y.] : b| Institute of Electrical and Electronics Engineers, c| 1963-
300			a| volumes : b| illustrations ; c| 28 cm
310			a| Monthly
336			a| text b| txt 2| rdacontent
337			a| unmediated b| n 2| rdamedia
338			a| volume b| nc 2| rdacarrier
362	0		a| Vol. 51, no. 1 (Jan. 1963)-
500			a| Title from cover.
510	2		a| Chemical abstracts x| 0009-2258
525			a| Vol. 100 also has a special issue called: 100th anniversary issue.
533			a| Microform. b| [New York, N.Y.? c| IEEE], d| 19__? e| microfiches ; 11 x 15 cm.
588	1		a| Vol. 90, no. 1 (Jan. 2002).
590			a| Binder's title: IEEE proceedings.
650		0	a| Radio v| Periodicals. 0| http://id.loc.gov/authorities/subjects/sh2008110405
650		0	a| Electronics v| Periodicals. 0| http://id.loc.gov/authorities/subjects/sh2008102897
650		6	a| Électronique v| Périodiques.
650		6	a| Électricité v| Périodiques.
650		7	a| Electronics. 2| fast 0| (OCoLC)fst00907538
650		7	a| Radio. 2| fast 0| (OCoLC)fst01087053
650	1	7	a| Elektrotechniek. 2| gtt
650	1	2	a| Medical Laboratory Science. 0| https://id.nlm.nih.gov/mesh/D013677
655		0	a| Electronic journals.

655 4 a| Electronic journals.
655 7 a| Periodicals. 2| aat
655 7 a| Periodicals. 2| fast 0| (OCoLC)fst01411641
655 7 a| Electronic journals. 2| lcgft
776 0 8 i| Online version: a| Institute of Electrical and Electronics Engineers. t| Proceedings of the IEEE (Online) x| 1558-2256 w| (DLC) 2005212484 w| (OCoLC)60638421
780 0 0 a| Institute of Radio Engineers. t| Proceedings of the IRE x| 0096-8390 w| (DLC) 86645262 w| (OCoLC)1753246
949 a| TK5700.I6 v.51 no.1-6 1963 w| LCPER c| 1 i| 000052233371 d| 9/22/2003 l| ACAD-BLDG m| UP-ANNEX n| 1 r| Y s| Y t| PERIODICAL u| 9/15/2003
949 a| TK5700.I6 v.51 no.7-12 1963 w| LCPER c| 1 i| 000069466250 l| ACAD-BLDG m| UP-ANNEX r| Y s| Y t| PERIODICAL u| 9/8/2010
949 a| TK5700.I6 v.52 no.1-6 1964 w| LCPER c| 1 i| 000069466267 l| ACAD-BLDG m| UP-ANNEX r| Y s| Y t| PERIODICAL u| 9/8/2010
949 a| TK5700.I6 v.52 no.7-12 1964 w| LCPER c| 1 i| 000069466274 l| ACAD-BLDG m| UP-ANNEX r| Y s| Y t| PERIODICAL u| 9/8/2010
949 a| TK5700.I6 v.53 no.1-6 1965 w| LCPER c| 1 i| 000069466281 l| ACAD-BLDG m| UP-ANNEX r| Y s| Y t| PERIODICAL u| 9/8/2010
949 a| TK5700.I6 v.53 no.7-12 1965 w| LCPER c| 1 i| 000069466298 l| ACAD-BLDG m| UP-ANNEX r| Y s| Y t| PERIODICAL u| 9/8/2010
949 a| TK5700.I6 v.54 no.1-6 1966 w| LCPER c| 1 i| 000046607492 d| 4/1/2002 e| 3/21/2002 l| ACAD-BLDG m| UP-ANNEX n| 1 r| Y s| Y t| PERIODICAL u| 3/21/2002
949 a| TK5700.I6 v.54 no.7-12 1966 w| LCPER c| 1 i| 000069466304 l| ACAD-BLDG m| UP-ANNEX r| Y s| Y t| PERIODICAL u| 9/8/2010
949 a| TK5700.I6 v.55 no.1-6 1967 w| LCPER c| 1 i| 000069466311 l| ACAD-BLDG m| UP-ANNEX r| Y s| Y t| PERIODICAL u| 9/8/2010
949 a| TK5700.I6 v.55 no.7-12 1967 w| LCPER c| 1 i| 000052238857 l| ACAD-BLDG m| UP-ANNEX r| Y s| Y t| PERIODICAL u| 12/23/2003
949 a| TK5700.I6 v.56 no.1-6 1968 w| LCPER c| 1 i| 000069466328 l| ACAD-BLDG m| UP-ANNEX r| Y s| Y t| PERIODICAL u| 9/8/2010
949 a| TK5700.I6 v.56 no.7-12 1968 w| LCPER c| 1 i| 000052242304 d| 6/22/2005 l| ACAD-BLDG m| UP-ANNEX n| 1 r| Y s| Y t| PERIODICAL u| 6/21/2005
949 a| TK5700.I6 v.57 no.1-6 1969 w| LCPER c| 1 i| 000052240683 d| 3/18/2004 l| ACAD-BLDG m| UP-ANNEX n| 1 r| Y s| Y t| PERIODICAL u| 3/17/2004
949 a| TK5700.I6 v.57 no.7-12 1969 w| LCPER c| 1 i| 000069466144 l| ACAD-BLDG m| UP-ANNEX r| Y s| Y t| PERIODICAL u| 9/8/2010
949 a| TK5700.I6 v.58 no.1-6 1970 w| LCPER c| 1 i| 000018898170 l| CATO-2 m| UP-ANNEX r| Y s| Y t| PERIODICAL u| 3/20/2003 z| 7764
949 a| TK5700.I6 v.58 no.7-12 1970 w| LCPER c| 1 i| 000018898187 l| CATO-2 m| UP-ANNEX r| Y s| Y t| PERIODICAL u| 3/20/2003 z| 7764
949 a| TK5700.I6 v.59 no.1-6 1971 w| LCPER c| 1 i| 000018898194 d| 2/16/2004 l| CATO-2 m| UP-ANNEX q| 1 r| Y s| Y t| PERIODICAL u| 3/20/2003 z| 7764
949 a| TK5700.I6 v.59 no.7-12 1971 w| LCPER c| 1 i| 000018898200 l| CATO-2 m| UP-ANNEX r| Y s| Y t| PERIODICAL u| 3/20/2003 z| 7764
949 a| TK5700.I6 v.60 no.1-6 1972 w| LCPER c| 1 i| 000018898217 d| 6/28/2005 e| 6/28/2005 l| CATO-2 m| UP-ANNEX n| 1 q| 1 r| Y s| Y t| PERIODICAL u| 3/20/2003 z| 7764
949 a| TK5700.I6 v.60 no.7-12 1972 w| LCPER c| 1 i| 000018898224 d| 5/24/2004 l| CATO-2 m| UP-ANNEX q| 1 r| Y s| Y t| PERIODICAL u| 3/20/2003 z| 7764
949 a| TK5700.I6 v.61 no.1-6 1973 w| LCPER c| 1 i| 000018898231 l| CATO-2 m| UP-ANNEX r| Y s| Y t| PERIODICAL u| 3/20/2003 z| 7764
949 a| TK5700.I6 v.61 no.7-12 1973 w| LCPER c| 1 i| 000018898248 d| 6/13/2005 l| CATO-2 m| UP-ANNEX q| 2 r| Y s| Y t| PERIODICAL u| 3/20/2003 z| 7764
949 a| TK5700.I6 v.62 no.1-6 1974 w| LCPER c| 1 i| 000018898255 d| 7/6/2015 e| 6/25/2015 l| CATO-2 m| UP-ANNEX q| 4 r| Y s| Y t| PERIODICAL u| 3/20/2003 z| 7764
949 a| TK5700.I6 v.62 no.7-12 1974 w| LCPER c| 1 i| 000018898262 d| 2/24/2004 l| CATO-2 m| UP-ANNEX q| 2 r| Y s| Y t| PERIODICAL u| 3/20/2003 z| 7764
949 a| TK5700.I6 v.63 no.1-6 1975 w| LCPER c| 1 i| 000051826017 l| CATO-2 m| UP-ANNEX r| Y s| Y t| PERIODICAL u| 3/20/2003 z| 7764
949 a| TK5700.I6 v.63 no.7-12 1975 w| LCPER c| 1 i| 000051826024 d| 5/11/2005 e| 5/11/2005 l| CATO-2 m| UP-ANNEX n| 2 r| Y s| Y t| PERIODICAL u| 3/20/2003 z| 7764
949 a| TK5700.I6 v.64 no.1-6 1976 w| LCPER c| 1 i| 000051826031 l| CATO-2 m| UP-ANNEX r| Y s| Y t| PERIODICAL u| 3/20/2003 z| 7764
949 a| TK5700.I6 v.64 no.7-12 1976 w| LCPER c| 1 i| 000051826048 l| CATO-2 m| UP-ANNEX r| Y s| Y t| PERIODICAL u| 3/20/2003 z| 7764
949 a| TK5700.I6 v.65 no.1-6 1977 w| LCPER c| 1 i| 000051826055 d| 12/2/2003 l| CATO-2 m| UP-ANNEX q| 1 r| Y s| Y t| PERIODICAL u| 3/20/2003 z| 7764
949 a| TK5700.I6 v.65 no.7-12 1977 w| LCPER c| 1 i| 000051826062 d| 7/16/2010 l| CATO-2 m| UP-ANNEX q| 3 r| Y s| Y t| PERIODICAL u| 3/20/2003 z| 7764
949 a| TK5700.I6 v.66 no.1-6 1978 w| LCPER c| 1 i| 000051826079 d| 8/24/2006 e| 11/17/2004 l| CATO-2 m| UP-ANNEX n| 2 q| 1 r| Y s| Y t| PERIODICAL u| 3/20/2003 z| 7764
949 a| TK5700.I6 v.66 no.7-12 1978 w| LCPER c| 1 i| 000051826086 d| 9/4/2003 l| CATO-2 m| UP-ANNEX q| 1 r| Y s| Y t| PERIODICAL u| 3/20/2003 z| 7764
949 a| TK5700.I6 v.67 no.1-6 1979 w| LCPER c| 1 i| 000051826093 l| CATO-2 m| UP-ANNEX r| Y s| Y t| PERIODICAL u| 3/20/2003 z| 7764
949 a| TK5700.I6 v.67 no.7-12 1979 w| LCPER c| 1 i| 000051826109 d| 7/2/2003 e| 7/2/2003 l| CATO-2 m| UP-ANNEX n| 2 q| 1 r| Y s| Y t| PERIODICAL u| 3/20/2003 z| 7764
949 a| TK5700.I6 v.68 no.1-6 1980 w| LCPER c| 1 i| 000051826116 d| 10/13/2004 l| CATO-2 m| UP-ANNEX q| 1 r| Y s| Y t| PERIODICAL u| 3/20/2003 z| 7764
949 a| TK5700.I6 v.68 no.7-12 1980 w| LCPER c| 1 i| 000051826123 d| 6/5/2005 e| 6/5/2005 l| CATO-2 m| UP-ANNEX n| 1 r| Y s| Y t| PERIODICAL u| 3/20/2003 z| 7764

949	a| TK5700.I6 v.69 no.1-6 1981 w| LCPER c| 1 i| 000051826130 d| 12/2/2003 l| CATO-2 m| UP-ANNEX q| 3 r| Y s| Y t| PERIODICAL u| 3/20/2003 z| 7764
949	a| TK5700.I6 v.69 no.7-12 1981 w| LCPER c| 1 i| 000051826147 d| 12/2/2003 l| CATO-2 m| UP-ANNEX q| 1 r| Y s| Y t| PERIODICAL u| 3/20/2003 z| 7764
949	a| TK5700.I6 v.70 no.1-6 1982 w| LCPER c| 1 i| 000051826154 d| 1/26/2005 l| CATO-2 m| UP-ANNEX q| 2 r| Y s| Y t| PERIODICAL u| 3/20/2003 z| 7766
949	a| TK5700.I6 v.70 no.7-12 1982 w| LCPER c| 1 i| 000051826161 d| 1/13/2005 l| CATO-2 m| UP-ANNEX q| 2 r| Y s| Y t| PERIODICAL u| 3/20/2003 z| 7766
949	a| TK5700.I6 v.71 no.1-6 1983 w| LCPER c| 1 i| 000051826178 d| 2/10/2005 l| CATO-2 m| UP-ANNEX q| 3 r| Y s| Y t| PERIODICAL u| 3/20/2003 z| 7766
949	a| TK5700.I6 v.71 no.7-12 1983 w| LCPER c| 1 i| 000051826185 d| 5/21/2007 e| 5/21/2007 l| CATO-2 m| UP-ANNEX n| 1 r| Y s| Y t| PERIODICAL u| 3/20/2003 z| 7766
949	a| TK5700.I6 v.72 no.1-4 1984 w| LCPER c| 1 i| 000051826192 l| CATO-2 m| UP-ANNEX r| Y s| Y t| PERIODICAL u| 3/20/2003 z| 7766
949	a| TK5700.I6 v.72 no.5-8 1984 w| LCPER c| 1 i| 000051826208 l| CATO-2 m| UP-ANNEX r| Y s| Y t| PERIODICAL u| 3/20/2003 z| 7766
949	a| TK5700.I6 v.72 no.9-12 1984 w| LCPER c| 1 i| 000051826215 l| CATO-2 m| UP-ANNEX r| Y s| Y t| PERIODICAL u| 3/20/2003 z| 7766
949	a| TK5700.I6 v.73 no.1-3 1985 w| LCPER c| 1 i| 000051826222 l| CATO-2 m| UP-ANNEX r| Y s| Y t| PERIODICAL u| 3/20/2003 z| 7766
949	a| TK5700.I6 v.73 no.4-7 1985 w| LCPER c| 1 i| 000051826239 d| 2/16/2004 l| CATO-2 m| UP-ANNEX q| 1 r| Y s| Y t| PERIODICAL u| 3/20/2003 z| 7766
949	a| TK5700.I6 v.73 no.8-12 1985 w| LCPER c| 1 i| 000051826246 l| CATO-2 m| UP-ANNEX r| Y s| Y t| PERIODICAL u| 3/20/2003 z| 7766
949	a| TK5700.I6 v.74 no.1-6 1986 w| LCPER c| 1 i| 000051826253 d| 7/1/2004 e| 7/1/2004 l| CATO-2 m| UP-ANNEX n| 1 q| 2 r| Y s| Y t| PERIODICAL u| 3/20/2003 z| 7766
949	a| TK5700.I6 v.74 no.7-12 1986 w| LCPER c| 1 i| 000051826260 l| CATO-2 m| UP-ANNEX r| Y s| Y t| PERIODICAL u| 3/20/2003 z| 7766
949	a| TK5700.I6 v.75 no.1-6 1987 w| LCPER c| 1 i| 000051826277 d| 2/1/2005 e| 2/1/2005 l| CATO-2 m| UP-ANNEX n| 1 q| 1 r| Y s| Y t| PERIODICAL u| 3/20/2003 z| 7766
949	a| TK5700.I6 v.75 no.7-12 1987 w| LCPER c| 1 i| 000051826284 l| CATO-2 m| UP-ANNEX r| Y s| Y t| PERIODICAL u| 3/20/2003 z| 7766
949	a| TK5700.I6 v.76 no.1-4 1988 w| LCPER c| 1 i| 000051826291 l| CATO-2 m| UP-ANNEX r| Y s| Y t| PERIODICAL u| 3/20/2003 z| 7766
949	a| TK5700.I6 v.76 no.5-8 1988 w| LCPER c| 1 i| 000051826307 l| CATO-2 m| UP-ANNEX r| Y s| Y t| PERIODICAL u| 3/20/2003 z| 7766
949	a| TK5700.I6 v.76 no.9-12 1988 w| LCPER c| 1 i| 000051826314 l| CATO-2 m| UP-ANNEX r| Y s| Y t| PERIODICAL u| 3/20/2003 z| 7766
949	a| TK5700.I6 v.77 no.1-6 1989 w| LCPER c| 1 i| 000051826321 l| CATO-2 m| UP-ANNEX r| Y s| Y t| PERIODICAL u| 3/20/2003 z| 7766
949	a| TK5700.I6 v.77 no.7-9 1989 w| LCPER c| 1 i| 000051826338 l| CATO-2 m| UP-ANNEX r| Y s| Y t| PERIODICAL u| 3/20/2003 z| 7766
949	a| TK5700.I6 v.77 no.10-12 1989 w| LCPER c| 1 i| 000051826345 l| CATO-2 m| UP-ANNEX r| Y s| Y t| PERIODICAL u| 3/20/2003 z| 7766
949	a| TK5700.I6 v.78 no.1-3 1990 w| LCPER c| 1 i| 000051826352 l| CATO-2 m| UP-ANNEX r| Y s| Y t| PERIODICAL u| 3/20/2003 z| 7766
949	a| TK5700.I6 v.78 no.4-6 1990 w| LCPER c| 1 i| 000051826369 l| CATO-2 m| UP-ANNEX r| Y s| Y t| PERIODICAL u| 3/20/2003 z| 7766
949	a| TK5700.I6 v.78 no.7-9 1990 w| LCPER c| 1 i| 000051826376 l| CATO-2 m| UP-ANNEX r| Y s| Y t| PERIODICAL u| 3/20/2003 z| 7766
949	a| TK5700.I6 v.78 no.10-12 1990 w| LCPER c| 1 i| 000051826383 l| CATO-2 m| UP-ANNEX r| Y s| Y t| PERIODICAL u| 3/20/2003 z| 7766
949	a| TK5700.I6 v.79 no.1-3 1991 w| LCPER c| 1 i| 000051826390 l| CATO-2 m| UP-ANNEX r| Y s| Y t| PERIODICAL u| 3/20/2003 z| 7766
949	a| TK5700.I6 v.79 no.4-6 1991 w| LCPER c| 1 i| 000051826406 l| CATO-2 m| UP-ANNEX r| Y s| Y t| PERIODICAL u| 3/20/2003 z| 7766
949	a| TK5700.I6 v.79 no.7-9 1991 w| LCPER c| 1 i| 000051826413 l| CATO-2 m| UP-ANNEX r| Y s| Y t| PERIODICAL u| 3/20/2003 z| 7766
949	a| TK5700.I6 v.79 no.10-12 1991 w| LCPER c| 1 i| 000051826420 l| CATO-2 m| UP-ANNEX r| Y s| Y t| PERIODICAL u| 3/20/2003 z| 7766
949	a| TK5700.I6 v.80 no.1-3 1992 w| LCPER c| 1 i| 000051826437 l| CATO-2 m| UP-ANNEX r| Y s| Y t| PERIODICAL u| 3/20/2003 z| 7766
949	a| TK5700.I6 v.80 no.4-6 1992 w| LCPER c| 1 i| 000051826444 l| CATO-2 m| UP-ANNEX r| Y s| Y t| PERIODICAL u| 3/20/2003 z| 7766
949	a| TK5700.I6 v.80 no.7-9 1992 w| LCPER c| 1 i| 000051826451 l| CATO-2 m| UP-ANNEX r| Y s| Y t| PERIODICAL u| 3/20/2003 z| 7766
949	a| TK5700.I6 v.80 no.10-12 1992 w| LCPER c| 1 i| 000051826468 l| CATO-2 m| UP-ANNEX r| Y s| Y t| PERIODICAL u| 3/20/2003 z| 7766
949	a| TK5700.I6 v.81 no.1-6 1993 w| LCPER c| 1 i| 000051826475 l| CATO-2 m| UP-ANNEX r| Y s| Y t| PERIODICAL u| 3/20/2003 z|

7766

949 a| TK5700.I6 v.81 no.7-12 1993 w| LCPER c| 1 i| 000051826482 l| CATO-2 m| UP-ANNEX r| Y s| Y t| PERIODICAL u| 3/20/2003 z| 7766

949 a| TK5700.I6 v.82 no.1-6 1994 w| LCPER c| 1 i| 000051826499 l| CATO-2 m| UP-ANNEX r| Y s| Y t| PERIODICAL u| 3/20/2003 z| 7766

949 a| TK5700.I6 v.82 no.7-12 1994 w| LCPER c| 1 i| 000051826505 l| CATO-2 m| UP-ANNEX r| Y s| Y t| PERIODICAL u| 3/20/2003 z| 7766

949 a| TK5700.I6 v.83 no.1-6 1995 w| LCPER c| 1 i| 000051826512 l| CATO-2 m| UP-ANNEX r| Y s| Y t| PERIODICAL u| 3/20/2003 z| 7766

949 a| TK5700.I6 v.83 no.7-12 1995 w| LCPER c| 1 i| 000051826529 l| CATO-2 m| UP-ANNEX r| Y s| Y t| PERIODICAL u| 3/20/2003 z| 7766

949 a| TK5700.I6 v.84 no.1-6 1996 w| LCPER c| 1 i| 000051826536 l| CATO-2 m| UP-ANNEX r| Y s| Y t| PERIODICAL u| 3/20/2003 z| 7766

949 a| TK5700.I6 v.84 no.7-12 1996 w| LCPER c| 1 i| 000051826543 l| CATO-2 m| UP-ANNEX r| Y s| Y t| PERIODICAL u| 3/20/2003 z| 7766

949 a| TK5700.I6 v.85 no.1-6 1997 w| LCPER c| 1 i| 000051826550 l| CATO-2 m| UP-ANNEX r| Y s| Y t| PERIODICAL u| 3/20/2003 z| 7766

949 a| TK5700.I6 v.85 no.7-12 1997 w| LCPER c| 1 i| 000051826567 l| CATO-2 m| UP-ANNEX r| Y s| Y t| PERIODICAL u| 3/20/2003 z| 7766

949 a| TK5700.I6 v.86 no.1-6 1998 w| LCPER c| 1 i| 000051826574 d| 8/13/2018 l| CATO-2 m| UP-ANNEX q| 3 r| Y s| Y t| PERIODICAL u| 3/20/2003 z| 7766

949 a| TK5700.I6 v.86 no.7-12 1998 w| LCPER c| 1 i| 000051826581 d| 10/7/2003 l| CATO-2 m| UP-ANNEX q| 1 r| Y s| Y t| PERIODICAL u| 3/20/2003 z| 7766

949 a| TK5700.I6 v.87 no.1-6 1999 w| LCPER c| 1 i| 000051826598 d| 12/2/2003 l| CATO-2 m| UP-ANNEX q| 2 r| Y s| Y t| PERIODICAL u| 3/20/2003 z| 7766

949 a| TK5700.I6 v.87 no.7-12 1999 w| LCPER c| 1 i| 000051826604 d| 12/2/2003 l| CATO-2 m| UP-ANNEX q| 1 r| Y s| Y t| PERIODICAL u| 3/20/2003 z| 7766

949 a| TK5700.I6 v.88 no.1-6 2000 w| LCPER c| 1 i| 000048232104 d| 12/2/2003 l| CATO-2 m| UP-ANNEX q| 1 r| Y s| Y t| PERIODICAL u| 4/12/2001 z| 7766

949 a| TK5700.I6 v.88 no.7-12 2000 w| LCPER c| 1 i| 000048232098 d| 12/2/2003 l| CATO-2 m| UP-ANNEX q| 2 r| Y s| Y t| PERIODICAL u| 9/26/2001 z| 7766

949 a| TK5700.I6 v.89 no.1-6 2001 w| LCPER c| 1 i| 000048462211 l| CATO-2 m| UP-ANNEX r| Y s| Y t| PERIODICAL u| 9/26/2002 z| 7766

949 a| TK5700.I6 v.89 no.7-12 2001 w| LCPER c| 1 i| 000048462204 l| CATO-2 m| UP-ANNEX r| Y s| Y t| PERIODICAL u| 9/26/2002 z| 7766

949 a| TK5700.I6 v.90 no.1-6 2002 w| LCPER c| 1 i| 000051871550 l| CATO-2 m| UP-ANNEX r| Y s| Y t| PERIODICAL u| 5/8/2003 z| 7766

949 a| TK5700.I6 v.90 no.7-12 2002 w| LCPER c| 1 i| 000051871543 l| CATO-2 m| UP-ANNEX r| Y s| Y t| PERIODICAL u| 5/8/2003 z| 7766

949 a| TK5700.I6 v.91 no.1-6 2003 w| LCPER c| 1 i| 000052806384 l| CATO-2 m| UP-ANNEX r| Y s| Y t| PERIODICAL u| 3/2/2004 z| 7766

949 a| TK5700.I6 v.91 no.7-12 2003 w| LCPER c| 1 i| 000052806391 d| 1/11/2007 l| CATO-2 m| UP-ANNEX q| 1 r| Y s| Y t| PERIODICAL u| 3/2/2004 z| 7760

949 a| TK5700.I6 v.92 no.1-6 2004 w| LCPER c| 1 i| 000054847743 l| CATO-2 m| UP-ANNEX r| Y s| Y t| PERIODICAL u| 4/7/2005 z| 7760

949 a| TK5700.I6 v.92 no.7-12 2004 w| LCPER c| 1 i| 000054847736 l| CATO-2 m| UP-ANNEX r| Y s| Y t| PERIODICAL u| 4/7/2005 z| 7760

949 a| TK5700.I6 v.93 no.1-4 2005 w| LCPER c| 1 i| 000054971325 l| CATO-2 m| UP-ANNEX r| Y s| Y t| PERIODICAL u| 3/27/2006 z| 7760

949 a| TK5700.I6 v.93 no.5-8 2005 w| LCPER c| 1 i| 000054971318 l| CATO-2 m| UP-ANNEX r| Y s| Y t| PERIODICAL u| 3/27/2006 z| 7760

949 a| TK5700.I6 v.93 no.9-12 2005 w| LCPER c| 1 i| 000054971578 l| CATO-2 m| UP-ANNEX r| Y s| Y t| PERIODICAL u| 3/27/2006 z| 7760

949 a| TK5700.I6 v.94 no.1-4 2006 w| LCPER c| 1 i| 000055213905 l| CATO-2 m| UP-ANNEX r| Y s| Y t| PERIODICAL u| 5/9/2007 z| 7760

949 a| TK5700.I6 v.94 no.5-8 2006 w| LCPER c| 1 i| 000055213929 l| CATO-2 m| UP-ANNEX r| Y s| Y t| PERIODICAL u| 5/9/2007 z| 7760

949 a| TK5700.I6 v.94 no.9-12 2006 w| LCPER c| 1 i| 000055213912 l| CATO-2 m| UP-ANNEX r| Y s| Y t| PERIODICAL u| 5/9/2007 z| 7760

949 a| TK5700.I6 v.95 no.1-4 2007 w| LCPER c| 1 i| 000059601432 l| CATO-2 m| UP-ANNEX r| Y s| Y t| PERIODICAL u| 1/23/2008 z| 7760

949 a| TK5700.I6 v.95 no.5-8 2007 w| LCPER c| 1 i| 000059601425 l| CATO-2 m| UP-ANNEX r| Y s| Y t| PERIODICAL u| 1/23/2008 z| 7760

949 a| TK5700.I6 v.95 no.9-12 2007 w| LCPER c| 1 i| 000059602040 l| CATO-2 m| UP-ANNEX r| Y s| Y t| PERIODICAL u| 1/23/2008 z| 7760

949 a| TK5700.I6 v.96 no.1-4 2008 w| LCPER c| 1 i| 000059737773 l| CATO-2 m| UP-ANNEX r| Y s| Y t| PERIODICAL u| 2/18/2009 z| 7760

949 a| TK5700.I6 v.96 no.5-8 2008 w| LCPER c| 1 i| 000059738398 l| CATO-2 m| UP-ANNEX r| Y s| Y t| PERIODICAL u| 2/18/2009 z| 7760

949 a| TK5700.I6 v.96 no.9-12 2008 w| LCPER c| 1 i| 000059738404 l| CATO-2 m| UP-ANNEX r| Y s| Y t| PERIODICAL u| 2/18/2009 z| 7760

852 0 1 a| PSt b| UP-ANNEX c| ANNEX h| TK5700 i| .I6

866 0 8| 0 a| v.51(1963)-v.96(2008)


PennState
Copyright @2019 The Pennsylvania State University. All rights reserved. Except where otherwise noted, this work is subject to a Creative Commons Attribution 4.0 license. Details and exceptions.
Legal Statements | PSU Hotlines
PENN STATE UNIVERSITY LIBRARIES
(814) 865-6368
Libraries Home
Libraries Intranet (Staff Only)
Accessibility Help
Website Feedback
Policies and Guidelines
Staff Directory

screenshot-catalog.libraries.psu.edu-2023.12.05-15_55_35
https://catalog.libraries.psu.edu/catalog/37409831/marc_view
05.12.2023

PennState University Libraries | Catalog

Bookmarks 0 Course Reserves My Account

Keyword Search... Search Advanced search Start Over

← Previous | 2 of 4,939 | Next →

Share Bookmark Report an Issue



Proceedings of the IEEE

Corporate Author: Institute of Electrical and Electronics Engineers

Additional Titles: Proc. I.E.E.E. and Proceedings of the Institute of Electrical and Electronics Engineers

Published: [New York, N.Y.] : Institute of Electrical and Electronics Engineers, 1963-

Physical Description: volumes : illustrations ; 28 cm

Read online at Google Books

Availability

Browse Nearby on Shelf I Want It

Library Storage (106 items)

Call number	Material	Location
Annexed Material: Holdings Summary v.51(1963)-v.96(2008)		
TK5700.I6 v.96 no.9-12 2008	Bound Journal	Annexed Material
TK5700.I6 v.96 no.5-8 2008	Bound Journal	Annexed Material
TK5700.I6 v.96 no.1-4 2008	Bound Journal	Annexed Material
TK5700.I6 v.95 no.9-12 2007	Bound Journal	Annexed Material
TK5700.I6 v.95 no.5-8 2007	Bound Journal	Annexed Material
TK5700.I6 v.95 no.1-4 2007	Bound Journal	Annexed Material
TK5700.I6 v.94 no.9-12 2006	Bound Journal	Annexed Material
TK5700.I6 v.94 no.5-8 2006	Bound Journal	Annexed Material
TK5700.I6 v.94 no.1-4 2006	Bound Journal	Annexed Material
TK5700.I6 v.93 no.9-12 2005	Bound Journal	Annexed Material
TK5700.I6 v.93 no.5-8 2005	Bound Journal	Annexed Material
TK5700.I6 v.93 no.1-4 2005	Bound Journal	Annexed Material
TK5700.I6 v.92 no.7-12 2004	Bound Journal	Annexed Material
TK5700.I6 v.92 no.1-6 2004	Bound Journal	Annexed Material
TK5700.I6 v.91 no.7-12 2003	Bound Journal	Annexed Material
TK5700.I6 v.91 no.1-6 2003	Bound Journal	Annexed Material
TK5700.I6 v.90 no.7-12 2002	Bound Journal	Annexed Material
TK5700.I6 v.90 no.1-6 2002	Bound Journal	Annexed Material
TK5700.I6 v.89 no.7-12 2001	Bound Journal	Annexed Material
TK5700.I6 v.89 no.1-6 2001	Bound Journal	Annexed Material
TK5700.I6 v.88 no.7-12 2000	Bound Journal	Annexed Material
TK5700.I6 v.88 no.1-6 2000	Bound Journal	Annexed Material
TK5700.I6 v.87 no.7-12 1999	Bound Journal	Checked out
TK5700.I6 v.87 no.1-6 1999	Bound Journal	Annexed Material
TK5700.I6 v.86 no.7-12 1998	Bound Journal	Annexed Material

TK5700.I6 v.86 no.1-6 1998	Bound Journal	Annexed Material
TK5700.I6 v.85 no.7-12 1997	Bound Journal	Annexed Material
TK5700.I6 v.85 no.1-6 1997	Bound Journal	Annexed Material
TK5700.I6 v.84 no.7-12 1996	Bound Journal	Annexed Material
TK5700.I6 v.84 no.1-6 1996	Bound Journal	Annexed Material
TK5700.I6 v.83 no.7-12 1995	Bound Journal	Annexed Material
TK5700.I6 v.83 no.1-6 1995	Bound Journal	Annexed Material
TK5700.I6 v.82 no.7-12 1994	Bound Journal	Annexed Material
TK5700.I6 v.82 no.1-6 1994	Bound Journal	Annexed Material
TK5700.I6 v.81 no.7-12 1993	Bound Journal	Annexed Material
TK5700.I6 v.81 no.1-6 1993	Bound Journal	Annexed Material
TK5700.I6 v.80 no.10-12 1992	Bound Journal	Annexed Material
TK5700.I6 v.80 no.7-9 1992	Bound Journal	Annexed Material
TK5700.I6 v.80 no.4-6 1992	Bound Journal	Annexed Material
TK5700.I6 v.80 no.1-3 1992	Bound Journal	Annexed Material
TK5700.I6 v.79 no.10-12 1991	Bound Journal	Annexed Material
TK5700.I6 v.79 no.7-9 1991	Bound Journal	Annexed Material
TK5700.I6 v.79 no.4-6 1991	Bound Journal	Annexed Material
TK5700.I6 v.79 no.1-3 1991	Bound Journal	Annexed Material
TK5700.I6 v.78 no.10-12 1990	Bound Journal	Annexed Material
TK5700.I6 v.78 no.7-9 1990	Bound Journal	Annexed Material
TK5700.I6 v.78 no.4-6 1990	Bound Journal	Annexed Material
TK5700.I6 v.78 no.1-3 1990	Bound Journal	Annexed Material
TK5700.I6 v.77 no.10-12 1989	Bound Journal	Annexed Material
TK5700.I6 v.77 no.7-9 1989	Bound Journal	Annexed Material
TK5700.I6 v.77 no.1-6 1989	Bound Journal	Annexed Material
TK5700.I6 v.76 no.9-12 1988	Bound Journal	Annexed Material
TK5700.I6 v.76 no.5-8 1988	Bound Journal	Annexed Material
TK5700.I6 v.76 no.1-4 1988	Bound Journal	Annexed Material
TK5700.I6 v.75 no.7-12 1987	Bound Journal	Annexed Material
TK5700.I6 v.75 no.1-6 1987	Bound Journal	Annexed Material
TK5700.I6 v.74 no.7-12 1986	Bound Journal	Annexed Material
TK5700.I6 v.74 no.1-6 1986	Bound Journal	Annexed Material
TK5700.I6 v.73 no.8-12 1985	Bound Journal	Annexed Material
TK5700.I6 v.73 no.4-7 1985	Bound Journal	Annexed Material
TK5700.I6 v.73 no.1-3 1985	Bound Journal	Annexed Material
TK5700.I6 v.72 no.9-12 1984	Bound Journal	Annexed Material
TK5700.I6 v.72 no.5-8 1984	Bound Journal	Annexed Material
TK5700.I6 v.72 no.1-4 1984	Bound Journal	Annexed Material
TK5700.I6 v.71 no.7-12 1983	Bound Journal	Annexed Material
TK5700.I6 v.71 no.1-6 1983	Bound Journal	Annexed Material
TK5700.I6 v.70 no.7-12 1982	Bound Journal	Annexed Material
TK5700.I6 v.70 no.1-6 1982	Bound Journal	Annexed Material
TK5700.I6 v.69 no.7-12 1981	Bound Journal	Annexed Material
TK5700.I6 v.69 no.1-6 1981	Bound Journal	Annexed Material
TK5700.I6 v.68 no.7-12 1980	Bound Journal	Annexed Material
TK5700.I6 v.68 no.1-6 1980	Bound Journal	Annexed Material
TK5700.I6 v.67 no.7-12 1979	Bound Journal	Annexed Material
TK5700.I6 v.67 no.1-6 1979	Bound Journal	Annexed Material
TK5700.I6 v.66 no.7-12 1978	Bound Journal	Annexed Material

TK5700.I6 v.66 no.7-12 1978	Bound Journal	Annexed Material
TK5700.I6 v.66 no.1-6 1978	Bound Journal	Annexed Material
TK5700.I6 v.65 no.7-12 1977	Bound Journal	Annexed Material
TK5700.I6 v.65 no.1-6 1977	Bound Journal	Annexed Material
TK5700.I6 v.64 no.7-12 1976	Bound Journal	Annexed Material
TK5700.I6 v.64 no.1-6 1976	Bound Journal	Annexed Material
TK5700.I6 v.63 no.7-12 1975	Bound Journal	Annexed Material
TK5700.I6 v.63 no.1-6 1975	Bound Journal	Annexed Material
TK5700.I6 v.62 no.7-12 1974	Bound Journal	Annexed Material
TK5700.I6 v.62 no.1-6 1974	Bound Journal	Annexed Material
TK5700.I6 v.61 no.7-12 1973	Bound Journal	Annexed Material
TK5700.I6 v.61 no.1-6 1973	Bound Journal	Annexed Material
TK5700.I6 v.60 no.7-12 1972	Bound Journal	Annexed Material
TK5700.I6 v.60 no.1-6 1972	Bound Journal	Annexed Material
TK5700.I6 v.59 no.7-12 1971	Bound Journal	Annexed Material
TK5700.I6 v.59 no.1-6 1971	Bound Journal	Annexed Material
TK5700.I6 v.58 no.7-12 1970	Bound Journal	Annexed Material
TK5700.I6 v.58 no.1-6 1970	Bound Journal	Annexed Material
TK5700.I6 v.57 no.7-12 1969	Bound Journal	Annexed Material
TK5700.I6 v.57 no.1-6 1969	Bound Journal	Annexed Material
TK5700.I6 v.56 no.7-12 1968	Bound Journal	Annexed Material
TK5700.I6 v.56 no.1-6 1968	Bound Journal	Annexed Material
TK5700.I6 v.55 no.7-12 1967	Bound Journal	Annexed Material
TK5700.I6 v.55 no.1-6 1967	Bound Journal	Annexed Material
TK5700.I6 v.54 no.7-12 1966	Bound Journal	Annexed Material
TK5700.I6 v.54 no.1-6 1966	Bound Journal	Annexed Material
TK5700.I6 v.53 no.7-12 1965	Bound Journal	Annexed Material
TK5700.I6 v.53 no.1-6 1965	Bound Journal	Annexed Material
TK5700.I6 v.52 no.7-12 1964	Bound Journal	Annexed Material
TK5700.I6 v.52 no.1-6 1964	Bound Journal	Annexed Material
TK5700.I6 v.51 no.7-12 1963	Bound Journal	Annexed Material
TK5700.I6 v.51 no.1-6 1963	Bound Journal	Annexed Material

Continues:
Proceedings of the IRE

Dates of Publication and/or Sequential Designation:
Vol. 51, no. 1 (Jan. 1963)-

Subject(s):
Radio—Periodicals
Electronics—Periodicals
Électronique—Périodiques
Électricité—Périodiques
Electronics
Radio
Elektrotechniek
Medical Laboratory Science

Genre(s):
Electronic journals
Periodicals

ISSN:
0018-9219

Publication Frequency:
Monthly

Note:

Note:
Title from cover.
Binder's title: IEEE proceedings.

Supplement Note:
Vol. 100 also has a special issue called: 100th anniversary issue.

Reproduction Note:
Microform. [New York, N.Y.? IEEE], 19__? microfiches ; 11 x 15 cm.

Selectively Indexed By:
Chemical abstracts 0009-2258

View MARC record | catkey: 37409831

PennState

Copyright @2019 The Pennsylvania State University. All rights reserved. Except where otherwise noted, this work is subject to a Creative Commons Attribution 4.0 license. Details and exceptions.

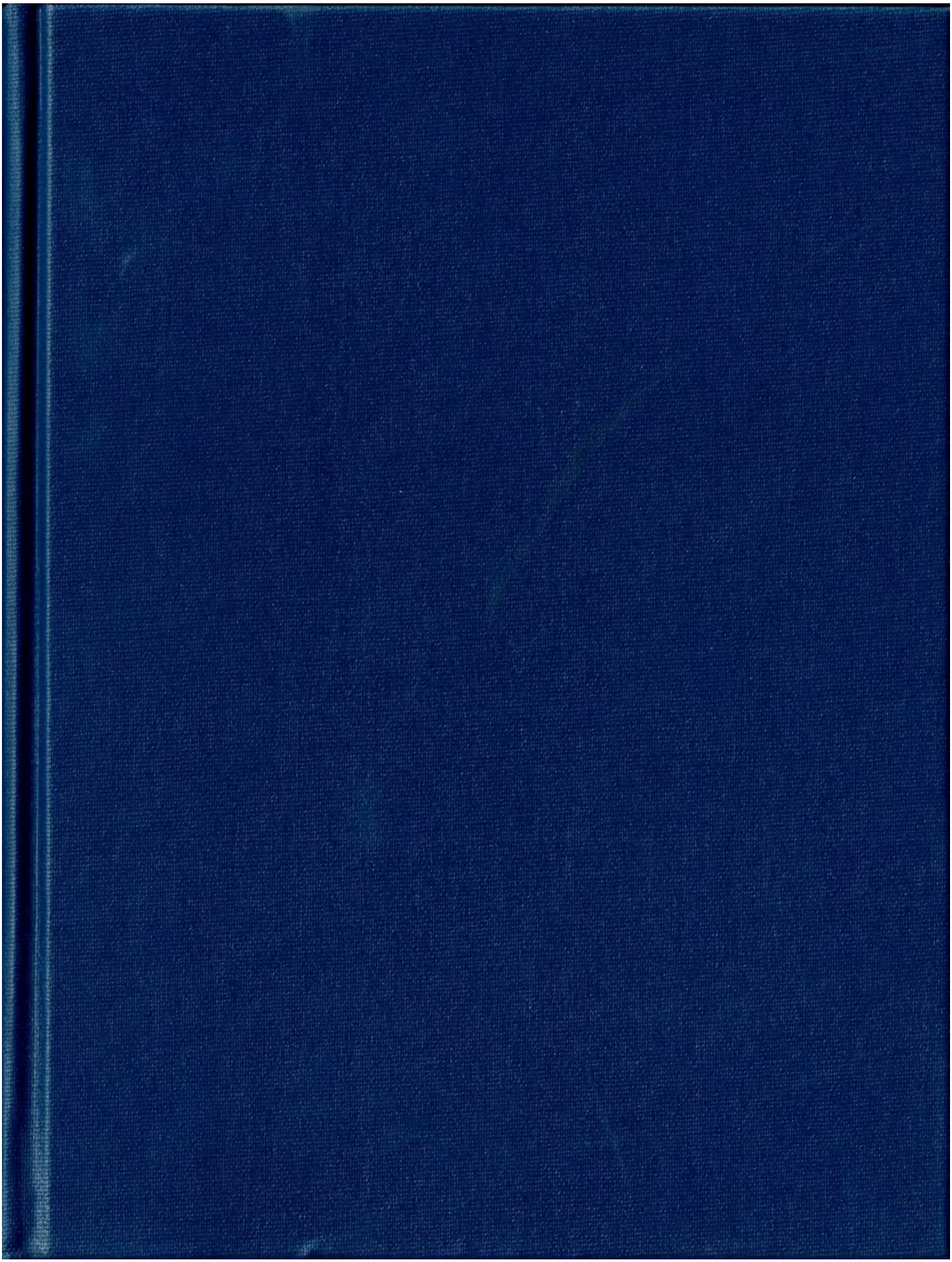
Legal Statements | PSU Hotlines

PENN STATE UNIVERSITY LIBRARIES

Libraries Home
Libraries Intranet (Staff Only)
Accessibility Help
Website Feedback
Policies and Guidelines
Staff Directory

(814) 865-6368

APPENDIX GIROD02



INSTITUTE OF ELECTRICAL AND ELECTRONICS ENGINEERS PROCEEDINGS OF THE IEEE
87 JULY-DEC 1999
ENGIN TK5700 .I6


A0000518266O4

ENGINEERING LIBRARY

SHELVED IN
BOUND
PERIODICAL
COLLECTION

PROCEEDINGS OF THE IEEE

THE INSTITUTE OF ELECTRICAL AND ELECTRONICS ENGINEERS, INC.

OCTOBER 1999

Special Issue

VIDEO TRANSMISSION FOR MOBILE MULTIMEDIA APPLICATIONS

Papers on:

* *Feedback Error Control* * *Robust Video Coding* * *Separate, Concatenated & Joint Source Channel Coding* * *Third-Generation Multipriority Video* * *Transmission Aspects of Wireless Multimedia* * *Broad-Band OFDM Radio Transmission* * *Wireless ATM Networks* * *Multicode CDMA Transport Architecture for MPEG-2 Video*

Classic 1919 Paper: Trans-Oceanic Radio Communication by Ernst F. W. Alexanderson

Predictive 1962 Paper & Update: Diagnostics by Urner Liddel

The Electrical Century: Biomedical Engineering

PROCEEDINGS OF THE IEEE 21st CENTURY TECHNOLOGY FORECAST



SEP 3 0 1999

PROCEEDINGS OF THE IEEE

published monthly by the Institute of Electrical and Electronics Engineers, Inc.

October 1999 Vol. 87 No. 10

SPECIAL ISSUE ON
VIDEO TRANSMISSION FOR MOBILE MULTIMEDIA APPLICATIONS
Edited by Hamid Gharavi and Lajos Hanzo

1703 Scanning the Special Issue on Video Transmission for Mobile Multimedia Applications, *H. Gharavi and L. Hanzo*

PAPERS

1707 Feedback-Based Error Control for Mobile Video Transmission *(Invited Paper)*, *B. Girod and N. Färber*

1724 Robust Video Coding Algorithms and Systems *(Invited Paper)*, *J. D. Villasenor, Y.-Q. Zhang, and J. Wen*

1734 Transport of Wireless Video Using Separate, Concatenated, and Joint Source-Channel Coding *(Invited Paper)*, *R. E. Van Dyck and D. J. Miller*

1751 Multipriority Video Transmission for Third-Generation Wireless Communication Systems, *H. Gharavi and S. M. Alamouti*

1764 Channel Coding and Transmission Aspects for Wireless Multimedia *(Invited Paper)*, *J. Hagenauer and T. Stockhammer*

1778 Broad-Band OFDM Radio Transmission for Multimedia Applications *(Invited Paper)*, *H. Rohling, T. May, K. Brüninghaus, and R. Grünheid*

1790 Wireless ATM Networks: Technology Status and Future Directions *(Invited Paper)*, *D. Raychaudhuri*

1807 Wireless ATM-Based Multicode CDMA Transport Architecture for MPEG-2 Video Transmission *(Invited Paper)*, *P.-R. Chang and C.-F. Lin*

1825 Introduction to "Trans-Oceanic Radio Communication" *(Invited Paper)*, *J. E. Brittain*

1829 Trans-Oceanic Radio Communication *(Classic Paper)*, *E. F. W. Alexanderson*

1838 Diagnostics *(Predictive Paper Reprint)*, *U. Liddel*

1839 Diagnostics Update: A Winding Road *(Predictive Paper)*, *L. S. Edelheit*

THE ELECTRICAL CENTURY

1842 The Bioelectrical Century: Bioelectrical Engineering and the "Inside Story" of the Electrical Century, *D. B. Geselowitz and M. N. Geselowitz*

1847 **FUTURE SPECIAL ISSUES/SPECIAL SECTIONS OF THE PROCEEDINGS**

1848 **PROCEEDINGS CLASSIC PAPER REPRINT SCHEDULE**

1848 **PROCEEDINGS "THE ELECTRICAL CENTURY" SCHEDULE**

OCTOBER

Feedback-Based Error Control for Mobile Video Transmission

BERND GIROD, FELLOW, IEEE, AND NIKO FÄRBER, MEMBER, IEEE

Invited Paper

We review feedback-based low bit-rate video coding techniques for robust transmission in mobile multimedia networks. For error control on the source coding level, each decoder has to make provisions for error detection, resynchronization, and error concealment, and we review techniques suitable for that purpose. Further, techniques are discussed for intelligent processing of acknowledgment information by the coding control to adapt the source coder to the channel. We review and compare error tracking, error confinement, and reference picture selection techniques for channel-adaptive source coding. For comparison of these techniques, a system for transmitting low bit-rate video over a wireless channel is presented and the performance is evaluated for a range of transmission conditions. We also show how feedback-based source coding can be employed in conjunction with precompressed video stored on a media server. The techniques discussed are applicable to a wide variety of interframe video schemes, including various video coding standards. Several of the techniques have been incorporated into the H.263 video compression standard recently, and this standard is used as an example throughout.

Keywords*—*Error correction, feedback, mobile communication, standards, video coding.

I. Introduction

Of all modalities desirable for future mobile multimedia systems, motion video is the most demanding in terms of bit rate. Even with state-of-the-art compression, television quality requires a few megabits per second (Mb/s), while for low-resolution, limited-motion video sequences typical for picturephones, a few tens of kilobits per second (kb/s) are required for satisfactory picture quality. Today's "second-generation" cellular telephony networks, such as the global system for mobile communications (GSM), typically provide 10–15 kb/s, suitable for compressed speech, but too little for motion video. Fortunately, the standardization of higher bandwidth networks, such as the universal mobile telecommunications system (UMTS) [1], [2], is well underway, and, together with continued progress in video compression technology, mobile video-communicators with picturephone functionality and Internet videoserver access will be possible.

Beyond the limited available bit rate, wireless video transmission offers a number of interesting technical challenges. A recent review has appeared in [3]. One of the issues is that mobile networks cannot provide guaranteed quality of service because high bit error rates occur during fading periods. Transmission errors in a mobile channel range from single bit errors to burst errors or even intermittent loss of the connection. These widely varying error conditions limit the effectiveness of classic forward error correction (FEC), since a worst-case design would lead to a prohibitive amount of redundancy. Closed-loop error control techniques like automatic repeat request (ARQ) [4] have been shown to be more effective than FEC and successfully applied to wireless video transmission [5], [6]. Retransmission of corrupted data frames, however, introduces additional delay, which might be unacceptable for real-time conversational services. Refinements of ARQ schemes proposed for video include the retransmission of more strongly compressed video [7] or the retransmission of multiple copies [8] in a packet network. Both techniques can be combined. Nevertheless, residual transmission errors cannot be avoided with a mobile radio channel, even when FEC and ARQ are combined.

The compressed video signal is extremely vulnerable against transmission errors, since low bit-rate video coding schemes rely on interframe coding for high coding efficiency. They use the previous encoded and reconstructed video frame to predict the next frame. Therefore, the loss of information in one frame has considerable impact on the quality of the following frames. Since some residual transmission errors inevitably corrupt the video bit stream, this vulnerability precludes the use of low bit-rate video coding schemes designed for error-free channels without special measures. These measures have to be built into the video coding and decoding algorithms themselves and form the "last line of defense" if techniques like FEC and ARQ fail. In this paper, we discuss such last-line-of-defense

Manuscript received January 27, 1998; revised March 11, 1998.
The authors are with the Telecommunications Laboratory, University of Erlangen-Nuremberg, Erlangen D-91058 Germany.
Publisher Item Identifier S 0018-9219(99)07472-1.

0018–9219/99$10.00 © 1999 IEEE

techniques that can be used to make low bit-rate video coders error resilient. We concentrate on techniques that use acknowledgment information provided by a feedback channel.

The use of a feedback channel is not the only approach to increase the robustness of low bit-rate video communications. A comprehensive review of the great variety of error control and concealment techniques that have been proposed during the last 10–15 years has been presented in an excellent paper by Wang and Zhu recently [8]. For example, one can partition the bit stream into classes of different error sensitivity (often referred to as data partitioning) to enable the use of unequal error protection [9]–[12]. Data partitioning has been included as an error resilience tool in the MPEG-4 standard [13]. Unequal error protection can significantly increase the robustness of the transmission and provide graceful degradation of the picture quality in case of a deteriorating channel. Since unequal error protection does not incorporate information about the current state of the mobile channel, the design of such a scheme is a compromise that accommodates a range of operating conditions. Feedback-based techniques, on the other hand, can adjust to the varying transmission conditions rapidly and make more effective use of the channel.

In this paper, we first review the principles of low bit-rate video coding briefly (Section II), emphasizing the aspects relevant for error-resilience techniques. In Section III, we discuss problems that arise when feeding an erroneous bit stream to an interframe video decoder. In particular, we analyze interframe error propagation. In Section IV, we then present techniques for the video coder to process acknowledgment information from a feedback channel. In Section V, we present simulation results for the transmission of video over a wireless channel to illustrate the effectiveness of feedback-based error control. Finally, in Section VI, we address feedback-based error control for streaming compressed video off a server.

The techniques discussed in this paper are relevant and applicable to a wide variety of interframe video coding schemes, both standard and nonstandard. We emphasize general principles where appropriate. As an illustrative example, we use the video compression standard H.263 [14] throughout. H.263 is not only a state-of-the-art low bit-rate video coder, but it has also been extended to include a variety of feedback-based error control mechanisms. Therefore, this article simultaneously provides an overview of error control techniques currently available in H.263.

II. Motion-Compensated Hybrid Coding

A. General Principles

Most state-of-the-art low bit-rate video codecs are motion-compensated hybrid codecs, as illustrated in Fig. 1. Two basic modes of operation can be selected, depending on the position of the switch S. These two modes allow the video signal in the current frame to be encoded either directly (INTRA coding), or with reference to previously encoded and reconstructed frames (INTER coding).

The INTER mode combines differential pulse code modulation (DPCM) along an estimated motion trajectory with intraframe encoding of the residual prediction error. Motion-compensated prediction is carried out by estimating the motion between successive frames, shifting the contents of a previously encoded, reconstructed frame accordingly, and transmitting the motion vector in addition to the prediction error residual as side information. Note that the output from the frame memory in Fig. 1 is identical to the decoded frames at the decoder for error-free transmission. Therefore, the same prediction can be formed at the encoder and decoder.

The residual prediction error is usually small and requires fewer bits than directly encoding the original video signal. For efficient encoding, a wide variety of intraframe coding schemes can be used, e.g., subband coding or blockwise vector quantization. In all current compression standards, the discrete cosine transform (DCT) is employed for this purpose with a blocksize of 8×8 pixels. The transform coefficients are quantized (Q) and typically encoded as a series of zero-runs and quantizer levels. Transform coefficients and motion vectors are entropy coded along with other side information resulting in variable-length code words, which are multiplexed to the video bit stream.

For most of a video signal, the INTER mode is the preferred mode because of its superior coding efficiency. However, some changes in successive frames, for example, due to uncovered background, new objects appearing in the scene, or after a scene cut, cannot be predicted well, and subtracting the prediction might lead to a prediction error that requires more bits than the original video signal. Therefore, the second basic encoding mode besides INTER coding is the INTRA mode, in which no reference to previous frames is made and the picture is directly intraframe coded. Again, a variety of schemes can be used, but typically a blockwise 8×8 DCT coder is employed.

The video codec shown in Fig. 1 is a forward-adaptive system. Decisions about INTER or INTRA mode, motion vector, or quantizer step size are made by the "intelligent" encoder and are transmitted as side information to the "dumb" decoder. This architecture not only reduces the complexity of the decoder but also leads to increased robustness in case of transmission errors, compared to backward-adaptive systems that avoid sending side information by deriving it from the decoded past available both at the encoder and the decoder. Moreover, the forward-adaptive system architecture provides great freedom for the optimization of the coding control since, unlike a backward-adaptive system, the same decoder can be used for a variety of control strategies. In particular, the switching between INTRA and INTER mode is not subject to a prior agreement between encoder and decoder. Feedback-based error control, discussed in Section IV, can exploit this feature. For more information on the general principles of digital video processing, the reader is referred to [15].

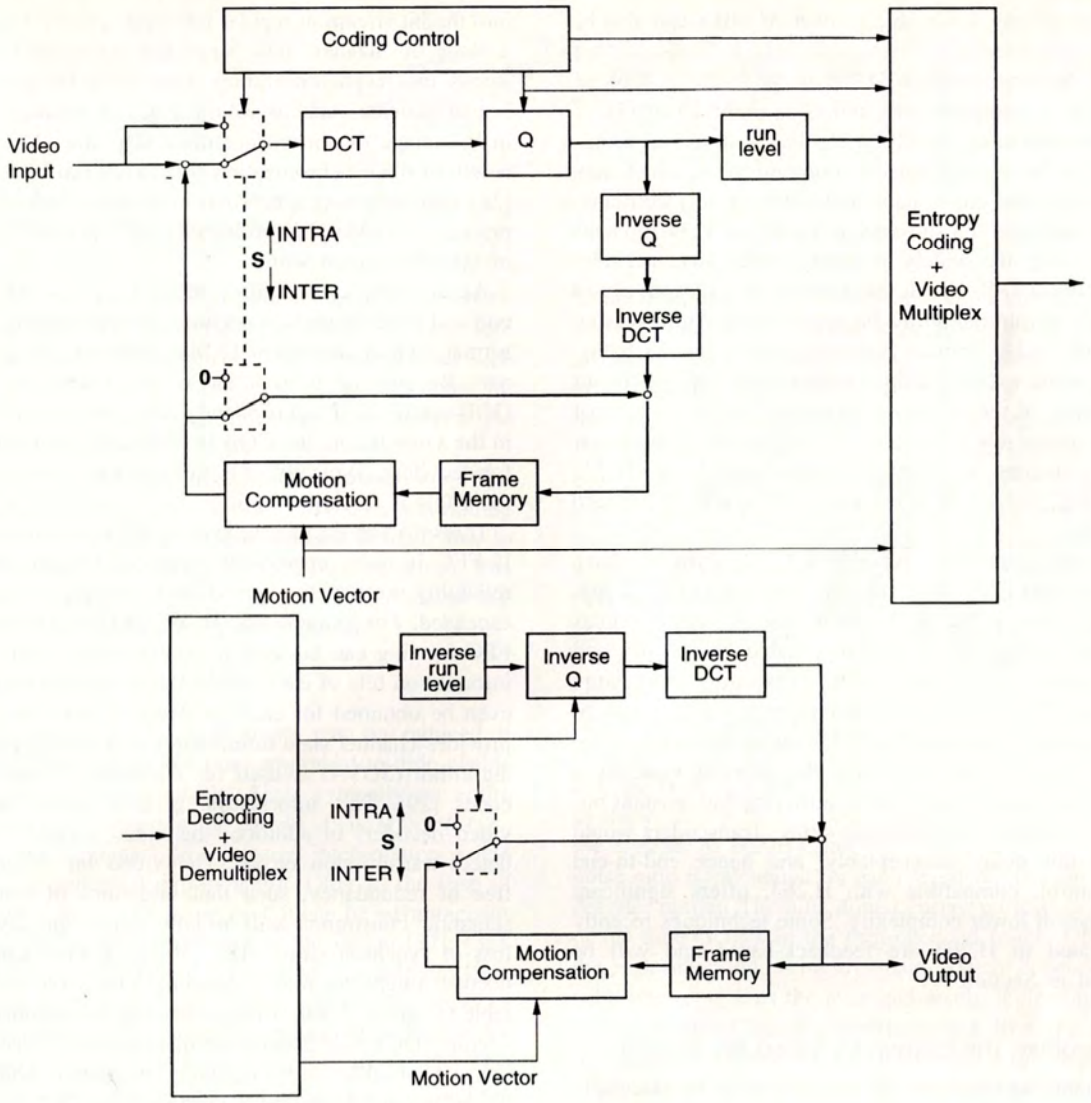


Fig. 1. (a) Motion-compensated hybrid encoder and (b) decoder.

B. The H.263 Coding Standard

The general principles discussed above are the basis for all video compression standards in use today, in particular the ISO standards MPEG-1 [16], MPEG-2 [17], and MPEG-4 [18], and the ITU-T Recommendations H.261 [19], H.262 (identical with MPEG-2), and H.263 [14]. We will use H.263 as an example throughout this paper. For video sequences with moderate motion, the H.263 algorithm can provide compression of at most 100:1 to 200:1 with acceptable picture quality [20]. To achieve even higher compression, as required for the transmission over mobile networks at very low bit rates, both the spatial resolution and the frame rate have to be reduced compared to standard television pictures. At bit rates below 64 kb/s, frame rates anywhere from 15 f/s (frames per second) down to 5 f/s are common. The picture resolution is often quarter common intermediate format (QCIF, 176 × 144 pixels), which is the most common input format at such low bit rates.

At QCIF resolution, each picture is divided into 11 × 9 macroblocks (MB's), which comprise 16 × 16 luminance samples, and two corresponding 8 × 8 blocks of chrominance samples. The luminance component of each MB is further subdivided into four 8 × 8 blocks, such that 8 × 8 DCT's can be applied to each block. Each MB is encoded either in INTRA or INTER mode. Motion compensation is carried out with half-pixel accuracy with one motion vector sent for each MB. Optionally, individual motion vectors can be provided for each 8 × 8 block, and blocks can be overlapped for motion compensation. A fixed number of successive MB's is usually grouped into a group of blocks (GOB) and side information that is appropriate for a larger number of MB's, but not for an entire frame, can be communicated efficiently on that level. In a similar but

more general way, a variable number of MB's can also be grouped into slices.

ITU-T Recommendation H.263 is the video portion of a series of recommendations under the umbrella of ITU-T Recommendation H.324 [21], [22]. H.324 describes terminals for low bit-rate multimedia communication, which may support real-time voice, data, and video, or any combination. Because the transmission is based on V.34 modems operating over the widely available public switched telephone network (PSTN), H.324 terminals are likely to play a major role in future multimedia applications. An increasing number of H.324 terminals is commercially available today. One important reason for this success is the state-of-the-art performance of the H.263 video coding standard [20] that achieves acceptable image quality at modem bit-rates. Other recommendations in the H.324 series include the H.223 multiplex [23], [24], H.245 control [25], and G.723 speech codec [26].

Standardization efforts for mobile H.324 terminals have already started [24]. Like cellular voice telephony, a major requirement is the ability to interwork with terminals connected to the PSTN at a reasonable complexity and with low delay. This precludes the transcoding architecture used today for cellular voice telephony, where a special speech codec is employed only for the mobile part of the network. For low bit-rate video, the delay is typically a few hundred milliseconds due to buffering for constant bit-rate transmission and processing delay. Transcoders would increase this delay unacceptably, and hence end-to-end error control, compatible with H.263, offers significant advantages at lower complexity. Some techniques recently incorporated in H.263 are feedback-based and will be discussed in Section IV.

III. Decoding the Erroneous Video Bit Stream

In general, an erroneous bit stream cannot be gracefully decoded by an "off-the-shelf" video decoder build for error-free transmission. Special provisions for error detection, resynchronization, and concealment are required. We discuss these measures and the interframe propagation of the remaining picture impairment in this section.

A. Error Detection and Resynchronization

Because the multiplexed video bit stream consists of variable length code (VLC) words, a single bit error may cause a loss of synchronization and a series of erroneous code words at the decoder. Residual redundancy in non-compact VLC's can be used to design self-synchronizing codes, such that valid symbols may be obtained again after some slippage [27]. However, even if resynchronization is regained quickly, the appropriate location of the decoded information within the frame is no longer known, since the number of missing symbols cannot be determined. Moreover, the subsequent code words are useless if the information is encoded differentially, as it is often the case, e.g., for motion vectors. The common solution to this problem is to insert unique synchronization code words into the bit stream in regular intervals, usually followed by a block of "header" bits. Since any conditional encoding across the resynchronization point must be avoided, the header provides anchor values, e.g., for absolute location in the image or current quantizer step size. Although the length of the synchronization code word can be minimized [28], relatively long synchronization code words are used in practice to reduce the probability of accidental emulation of synchronization words.

As an example, we again consider H.263, which supports optional GOB-headers as resynchronization points. In QCIF format, a GOB consists of 11 MB's that are arranged in one row. Because all information within a correctly decoded GOB can be used independently from previous information in the same frame, the GOB is often used as the basic unit for decoding. Typically, if a transmission error is detected, the GOB is discarded entirely.

Transmission errors can be detected in a variety of ways. If FEC is used, errors can often be detected with high reliability, even if the correction capability of the code is exceeded. For example, in H.261 and H.263 an optional FEC framing can be used to detect errors within the 493 information bits of each block. Reliability information can even be obtained for each received bit when the receiver provides channel state information or a soft output Viterbi algorithm (SOVA) is used for decoding of convolutional codes [29]. This information is then passed on to the video decoder. In addition, the video decoder itself can detect transmission errors. The video bit stream is not free of redundancy, such that violations of syntactic or semantic constraints will usually occur quickly after a loss of synchronization [13], [30]–[32]. For example, the decoder might not find a matching VLC word in the code table (a syntax violation) or detect that the decoded motion vectors, DCT coefficients, or quantizer step sizes exceed their permissible range (semantic violations). Additionally, the accumulated run that is used to place DCT coefficients into an 8×8 block might exceed 64, or the number of MB's in a GOB might be too small or too large. Especially for severe errors, the detection of errors can be further supported by localizing visual artifacts that are unlikely to appear in natural video signals.

Recently, more advanced techniques for improved resynchronization have been developed in the context of MPEG-4. Among several error resilience tools, data partitioning has been shown to be effective [13]. Especially when combined with reversible VLC (RVLC), which allow bit streams to be decoded in either the forward or reverse direction, the number of symbols that have to be discarded can be reduced significantly. Because RVLC's can be matched well to the statistics of image and video data, only a small penalty in coding efficiency is incurred [33], [34]. A recently proposed technique can even approach the efficiency of Huffman codes by combining a prefix and suffix code word stream by delayed XORing [35]. Another elegant technique that is not part of any current video coding standard has been proposed by Kingsbury *et al.* as error-resilient entropy coding (EREC) [36]. Similar to

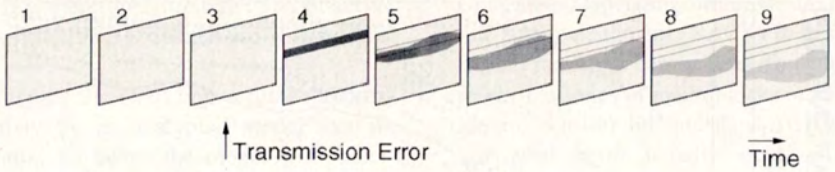


Fig. 2. Illustration of spatiotemporal error propagation.

data partitioning, a reordering of the bit stream is involved. Instead of clustering all symbols of the same type into one partition, EREC reorganizes VLC image blocks such that each block starts at a known position within the bit stream and the most important information is closest to the synchronization points.

However, even when GOB-headers are placed more frequently or more advanced techniques like data partitioning or EREC are applied, a certain amount of data has to be discarded when decoding an erroneous bit stream. The corresponding region in the image is then marked as lost and further processed by error concealment.

B. Error Concealment

The severeness of residual errors can be reduced if error concealment techniques are employed to hide visible distortion as well as possible. Since typically an entire GOB, or at least a significant part of it, is affected (i.e., 16 successive luminance lines) spatial interpolation is less efficient than temporal extrapolation. Only in the case of very complex motion or scene cuts, it can be advantageous to rely on the spatial correlation in the image [37], [38], or switch between temporal and spatial concealment [39], [32]. In the simplest and most common approach, previous frame concealment, the corrupted image content is replaced by corresponding pixels from the previous frame. This simple approach yields good results for sequences with little motion [30]. However, severe distortions are introduced for image regions containing heavy motion.

If data partitioning and strong error protection for the motion vector is used, one might rely on the transmitted motion vectors for motion-compensated concealment. If motion vectors are lost, they can be reconstructed by appropriate techniques, for example, by spatial interpolation of the motion vector field [40], which can be enhanced by additionally considering the smoothness of the concealed macroblock along the block boundaries [41], [42]. The interested reader is referred to [8] for a comprehensive overview of concealment techniques. All the feedback-based error control approaches discussed in the sequel benefit similarly from better concealment. Hence, it suffices to select one technique, and we present experimental results for the simple previous frame concealment in the following.

C. Interframe Error Propagation

Errors remaining after concealment propagate to successive frames and remain visible for a longer period of time, which makes the resulting artifacts particularly annoying. In addition, the accumulation of several errors can result in very poor image quality, even if the individual errors are small. Fig. 2 illustrates the typical transmission error effects for the loss of one GOB in frame 4. Not only does the error propagate temporally, but it also spreads spatially due to motion-compensated prediction. To some extent, the impairment caused by transmission errors decays over time due to leakage in the prediction loop. Leaky prediction is a well-known technique to increase the robustness of DPCM systems by attenuating the energy of the prediction signal [43]. For hybrid video coding, leakage is introduced by spatial filtering, as discussed in detail in the following.

Fig. 3 quantitatively illustrates the interframe error propagation after the loss of one GOB when previous frame concealment is used. The QCIF sequence *Foreman* is coded with H.263 at 100 kb/s and 12.5 f/s, resulting in an average peak signal-to-noise ratio (PSNR) of about 34 dB in the error-free case. Using the reconstructed frames at the encoder as the baseline, the loss ΔPSNR in signal-to-noise ratio is calculated for each reconstructed frame at the decoder output. The nine dotted curves correspond to each of the nine GOB's in the fifth encoded frame. Obviously, the error magnitude is highly image content dependent. The solid line represents the averaged result, indicating that an average residual loss of approximately 1 dB still remains in the sequence after 3 s due to interframe error propagation.

The decay of propagated errors is determined by two effects:

- some blocks are encoded in INTRA mode, i.e., without reference to the previous frame;
- repeated spatial filtering in the motion-compensated predictor, especially for half-pixel interpolation, attenuates the high spatial frequency components of the superimposed transmission error.

We can isolate the influence of these effects by experimental results shown in Fig. 4. We performed five simulations (A–E) with a baseline H.263 coder and decoder under different constraints with respect to spatial filtering and the use of INTRA mode. The general simulation conditions are identical to those in Fig. 3. All macroblocks are encoded in the INTER mode, except for simulation E, where nine out of 99 macroblocks per frame are randomly coded in INTRA mode. In simulation A, the subpixel fractions of the vector are forced to (0,0), i.e., motion compensation is carried out with integer–pixel accuracy and no spatial interpolation is required. In this case, the error due to a lost GOB does not decay over time. In simulation B, the subpixel fractions of the motion vector are forced

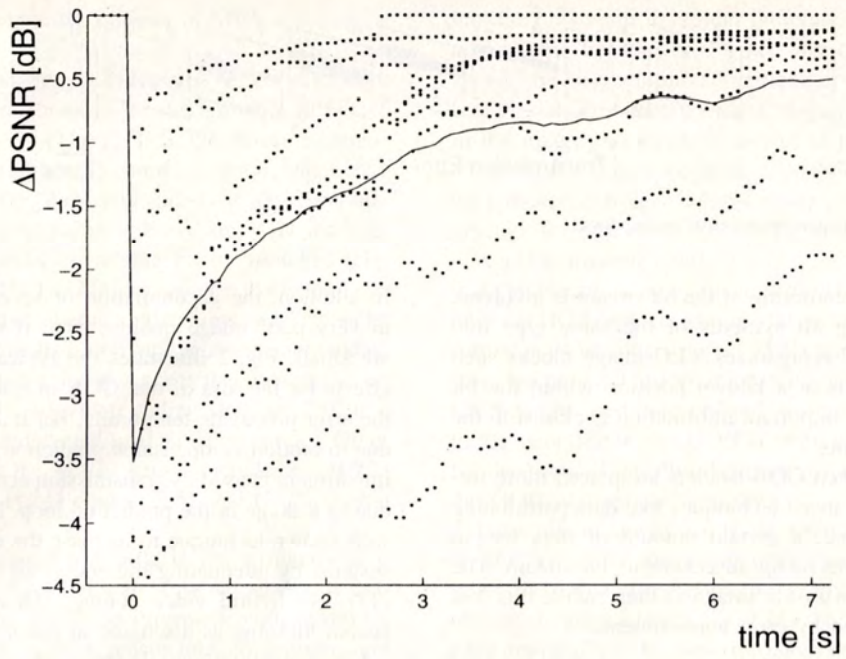


Fig. 3. Loss in SNR of the decoded video signal after previous frame concealment of one GOB.

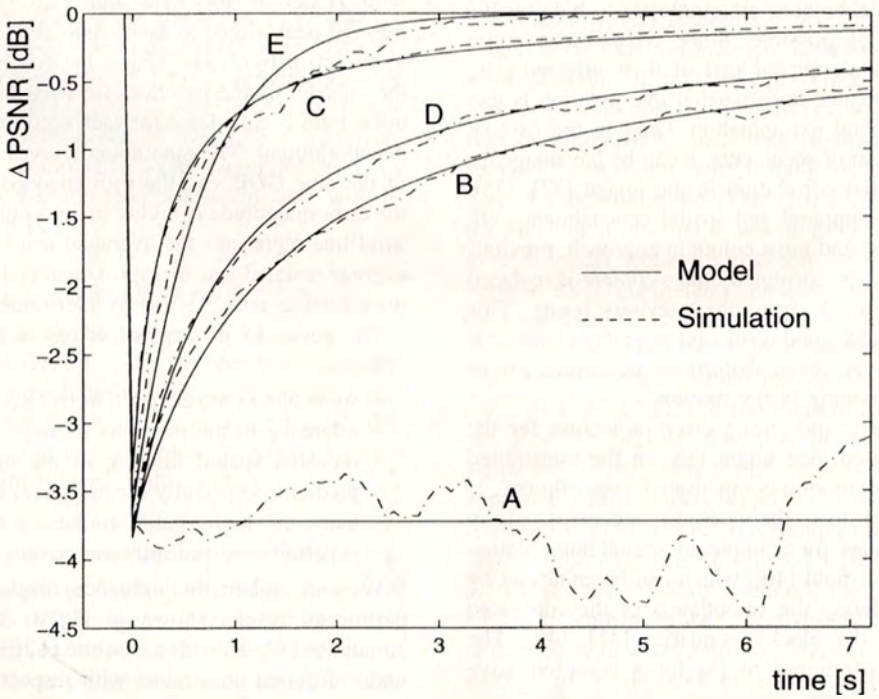


Fig. 4. Loss in PSNR of the decoded video-signal for different spatial interpolations (SI) in the prediction loop. A: no SI, B: horizontal SI, C: horizontal and vertical SI, D: SI not altered, E: SI not altered with 10% INTRA update.

to (0.5, 0.0), such that horizontal interpolation has to be performed for the entire image. Similarly, in simulation C the subpixel fractions are forced to (0.5, 0.5), such that horizontal and vertical interpolation must be performed for the entire image. H.263 employs bilinear interpolation for sub-pixel motion compensation, which acts as a low-pass filter, and the interframe error propagation decays faster, if more severe low-pass filtering is applied. For the remaining simulations D and E, the subpixel fractions are not altered but remain as selected by the encoder for best compression

performance. Curve D is therefore a mixture of A, B, and C, while curve E decays faster then D due the use of intraframe coding.

The experimental curves shown in Fig. 4 can be approximated quite accurately by an analytical model that we derive in the Appendix. To match the model with experimental results, two parameters are necessary to describe the introduced error which remains after previous frame concealment. The first parameter is the average energy of the error, and the second parameter describes the shape of the power spectral density (PSD) when approximated by a Gaussian function. Both parameters can be derived from the true PSD of the error which has significant influence on interframe error propagation. The model predicts that for case B, the energy decreases with $\sqrt{1/t}$ for large t, or with $1/t$ for case C. Such analytical models are important to understand interframe error propagation and can be built into error tracking algorithms, as discussed in Section IV.

Spatial filtering in the motion-compensated predictor is a necessary ingredient for good compression performance of a hybrid coder [44], [45]. Even with integer-pixel accurate motion compensation, a "loop filter" should be employed. For example, in H.261, which uses integer-pixel motion compensation, the PSNR gain due to the loop filter is up to 2 dB [20]. While error recovery is also improved significantly at the same time, this is really a side-effect, and, as Fig. 4 shows, the leakage in the DPCM loop of standardized video codecs by itself is not strong enough for error robustness. For this purpose, additional leakage could be introduced at the cost of coding efficiency [46], [40]. On the other hand, quick error recovery is also possible when INTRA coding is used as illustrated by curve E.

A safe method to stop interframe error propagation that is used in MPEG is the regular insertion of I-frames, i.e., pictures that are encoded entirely in INTRA mode. Unfortunately, I-frames typically require several times more bits than P-frames (the MPEG term for pictures encoded with reference to previous frames). While this is acceptable for higher bit-rate applications, or even necessary for broadcasting, where many receivers need to resynchronize at random times, the use of the INTRA mode should be restricted as much as possible in point-to-point transmission at low bit rates, as typical for mobile multimedia networks. Feedback-based methods described in the following section can efficiently minimize the use of the INTRA mode and therefore maintain higher coding efficiency for hostile channels.

IV. Error Mitigation by Feedback

As shown in the previous section, the remaining distortion after error concealment of corrupted image regions may remain visible in the image sequence for several seconds. In this section, we discuss error resilience techniques that utilize a feedback channel from the receiver to the transmitter. Such a feedback channel indicates which parts of the bit stream were received intact and/or which parts of the video signal could not be decoded and had to be concealed. Depending on the desired error behavior, negative acknowledgment (NACK) or positive acknowledgment (ACK) messages can be sent. Typically, an ACK or NACK refers to a series of macroblocks or an entire GOB. NACK's require a lower bit rate than ACK's, since they are only sent when errors actually occur, while ACK's have to be sent continuously. In either case, the requirements on the bit rate are very modest compared to the video bit rate of the forward channel. The feedback message is usually not part of the video syntax but transmitted in a different layer of the protocol stack where control information is exchanged. For example, in conjunction with H.263, ITU-T Recommendation H.245 [25] allows reporting of the temporal and spatial location of MB's that could not be decoded successfully and had to be concealed. Since the information is transmitted using a retransmission protocol, the error-free reception is guaranteed. However, additional delay my be introduced in the case of errors. In the following we assume that ACK's/NACK's are received error free after a relatively large round trip delay, e.g., 300 ms. This delay covers several retransmission attempts and may be considered as a worst case estimate for the actual delay. An alternative approach would be to sacrifice the reliable transmission of acknowledgment information at the advantage of reduced delay. Though this approach may be advantageous in some situations, we only consider reliable transmission of ACK's/NACK's in the following.

A. Error Tracking

The error tracking approach uses the INTRA mode for some MB's to stop interframe error propagation but limits its use to severely affected image regions only. During error-free transmission, the more effective INTER mode is used and the system therefore adapts effectively to varying channel conditions. This is accomplished by processing the NACK's from a feedback channel in the coding control of the encoder (Fig. 1). Based on the information of an NACK, the encoder can reconstruct the resulting error distribution in the current frame as described below. The coding control of a forward-adaptive encoder can then effectively stop interframe error propagation by selecting the INTRA mode whenever a MB is severely distorted. On the other hand, if error concealment was successful and the error of a certain MB is small, the encoder may decide that INTRA coding is not necessary. For severe errors however, a large number of MB's is selected, and the encoder may have to use a coarser quantizer to maintain a constant frame rate and bit rate. In this case, the overall picture quality decreases with a higher frequency of NACK's. Unlike retransmission techniques such as ARQ, error tracking does not increase the delay between encoder and decoder. It is therefore particularly suitable for applications that require a short latency.

Fig. 5 illustrates error tracking for the same example as in Fig. 2. As soon as the NACK is received with a system-dependent round-trip delay, the impaired MB's are determined and error propagation can be terminated by INTRA coding these MB's (frames 7–9). Fig. 6 shows the averaged PSNR loss for an assumed round-trip delay

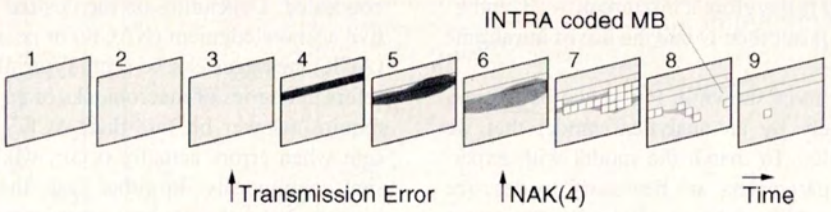


Fig. 5. Illustration of error propagation when error tracking is used.

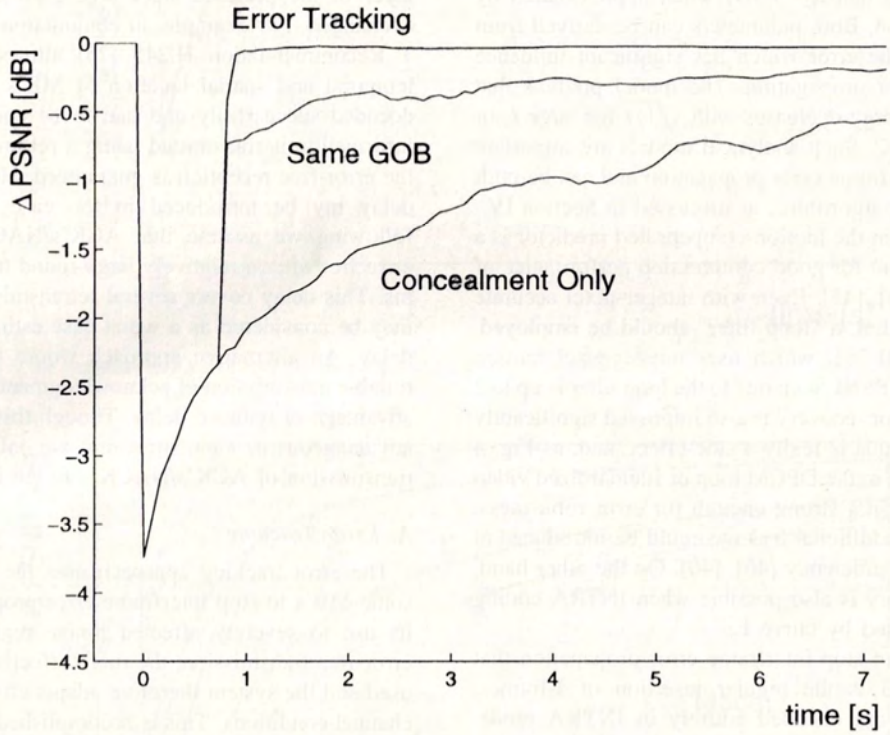


Fig. 6. Error recovery with feedback channel.

of 800 ms. The same simulation conditions as in Fig. 3 are used. Compared to the case without error tracking, the picture quality recovers rapidly as soon as INTRA coded MB's are inserted into the bit stream. A longer round-trip delay just results in a later start of the error recovery. Considering the slow recovery for concealment only, NACK's may still be useful after several seconds. In order to illustrate the importance of actually tracking the shifting location of the error, we also show results for the simple same GOB strategy, where the error is assumed to remain in the GOB were it originally occurred. When errors are dragged out of the original GOB along with vertical motion of picture contents, the same GOB strategy cannot remove it successfully, and annoying artifacts remain. Only when error tracking is employed, the propagation is stopped effectively. This is also demonstrated in Fig. 7, which shows example frames of the H.263 encoded test sequence *Foreman* directly after the NACK is received.

In order to reconstruct the interframe error propagation that has occurred at the decoder, the encoder could store its own output bit stream and decode it again, taking into account the reported loss of GOB's. While this approach is not feasible for a real-time implementation, it illustrates that the encoder, in principle, possesses all the information necessary to reconstruct the spatiotemporal error propagation at the decoder, once the NACK's have been received. For a practical system, the interframe error propagation has to be estimated with a low-complexity algorithm, as described in [47]–[49] for a macroblock-based coder, such as H.263.

The basic idea of the low-complexity algorithm is to carry out the error tracking with macroblock resolution rather than pixel resolution. This is sufficient since the INTRA/INTER mode decision at the coder and the error concealment decision at the decoder are carried out for entire MB's as well. In a cyclical buffer that covers all the MB's of the last several frames, the spatial overlap of MB's in successive frames due to motion-compensated prediction is stored, along with the error energy that would be introduced if concealment had to be used. If an NACK is received that indicates an error a few frames back, this



Fig. 7. Reconstructed frames of test sequence *Foreman*: (a) frame 90 after previous frame concealment of two GOB's in frame 75; (b) as (a) with INTRA update in frame 90 according to Same GOB strategy; (c) as (a) with INTRA update in frame 90 according to error tracking strategy; (d) frame 90 without GOB loss in frame 75.

error energy is "released" and "ripples" through the directed graph of frame-to-frame dependencies to the macroblocks of the current frame. The interframe error propagation model derived in the Appendix can be incorporated for more accurate prediction. Since all calculations are carried out on the MB level, the computational burden and memory requirements are small compared to the actual encoding of the video. For example, at QCIF resolution, there are only 99 MB's in each frame, as opposed to 38 016 luminance and chrominance samples.

The above error tracking scheme is a refinement of Wada's "selective recovery method" [50]. Wada's method marks all potentially damaged image blocks by one bit and prevents their use for interframe prediction. The method described here also calculates the severeness of the impairment and can thus use the extra bits required for INTRA coding more sparingly. Note that the coder has to know the decoder's concealment technique for that. On the other hand, Wada's method only considers the worst possible interframe error propagation and hence does not require an agreed concealment technique.

Error tracking is particularly attractive since it does not require any modifications of the bit stream syntax of the motion-compensated hybrid coder. It is therefore fully compatible with standards such as H.261, H.263, or MPEG. The ITU-T recommends using previous frame concealment and error tracking with baseline H.263 and has included an informative appendix with Recommendation H.263. In addition, minor extensions of the H.245 control standard were adopted to include the appropriate NACK messages.

B. Error Confinement

While interframe error propagation can be tracked reliably and with low complexity, a number of proposals for feedback-based error control technique do not rely on this technique but confine the error to a well-defined subregion of the frame instead. For example, in MPEG-4, arbitrarily shaped video object planes (VOP's) can be

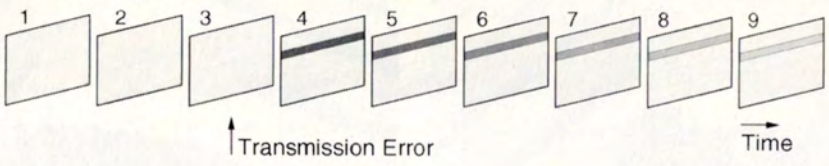


Fig. 8. Illustration of error propagation when error confinement is used.

encoded independently and superimposed at the decoder [13], [18]. If an error occurs in the bit stream of one VOP, the interframe error propagation is confined to that VOP since other VOP's will not refer to it for motion-compensated prediction. Basically, the video sequence is partitioned into independent subvideos.

Such a subvideo technique has also been included in H.263+ as an optional extension. The "independent segment decoding" (ISD) mode is described in Annex R of H.263. It can also be combined with slices, but we restrict the discussion to the case in which a segment is identical to a GOB. In the ISD mode, each GOB is encoded as an individual picture (or subvideo) independently from other GOB's. In particular, all GOB boundaries are treated just like picture boundaries. This approach significantly reduces the efficiency of motion compensation, particularly for vertical motion, since image content outside the current GOB must not be used for prediction. To reduce the loss of coding efficiency the ISD mode is therefore often combined with the "unrestricted motion vector" (UMV) mode which allows motion vectors pointing outside the coded picture area by extrapolating the image (or subvideo) borders. In spite of the UMV mode, typical losses in PSNR in the range from 0.2 to 1.0 dB often have to be accepted.

In case of transmission errors, the ISD mode assures that errors inside a GOB will not propagate to other GOB's, as illustrated in Fig. 8. Of course, the ISD mode alone does not solve the problem of temporal error propagation. It only simplifies keeping track of the error effects. The error propagation itself must be combatted by feedback based INTRA updates, or by the use of reference picture selection (RPS).

C. Reference Picture Selection

Rather than switching to INTRA mode at the encoder to stop interframe error propagation at the decoder, the coder could also encode the current frame with reference to a previous frame that has been successfully decoded. This RPS approach can lower the excess bit-rate due to NACK-induced INTRA coding [51], [52].

H.263+ has included RPS as an option, described in Annex N. As for the discussion of the ISD mode, we again consider the case that GOB headers are used. Then, in H.263, the reference picture is selected on a GOB basis, i.e., for all MB's within one GOB the same reference picture is used. In order to stop error propagation while maintaining the best coding efficiency, the last frame available without errors at the decoder should be selected. The RPS mode can be combined with the ISD mode to avoid spatial error propagation, or, for better coding efficiency, with an error tracking algorithm.

RPS can be operated in two different modes. When the encoder receives only negative acknowledgments, the operation of the encoder is not altered during error-free transmission, and the GOB's of the previous frame are used as a reference. After a transmission error, the decoder sends an NACK for an erroneous GOB and thereby requests that older, intact frames provide the reference-GOB. The typical transmission error effects are illustrated in Fig. 9, where the selection of reference-GOB's is indicated by arrows. Note that the use of the ISD mode is assumed and the indicated selection is only valid for the erroneous GOB. The encoder receives an NACK for frame 4 before the encoding of frame 7. The NACK includes the explicit request to use frame 3 for prediction, which is observed by the encoder. Similar to the error tracking approach, the quality degrades until the requested GOB arrives at the decoder, i.e., for the period of one round trip delay. Therefore, the loss of picture quality after a transmission error and the recovery after receiving an NACK behaves very similarly to basic error tracking. The advantage of the RPS mode versus simply switching to INTRA mode lies in the increased coding efficiency. Fewer bits are needed for encoding the motion-compensated prediction error than for the video signal itself, even if the time lag between the reference frame and the current frame is several frame intervals.

In the positive acknowledgment mode, all correctly received GOB's are acknowledged and the encoder uses only confirmed GOB's as a reference. Since the encoder has to use older reference pictures for motion-compensated prediction with increasing round-trip time, the coding performance decreases, even if no transmission errors occur. On the other hand, error propagation is avoided entirely since only error free pictures are used for prediction.

RPS requires additional frame buffers at the encoder and decoder to store enough previous frames to cover the maximum round trip delay of NACK's or ACK's. In the NACK mode, the storage requirements of the decoder can be reduced to two frame buffers. Furthermore, if only error-free GOB's shall be displayed, one frame buffer is sufficient. In the ACK mode no such storage reduction is possible, unless a combination of both modes is allowed [52]. Increased storage requirements may still be considered a problem for inexpensive mobile terminals for some time.

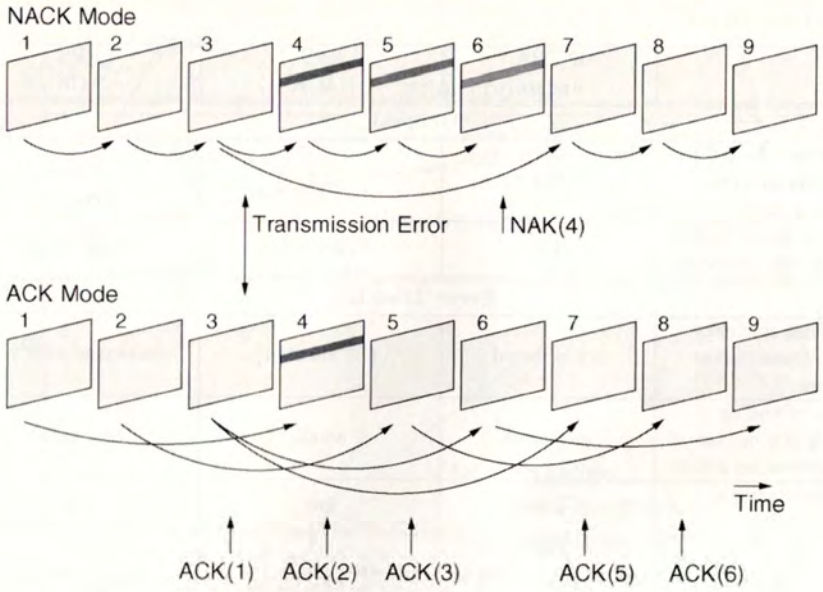


Fig. 9. Illustration of error propagation when RPS is used together with error confinement.

On the other hand, there are proposals for increased coding efficiency in low bit-rate video codecs which use several or even many previous frames for prediction [53]–[55]. When using RPS, the additional frames can then be used to simultaneously increase error robustness.

The different techniques for feedback-based error control that have been discussed in this section can be used in various combinations. Either error propagation is stopped by an INTRA update of affected regions or by selecting an error-free reference frame. Either the ACK mode or the NACK mode can be used for the latter option. Furthermore, either error tracking is used to identify affected regions or error propagation is confined. The advantages and disadvantages of possible combinations are summarized in Table 1.

V. Video Transmission over a Wireless DECT Channel

In this section, we illustrate the performance of feedback-based error mitigation in a mobile environment by simulating the transmission over a wireless channel. The channel model is related to the Digital European Cordless Telecommunications (DECT) standard, which provides a wide range of services for cordless personal communications [56], [57]. Our simulations are based on bit error sequences that are generated assuming Rayleigh fading and a Doppler frequency of 62 Hz. Carrier-to-noise ratios (E_b/N_0) ranging from 20 to 30 dB are considered with corresponding bit error rates as summarized in Table 2. The bit error sequences exhibit severe burst errors at a total bit rate of 80 kb/s, corresponding to the double slot format of DECT.

We apply FEC directly to the video bit stream using a BCH code of block size $n = 255$ bits with $k = 179$ information bits and $t = 10$ correctable errors per block. Due to the burstyness of the channel, not all errors can be corrected, and a significant block error rate remains, as also shown in Table 2. If the errors within a block cannot be corrected by FEC, all affected GOB's of the video bit stream are discarded and the video decoder invokes error concealment. We compare the error robustness of a baseline H.263 codec with and without error tracking to an H.263+ codec that uses NACK's, reference picture selection and error confinement by ISD in conjunction with the UMV mode. The feedback channel is assumed to be error-free with a constant delay of 100 ms. The round-trip delay, measured from encoding a frame to receiving an NACK, is about 300 ms due to the processing delay and buffering for constant transmission bit rate.

Twelve seconds of a typical videophone sequence *(Mother and Daughter)* are encoded at 12.5 f/s and transmitted over 30 different realizations of each test channel. Fig. 10 shows the average PSNR of the reconstructed frames at the encoder (after coding) and decoder (after transmission). The results are averaged values for all frames and realizations at each E_b/N_0. Note that for error tracking the picture quality after coding increases with increasing E_b/N_0 because fewer NACK's are received at better channel conditions and fewer MB's have to be coded in INTRA mode. Similarly, in the RPS mode, fewer GOB's have to be predicted with a higher time lag at better channel conditions. Both channel-adaptive approaches perform significantly better than the baseline mode of H.263 without feedback (NO). For lower E_b/N_0 the performance of the RPS mode in terms of $\overline{\text{PSNR}}$ is slightly superior to error tracking, since the INTRA mode can often be avoided. For higher E_b/N_0 this situation is reversed, because motion compensation is less efficient with the ISD mode. In summary, both channel-adaptive schemes perform very similarly and clearly outperform the nonadaptive scheme.

Table 1
Summary of Feedback-Based Error Control

	INTRA update	RPS NACK	RPS ACK
General			
Frames affected by interframe error propagation	N-1	N-1	0
Extra frame buffers at encoder/decoder	0/0	N/0 (N/1)	N/N
Error Tracking			
Coding efficiency w/o transmission errors	not affected	not affected	decreases with rtd
Loss of coding efficiency in case of transmission errors	moderate	small	very small
Computational complexity	low	low	low
Standards compliance	H.261, H.263, MPEG-1, MPEG-2, MPEG-4	H.263+ (Annex N)	H.263+ (Annex N)
Error Confinement			
Coding efficiency w/o transmission errors	somewhat reduced	somewhat reduced	somewhat reduced, decreases further with rtd
Loss of coding efficiency in case of transmission errors	significant	small	very small
Computational complexity	very low	very low	very low
Standards compliance	H.263+ (Annex R) MPEG-4	H.263+ (Annex N+R)	H.263+ (Annex N+R)

rtd: round-trip delay
N: number of encoded frames during one round-trip delay

Table 2
Summary of Test Channel Parameters

SNR [dB]	Bit Error Rate	Block Error Rate
20	0.002578	0.017075
22	0.001646	0.011250
24	0.001025	0.007575
26	0.000644	0.004675
28	0.000390	0.002775
30	0.000234	0.001725

VI. Feedback-Based Error Control for Precompressed Video

In the above channel-adaptive schemes, acknowledgment information is incorporated during the encoding process. Therefore, these approaches are particularly relevant for conversational services or surveillance where video is encoded while being transmitted. However, feedback-based error mitigation can also be used for applications involving precompressed stored video, like video-on-demand for mobile clients. In this case, a direct influence on the coding control is no longer possible. To still adapt the bit stream to the error conditions of the channel, multiple bit streams have to be stored that are assembled dynamically for transmission [58], [59].

Assume that two bit streams are stored at the video server. The first stream (P-stream) results from regular encoding of the video sequence and consists of INTER-coded frames (P-frames). In normal operation, the video server transmits the P-stream only. The second stream (I-stream) consists of INTRA-coded frames (I-frames) and is used for resynchronization after transmission errors. The I-stream can be encoded at a lower frame rate to reduce the storage requirements at the video server. Upon receiving an NACK, the video server uses an error tracking algorithm to identify damaged image regions. These regions are then extracted from the next I-frame in the I-stream and inserted into the transmitted bit stream at the corresponding position. If predictive encoding of symbols (e.g. motion vectors) is used, as is the case for H.263 or MPEG, the bit stream has to be assembled on the slice or GOB level rather than the MB level. In this fashion, error propagation is limited almost as for real-time encoding. Of course, the selection of INTRA-coded regions happens at a coarser level.

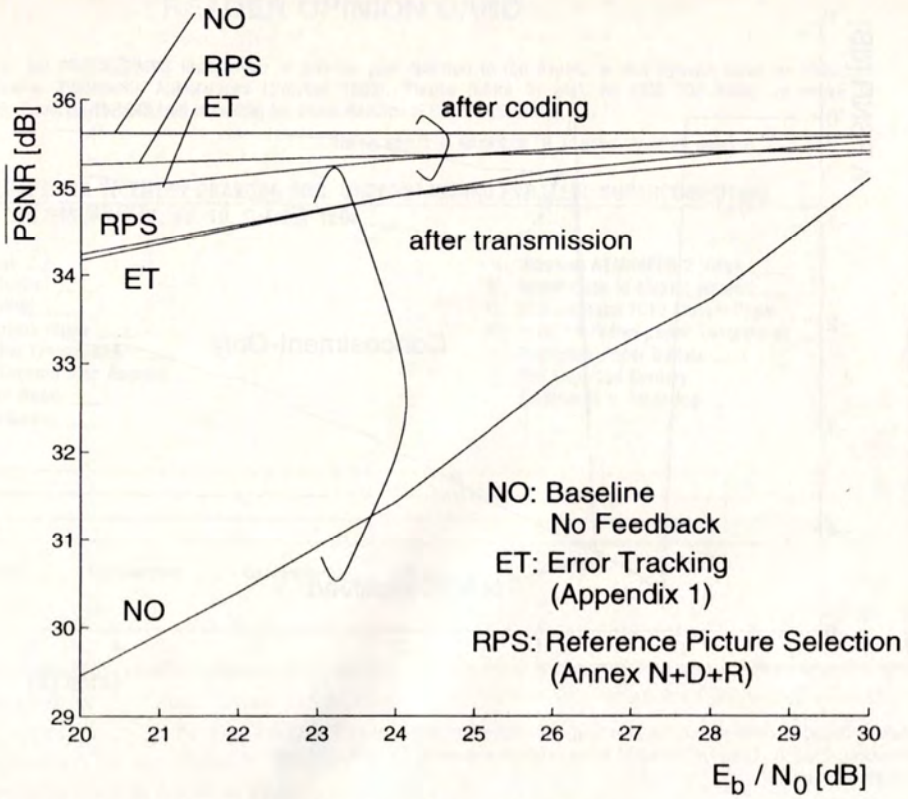


Fig. 10. Average PSNR of reconstructed frames at encoder (after coding) and decoder (after transmission) for the simulated transmission of H.263 coded video over a wireless DECT channel.

Note that the NACK-induced switching between the I-stream and the P-stream stops error propagation, but introduces a new mismatch error which results from the difference of the reconstructed P-frame and its corresponding reconstructed I-frame. If the difference is only minor, it will fade away over the following few P-frames as discussed in Section III-C. However, when there is a considerable difference and only weak filtering is applied in the coding loop, the mismatch error will cause annoying visual artifacts. To reduce the mismatch error, the reconstructed I-frame should be as close as possible to its corresponding P-frame. To achieve this, the I-stream is encoded using the reconstructed frames of the P-stream as the input instead of the original sequence.

Again, we demonstrate the feasibility of the approach in the framework of H.263. Fig. 11 shows the average loss of PSNR due to a burst error with the familiar recovery process in the case of no available feedback information. As soon as the NACK arrives and INTRA-coded GOB's are inserted, the picture quality improves similarly to the simulation results shown in Fig. 6. If the I-stream is generated by encoding the original sequence (case A), a good picture quality can be observed directly after the insertion. However, after several frames from the P-stream are transmitted, the mismatch between the reconstructed I-frame and the corresponding reconstructed P-frame dominates. This effect can be reduced if the I-stream is generated by encoding the reconstructed frames from the P-stream (case B).

Interestingly, this approach also offers a very efficient solution to random access. In the common approach, I-frames are inserted periodically into the bit stream to provide random access. In this case, I-frames also have to be transmitted during normal-speed playback, even though they do not provide any additional functionality. However, when the bit stream is assembled dynamically at the server, the higher efficiency of the INTER mode can be fully exploited during normal-speed playback. Random access, fast forward, and fast reverse can still be supported, because I-frames may be inserted whenever requested by the client. Note that this approach is fully standard compliant with H.261, H.263, or MPEG and requires only little additional complexity and storage overhead at the video server. It has also been extended to support bit rate and resolution scalability [60].

VII. Concluding Remarks

In this paper, we have reviewed feedback-based techniques for robust transmission of video in mobile multimedia systems. We argue that transcoders significantly increase complexity and add unacceptable delay, and that therefore end-to-end error control has to be used. Each decoder therefore has to make provisions for error detection, resynchronization and error concealment. Additionally, we

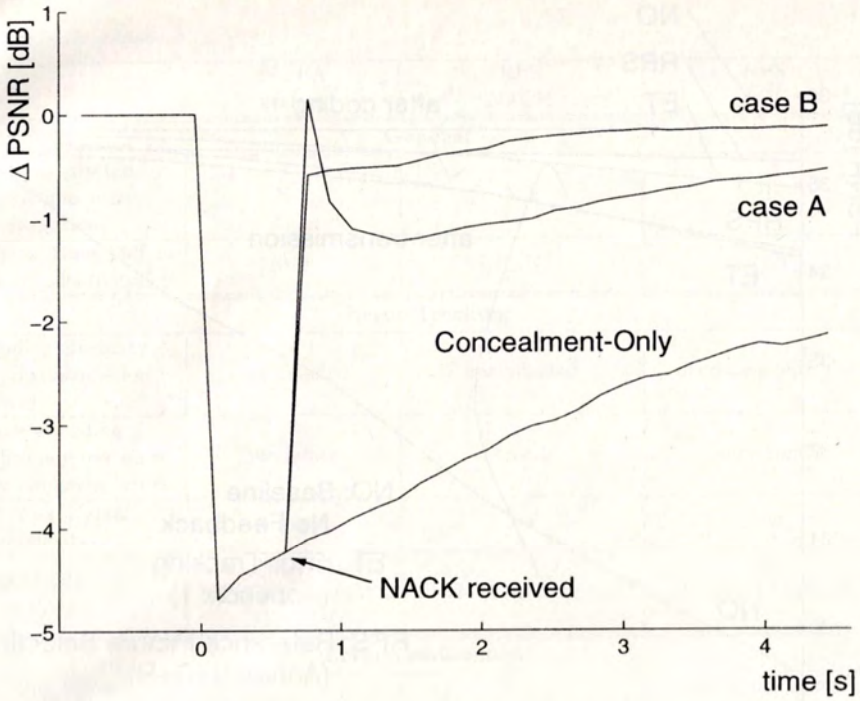


Fig. 11. Loss in PSNR of decoded video signal for inserting I-stream information into a P-stream in a video server application. Case A: I-stream encoded from original sequence. Case B: I-stream encoded from reconstructed P-stream.

advocate the intelligent processing of acknowledgment information by the coding control to adapt the source coder to the channel.

Error tracking allows the encoder to estimate interframe error propagation accurately and adapt its encoding strategy to mitigate the effects of past transmission errors. While error tracking is possible with low complexity, it can be simplified by error confinement techniques, at the expense of compression efficiency. Compression efficiency in case of transmission errors can be improved, however, if multiple previous pictures are kept in an RPS scheme. The simulation of a video transmission over a wireless channel indicates that different channel-adaptive schemes perform very similar but have a significant advantage over schemes that are not feedback-based.

The ITU-T Study Group 16 has adopted feedback-based error control in their effort toward mobile extensions of the successful Recommendation H.263. The first version of H.263 included basic error tracking as described in Section IV-A. The second version, which is informally known as H.263+, was adopted by ITU-T in February 1998. Among many other enhancements, it contains two new options supporting RPS (Annex N) and ISD (Annex R), both discussed in more detail in this article. Future enhancements, e.g., data partitioning, unequal error protection, and reversible variable length coding, are under consideration for future versions of the standard, informally known as H.263++ and H.26L.

Feedback schemes are suitable for interactive, individual communications, but they have inherent limitations outside this domain. They are particularly powerful if the round-trip delay is short. If the round-trip delay increases they become less efficient and ultimately useless. Also, feedback schemes are particularly advantageous for point-to-point communications. For schemes like error tracking that use INTRA updates to stop error propagation, extensions to few users are possible at a loss in performance. In the case of RPS, multipoint communication may even become impossible, because different decoders may require different reference frames. On the other hand, the objection that feedback-based source coding can only be used with real-time encoding is not valid, as shown in Section VI.

While most of the discussed feedback-based error control schemes are pragmatic engineering solutions to a problem at hand, there is an unsolved theoretical problem of fundamental importance underneath. Traditionally, error control has been performed without regard to the contents of the bit stream, e.g., by FEC or transport layer retransmission schemes. Using channel-adaptive source coding for robust transmission is a relatively new idea. In our work, we have learned that well-designed mobile video systems should combine all these techniques, as exemplified in Section V. The tradeoffs in such a system design, however, are not at all well understood, and a general theoretical framework for feedback-based error control is needed.

APPENDIX
ANALYSIS OF INTERFRAME ERROR PROPAGATION

In the following we derive an analytical model for the distortion that is caused by transmission errors and propa-

gates due to the recursive DPCM structure in the decoder. We are interested in the signal $v[x, y, t]$, which is the frame difference of the reconstructed frames at the encoder and decoder at time step t. We assume that the residual error $u[x, y]$ is introduced at $t = 0$ (after resynchronization and error concealment) such that $v[x, y, 0] = u[x, y]$. In particular, we are interested in the variance $\sigma_v^2[t]$ of the propagated error signal.

A. Two-Dimensional Case

First we consider the two-dimensional case with the discrete spatial and temporal variables x and t. When the decoder is regarded as a linear system $H_t(\omega_x)$ with parameter t, the variance of $v[x, t]$ can be obtained as

$$\sigma_v^2[t] = \frac{1}{2\pi} \int_{-\pi}^{+\pi} |H_t(\omega_x)|^2 \Phi_{uu}(\omega_x)\, d\omega_x \qquad (1)$$

where Φ_{uu} is the power spectral density (PSD) of the signal $u[x]$. We assume that a spatial filter $F(\omega_x)$ is applied in each time step. Then the impulse response of the decoder $h_t[x]$ can be defined recursively as $h_t[x] = h_{t-1}[x] * f[x]$, where "$*$" denotes discrete spatial convolution and $f[x]$ is the impulse response of the filter. Based on the central limit theorem we expect $h_t[x]$ to be Gaussian for large t. Therefore, the magnitude of the transfer function of the decoder can be approximated in the base band $|\omega_x| < \pi$ by

$$|\hat{H}_t(\omega_x)| = \exp\left(-\frac{\omega_x^2 t \sigma_f^2}{2}\right) \qquad (2)$$

where σ_f^2 is defined as

$$\sigma_f^2 = \sum_x x^2 f[x] - \left(\sum_x x f[x]\right)^2. \qquad (3)$$

In the case of linear interpolation, as commonly used for half-pel motion compensation, we obtain $\sigma_f^2 = 1/4$. In addition to the Gaussian approximation for $H_t(\omega_x)$ we also approximate the PSD of the introduced error signal $u[x]$ by

$$\hat{\Phi}_{uu}(\omega_x) = \sigma_u^2 \sqrt{4\pi\sigma_g^2} \exp\left(-\omega_x^2 \sigma_g^2\right) \qquad (4)$$

i.e., a Gaussian PSD with the energy σ_u^2. The parameter σ_g^2 determines the shape of the PSD and can be used to match (4) with the true PSD. With the given approximations for $|H_t(\omega_x)|$ and $\Phi_{uu}(\omega_x)$ we can solve (1) directly yielding

$$\hat{\sigma}_v^2[t] = \sigma_u^2 \sqrt{\frac{\sigma_g^2}{\sigma_g^2 + t\sigma_f^2}} = \sigma_u^2 \alpha[t] \qquad (5)$$

where $\alpha[t]$ is the power transfer factor after t time steps.

B. Extension to Three-Dimensional Case

In the following we focus on spatial filtering caused by motion compensated prediction with half-pel accuracy and bilinear interpolation. For the extension of the above results to the three-dimensional case with the discrete variables x, y, and t, it has to be considered that individual image regions undergo different filtering operations. For each macroblock a different motion vector is selected, and depending on its sub-pel fractions either no filtering, only horizontal, only vertical, or horizontal and vertical spatial filtering is applied.

In the process of encoding, different combinations of filters are applied to an individual image region after t time steps. The probability that an image region is filtered h times horizontally and v times vertically can be described by a two dimensional probability density function (pdf) $p_t[h, v]$ with parameter t. For $t = 0$ no filter operations have yet been performed, i.e., $p_0[0, 0] = 1$ and otherwise zero. For $t = 1$ the pdf is given by $p_1[0, 0]$, $p_1[1, 0]$, $p_1[0, 1]$, and $p_1[1, 1]$, with all other probabilities being equal to zero. In general, these four probabilities are equal to $1/4$ in moving areas unless specific sub-pel fractions are enforced. For $t > 1$ the pdf can be defined recursively according to

$$p_t[h, v] = p_{t-1}[h, v] * p_1[h, v] \qquad (6)$$

under the assumption that the subpel fractions are independent in each frame at a given location. With this assumption and the definition of the power transfer factor $\alpha[\cdot]$ in (5), we obtain the variance of the signal v for the three-dimensional case as

$$\hat{\sigma}_v^2[t] = \sigma_u^2 \sum_h \sum_v \alpha[h]\alpha[v] p_t[h, v]. \qquad (7)$$

This equation does not consider INTRA coded macroblocks, which will cause a faster decrease in error energy. If the INTRA mode is selected randomly for n out of N macroblocks per frame, the effect on the variance can be modeled as an additional leakage $\beta = 1 - n/N$ resulting in

$$\hat{\sigma}_v^2[t] = \beta^t \sigma_u^2 \sum_h \sum_v \alpha[h]\alpha[v] p_t[h, v]. \qquad (8)$$

REFERENCES

[1] E. Berruto, M. Gudmundson, R. Menolascino, W. Mohr, and M. Pizarroso, "Research activities on UMTS radio interface, network architectures, and planning," *IEEE Commun. Mag.*, vol. 36, pp. 82–95, Feb. 1998.

[2] D. Grillo, Ed., "Special section on third-generation mobile systems in Europe," *IEEE Personal Commun. Mag.*, vol. 5, pp. 5–38, Apr. 1998.

[3] P. Bahl and B. Girod, Eds., "Special section on wireless video," *IEEE Commun. Mag.*, vol. 36, pp. 92–151, June 1998.

[4] S. Lin, D. J. Costello, and M. J. Miller, "Automatic repeat error control schemes," *IEEE Commun. Mag.*, vol. 22, pp. 5–17, Dec. 1984.

[5] A. Heron and N. MacDonald, "Video transmission over a radio link using H.261 and DECT," in *Inst. Elect. Eng. Conf. Publications*, 1992, no. 354, pp. 621–624.

[6] M. Khansari, A. Jalali, E. Dubois, and P. Mermelstein, "Low bit-rate video transmission over fading channels for wireless microcellular systems," *IEEE Trans. Circuits Syst. Video Technol.*, vol. 6, pp. 1–11, Feb. 1996.

[7] P. Cherriman and L. Hanzo, "Programable H.263-based video transceivers for interference-limited environments," *IEEE Trans. Circuits Syst. Video Technol.*, vol. 8, pp. 275–286, June 1998.

[8] Y. Wang and Q.-F. Zhu, "Error control and concealment for video communication: A review," *Proc. IEEE*, vol. 86, pp. 974–997, May 1998.

[9] R. Fischer, P. Mangold, R. M. Pelz, and G. Nitsche, "Combined source and channel coding for very low bitrate mobile visual

communication systems," in *Proc. Int. Picture Coding Symp. (PCS)*, Melbourne, Australia, Mar. 1996, pp. 231–236.
[10] K. Illgner and D. Lappe, "Mobile multimedia communications in a universal telecommunications network," in *Proc. SPIE Conf. Visual Communications and Image Processing (VCIP)*, vol. 2501, Taipei, Taiwan, May 1995, pp. 1034–1043.
[11] B. Girod, U. Horn, and B. Belzer, "Scalable video coding with multiscale motion compensation and unequal error protection," in *Multimedia Communications and Video Coding*, Y. Wang, S. Panwar, S. P. Kim, and H. L. Bertoni, Eds. New York: Plenum, 1996, pp. 475–482.
[12] R. M. Pelz, "An unequal error protected $p \times 8$ kbit/s video transmission for dect," in *Proc. IEEE Vehicular Technology Conf. (VTC)*, Stockholm, Sweden, June 1994, pp. 1020–1024.
[13] R. Talluri, "Error-resilient video coding in the MPEG-4 standard," *IEEE Commun. Mag.*, vol. 36, pp. 112–119, June 1998.
[14] *Video Coding for Low Bitrate Communication*, ITU-T Recommendation H.263, 1996.
[15] A. M. Tekalp, *Digital Video Processing*. Upper Saddle River, NJ: Prentice Hall, 1995.
[16] *Coding of Moving Pictures and Associated Audio for Digital Storage Media at up to About 1.5 Mbit/s (MPEG-1)*, International Standard ISO/IEC 11172-2, 1994.
[17] *Generic Coding of Moving Pictures and Associated Audio. Recommendation H.262 (MPEG-2)*, International Standard ISO/IEC 13818-2, 1995.
[18] *Coding of Audio-Visual Objects: Visual (MPEG-4 Video)*, Committee Draft ISO/IEC 14496-2, Oct. 1997.
[19] *Video Coding for Audiovisual Services at $p \times 64$ kbit/s*, ITU-T Recommendation H.261, 1990.
[20] B. Girod, N. Färber, and E. Steinbach, "Performance of the H.263 video compression standard," *J. VLSI Signal Processing: Syst. Signal, Image, Video Technol.*, vol. 17, pp. 101–111, Nov. 1997.
[21] *Terminal for Low Bitrate Multimedia Communication*, ITU-T Recommendation H.324, 1995.
[22] D. Lindberg, "The H.324 multimedia communication standard," *IEEE Commun. Mag.*, vol. 34, pp. 46–51, Dec. 1996.
[23] *Multiplexing Protocol for Low Bitrate Multimedia Communication*, ITU-T Recommendation H.223, 1996.
[24] N. Färber, B. Girod, and J. Villasenor, "Extensions of ITU-T recommendation H.324 for error-resilient video transmission," *IEEE Commun. Mag.*, vol. 36, pp. 120–128, June 1998.
[25] *Control Protocol for Multimedia Communication*, ITU-T Recommendation H.245, 1996.
[26] *Dual Rate Speech Coder for Multimedia Communications Transmitting at 5.3 and 6.3 kbit/s*, ITU-T Recommendation G.723.1, 1996.
[27] T. J. Ferguson and J. H. Rabinowitz, "Self-synchronizing Huffman codes," *IEEE Trans. Inform. Theory*, vol. IT-30, pp. 687–693, July 1984.
[28] W.-M. Lam and A. R. Reibman, "Self-synchronizing variable length codes for image transmission," in *Proc. IEEE Int. Conf. Acoustics, Speech, and Signal Processing (ICASSP'92)*, vol. 3, San Francisco, CA, Mar. 1992, pp. 477–480.
[29] J. Hagenauer and P. Höher, "A Viterbi algorithm with soft-decision output and its applications," in *Proc. IEEE Global Telecommunications Conf. (GLOBECOM)*, Dallas, TX, Nov. 1989, pp. 47.1.1–47.1.7.
[30] C. Chen, "Error detection and concealment with an unsupervised MPEG2 video decoder," *J. Visual Commun. Image Representation*, vol. 6, no. 3, pp. 265–278, Sept. 1995.
[31] W.-M. Lam and A. R. Reibman, "An error concealment algorithm for images subject to channel errors," *IEEE Trans. Image Processing*, vol. 4, pp. 533–542, May 1995.
[32] J. W. Park, J. W. Kim, and S. U. Lee, "DCT coefficients recovery-based error concealment technique and its application to the MPEG-2 bit stream," *IEEE Trans. Circuits Syst. Video Technol.*, vol. 7, pp. 845–854, Dec. 1997.
[33] J. Wen and J. D. Villasenor, "A class of reversible variable length codes for robust image and video coding," in *Proc. 1997 IEEE Int. Conf. Image Processing (ICIP)*, vol. 2, Santa Barbara, CA, Oct. 1997, pp. 65–68.
[34] J. Wen and J. D. Villasenor, "Reversible variable length codes for efficient and robust image and video coding," in *Proc. IEEE Data Compression Conf. (DCC)*, Mar. 1998, Snowbird, UT, pp. 471–480.
[35] B. Girod, "Bidirectionally decodable streams of prefix code words," *IEEE Commun. Lett.*, to be published.
[36] D. W. Redmill and N. G. Kingsbury, "The EREC: An error-resilient technique for coding variable-length blocks of data," *IEEE Trans. Image Processing*, vol. 5, pp. 565–574, Apr. 1996.
[37] Y. Wang, Q.-F. Zhu, and L. Shaw, "Maximally smooth image recovery in transform coding," *IEEE Trans. Commun.*, vol. 41, pp. 1544–1551, Oct. 1993.
[38] H. Sun and W. Kwok, "Concealment of damaged block transform coded images using projection onto convex sets," *IEEE Trans. Image Processing*, vol. 4, pp. 470–477, Apr. 1995.
[39] H. Sun and J. Zedepski, "Adaptive error concealment algorithm for MPEG compressed video," in *Proc. SPIE Conf. Visual Communications and Image Processing (VCIP)*, vol. 1818, Boston, MA, Nov. 1992, pp. 814–824.
[40] P. Haskell and D. Messerschmitt, "Resynchronization of motion compensated video affected by ATM cell loss," in *Proc. IEEE Int. Conf. Acoustics, Speech, and Signal Processing (ICASSP)*, vol. 3, San Francisco, CA, Mar. 1992, pp. 545–548.
[41] W.-M. Lam, A. R. Reibman, and B. Lin, "Recovery of lost or erroneously received motion vectors," in *Proc. IEEE Int. Conf. Acoustics, Speech, and Signal processing (ICASSP)*, vol. 5, Minneapolis, MN, Apr. 1993, pp. 417–420.
[42] P. Salama, N. Shroff, and E. J. Delp, "A fast suboptimal approach to error concealment in encoded video streams," in *Proc. IEEE Int. Conf. Image Processing (ICIP)*, vol. 2, Santa Barbara, CA, Oct. 1997, pp. 101–104.
[43] N. S. Jayant and P. Noll, *Digital Coding of Waveforms*. Englewood Cliffs, NJ: Prentice Hall, 1984.
[44] B. Girod, "The efficiency of motion-compensating prediction for hybrid coding of video sequences," *IEEE J. Select. Areas Commun.*, vol. SAC-5, pp. 1140–1154, Aug. 1987.
[45] ——, "Motion-compensating prediction with fractional-pel accuracy," *IEEE Trans. Commun.*, vol. 41, pp. 604–612, Apr. 1993.
[46] D. J. Connor, "Techniques for reducing the visibility of transmission errors in digitally encoded video signals," *IEEE Trans. Commun.*, vol. COM-21, pp. 695–706, June 1973.
[47] N. Färber, E. Steinbach, and B. Girod, "Robust H.263 compatible video transmission over wireless channels," in *Proc. Int. Picture Coding Symp. (PCS)*, Melbourne, Australia, Mar. 1996, pp. 575–578.
[48] E. Steinbach, N. Färber, and B. Girod, "Standard compatible extension of H.263 for robust video transmission in mobile environments," *IEEE Trans. Circuits Syst. Video Technol.*, vol. 7, pp. 872–881, Dec. 1997.
[49] B. Girod, N. Färber, and E. Steinbach, "Error-resilient coding for H.263," in *Insights into Mobile Multimedia Communication*, D. Bull, N. Canagarajah, and A. Nix, Eds. New York: Academic, 1999, pp. 445–449.
[50] M. Wada, "Selective recovery of video packet loss using error concealment," *IEEE J. Select. Areas Commun.*, vol. 7, pp. 807–814, June 1989.
[51] S. Fukunaga, T. Nakai, and H. Inoue, "Error resilient video coding by dynamic replacing of reference pictures," in *Proc. IEEE Global Telecommunications Conf. (GLOBECOM)*, London, U.K., Nov. 1996, vol. 3, pp. 1503–1508.
[52] Y. Tomita, T. Kimura, and T. Ichikawa, "Error resilient modified inter-frame coding system for limited reference picture memories," in *Proc. Int. Picture Coding Symp. (PCS)*, Berlin, Germany, Sept. 1997, pp. 743–748.
[53] T. Wiegand, X. Zhang, and B. Girod, "Motion-compensating long-term memory prediction," in *Proc. IEEE Int. Conf. Image Processing (ICIP)*, Santa Barbara, CA, Oct. 1997, pp. 53–56.
[54] T. Wiegand, X. Zhang, and B. Girod, "Long-term memory motion-compensated prediction," *IEEE Trans. Circuits Syst. Video Technol.*, vol. 9, pp. 70–84, Feb. 1999.
[55] B. Girod, T. Wiegand, E. Steinbach, M. Flierl, and X. Zhang, "High-order motion compensation for low bit-rate video," in *Proc. Europ. Signal Processing Conf.*, Rhodes, Greece, Sept. 1998, pp. 253–256.
[56] J. E. Padgett, C. Günther, and T. Hattori, "Overview of wireless personal communications," *IEEE Commun. Mag.*, vol. 33, pp. 28–41, Jan. 1995.
[57] P. Wong and D. Britland, *Mobile Data Communications Systems*. Norwood, MA: Artech House, 1995.
[58] N. Färber, E. Steinbach, and B. Girod, "Robust H.263 compatible transmission for mobile video server access," in *Proc. 1st Int. Workshop Wireless Image/Video Communications*, Lough-

borough, U.K., Sept. 1996, pp. 8–13.
[59] N. Färber and B. Girod, "Robust H.263 compatible video transmission for mobile access to video servers," in *Proc. IEEE Int. Conf. Image Processing (ICIP)*, vol. 2, Santa Barbara, CA, Oct. 1997, pp. 73–76.
[60] B. Girod, N. Färber, and K. Stuhlmüller, "Internet video streaming," in *Multimedia Communications*, F. DeNatale and S. Pupolin, Eds. Berlin, Germany: Springer, 1999, pp. 547–556.



Bernd Girod (Fellow, IEEE) received the M.S. degree in electrical engineering from Georgia Institute of Technology, Atlanta, in 1980 and the Doctoral degree (with highest honors) from the University of Hannover, Germany, in 1987.

He is currently a Chaired Professor of Telecommunications in the Electrical Engineering Department and Head of the Telecommunications Institute I at the University of Erlangen-Nuremberg, Erlangen, Germany. Until 1987, he was a Member of the Research Staff at the Institut für Theoretische Nachrichtentechnik und Informationsverarbeitung, University of Hannover, working on moving image coding, human visual perception, and information theory. In 1988, he joined Massachusetts Institute of Technology, Cambridge, first as a Visiting Scientist with the Research Laboratory of Electronics, then as an Assistant Professor of Media Technology at the Media Laboratory. From 1990 to 1993, he was Professor of Computer Graphics and Technical Director of the Academy of Media Arts in Cologne, Germany, jointly appointed with the Computer Science Section of Cologne University. He was a Visiting Adjunct Professor with the Digital Signal Processing Group at Georgia Institute of Technology in 1993. Since 1997, he has codirected the newly found Telecommunications Laboratory at the University of Erlangen-Nuremberg. He served as the Chairman of the Electrical Engineering Department from 1995 to 1997, and as Director of the Center of Excellence "3-D Image Analysis and Synthesis" since 1995. He was a Visiting Professor with the Information Systems Laboratory of Stanford University, Stanford, CA, in 1997–1998 academic year. His research interests include image communication, video signal compression, human and machine vision, computer graphics and animation, as well as interactive media. For several years, he has served as a consultant to government agencies and companies, with special emphasis on start-up ventures. He has been a founder and Chief Scientist of Vivo Software, Inc., Waltham, MA (1993–1998), Chief Scientist of RealNetworks, Inc., Seattle, WA, (since 1998), and a board member of 8×8, Inc., Santa Clara, CA since 1996.

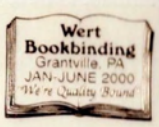
Dr. Girod was recently elected Fellow of the IEEE "for his contributions to the theory and practice of video communications."



Niko Färber (Member, IEEE) received the Dipl.-Ing. degree in electrical engineering from the Technical University of Munich, Germany, in 1993.

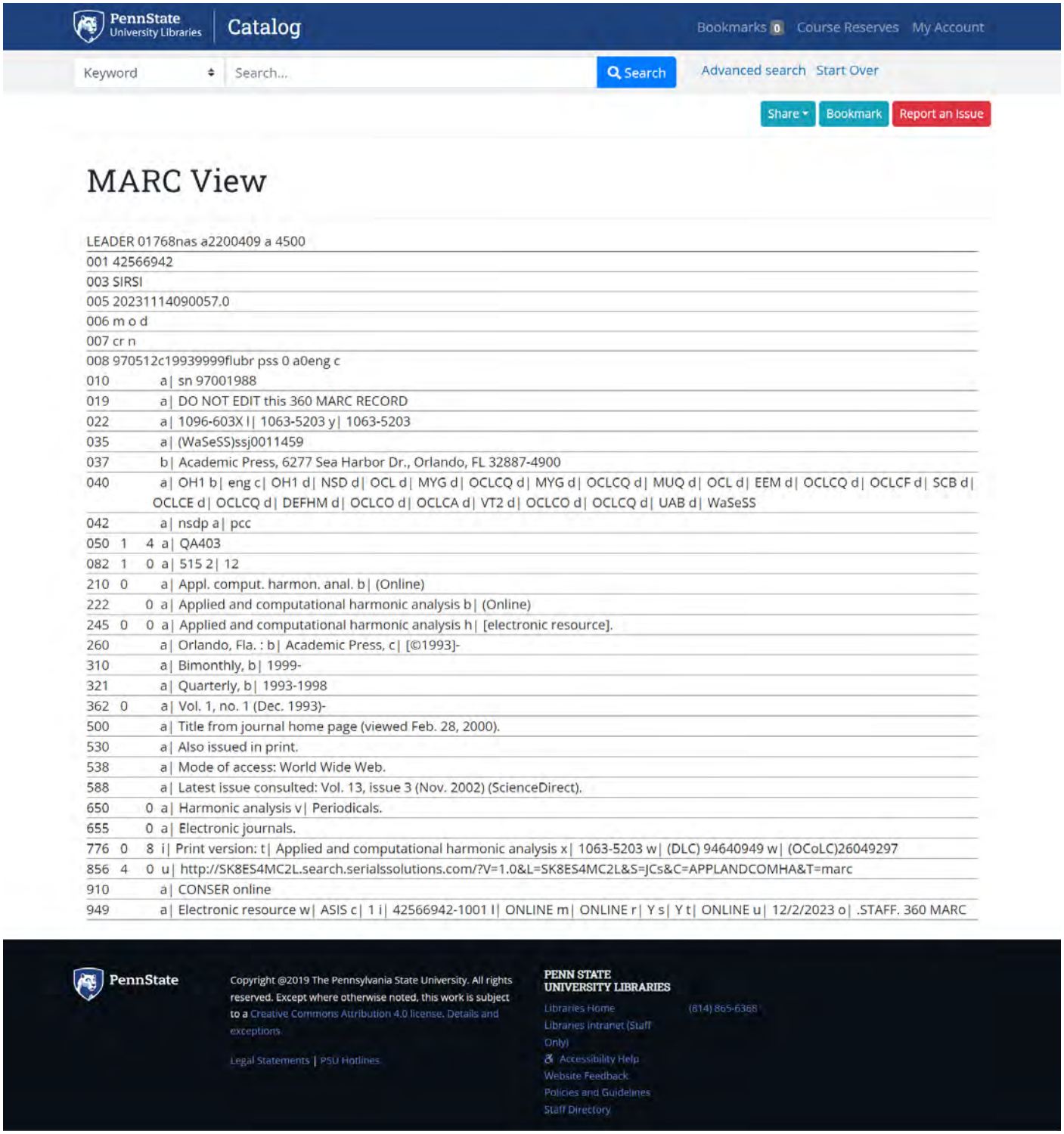
He was then with the Research Laboratory Mannesmann Pilotentwicklung, where he developed system components for satellite based vehicular navigation. In October 1993, he joined the Telecommunications Laboratory at the University of Erlangen-Nuremberg, Erlangen, Germany, where he is now a member of the Image Communication Group. He started his research on robust video transmission as a Visiting Scientist at the Image Processing Laboratory of University of California, Los Angeles, CA. Since then he has published several conference and journal papers on the subject and has contributed successfully to the ITU-T Study Group 16 efforts for robust extensions of the H.263 standard. He has also served as the Publicity Vice Chair for ICASSP-97 in Munich, Germany, and performed research for 8×8, Inc., Santa Clara, CA, and RealNetworks, Inc., Seattle, WA. In cooperation with RealNetworks, he holds a U.S. patent in the area of scalable video coding. His other research interests include combined source and channel coding and software only video coding.

ENGINEERING LIBRARY



APPENDIX SAITO01

screenshot-catalog.libraries.psu.edu-2023.12.05-15_39_10
https://catalog.libraries.psu.edu/catalog/42566942
05.12.2023



PennState University Libraries | Catalog

Bookmarks 0 Course Reserves My Account

Keyword Search... Search Advanced search Start Over

Share Bookmark Report an Issue

MARC View

LEADER 01768nas a2200409 a 4500				
001 42566942				
003 SIRSI				
005 20231114090057.0				
006 m o d				
007 cr n				
008 970512c19939999flubr pss 0 a0eng c				
010				a| sn 97001988
019				a| DO NOT EDIT this 360 MARC RECORD
022				a| 1096-603X l| 1063-5203 y| 1063-5203
035				a| (WaSeSS)ssj0011459
037				b| Academic Press, 6277 Sea Harbor Dr., Orlando, FL 32887-4900
040				a| OH1 b| eng c| OH1 d| NSD d| OCL d| MYG d| OCLCQ d| MYG d| OCLCQ d| MUQ d| OCL d| EEM d| OCLCQ d| OCLCF d| SCB d| OCLCE d| OCLCQ d| DEFHM d| OCLCO d| OCLCA d| VT2 d| OCLCO d| OCLCQ d| UAB d| WaSeSS
042				a| nsdp a| pcc
050	1	4		a| QA403
082	1	0		a| 515 2| 12
210	0			a| Appl. comput. harmon. anal. b| (Online)
222		0		a| Applied and computational harmonic analysis b| (Online)
245	0	0		a| Applied and computational harmonic analysis h| [electronic resource].
260				a| Orlando, Fla. : b| Academic Press, c| [©1993]-
310				a| Bimonthly, b| 1999-
321				a| Quarterly, b| 1993-1998
362	0			a| Vol. 1, no. 1 (Dec. 1993)-
500				a| Title from journal home page (viewed Feb. 28, 2000).
530				a| Also issued in print.
538				a| Mode of access: World Wide Web.
588				a| Latest issue consulted: Vol. 13, issue 3 (Nov. 2002) (ScienceDirect).
650		0		a| Harmonic analysis v| Periodicals.
655		0		a| Electronic journals.
776	0	8		i| Print version: t| Applied and computational harmonic analysis x| 1063-5203 w| (DLC) 94640949 w| (OCoLC)26049297
856	4	0		u| http://SK8ES4MC2L.search.serialssolutions.com/?V=1.0&L=SK8ES4MC2L&S=JCs&C=APPLANDCOMHA&T=marc
910				a| CONSER online
949				a| Electronic resource w| ASIS c| 1 i| 42566942-1001 l| ONLINE m| ONLINE r| Y s| Y t| ONLINE u| 12/2/2023 o| .STAFF. 360 MARC

PennState

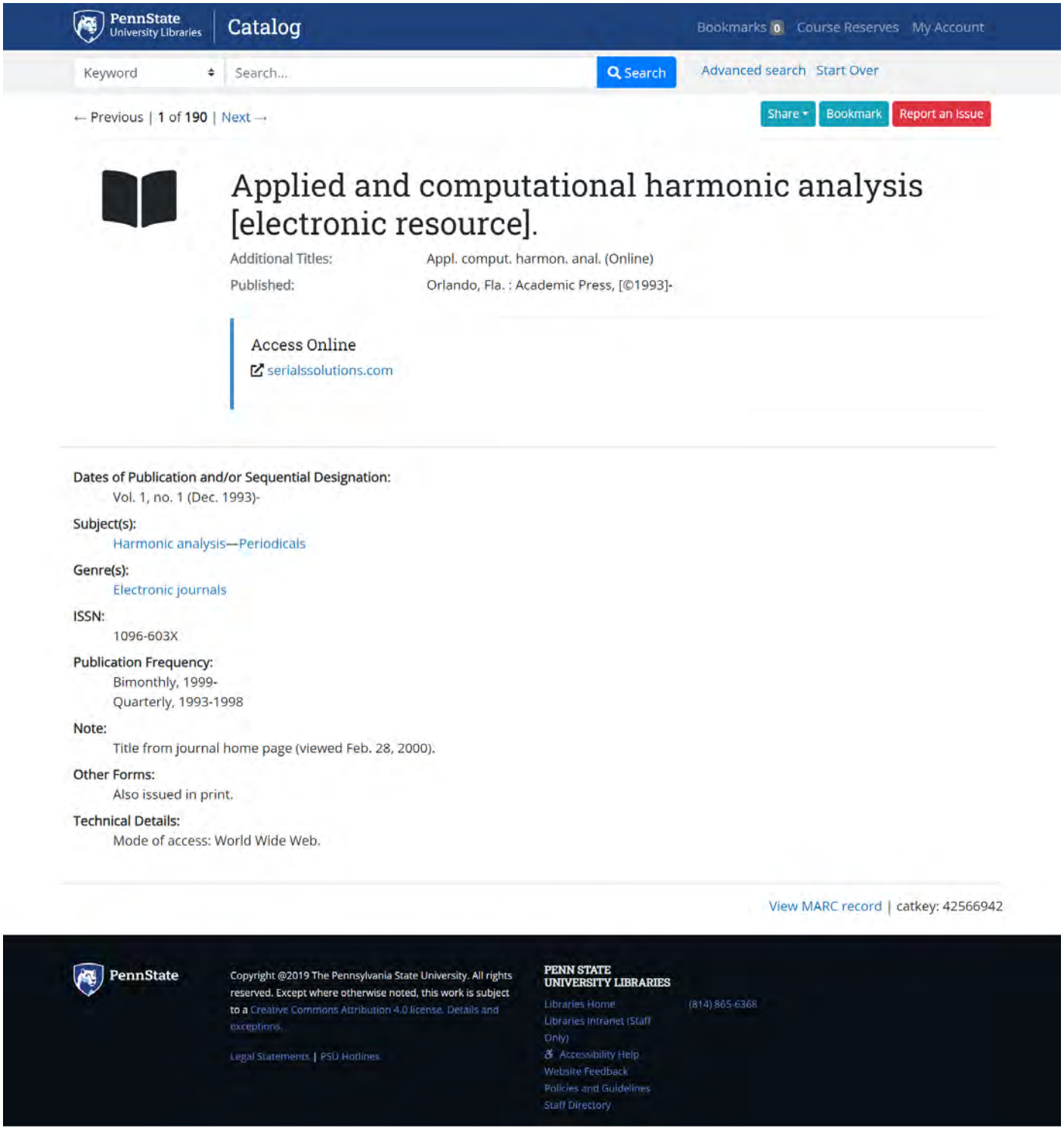
Copyright @2019 The Pennsylvania State University. All rights reserved. Except where otherwise noted, this work is subject to a Creative Commons Attribution 4.0 license. Details and exceptions.

Legal Statements | PSU Hotlines

PENN STATE UNIVERSITY LIBRARIES

Libraries Home (814) 865-6368
Libraries Intranet (Staff Only)
Accessibility Help
Website Feedback
Policies and Guidelines
Staff Directory

screenshot-catalog.libraries.psu.edu-2023.12.05-15_39_10
https://catalog.libraries.psu.edu/catalog/42566942
05.12.2023



ScienceDirect

Applied and Computational Harmonic Analysis

Supports *open access* • *Open archive*

5.3 CiteScore 2.5 Impact Factor

Submit your article | Guide for authors

Menu Search in this journal

Computational Harmonic Analysis - Part 2

Edited by

- Akram Aldroubi - Vanderbilt University, 1326 Stevenson Center, 13 South Dr., MSC 5766, Building 13/3N17, Nashville, TN 37240
- Charles Chui - Stanford University, Stanford, CA 94305

Volume 20, Issue 1,

Pages 1-158 (January 2006)

Download full issue

Previous vol/issue Next vol/issue

Receive an update when the latest issues in this journal are published

Sign in to set up alerts

Open archive

Editorial Board

Page CO2

View PDF

Editorial *Open archive*

Special issue on computational harmonic analysis, Part II

Akram Aldroubi, Charles Chui

Pages 1-2

FEEDBACK

View PDF

Research article *Open archive*

Robust reprojection methods for the resolution of the Gibbs phenomenon

Anne Gelb, Jared Tanner

Pages 3-25

View PDF Article preview

Research article *Open archive*

Frame expansions for Gabor multipliers

John J. Benedetto, Götz E. Pfander

Pages 26-40

View PDF Article preview

Research article *Open archive*

The polyharmonic local sine transform: A new tool for local image analysis and synthesis without edge effect

Naoki Saito, Jean-François Remy

Pages 41-73

View PDF Article preview

Research article *Open archive*

Affine frame decompositions and shift-invariant spaces

Charles K. Chui, Qiyu Sun

Pages 74-107

View PDF Article preview

Research article *Open archive*

The geometry of sets of parameters of wave packet frames

Wojciech Czaja, Gitta Kutyniok, Darrin Speegle

Pages 108-125

View PDF Article preview

Research article *Open archive*

Second-order Sigma–Delta ($\Sigma\Delta$) quantization of finite frame expansions

John J. Benedetto, Alexander M. Powell, Özgür Yılmaz

Pages 126-148

View PDF Article preview

Correspondence *Open archive*

Some properties of spectral measures

Izabella Łaba, Yang Wang

Pages 149-157

View PDF Article preview

Previous vol/issue Next vol/issue

ISSN: 1063-5203

Copyright © 2023 Elsevier Inc. All rights reserved

ELSEVIER

All content on this site: Copyright © 2023 Elsevier B.V., its licensors, and contributors. All rights are reserved, including those for text and data mining, AI training, and similar technologies. For all open access content, the Creative Commons licensing terms apply.

RELX™

APPENDIX SAITO02

Available online at www.sciencedirect.com
SCIENCE DIRECT®
Appl. Comput. Harmon. Anal. 20 (2006) 41–73
Applied and Computational Harmonic Analysis
www.elsevier.com/locate/acha

The polyharmonic local sine transform: A new tool for local image analysis and synthesis without edge effect ☆

Naoki Saito *, Jean-François Remy [1]

Department of Mathematics, University of California, Davis, CA 95616, USA

Received 9 November 2004; revised 15 January 2005; accepted 25 January 2005

Available online 15 August 2005

Communicated by Charles K. Chui

Abstract

We introduce a new local sine transform that can completely localize image information both in the space domain and in the spatial frequency domain. This transform, which we shall call the *polyharmonic local sine transform* (PHLST), first segments an image into local pieces using the characteristic functions, then decomposes each piece into two components: the *polyharmonic component* and the *residual*. The polyharmonic component is obtained by solving the elliptic boundary value problem associated with the so-called polyharmonic equation (e.g., Laplace's equation, biharmonic equation, etc.) given the boundary values (the pixel values along the boundary created by the characteristic function). Subsequently this component is subtracted from the original local piece to obtain the residual. Since the boundary values of the residual vanish, its Fourier sine series expansion has quickly decaying coefficients. Consequently, PHLST can distinguish *intrinsic* singularities in the data from the artificial discontinuities created by the local windowing. Combining this ability with the quickly decaying coefficients of the residuals, PHLST is also effective for image approximation, which we demonstrate using both synthetic and real images. In addition, we introduce the *polyharmonic local Fourier transform* (PHLFT) by replacing the Fourier sine series above by the complex Fourier series. With a slight sacrifice of the decay rate of the expansion coefficients,

☆ Dedicated to the memory of our fathers, Toshiki Saito and Christian Remy, both of them passed away in 2003. A preliminary version of the material was presented at the SPIE Conference on Wavelets: Applications in Signal and Image Processing X (San Diego, CA, August 2003), and the 2nd International Conference on Computational Harmonic Analysis (Nashville, TN, May 2004).

* Corresponding author.
E-mail addresses: saito@math.ucdavis.edu (N. Saito), jeanfrancois.remy@francetelecom.com (J.-F. Remy).

[1] Present address: France Telecom, Batiment Equinoxe, 4, avenue du 8 mai 1945, 78284 Guyancourt Cedex, France.

1063-5203/$ – see front matter © 2005 Elsevier Inc. All rights reserved.
doi:10.1016/j.acha.2005.01.005

PHLFT allows one to compute local Fourier magnitudes and phases without revealing the edge effect (or Gibbs phenomenon), yet is invertible and useful for various filtering, analysis, and approximation purposes.
© 2005 Elsevier Inc. All rights reserved.

Keywords: Polyharmonic equation; Laplace equation; Local sine transform; Local Fourier transform; Image approximation

1. Introduction

For smooth periodic signals and images, the conventional Fourier series expansion can give us almost everything we need. Simply manipulating the Fourier coefficients, we can shift them, differentiate/integrate them, and filter/attenuate them at our disposal. We can also measure the smoothness class (the Lipschitz/Hölder exponents) of a signal by checking the rate of the decay of its Fourier coefficients, which is related to sparsity since the faster decay of the expansion coefficients leads to a sparser representation. See the standard references on Fourier series [1–3] for the details. It is very important to realize that we lose everything once we have to deal with *nonperiodic* signals. The mismatch caused by the brute-force periodization (i.e., the head and the tail of an input signal do not match) kills every nice property we would have in the case of the smooth periodic signals. For example, the Fourier series expansion coefficients of nonperiodic data decay slowly, i.e., $O(\|\boldsymbol{k}\|^{-1})$, where $\boldsymbol{k}$ is the frequency index vector, and reveal the Gibbs phenomenon. Dealing with nonperiodic signals in a proper manner is of paramount importance in many applications that require analysis of local signal features such as data compression and discrimination. First of all, real signals are often nonperiodic. Second, even if the original signal is perfectly periodic, its locally segmented pieces (for local analysis of such pieces) are almost always not periodic. Thus, what we must do is not to create artificial discontinuities due to the local windowing or the brute-force periodization so that we can focus on the analysis of *intrinsic* discontinuities and singularities in the signal if any. Our goal is to develop a transform that can eliminate the interference of the boundary of a local window imposed by a user with the Fourier analysis of the information inside of such a window as much as possible.

We note that the wavelets/wavelet packets do not really solve this problem because in order to use wavelets or wavelet packets one needs to follow one of the following recipes: (1) periodize a signal and apply the standard wavelets/wavelet packets; or (2) design special wavelets near the boundaries (called "wavelets on the interval") as Cohen, Daubechies, and Vial proposed in [4]; or (3) use the so-called "multiwavelets" developed by Alpert [5], which essentially use segmented orthogonal polynomials. Unfortunately, none of them is really satisfactory for the applications we are interested in. The brute-force periodization (1) again creates the mismatch/discontinuity at the end points, and this generates large wavelet/wavelet packet coefficients. The wavelets on the interval (2) are rather complicated to implement in practice, particularly if one wants to use these in the wavelet packet mode or for images. Finally, the multiwavelets (3) are unfortunately not efficient for oscillatory signals such as textured images.

Coifman and Meyer [6] and Malvar [7,8] independently developed the so-called lapped orthogonal transform (LOT) (also known as local trigonometric transform (LTT) or Malvar wavelets) in an attempt to solve the above problems. However, it turned out that they were not completely satisfactory either, particularly for local signal analysis. The primary reason is the lack of the true localization capability of LTT: it cannot split an input signal into a set of nonoverlapping (disjoint) regions without the influence of their adjacent regions due to its use of the folding operations. (We shall call this a "crosstalk" problem.)

In this respect, the block discrete cosine transform (DCT) used in the JPEG Baseline standard is better because it chops a signal with the characteristic functions, i.e., no influence from the adjacent regions. Chopping the signal with the characteristic functions, however, makes the representation of the signal segment less sparse due to the sharp cutoff at the boundaries of the segment. If the signal segment does not contain any intrinsic discontinuity, the Fourier cosine coefficients decay with the rate $O(\|\boldsymbol{k}\|^{-2})$, which may not be fast enough, although this is better than the complex Fourier series expansion or Fourier sine series expansion, which provide only $O(\|\boldsymbol{k}\|^{-1})$ decay. In the case of LTT, we can tune the width of the overlap in the folding operations to get a faster decay rate, but there is another dilemma. The wider the overlap, the better in terms of sparsity, but the worse in terms of crosstalks (i.e., more statistically dependent). Fang and Séré developed the so-called "multiple folding" local trigonometric transforms (MLTT) [9] to overcome one of the problems. In terms of sparsity, MLTT provides a better representation than the conventional LTT. However, in terms of crosstalk problems, MLTT is definitely worse than LTT because MLTT has wider overlaps, especially in the early stage of the hierarchical split, and that creates more and more crosstalks down in the hierarchy. Villemoes proposed a further improvement in [10], which provides us with a set of local cosines satisfying the uniform bounds on their time–frequency concentrations, which was not possible by LTT and MLTT. However, this method constrains the arrangement of the dyadic blocks: it only allows each block to have adjacent blocks of either the same size or the twice as large or small in each dimension. In other words, around each block, we cannot place its adjacent blocks whose sizes are very different from it. Thus, this method generates a set of blocks similar to the Whitney decomposition [11]. However, this constraint may reduce the efficiency in approximation and compression. In principle, there should not be such a constraint; we should be able to arrange the blocks with different sizes freely. This constraint is due to the specific requirement of the action regions and bell functions which are the essence of the LTT construction.

All these problems essentially boil down to how to treat the boundaries that define those subintervals and regions. To attack this fundamental problem, we developed a new version of the local Fourier transform called "continuous boundary local Fourier transform" (CBLFT) a few years ago [12,13]. CBLFT does not create any crosstalks among the subintervals and any discontinuities in the signal values at the boundaries of those subintervals. For simplicity, let us describe the one-dimensional version of CBLFT here. It first chops a signal into segments with the characteristic functions. Let $I = [0, 1]$ be one of such segments. Then, let us periodize the segmented signal on I, say, $f(x)$ with period 1. Let us assume that f is continuous on I. At this point, the head and tail of f on I does not match, so the periodized signal has two discontinuities at $x = 0$ and $x = 1$. Consider now this periodized function on the extended interval $[-1, 2]$. We add the constant $f(0) - f(1)$ to this periodized signal only over $[-1, 0)$, and similarly $f(1) - f(0)$ only over $(1, 2]$. This makes this extended signal continuous over $[-1, 2]$ although this is not periodic with period 1 anymore. CBLFT then applies the folding operations at $x = 0$ and $x = 1$ and follows the usual LFT recipe of Wickerhauser ([14], [15, Chapter 4]). This procedure guarantees the decay rate of $O(|k|^{-2})$, generates no crosstalk since it only uses the signal information over I, and moreover, allows us to use the complex exponentials instead of real-valued cosine functions, which may be advantageous for certain applications such as computing locally analytic signals. However, CBLFT is not yet satisfactory: it does not deal with discontinuities in the derivatives at $x = 0$ and 1 so that the speed of the decay of the expansion coefficients is not fast enough. Moreover, due to its use of the folding operators, CBLFT is not too effective for analyzing very short segments of a signal.

We shall propose the *polyharmonic local sine transform* (PHLST) in the next section, which is a fundamentally better transform in the sense that it does not suffer from any of these problems compared to

the other methods mentioned above. It can also be generalized easily and hierarchically to higher dimensions. In essence, PHLST first segments an image into local pieces using the characteristic functions, then decomposes each piece into two components: the *polyharmonic component* and the *residual*. The polyharmonic component is obtained by solving the elliptic boundary value problem associated with the so-called polyharmonic equation (e.g., Laplace's equation, biharmonic equation, etc.) given the boundary values (the pixel values along the boundary created by the characteristic function) possibly with the estimates of normal derivatives at the boundary. Subsequently, this component is subtracted from the original local piece to obtain the residual. Because the boundary values of the residual (possibly with their normal derivatives) vanish, its Fourier sine series expansion has quickly decaying coefficients i.e., $O(\|\boldsymbol{k}\|^{-3})$ or faster. Using this transform, we can distinguish *intrinsic* singularities in the data from the artificial discontinuities created by the local windowing using the characteristic functions.

The organization of this paper is as follows. We describe the basic idea of PHLST in the next section. Section 3 describes important practical information, in particular, implementation issues. Section 4 reports the results of our simple image approximation experiments using DCT, local cosine transform (LCT; one version of LTT), discrete wavelet transform (DWT), and PHLST. In Section 5, we introduce the polyharmonic local Fourier transform (PHLFT) by replacing the Fourier sine series expansion of the residuals by the ordinary Fourier series expansion using the complex exponentials. With a slight sacrifice in the decay rate of the expansion coefficients, we gain many nice properties of the complex Fourier series such as the ability to represent local image patches by its Fourier magnitudes and phases without suffering from the Gibbs phenomenon. Finally, we conclude this paper in Section 6 where we discuss the open issues and our future plans, as well as the relation of PHLST to the previous works done by other scientists.

2. Our proposed method: polyharmonic local sine transform

Instead of constructing an orthonormal basis, we first segment a signal $f(\boldsymbol{x})$, $\boldsymbol{x} \in \mathbb{R}^d$ into local pieces using the characteristic functions, then split each piece into two components: the polyharmonic component and the residual. Let $\Omega \in \mathbb{R}^d$ be the overall domain where the signal is supported, and let $\bar{\Omega} = \bigcup_{j=1}^{J} \bar{\Omega}_j$ be a decomposition of the domain Ω into a set of disjoint subdomains $\{\Omega_j\}$. Note that Ω_j's are open and disjoint whereas $\bar{\Omega}_j$'s are closed and may share the boundaries. Let f_j be the restriction of f to $\bar{\Omega}_j$, i.e., $f_j = \chi_{\bar{\Omega}_j} f$. Let us now consider the local decomposition $f_j = u_j + v_j$ on Ω_j. We shall call u_j the *polyharmonic component* of f_j and v_j the *residual*. Let Δ be the Laplace operator in $\mathbb{R}^d$. Then the polyharmonic component is obtained by solving the following polyharmonic equation:

$$\Delta^m u_j = 0 \quad \text{in } \Omega_j, \quad m = 1, 2, \ldots, \tag{1}$$

with given boundary values and normal derivatives

$$\frac{\partial^{q_\ell} u_j}{\partial \nu^{q_\ell}} = \frac{\partial^{q_\ell} f}{\partial \nu^{q_\ell}} \quad \text{on } \partial\Omega_j, \quad \ell = 0, \ldots, m-1, \tag{2}$$

where q_ℓ is the order of the normal derivatives yet to be specified. The parameter q_0 is normally set to 0, which means that $u_j = f$ on the boundary $\partial\Omega_j$. These boundary conditions enforce the function values and the normal derivatives of orders $q_1, \ldots, q_{m-1}$ of the solution u_j along the boundary $\partial\Omega_j$ to match those of the original signal f over there. If the Ω_j's are all rectangles (of possibly different sizes),

then we take $q_\ell = 2\ell$, i.e., the *even order* normal derivatives. It is not necessary to match the odd order normal derivatives for the rectangular domain case because the Fourier sine series of v_j is equivalent to the Fourier series expansion of the extension of v_j by odd reflection with respect to the boundary $\partial\Omega_j$ and *the continuity of the odd order normal derivatives* (*up to order* $2m-1$) *is automatically guaranteed*. For $m = 1$, Eq. (1) becomes the following familiar form:

$$\begin{cases} \Delta u_j = 0 & \text{in } \Omega_j, \\ u_j = f & \text{on } \partial\Omega_j, \end{cases} \tag{3}$$

which is the *Laplace equation with the Dirichlet boundary condition*. For $m = 2$, we have the following *biharmonic equation with the mixed boundary condition*:

$$\begin{cases} \Delta^2 u_j = 0 & \text{in } \Omega_j, \\ u_j = f,\ \frac{\partial^\ell u_j}{\partial \nu^\ell} = \frac{\partial^\ell f}{\partial \nu^\ell} & \text{on } \partial\Omega_j, \end{cases} \tag{4}$$

where $\ell = 1$ or 2 depending on the shape of Ω_j. For the rectangular-shaped Ω_j, we take $\ell = 2$ as explained above. Note that in 1D ($d = 1$), the solution of (3) is simply a straight line connecting two boundary points of an interval $\bar{\Omega}_j$ whereas that of (4) is a cubic polynomial. However, in higher dimensions ($d \geqslant 2$), the solutions of (3), (4), and more generally (1) with (2) are not a tensor product of algebraic polynomials in general.

Subtracting such u_j from f_j gives us the residual $v_j = f_j - u_j$ satisfying:

$$\frac{\partial^{q_\ell} v_j}{\partial \nu^{q_\ell}} = 0 \quad \text{on } \partial\Omega_j, \quad \ell = 0, \ldots, m-1. \tag{5}$$

Since the values and the normal derivatives of v_j on $\partial\Omega_j$ vanish, its Fourier sine expansion coefficients decay rapidly, i.e., $O(\|\boldsymbol{k}\|^{-2m-1})$, if there is no other intrinsic singularity in Ω_j. In fact, we have the following theorem.

Theorem 1. *Let Ω_j be a bounded rectangular domain in $\mathbb{R}^d$, and let $f_j \in C^{2m}(\bar{\Omega}_j)$, but nonperiodic. Assume further that $(\partial/\partial x_i)^{2m+1} f$, $i = 1, \ldots, d$, exist and are of bounded variation. Furthermore, let $f_j = u_j + v_j$ be the PHLST representation, i.e., the polyharmonic component u_j is the solution of the polyharmonic equation* (1) *of degree m with the boundary condition* (2) *with $q_\ell = 2\ell$, $\ell = 0, 1, \ldots, m-1$, and $v_j = f_j - u_j$ is the residual component. Then, the Fourier sine coefficient $b_{\boldsymbol{k}}$ of the residual v_j is of $O(\|\boldsymbol{k}\|^{-2m-1})$ for all $\boldsymbol{k} \neq \boldsymbol{0}$, where $\boldsymbol{k} = (k_1, \ldots, k_d) \in \mathbb{Z}_+^d$, and $\|\boldsymbol{k}\|$ is the usual Euclidean (i.e., ℓ^2) norm of $\boldsymbol{k}$.*

The proof of this theorem is in Appendix A. Note that if we employ the straightforward Fourier series expansion of nonperiodic f_j by brute-force periodization, the decay rate becomes only $O(\|\boldsymbol{k}\|^{-1})$ even if $f_j \in C^{2m}(\bar{\Omega}_j)$. If we use the Fourier cosine series expansion of f_j, we can get $O(\|\boldsymbol{k}\|^{-2})$.

We call this new way of decomposing a function f into a set of functions $\{f_j = u_j + v_j\}_{j=1}^J$ the *polyharmonic local sine transform* (PHLST) of polyharmonicity m. For $m = 1$ and 2, we use the special abbreviations, LLST (Laplace LST) and BLST (biharmonic LST).

Remark 2. The polyharmonic component u_j is smooth particularly in the middle of the region Ω_j and as $\boldsymbol{x}$ approaches the boundary $\partial\Omega_j$, $u_j(\boldsymbol{x})$ approaches $f(\boldsymbol{x})$. In fact, u_j is also the minimizer of the following optimization problem (see, e.g., [16]):

$$\min_{u\in H^m(\Omega_j)} \sum_{|\alpha|=m} \binom{m}{\alpha} \int_{\Omega_j} \left|D^\alpha u\right|^2 \mathrm{d}\boldsymbol{x} \quad \text{subject to the boundary condition (2)}, \tag{6}$$

where $H^m(\Omega_j)$ is an L^2-Sobolev space of order m over Ω_j, $\alpha = (\alpha_1, \ldots, \alpha_d)$ is a multi-index of a d-dimensional variable with the following definitions: $|\alpha| = \alpha_1 + \cdots + \alpha_d$, $\binom{m}{\alpha} = m!/(\alpha_1! \cdots \alpha_d!)$, and $D^\alpha = \partial_1^{\alpha_1} \cdots \partial_d^{\alpha_d}$, where $\partial_i = \partial/\partial x_i$. This means that the polyharmonic component minimizes the *roughness* measured by the objective function in (6) while satisfying the boundary condition (2). The larger the polyharmonicity m is, the smoother the solution u_j gets.

Remark 3. Because the u_j component becomes very smooth away from the boundary and only carries the low frequency information in the middle of the region as discussed in Remark 2, the frequency content of the v_j component is close to that of f_j, particularly, around the mid to higher frequency band, where textures are well represented. Therefore, the v_j component retains the original texture information almost intact and is more suitable for texture analysis than the original image patch f_j.

Remark 4. Our PHLST belongs to a larger class of models, to which Yves Meyer refers as the $u + v$ models [17]. In a $u + v$ model, the original data f is assumed to be a sum of the two components u and v. The first component u is aimed at modeling the objects present in the data (often they are assumed to be in some specific function spaces such as the Besov spaces or the functions of bounded variation BV) whereas the v term is responsible for texture and noise in the data. In our PHLST model, one can also interpret u as "trend" and v as "fluctuation" of the original data f, which are commonly-used terms in the wavelet literature [18]. Yet another interpretation of this decomposition is the following: the polyharmonic component u represents the part of f that is *predictable from the boundary data only*, whereas the residual v represents the *unpredictable* part of f.

3. Practical aspects of PHLST

If Ω and Ω_j's are rectangular regions in $\mathbb{R}^d$ and the functions defined over there are sampled on a regular lattice (which is the most efficient case in terms of numerical implementation), we can employ the discrete sine transform (DST) based on the FFT algorithm to rapidly compute both the polyharmonic components and the Fourier sine series expansion of the residual components. In particular, we use the algorithm proposed by Averbuch and co-workers [19,20], which seems to us the most natural and practical Laplace/Poisson equation solver on rectangles. This ABIV method gives us more accurate solutions (in fact an arbitrary order of accuracy in principle) than those based on the finite difference (FD) approximation of the Laplace operator followed by FFT, which only gives us the solutions with accuracy $O(h^2)$ or $O(h^4)$, depending on the 5-point FD scheme or the modified 9-point FD scheme is used ([21, Section 7.1], [22, Chapter 12]) (h is, of course, the grid spacing here). Yet, the computational cost of the ABIV algorithm is still $O(N^d \log N)$, where N is the number of grid points in each direction of a rectangular domain. We also note that we use the $(d-1)$-dimensional version of PHLST to represent the

boundary function $f(\boldsymbol{x})$ for $\boldsymbol{x} \in \partial\Omega_j$, which can be recursively computed starting from the 1D version. To describe the ABIV method more simply and precisely, let us now consider the LLST decomposition $f(x, y) = u(x, y) + v(x, y)$ on the unit square $\bar{\Omega} = [0, 1]^2 \subset \mathbb{R}^2$. There are several options in the ABIV method, but the simplest and most practical version to compute the solution to (3) that does not require any derivative estimate can be written as follows.

$$u(x, y) = p(x, y) + \sum_{k \geqslant 1} \left\{ b_k^{(1)} h_k(x, 1-y) + b_k^{(2)} h_k(y, 1-x) + b_k^{(3)} h_k(x, y) + b_k^{(4)} h_k(y, x) \right\}, \tag{7}$$

where $p(x, y)$ is a harmonic polynomial that agrees with $f(x, y)$ at the four corner points of the domain, and its simplest form is:

$$p(x, y) = a_3 xy + a_2 x + a_1 y + a_0, \tag{8}$$

where the parameters a_j's can be easily and uniquely determined using the function values at the four corners. The function $h_k(x, y)$ is defined as

$$h_k(x, y) \stackrel{\Delta}{=} \sin(\pi k x) \frac{\sinh(\pi k y)}{\sinh(\pi k)}, \tag{9}$$

and $b_k^{(j)}$, $j = 1, 2, 3, 4$, are the kth 1D Fourier sine coefficients of the boundary functions $f(x, 0) - p(x, 0)$, $f(0, y) - p(0, y)$, $f(x, 1) - p(x, 1)$, and $f(1, y) - p(1, y)$, respectively, where $0 \leqslant x \leqslant 1$, $0 \leqslant y \leqslant 1$. One can easily verify that each sum involving h_k functions in (7) is a solution of the Laplace equation with the nonzero boundary values on only one side of the square. For example, $u^{(1)}(x, y) = \sum_{k \geqslant 1} b_k^{(1)} h_k(x, 1-y)$ satisfies the boundary condition:

$$u^{(1)}(x, 0) = f(x, 0) - p(x, 0), \quad u^{(1)}(x, 1) = 0, \quad u^{(1)}(0, y) = 0, \quad u^{(1)}(1, y) = 0.$$

One the other hand, the v component can be written as

$$v(x, y) = \sum_{m \geqslant 1} \sum_{n \geqslant 1} \beta_{mn} \sin(m\pi x) \sin(n\pi y), \tag{10}$$

where β_{mn} is the 2D Fourier sine coefficients of $v(x, y) = f(x, y) - u(x, y)$. We also note that we use the gridpoint formulation rather than the midpoint formulation for our discretization. Therefore, we use DST-I rather than the DST-II/III combination in this paper. See, e.g., [15, Chapter 4], [23] for the details of gridpoint vs midpoint formulations.

Let us show a simple example of the effect of removing the polyharmonic component. Figure 1 demonstrates this. We first use the global version of LLST, i.e., no further split of the image. One may wonder what is the difference between the original and the residual v component in this case because they look very similar. We would like to point out that the v component is displayed in a shifted dynamic range (i.e., $[-127, 127]$ instead of $[0, 255]$) to see the details. Moreover, if we examine them carefully, we can observe that the overall shading is gone in the v component. The bottom row of Fig. 1 clarifies this by displaying them as 3D perspective plots.

Figure 2 shows the results of LLST decomposition by splitting the original into a set of homogeneous square regions each of which has 17×17 pixels.

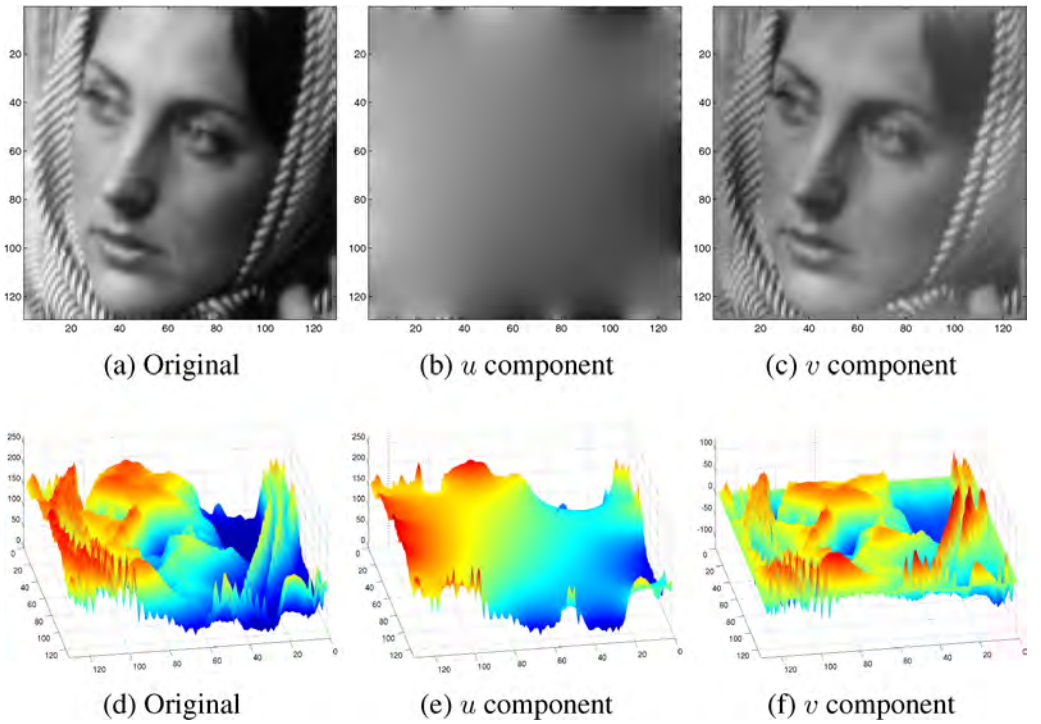


Fig. 1. The global version of LLST applied to the face part (129×129 pixels) of the Barbara image. Note that the display dynamic range of (a) and (b) are set to $[0, 255]$ whereas that of (c) is set to $[-127, 127]$. Figures (d)–(f) are the 3D perspective plots of the top row. It is easier to see in (f) that the overall shading of the face is removed in the v component.

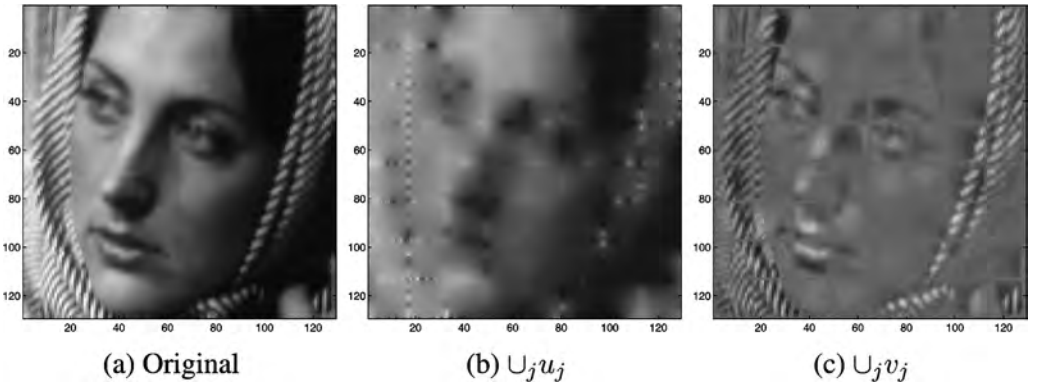


Fig. 2. The hierarchical LLST decomposition of the Barbara face image: (a) Original image; (b) the union of the u_j components $\bigcup_j u_j$ where each $\tilde{\Omega}_j$ is a square of 17×17 pixels; (c) the union of the v_j components $\bigcup_j v_j$.

4. Image approximation using PHLST

Since PHLST can represent smooth regions of an image very efficiently (i.e., faster decay of the DST coefficients of the residual components), image approximation and compression are immediate

and important applications of PHLST. In the field of image approximation, a great theoretical progress and understanding has been made. Nonlinear approximation of functions belonging to various function spaces, in particular, using the orthonormal wavelet bases or splines are now well understood [24]. However, as we shall discuss in Section 6.1.3, obtaining precise nonlinear approximation results for PHLST remains elusive. Therefore, in this paper, we shall report the results of our numerical experiments using PHLST and demonstrate its superiority over the other representative transforms such as DCT, LCT, and wavelets, which will hopefully illuminate our theoretical investigation.

In the rest of the paper, the dimension is set to $d = 2$, and the domain Ω and its subdomains Ω_j are all rectangles. We shall also limit our investigation to the specific version of PHLST with $m = 1$, i.e., LLST, rather than the PHLST of a higher polyharmonicity. We shall report the other settings (e.g., on more general domains, PHLST with $m > 1$, and investigation on PHLST-based image compression with quantization) at a later date. In our experiments, we shall examine how the intrinsic discontinuities and the smoothness and oscillation of the data away from the discontinuities affect the approximation performance.

Let us first describe the details of the LLST representation of a given image for a given split of the domain $\bar{\Omega} = \bigcup_j \bar{\Omega}_j$. In each subdomain Ω_j, we have an image patch f_j, which is decomposed into u_j and v_j components. Recall that each harmonic component u_j can be completely represented by the boundary values $f_j|_{\partial\Omega_j}$ that in turn can be represented by 1D version of LLST. As (7) shows, the u_j can be further decomposed into the harmonic polynomial p_j (8) and the rest using the h_k functions (9). The p_j component can be completely represented by (or recovered from) the four corner values of $\bar{\Omega}_j$. The rest of the u_j component is completely determined by 1D DST coefficients of the four boundary functions. Therefore, we represent the u_j component as the four corner values and the four sets of the 1D DST coefficients of the boundary values. We note that these four corner points and four sets of the 1D DST coefficients are shared by the adjacent blocks, so we should not duplicate them for storage efficiency. For example, if we split an image of size $(2^M + 1) \times (2^N + 1)$ pixels into a set of homogeneous blocks of size $(2^m + 1) \times (2^n + 1)$ pixels, then the total number of the corner points without duplication is $(2^{M-m} + 1) \times (2^{N-n} + 1)$. Another thing to note here is about the values of these corner points. The range of the corner pixel values are between 0 and 255 for a typical 8 bit gray scale image, which is quite different from that of the DST coefficients. This difference should be taken into account when the image compression including quantization is considered. Once the u_j component is taken care of, the v_j component is simply obtained by 2D DST (more precisely, 2D DST-I) in a straightforward manner.

As for the performance comparison, we compare LLST with: (1) the block DCT-II (abbreviated as "BDCT" below), which is used in the JPEG Baseline standard [23]; (2) LCT, which uses DCT-IV after the folding operations [15, Chapter 4]; and (3) C6 discrete wavelet transform (C6DWT), which is based on the 'Coiflet' 6-tap conjugate quadrature filter [25], [26, Chapter 8]. Note that the C6 wavelet functions has two vanishing moments, which means that any locally linear part of an input image generates negligible coefficients. Thus, we believe that it is a fair comparison with LLST since the u_j components of LLST also take care of locally linear parts.

Note also that if the size of an original image is $(2^M + 1) \times (2^N + 1)$, which is suitable for LLST, then we remove its last column and row to make it suitable for BDCT, LCT, and C6DWT. On the other hand, if an original image is of size $2^M \times 2^N$ pixels, then we duplicate the last column and row to make it suitable for LLST. Note also that the block size $(2^m + 1) \times (2^n + 1)$ pixels used for LLST correspond to $2^m \times 2^n$ pixels for BDCT and LCT.

Now let us describe our approximation strategy. We first retain all the corner pixel values for LLST, all the "DC" components for BDCT and LCT, and all the coefficients of the coarsest scaling function (i.e., the lowest frequency band) for C6DWT. Starting from those number of retained coefficients, we do the "nonlinear approximation," i.e., we select the coefficient with the largest energy among all the coefficients not yet used, add it to the retained set of coefficients, reconstruct an approximation from this set, and evaluate its quality of approximation. We repeat this process until we use up all the coefficients. The quality of approximation in this paper is measured by *PSNR* (or *peak signal-to-noise ratio*), which is normally considered as a better metric for evaluating image quality than SNR (signal-to-noise ratio) and defined as

$$20\log_{10}\Big(\max_{\boldsymbol{x}\in\bar{\Omega}}\big|f(\boldsymbol{x})\big|\big/\mathrm{RMSE}\Big),$$

where RMSE (the root mean square error) is the absolute ℓ^2 error between the original and the approximation divided by the square root of the number of pixels. The unit of PSNR is decibel (dB). Thus, PSNR $= 0$ dB corresponds to RMSE $= \max|f(\boldsymbol{x})|$, and PSNR $= 350$ dB corresponds to RMSE $\approx 10^{-17.5}\times\max|f(\boldsymbol{x})|$, which is essentially the machine precision, i.e., no error in practice. In our experiments, PSNR is computed as a function of the ratio R of the number of the retained coefficients to the total number of pixels of the input image.

4.1. Approximation of synthetic smooth images with and without discontinuity

In order to demonstrate the power of LLST, we shall conduct simple approximation experiments using synthetic data. We shall first examine the effect of intrinsic discontinuity in otherwise smooth data to the transforms under consideration.

4.1.1. A case without discontinuity

We first synthesize the 2D Gaussian function $\exp(-(x+1/3)^2-(y+1/3)^2)$ over the region $\bar{\Omega}=[-1,1]\times[-1,1]$, which does not have any intrinsic discontinuity. We sample this function with rate $\Delta x=\Delta y=1/128$, yielding discrete data of 257×257 pixels. If $\Omega=\mathbb{R}^2$, then this Gaussian function is in $C^\infty(\Omega)$. However, once we restrict this on a finite rectangle such as $[-1,1]\times[-1,1]$, its periodic extension is not in $C^\infty(\mathbb{R}^2)$ anymore, in fact, not even in $C(\mathbb{R}^2)$! This is due to the domain boundary we discussed in Introduction and by all means we need to remove this boundary effect in order to efficiently represent and characterize this dataset. On the other hand, we really do not need to split Ω into a set of smaller segments in this case since there is no intrinsic discontinuities in the data and it is homogeneous and isotropic. In order to confirm this, we also segment Ω into a set of homogeneous blocks of $2^j\times 2^j$ pixels for BDCT and LCT and $(2^j+1)\times(2^j+1)$ pixels for LLST where $j=7,6,5$, and check their approximation performance. We can view them as the quadtree-structured splits with the original image as the root node and those homogeneous blocks as the leaf nodes. Then, the maximum depth (or level) J of the quadtree is $J=1,2,3$, respectively. Note that $J=0$ implies no split of the domain Ω. For C6DWT, to match the number of the coefficients in the lowest frequency band with that of the DC components in the BDCT/LCT representations, the maximum depth of decomposition needs to be $J=7,6,5$, respectively. In general, for an image of $2^N\times 2^N$ pixels, the maximum depth J in the BDCT/LCT tree corresponds to the maximum depth $N-J$ in the wavelet tree.

Figure 3 shows these approximation results. As we have expected, LLST with no segmentation ($J=0$) outperforms all the other transforms with various depths of decomposition except that it is defeated

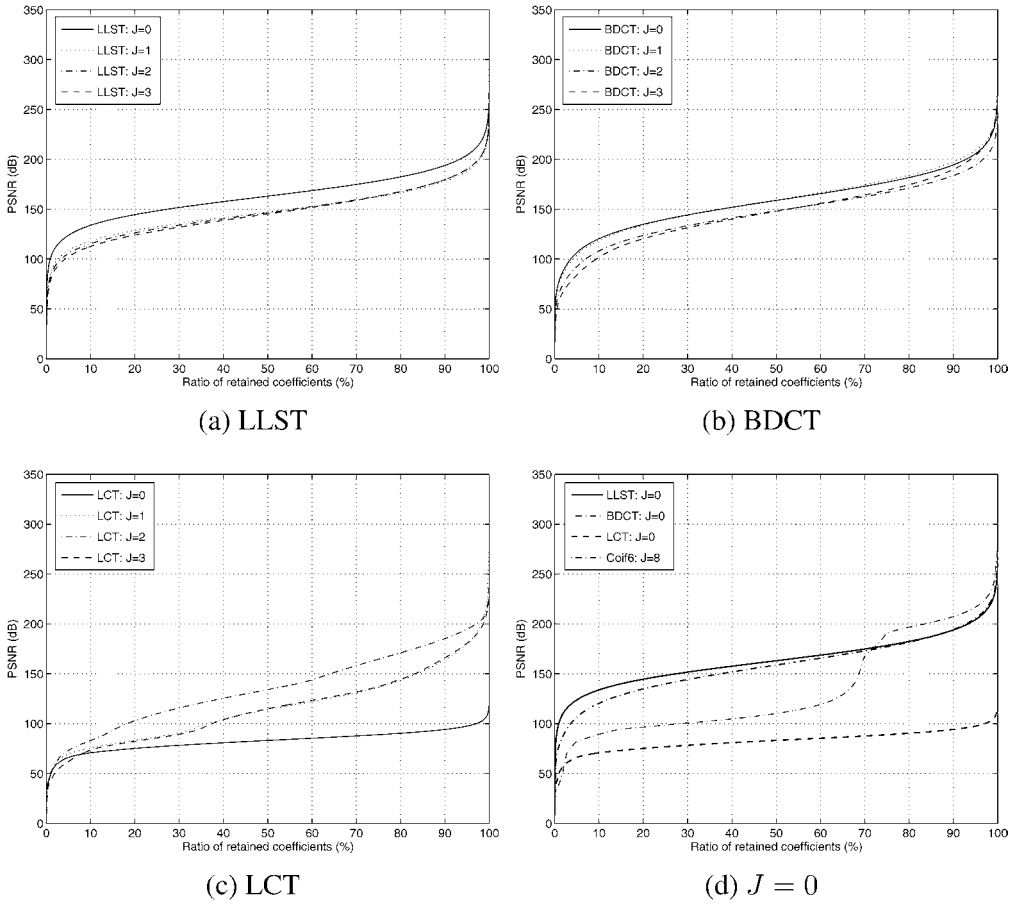


Fig. 3. Quality of approximation of the 2D Gaussian data measured by PSNR values. The index J represents the depth of the quadtree decomposition. Note that $J = 0$ means no splitting (i.e., the original domain is used).

by C6DWT if the ratio of the retained coefficients R is higher than about 72%. However, such a high ratio range is of no interest for the purpose of efficient approximation. We also observe that the more we subdivide the original domain, the more the performance of LLST and that of BDCT degrade. This superior performance of LLST with $J = 0$ over BDCT with $J = 0$ demonstrates the importance of having the coefficients decaying with $O(\|\boldsymbol{k}\|^{-3})$ rather than $O(\|\boldsymbol{k}\|^{-2})$.

The behavior of LCT is markedly different from that of LLST and BDCT. This is due to the folding operations and the use of DCT-IV as the underlying base transform in LCT [15, Chapter 4]. In essence, the folding operations split the data on the original domain into blocks smoothly using the appropriate bell function so that the data on each block become suitable for DCT-IV. In fact, the folding operations make the data locally even at the upper and left boundary and locally odd at the lower and right boundary of each block since each DCT-IV basis function behaves like cosines at the upper and left boundary and like sines at the lower and right boundary. These folding operations, however, need the data outside of the blocks. This means that we have a trouble at the blocks that share the boundary of the original domain because we do not know the data outside of the original domain. In particular, we cannot apply

the folding operation with $J = 0$, unless we can estimate a smooth extension of the data from the original domain. Note also that extending the input data by the brute-force periodization and then performing the folding do not solve the problem at all: such an operation does not match the polarity of the data at the domain boundary to what DCT-IV prefers. For simplicity, we use the so-called "free" boundary condition in our experiments. We do not assume any data outside of the domain, and do not perform any folding at the boundaries of the original domain. Therefore, LCT with $J = 0$ is equivalent to applying DCT-IV to the original image. Consequently, it senses the discontinuity at the lower and right boundaries unlike the simple DCT-II that views the data outside as the even-reflected version of the data inside. Thus, the LCT coefficients for $J = 0$ only decay as $O(\|\boldsymbol{k}\|^{-1})$, and that is the reason why LCT with $J = 0$ performs poorly. This is clearly worse than simply using DCT-II, and that is the main reason why DCT-IV is not used in the JPEG Baseline standard. On the other hand, if we use the smaller blocks such as the $J = 3$ case, then the influence of the boundary effect of the original domain is localized to the out-most blocks sharing the boundary of the original domain. However, the width of the bell function gets too short and the decay rate of the LCT coefficients becomes slow. That is the reason why LCT with $J = 2$ performs better than that with $J = 3$. See also [12,13] for the details of the boundary effects due to the folding operations.

As for the performance of C6DWT, we only plot $J = 8$ case in Fig. 3 (d) because the PSNR curves for the other values $J = 7, 6, 5$ are almost identical to that for $J = 8$ with very small differences in the low ratio region. This is due to the fact that the higher frequency finer scale coefficients are identical for these values of J. C6DWT performs reasonable for this dataset, but it is beaten by LLST and BDCT except at the very high ratios such as the region of $R \geqslant 72\%$ as mentioned above. Note also that this implementation of C6DWT assumes the periodic boundary condition at the domain boundary. Therefore, it too views the domain boundary as discontinuity in general.

Remark 5. The above observations on LCT and C6DWT suggest that removing the u component for $J = 0$ from the original data would help these transforms. In fact, if we remove the boundary by subtracting the u component, the performance of both LCT and C6DWT improves. In particular, for wavelets, this can be an alternative to "wavelets on the intervals" [4] provided that the pixels along the domain boundary (or their transformed version) are retained.

4.1.2. A case with discontinuity

Let us now introduce simple discontinuity in this dataset, and examine how the approximation performance changes by that. We multiply a scalar factor 2 to the circular region satisfying $\{(x, y) \mid (x + 1/3)^2 + (y + 1/3)^2 < 0.2\} \subset \Omega$.

Figure 4 shows these approximation results. Due to the discontinuity, the global methods ($J = 0$) are now inferior to the segmented cases for LLST, BDCT, and LCT. In fact, from Fig. 4 (a) and (b), we can see that the performance steadily improves as J increases. This is obvious since the discontinuity affects all the coefficients for $J = 0$ and makes their decay as $O(\|\boldsymbol{k}\|^{-1})$. On the other hand, for $J = 3$, the effect of the discontinuity is localized to the blocks where the discontinuity passes through. Note that in the continuum, whether covering the discontinuity by a large block or by a set of small or narrow blocks does not matter since the discontinuity results in the countable number of slowly decaying coefficients anyway. However, we are dealing with the finite dimensional sampled data. Consequently, localizing the discontinuity with a set of small size blocks reduces the number of slowly decaying coefficients.

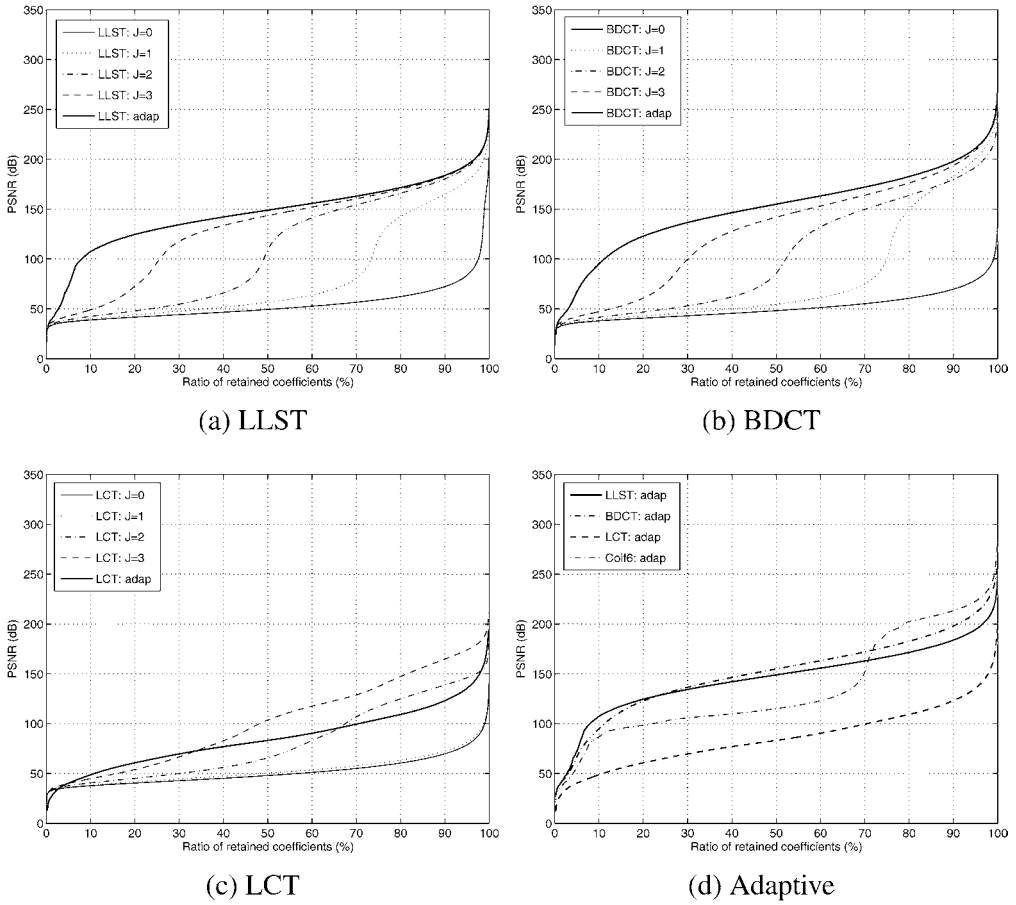


Fig. 4. Quality of approximation of the Gaussian data with circular discontinuity measured by PSNR values.

This observation leads us to the following expectation: grabbing smooth regions by largest possible blocks and using narrow blocks around the singularity should give us more efficient approximation than splitting the domain into a set of homogeneous blocks. There is no need to divide a smooth region into a set of smaller blocks, and in fact, that is wasteful due to the storage of the corner and boundary information in each block as demonstrated earlier. Therefore, we examine the power of the adaptive split of the domain honoring the geometry of (or the singularity in) the data. Figure 5 shows such an adaptive segmentation: smaller blocks around the singularity and progressively larger blocks away from the singularity, which is somewhat similar to the Whitney decomposition [11]. This particular segmentation has been done manually using our Java-based "Interactive Picture Partition" (IPP) program developed by Gary Zhong. We are currently developing an automatic adaptive segmentation algorithm using PHLST, and will report the details at a later date. Figure 4 also shows the performance of the approximations based on this adaptive segmentation. Of course, we use the same segmentation for LLST, BDCT, and LCT. As for adaptive version of C6DWT, we compute the so-called *best sparsifying basis* (BSB) via ℓ^1 norm minimization [27,28] from the C6 wavelet packet tree, and approximate by sorting out the BSB coefficients. However, our numerical computation shows that the BSB for this dataset turns out to be the

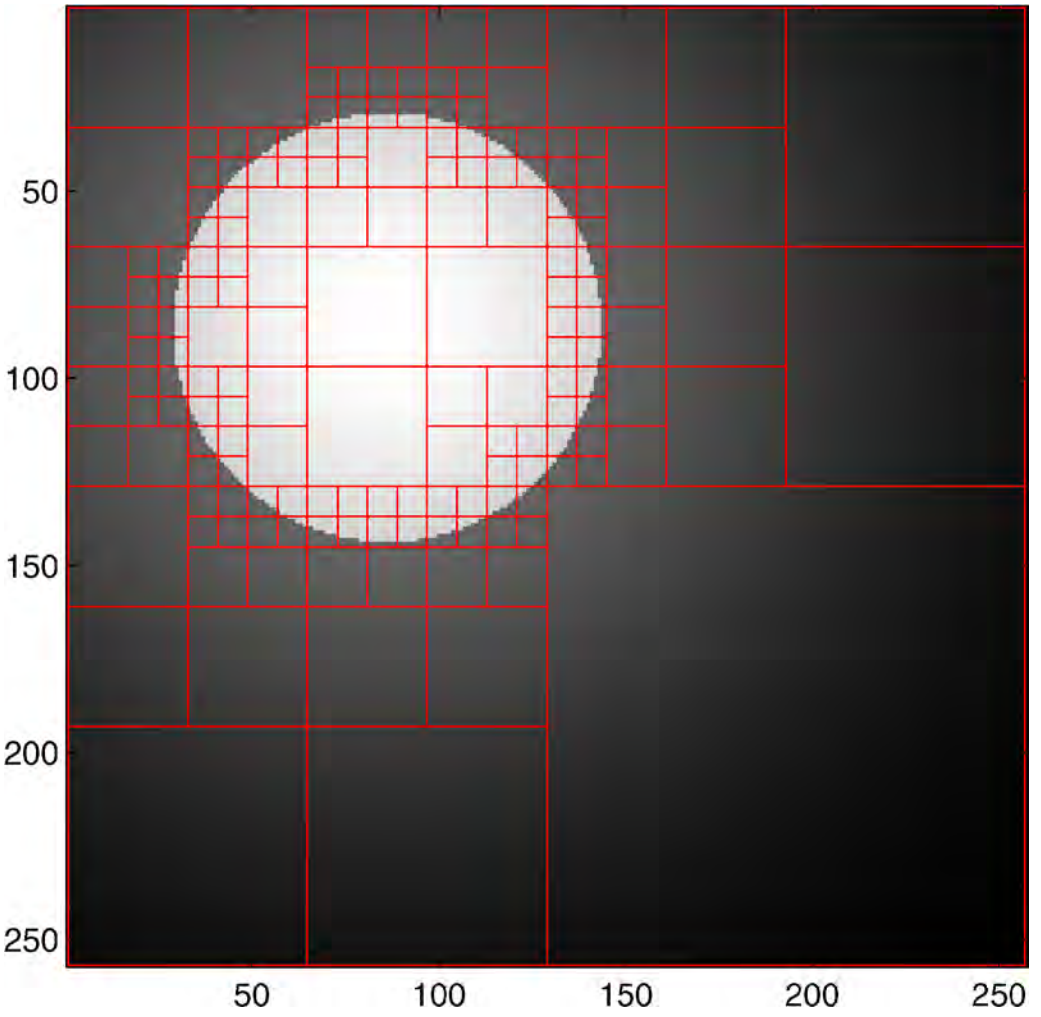


Fig. 5. Adaptive dyadic segmentation of the 2D Gaussian data with circular discontinuity, which honors the geometry of the discontinuity.

standard wavelet decomposition. This confirms the well-known fact that the wavelet transform performs well on piecewise smooth data. As we can easily see, the adaptive segmentation improves the performance of LLST and BDCT. Without adaptive segmentation, C6DWT performed best for $R \leqslant 25\%$ and $R \geqslant 72\%$, which can be seen by comparing the curve of LLST with $J = 3$ in subplot (a) with that of C6BSB ('Coif6: adap') in subplot (d) in Fig. 4.

With adaptive segmentation, however, LLST outperformed both BDCT and C6BSB for $R \leqslant 25\%$, which is the range of our interest.

Interestingly enough, the adaptive segmentation does not improve the performance of LCT so much from that of nonadaptive homogeneous split; it is slightly better only in the range $R \in [0, 30]$. The reason is that the adaptive segmentation uses many small blocks of size 8×8 pixels, as shown in Fig. 5. The version of LCT in our experiments uses the so-called "fixed" folding whose bell function width is com-

pletely determined by the smallest block size [15, Chapter 4]. Since the same bell function is also used for processing larger blocks, LCT loses its effectiveness as we discussed in Introduction and Section 4.1.1. To avoid such a problem, one needs to use multiple folding LCT of Fang and Séré [9], or better yet, the time–frequency LCT of Villemoes [10], which unfortunately constrains possible segmentation patterns as we discussed in Introduction. We shall not pursue these alternative versions of LCT here.

4.2. Approximation of synthetic oscillatory images with and without discontinuity

We shall now examine the performance of these transforms on an oscillatory function, in fact, a Gabor (i.e., a modulated Gaussian) function, with and without discontinuity as in the simple Gaussian case.

4.2.1. A case without discontinuity

We generate the data according to the formula: $f(x, y) = \exp(-(x+1/3)^2 - (y+1/3)^2) \cdot \sin(5\pi(2x + 3y))$, where $(x, y) \in [0, 1]^2$, and sample this with the same rate as before.

Figure 6 shows the approximation results. Again, in principle, there should not be any gain by splitting the data into a set of smaller blocks because the data do not have any intrinsic singularity. In fact, both LLST and BDCT, the $J = 0$ case outperforms the other values of J, and LLST with $J = 0$ remains as the best performer. Most obvious difference from the simple Gaussian case is the degradation of the performance of C6DWT, which confirms the well-know fact that the wavelet is not efficient for handling oscillatory data and textures. Another interesting observation is that LCT with $J = 2, 3$ performs quite well for this dataset. In fact, LCT with $J = 2, 3$ defeats LLST with $J = 0$ for the range $R > 42\%$; compare Fig. 6 (a) and (c). However, the range of our interest for efficient approximation, LLST with $J = 0$ still performs the best.

4.2.2. A case with discontinuity

Finally, we shall examine the toughest scenario so far: the Gabor function with the same circular discontinuity as the one used in Section 4.1.2. We shall not only use the homogeneous splits, but also the same segmentation pattern shown in Fig. 5 for the adaptive segmentation. We shall also compute the BSB from the C6 wavelet packet tree.

Figure 7 shows the approximation results. The performance of the approximation are degraded for all the transforms compared to the other scenarios considered so far, as expected. However, the overall best performer is LLST with adaptive segmentation, except for the range $R < 6\%$ where BDCT with adaptive segmentation performs slightly better. LCT with adaptive segmentation does not perform better than LCT with $J = 3$ as in the case of the Gaussian with discontinuity for the same reason: the width of the bell function is too narrow due to the smallest block size in this adaptive segmentation. We note that C6BSB in this case tries to subdivide the high frequency bands and performs better than the standard wavelet transform C6DWT unlike the case of Section 4.1.2 where C6BSB is in fact C6DWT.

In summary, our experiments with these synthetic images have shown that LLST is: (1) the best overall performer in the low ratio region of our interest; and (2) most effective if the adaptive segmentation of the domain honoring the geometry of the singularity in the data is used.

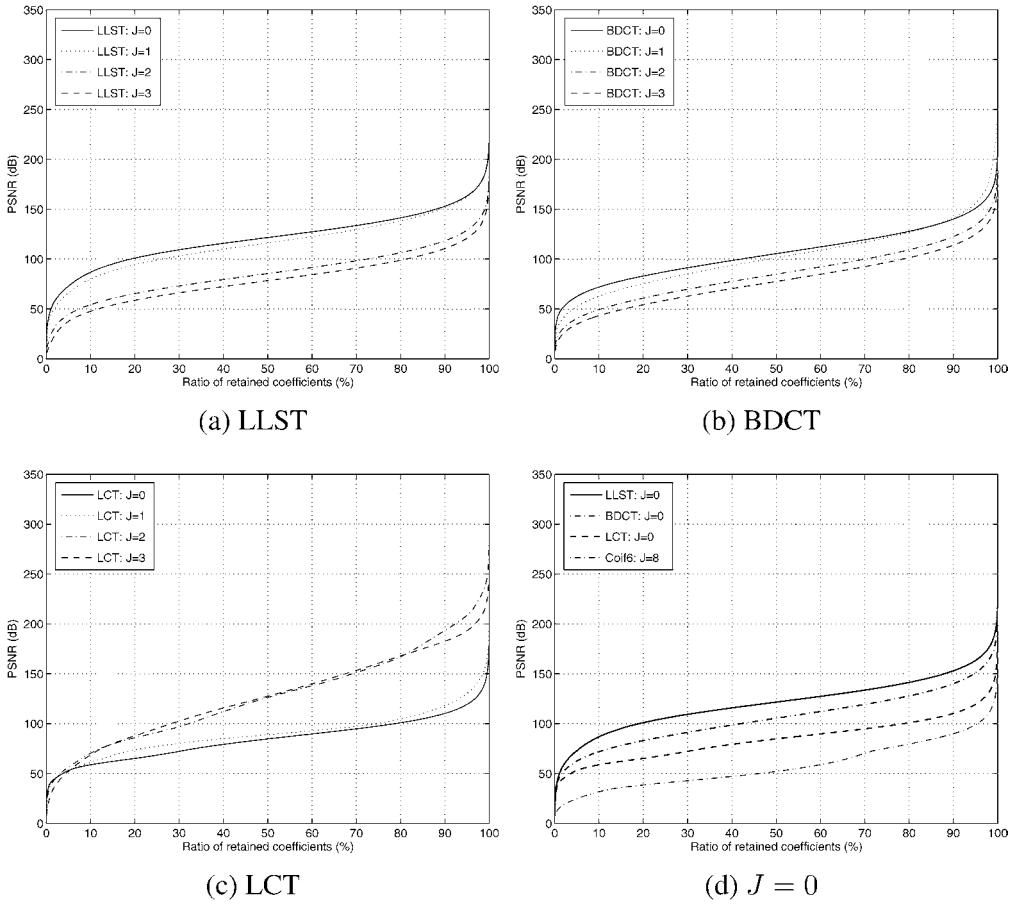


Fig. 6. Quality of approximation of the 2D Gabor (i.e., modulated Gaussian) data measured by PSNR values.

4.3. Barbara face image

Finally, we shall examine the approximation performance of various transforms using a real image. We shall use a face part of the famous image "Barbara," shown in Fig. 1 (a), which has been frequently used for image approximation and compression tests. The size of this face part of the Barbara image is 129×129 pixels. This is much more difficult to approximate than the simple Gaussian/Gabor datasets in the previous subsections because it contains a variety of regions: smooth regions (forehead and cheeks); more complicated regions (eyes, nose, mouth); and regions with oscillatory patterns (scarf). In this experiment, we shall use five different homogeneous splits $J = 0, 1, 2, 3, 4$. Note that the $J = 4$ case corresponds to the block size of 8×8 pixels, i.e., the standard JPEG-DCT scenario. We shall also examine the adaptive segmentation.

Figure 8 shows our results. The zoomed-up versions in the range $R \in [0, 20]$ are shown in Fig. 9. We use the IPP program as before to generate the adaptive segmentation for LLST, BDCT, and LCT, which is shown in Fig. 10.

From these figures, we observe the following:

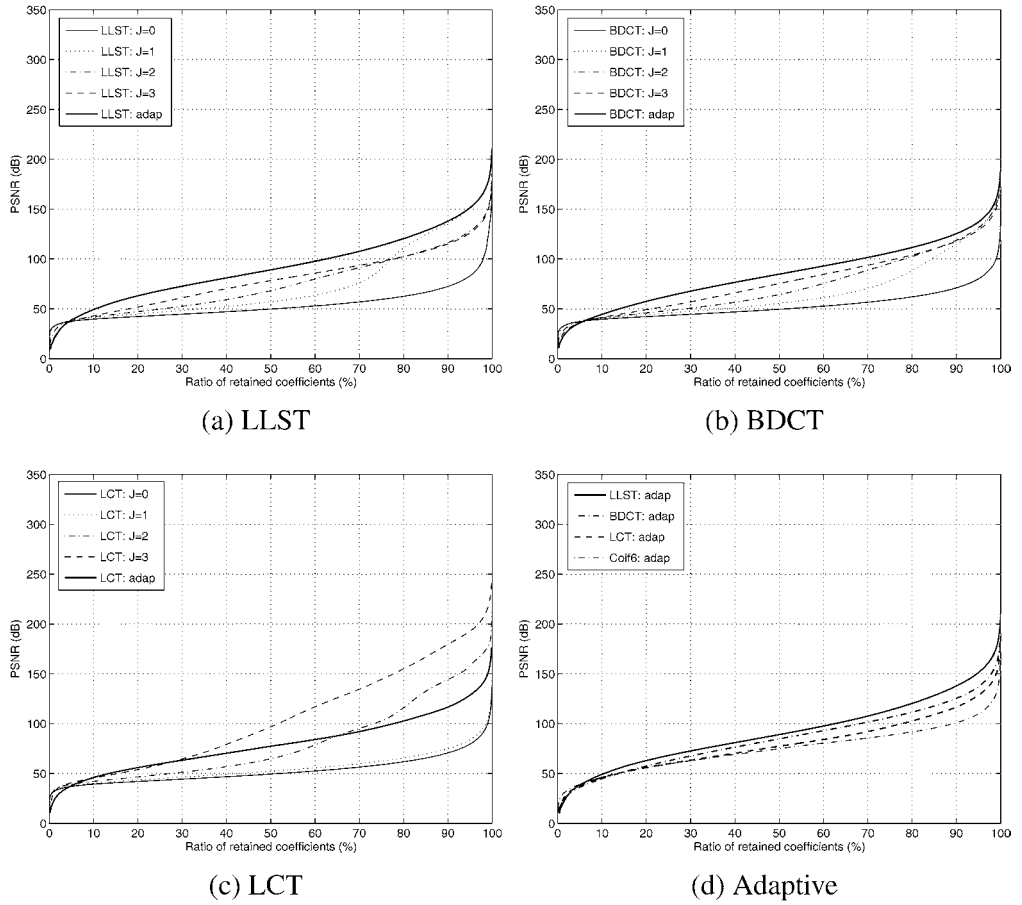


Fig. 7. Quality of approximation of the 2D Gabor data with circular discontinuity measured by PSNR values.

- The performance of LLST and BDCT with the adaptive segmentation and that of the homogeneous splits with $J = 2, 3$ are virtually the same.
- LLST and BDCT (with the adaptive segmentation or the homogeneous splits with $J = 2, 3$) outperform C6BSB except in the range $R \in [0, 5]$.
- The PSNR values of C6BSB in the range of $R \in [2, 20]$ are 1 dB higher than those of C6DWT with $J = 7$ (but not shown in the plots).
- LCT with adaptive segmentation is defeated by LCT with $J = 2, 3$, especially in the low range $R \leqslant 20\%$, by exactly the same reason as the Gaussian/Gabor cases.
- BDCT with $J = 4$ is defeated by BDCT with $J = 3$. This shows the nonoptimality (at least for this image) of the strategy of homogeneously splitting a target image into a set of blocks of size 8×8 pixels, which is adopted in the JPEG Baseline standard.
- Advantage of the adaptive segmentation is less obvious except the C6BSB case for this particular image.

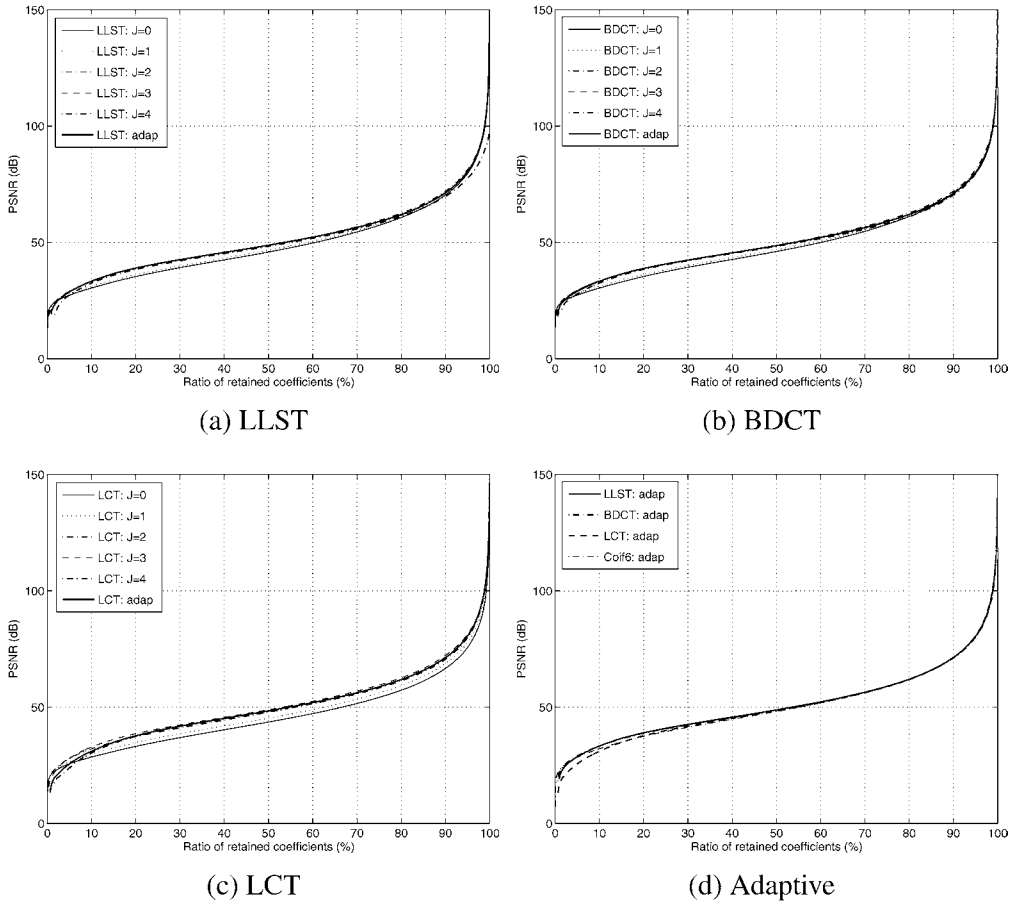
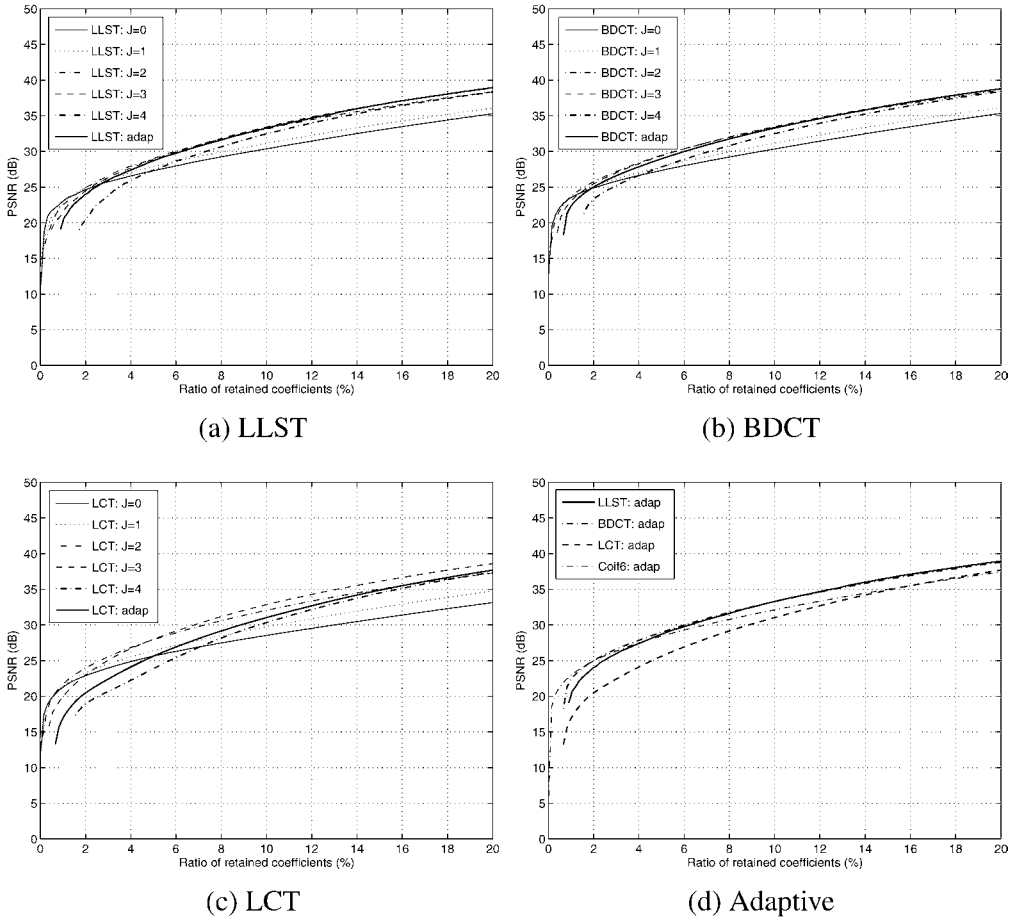


Fig. 8. Quality of approximation of the Barbara face image measured by PSNR values.

From these observations, unlike the synthetic datasets in Sections 4.1 and 4.2, we can claim neither the superiority of the adaptive segmentation over the homogeneous splits nor that of LLST over the other transforms, in particular, over BDCT *for this particular image and in terms of the PSNR values*. We shall therefore compare the perceptual quality of these approximations further by displaying the reconstructed images. Figure 11 shows the approximations using the top 5% of the coefficients by these transforms with the adaptive segmentation. Figure 12 shows the zoomed-up versions to see the quality of those approximations in details. It is clear that the visual quality of the LLST approximation is closest to the original among these transforms. The BDCT approximation reveals the annoying blocking artifact. The LCT approximation is the worst due to the artifact generated by the folding procedure. The C6BSB approximation is perhaps the next best, but the forehead and cheek portions are less smooth than the LLST approximation, and the stripes of the scarf, especially those in the right-hand side, are not well approximated. These experiments suggest that PSNR is not necessarily the best metric for judging the quality of displayed images. In the near future, we plan to use the more perceptually correct metric such as *mean structural similarity index* (MSSIM) [29], which is based on the comparison of the local patterns of pixel intensities normalized for luminance and contrast.



(a) LLST (b) BDCT

(c) LCT (d) Adaptive

Fig. 9. Zoomed up versions of Fig. 8 when 0% to 20% of the original coefficients are retained.

5. Polyharmonic local Fourier transform: use of the complex exponentials

As we discussed in Section 2, the Fourier sine coefficients of the v_j component of the PHLST decomposition posed as (1), (2), and (5) have the good decay rate, i.e., $O(\|\boldsymbol{k}\|^{-2m-1})$, $m = 1, 2, \ldots$. The main motivation of using the sine functions was the extra gain in the decay speed of the expansion coefficients via odd reflection at the boundary of the domain, which in turn is the consequence of the vanishing boundary values of v_j. However, it is well understood now that the *oriented patterns* are not efficiently captured and represented by using only sines (or only cosines). It is much more efficient to use *complex exponentials* for representing oriented patterns than sines alone. Because the boundary values of v_j vanish, it is possible to use the *complex exponentials* instead of sines, i.e., the ordinary Fourier series expansion instead of the Fourier sine series expansion, if one can tolerate slower decay rate of the coefficients. This slower decay is due to the periodization of the v_j component without the odd reflection. We shall call this the *polyharmonic local Fourier transform* (PHLFT). More precisely, let Ω_j be a box of the form $\Omega_j = \boldsymbol{x}_0^j + \prod_{k=1}^d (a_k^j, b_k^j)$, where $\boldsymbol{x}_0^j$ is the vertex of the box closest to the origin (i.e., the lower

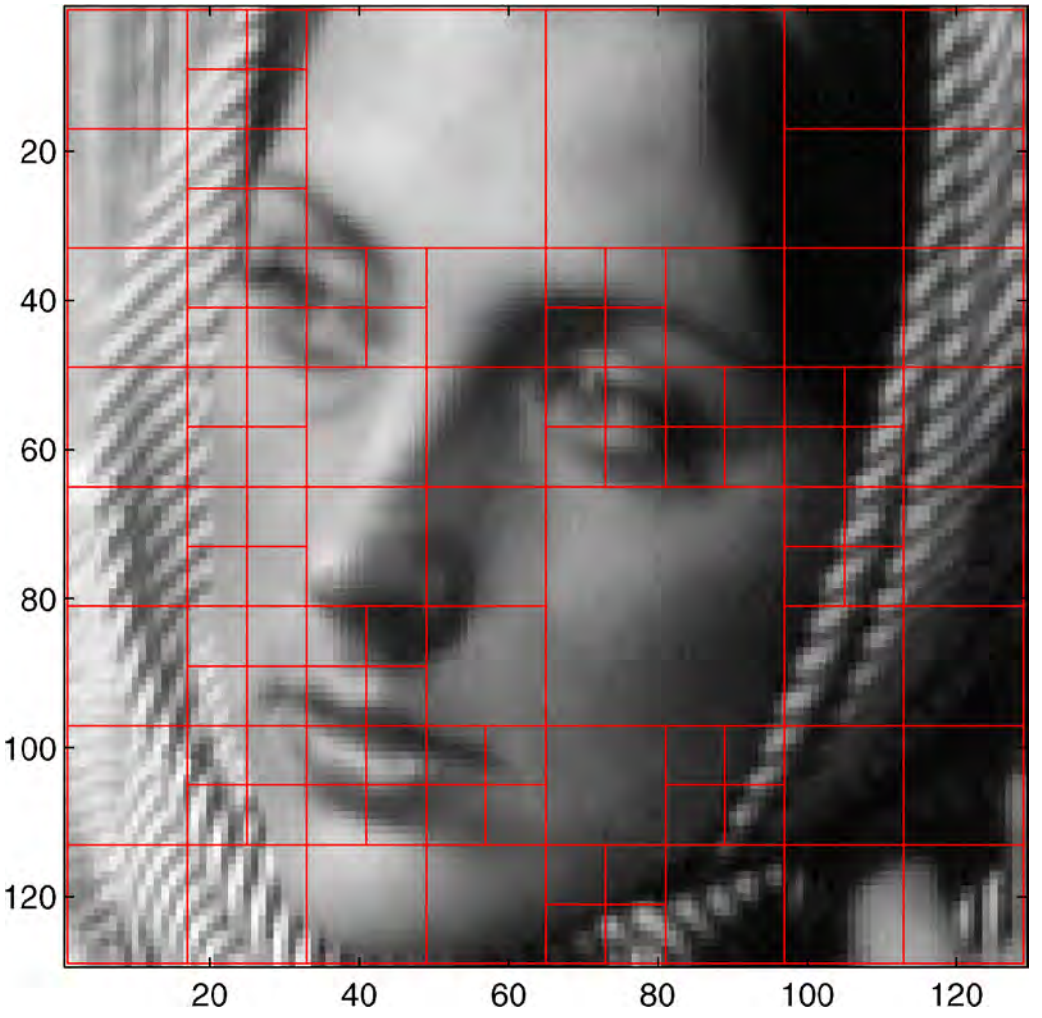


Fig. 10. Adaptive dyadic segmentation of the Barbara face image performed interactively using the Java-based IPP program.

left corner in the case of 2D), and $\ell_k^j \triangleq b_k^j - a_k^j$ is the length of the kth side of this box. Furthermore, let us assume that f is locally C^{2m} on $\bar{\Omega}_j$ with $m \geqslant 1$. If we use the following boundary condition instead of (2) to solve for the u_j component (1):

$$\frac{\partial^\ell u_j}{\partial \nu^\ell} = \frac{\partial^\ell f}{\partial \nu^\ell} \quad \text{on } \partial\Omega_j, \quad \ell = 0, \ldots, m-1, \tag{11}$$

then the resulting v_j component can be extended periodically and becomes $C^{m-1}(\mathbb{R}^d)$. Therefore, we can expand v_j into the Fourier series:

$$v_j(\boldsymbol{x}) \sim \sum_{\boldsymbol{k}\in\mathbb{Z}^d} c_{\boldsymbol{k}} \mathrm{e}^{2\pi \mathrm{i}\langle \boldsymbol{k}, L_{\Omega_j}^{-1}(\boldsymbol{x}-\boldsymbol{x}_0^j)\rangle}, \quad \boldsymbol{x} \in \Omega_j,$$

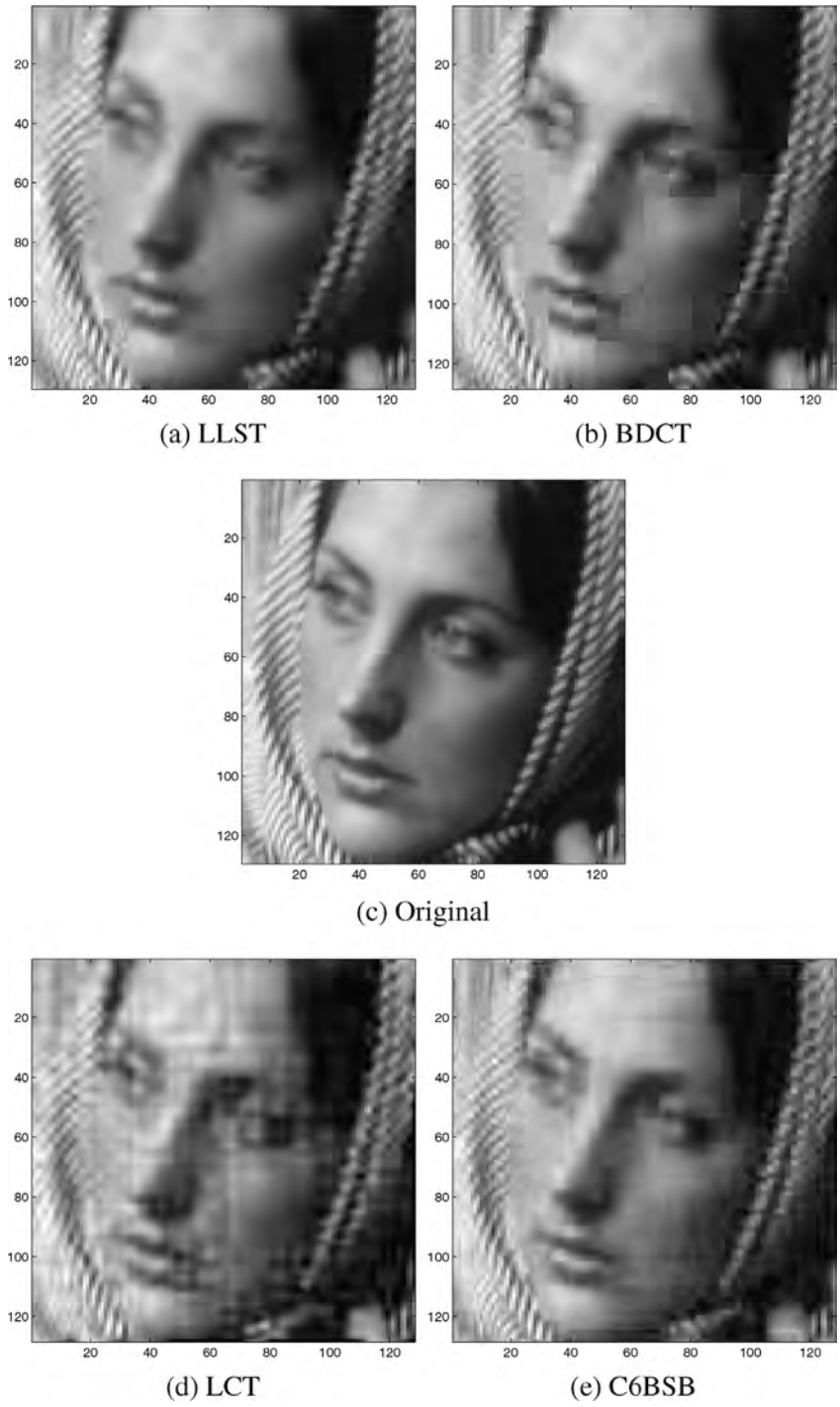


Fig. 11. Approximation of the Barbara face image by LLST, BDCT, LCT, and C6BSB using top 5% of the representations. The adaptive segmentation shown in Fig. 10 was used for LLST, BDCT, and LCT. C6BSB was computed from the C6 wavelet packet tree.

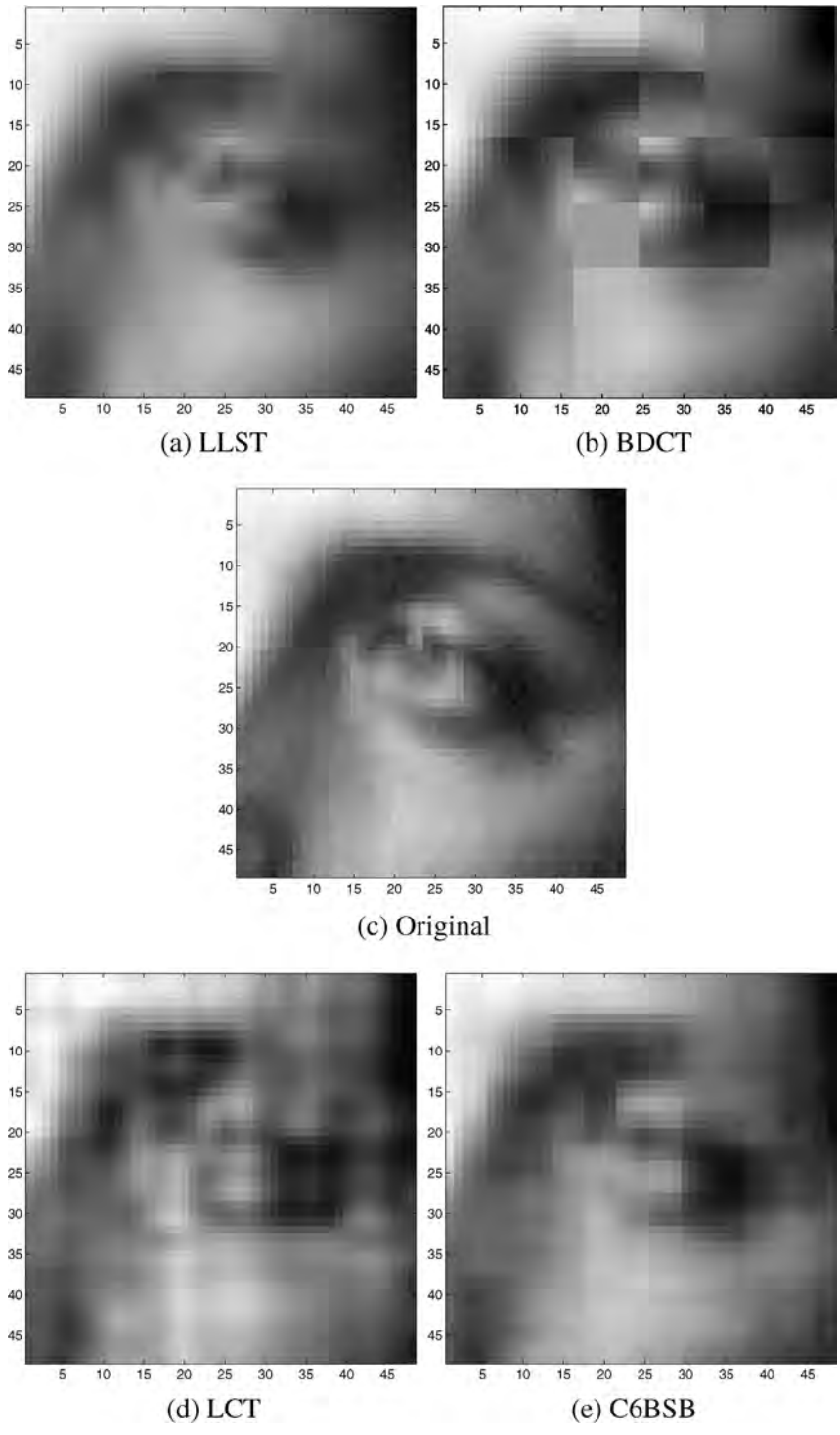


Fig. 12. Zoomed-up versions of Fig. 11.

where $L_{\Omega_j} = \mathrm{diag}(\ell_1^j, \ldots, \ell_d^j)$, with the coefficients $|c_{\boldsymbol{k}}|$ decaying as $O(\|\boldsymbol{k}\|^{-m-1})$; see Theorem A.2 in Appendix A. Accordingly, the case with $m = 1$, which we shall call *Laplace local Fourier transform* (LLFT), has the decay of order $O(\|\boldsymbol{k}\|^{-2})$, which is the same as BDCT. But we gain the ability to easily detect and interpret oriented patterns instead, which is difficult with BDCT or LLST. Figure 13 demonstrates this point. If one uses the block discrete Fourier transform (BDFT) without removing the u_j components, the DFT coefficients are all contaminated by the Gibbs phenomenon due to the block boundaries as shown in Fig. 13 (b). If one uses LLST or BDCT, it is difficult to decipher the orientation information from the coefficients; see Fig. 13 (c), (d). On the other hand, LLFT clearly reveals the ori-

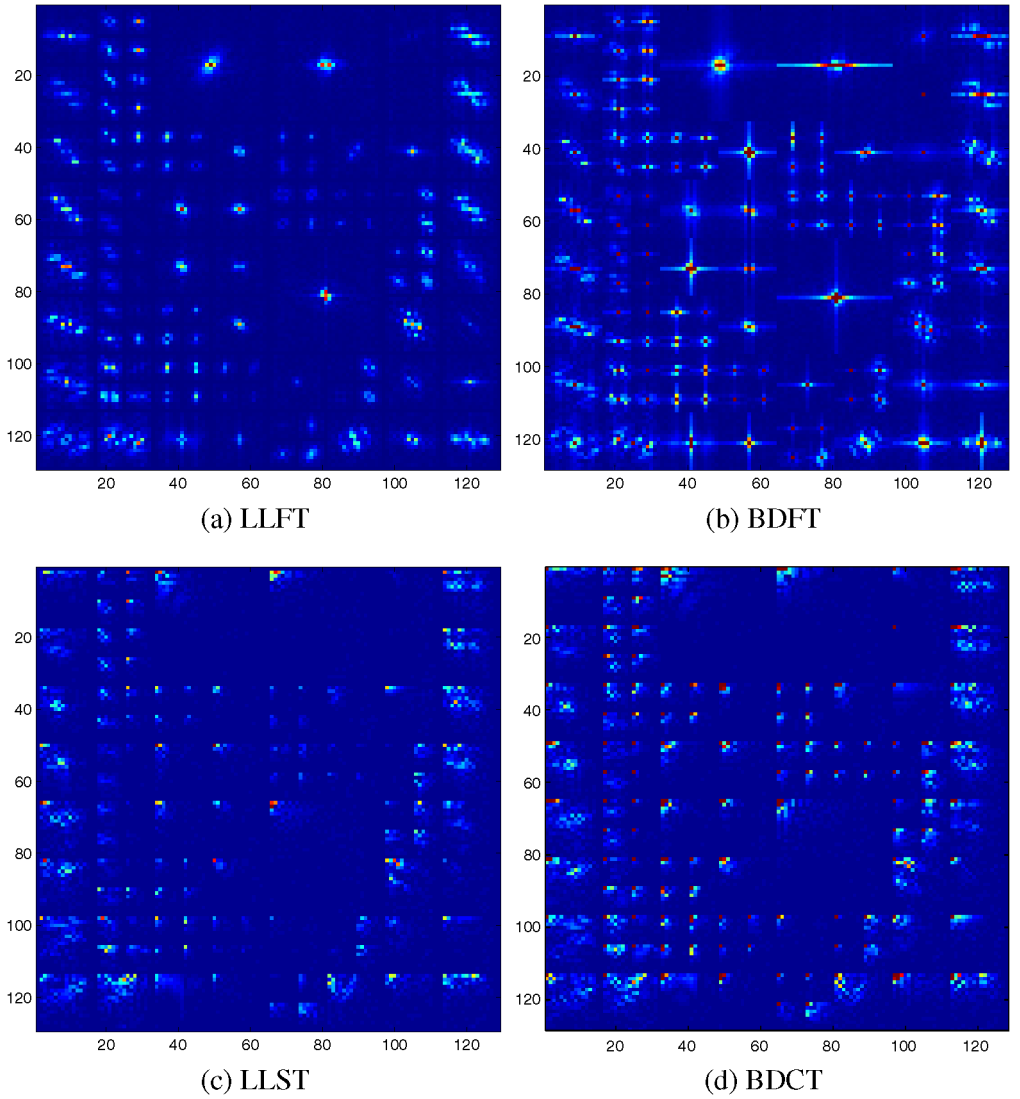


Fig. 13. Magnitude of the coefficients in LLFT, BDFT, LLST, and BDCT of the Barbara face image with the adaptive segmentation of Fig. 10. Note that the corner pixel values and 1D DST coefficients of the boundaries are not shown in LLFT and LLST here.

entation information as shown in Fig. 13 (a). We note that, in practice, one only needs to store the LLFT coefficients in the upper half plane in each block thanks to their symmetry, assuming that an input image is real-valued. LLFT also permits us to compute locally analytic signal, instantaneous frequency, etc., which we will explore at a later date.

6. Discussion

In this section, we shall first discuss issues that are left open in PHLST. Then we shall describe possible extensions and applications using PHLST and its relatives. We shall also discuss the related concepts and methods proposed previously by other researchers and conclude this article by describing the difference of their work from ours.

6.1. Open issues

6.1.1. Compression with quantization

A strategy for lossy image compression using PHLST remains an open issue. Unlike the image approximation, which simply keeps a subset of the exact expansion coefficients and corner pixel values as we discussed in Section 4, lossy image compression truly reduces the number of "bits" required to represent a given image approximately and converts it to a stream of bits via the process of *quantization*. In the JPEG Baseline standard [30,31], the DCT-II coefficients in each block of 8×8 pixels are divided by the entries of the so-called luminance quantization table (LQT) and further rounded into the nearest integers. This quantization process tends to suppress the higher frequency coefficients than the lower frequency coefficients so that this process can result in many zeros (i.e., more compression) without sacrificing visual fidelity too much. In fact, LQT was determined by psychophysical experiments on the visibility of the DCT-II basis vectors [30, Section 4.1.3] for the square block of 8×8 pixels. The Baseline method further uses the zigzag search of the quantized coefficients in each block to record the end of the block position instead of recording all the subsequent zeros in the block. Finally, this quantized sequence (integers) are encoded by some entropy coder (e.g., the Huffman coder or the arithmetic coder) for further compression in a "lossless" manner.

Unfortunately, we cannot directly use this LQT adopted in the JPEG Baseline standard for PHLST because it is optimized only for DCT-II of 8×8 pixel blocks, and not optimal for any other settings. In fact, it is not optimal even for DCT-II if the size of a block is different from 8×8 pixels. Therefore, if we wish to follow this approach, we would need to calibrate the LQT specifically for DST used in PHLST for various pixel sizes such as 9×9, 17×17, 33×33, etc. It would be too costly (in human resources) to conduct such psychophysical experiments. Also, the PHLST representation consists of three different items in each block: four corner pixel values, the 1D DST coefficients of the block boundary; and the 2D DST coefficients of the residual component. We need to examine whether these three components should be quantized separately or not.

We are currently investigating simpler uniform quantizers with "dead zone" (a special bin covering the zero value). This dead zone can get rid of noise in input data if its width is appropriately chosen because any coefficients within this zone are quantized to zero, i.e., killed. Thus, the width of the dead zone plays the role of the threshold in denoising algorithms. The subtle and interesting issue here is how to choose the width of the dead zone as well as that of the uniform bins outside of the dead zone, which determines

the resolution of the quantization. Yet another open issue is that of encoding after quantization. Just like the JPEG Baseline standard, it is possible to use the zigzag search to detect the trailing zeros in each block, and encode the resulting quantized sequences via Huffman coder. However, it still remains to be investigated whether such an approach is most suitable for PHLST.

6.1.2. Segmentation and denoising

Another open problem is how to automatically and adaptively segment a given input image to achieve more efficient approximation and compression. Note that what we mean segmentation here is different from usual image segmentation studied in the image analysis and computer vision literature where one wishes to faithfully segment an image into a set of objects or domains whose boundaries are general smooth curves. What we want to do here is to simply split an image into a set of adaptive dyadic blocks honoring the geometric structure of input data as much as possible. For example, we wish to obtain segmentations like those shown in Figs. 5 and 10 completely automatically rather than manually using an interactive program like IPP. We already demonstrated that such adaptive dyadic splits help image approximation in Section 4. We need to confirm that the same is true for image compression, which necessarily includes the cost of recording the geometry of adaptive splits.

We are currently investigating a hierarchical and recursive split-and-merge strategy similar to the best-basis algorithm of Coifman and Wickerhauser [32] in spirit. Clearly, the key is what criterion we should employ to judge whether smaller blocks should be merged into larger blocks. One of the most promising and natural criteria is the *minimum description length* (MDL) criterion [33–36]. Viewing each split pattern of an image in PHLST as a *model*, the MDL criterion suggests that we should choose among many possible models the one giving the shortest description (counted in bits) of the data *and* the model. This leads to the minimization of the infidelity of the model to the data and the complexity of the model itself in a balanced manner. In the case of PHLST, the MDL criterion is particularly appealing since PHLST does not provide an orthonormal basis. Instead, it provides "nonhomogeneous" representations using the corner pixels, 1D DST coefficients of the boundaries, and the 2D DST coefficients of the residuals, as explained in Section 4. Thus, the sparsity criterion using ℓ^p norm with $0 < p \leqslant 1$ makes less sense contrary to the case of the libraries of orthonormal bases such as local cosines and wavelet packets. It makes more sense to count the description length in bits needed to encode such nonhomogeneous representations.

There are several additional advantages to use the MDL criterion here. First, it forces us to incorporate a quantization procedure to convert the representation into a sequence of bits. Second, it can achieve *simultaneous compression and denoising* of input data. Similarly to the case of wavelets and the libraries of orthonormal bases shown by Saito [36], Chang et al. [37], and Hansen and Yu [38] among others, we expect that the MDL-based method will achieve the desired results for PHLST. Finally, the MDL formulation allows us to incorporate easily various noise models and prior models for distribution of the expansion coefficients: it can automatically select the most suitable noise model and coefficient distribution models out of many competing models. This is advantageous since it is well known that the Laplace (or double exponential) distribution or the generalized Gaussian distribution are more suitable to model the wavelet coefficients [38] and DCT coefficients [39] of natural images than the Gaussian distribution. The DST coefficients in PHLST are expected to behave in a similar manner.

6.1.3. Nonlinear approximation with PHLST

Another open issue is to obtain precise nonlinear approximation results using PHLST. Such a task remains elusive compared to the case of the orthonormal wavelets or splines. Let us briefly explain why

this is so. First, let us introduce some important concepts of the nonlinear approximation. Let X be some function space (e.g., the Besov space) defined on a domain $\Omega \subset \mathbb{R}^d$, and let $\Sigma_n \subset X$ be a nonlinear manifold so that any function belonging to Σ_n can be exactly representable by at most n parameters. Examples of such Σ_n include a set of functions that can be exactly specified by at most n basis functions selected from a basis set for X and a set of piecewise constant functions with n knots or breakpoints for $d = 1$. We now define the n-term approximation error of $f \in X \subset L^p(\Omega)$ as follows:

$$\sigma_n(f)_p \stackrel{\Delta}{=} \inf_{g \in \Sigma_n} \|f - g\|_p,$$

where $1 \leqslant p \leqslant \infty$. In the nonlinear approximation setting, the goodness of Σ_n is measured by the decay rate of the worst case n-term approximation error as n increases:

$$\sigma_n(X)_p \stackrel{\Delta}{=} \sup_{f \in X} \sigma_n(f)_p \leqslant C n^{-\alpha}, \tag{12}$$

where $\alpha > 0$. Clearly, the larger the value of α, the better the manifold Σ_n. The primary difficulty in obtaining n-term approximation results for PHLST lies in the strategy to optimally distribute the resources of n terms (or numbers) to the geometry information $\{\Omega_j\}$, the polyharmonic components $\{u_j\}$, and the residuals $\{v_j\}$. Even with a homogeneous split of Ω, it is challenging to derive an optimal allocation of n terms into the $\{u_j\}$ and $\{v_j\}$ components. Another difficulty, which is clearly related to the primary one above, is to determine a good function space X that allows us to obtain the best possible n-term approximation results, i.e., the largest $\alpha > 0$ in (12). We need to start attacking a simpler case of 1D functions here since DeVore in his plenary lecture [40] pointed out that obtaining nonlinear approximation results for an even simpler "Spline-Fourier" method with $d = 1$ (where a target function is segmented into several pieces brutally and each piece is approximated by the truncated Fourier series) is still open. On the other hand, it is encouraging to know that if $\Omega = [0, 1]^d$ without any further split, then the precise nonlinear approximation results are known [41].

6.2. Extensions and applications

In this section, we shall list possible extensions and applications of PHLST and its relatives.

6.2.1. PHLST/PHLFT in the frequency domain

Nothing prevents us from operating PHLST/PHLFT in the frequency domain. In fact, this strategy may be an excellent alternative to the wavelet packets and the brushlets [42]. The frequency support of each wavelet packet basis function is not completely localized except for the Shannon wavelet packets. On the other hand, each of the Shannon wavelet packets has unbounded support in the spatial domain, which makes them less useful. The frequency support of each brushlet basis functions is more localized than that of the wavelet packets, but still overlaps with that of the adjacent brushlets due to the use of the folding operations in the frequency domain. The PHLST/PHLFT in the frequency domain may overcome these shortcomings of the wavelet packets and the brushlets. We note that it is important to subtract the global u component from the original image f before converting it to the frequency domain. Otherwise, sharp horizontal and vertical lines crossing at the origin (the DC component) are generated due to the Gibbs phenomenon from the domain boundary, which interfere our analysis of the frequency information of the image. This is evident from Fig. 13 (b), which shows the local version of this annoying interference.

6.2.2. Use of the Neumann boundary condition

It is possible to use the *Neumann boundary condition* instead of the Dirichlet condition in (3). This will give us the $O(\|\boldsymbol{k}\|^{-4})$ decay rate of the v_j components instead of $O(\|\boldsymbol{k}\|^{-3})$ in the case of the Dirichlet boundary condition. To do so, we need to modify (3); we shall solve the following *Poisson equation* with the Neumann boundary condition:

$$\begin{cases} \Delta u_j = K_j & \text{in } \Omega_j, \\ \frac{\partial u_j}{\partial \nu} = \frac{\partial f_j}{\partial \nu} & \text{on } \partial\Omega_j, \end{cases} \tag{13}$$

where K_j is a constant that needs to be computed as follows:

$$K_j = \frac{1}{|\Omega_j|} \int_{\partial\Omega_j} \frac{\partial f_j}{\partial \nu}\, \mathrm{d}s,$$

which is the boundary integral of $\partial f_j/\partial\nu$ normalized by $|\Omega_j|$ (the volume of the domain). This constant K_j is necessary for (13) to have a unique solution (modulo an additive constant); see, e.g., [43, p. 84]. The solution u_j is not just a function having the same normal derivative at the boundary with the original function f_j; one can show that it is *the minimizer of the total squared curvature integral* on the domain Ω_j. Once we get the solution u_j, the residual function $v_j = f_j - u_j$ clearly satisfies $\partial v_j/\partial\nu = 0$ on $\partial\Omega_j$. Assuming that $f_j \in C^2(\bar{\Omega}_j)$, we can show that the residual v_j has at least C^2 smoothness across the block boundary when it is extended by the even reflection. Therefore, if we use the Fourier *cosine* series expansion of v_j we get the coefficients with decay rate $O(\|\boldsymbol{k}\|^{-4})$. See also Theorem A.2 in Appendix A. We naturally call this version of the transform the *polyharmonic local cosine transform* (PHLCT). However, this method of course requires to estimate the first order normal derivative of data at the boundary. We are currently investigating this issue with our collaborator, Katsu Yamatani, and getting encouraging results [44].

6.2.3. Extension to higher orders of polyharmonicity

We believe that PHLST of polyharmonicity $m > 2$ is not practical considering the need to estimate $\partial^{2(m-1)} f_j/\partial\nu^{2(m-1)}$ in (2) and the numerical sensitivity to compute these high order derivatives. However, the case of $m = 2$, i.e., BLST (biharmonic local sine transform), remains to be investigated; we are interested in knowing whether BLST is of practical interest for image approximation and compression or not. In theory, the Fourier sine coefficients of the v_j components in BLST should decay as $O(\|\boldsymbol{k}\|^{-5})$ instead of $O(\|\boldsymbol{k}\|^{-3})$ in LLST. However, the effectiveness of BLST still hinges on the accuracy of the second order normal derivative estimates at the boundary. Thus developing a robust method to estimate those derivatives from noisy data will be an challenging but important project. Note that such a method will also be useful for other purposes, for example, edge detection.

6.2.4. Extension to higher dimensions

It is important to realize that the information contained in the boundary becomes more and more meaningful as the dimension increases. For example, in 1D, the boundary of an interval simply consists of two endpoints. In 2D, the boundary of a domain becomes a 1D curve whereas in 3D, this becomes a 2D surface. If the data is supported in a 3D cube, then the boundary consists of six faces of that cube. It is also important to recognize that the boundary structure is *recursively organized*. For example, the boundary of each 2D face of a 3D cube consists of four 1D edges, and the boundary of each 1D edge

in turn consists of two corners. We can take advantage of this recursive structure: we can process each component, i.e., edges, faces, bodies, etc., by PHLST of the corresponding dimensions. The simple, hierarchical, and recursive algorithmic structure of PHLST can be carried over to higher dimensions in a straightforward manner. In particular, PHLST for 3D datasets is promising for efficient approximation, compression, and local feature computation for 3D medical images and 3D geophysical data, which we are currently investigating in collaboration with our graduate student Noel Smith [45].

6.2.5. Other potential applications

Because of its ability to completely localize the analysis of an input image and sparsify its representation equipped with a fast algorithm, there are many potential applications of PHLST. For example, its application to image zooming and interpolation is promising since PHLST does not suffer from the boundary effect/the Gibbs phenomenon, which is often a nuisance in image zooming. Commonly used image zooming/interpolation techniques such as pixel replication, bilinear interpolation, bi-cubic interpolation have all drawbacks, especially with large magnifications. The pixel replication is computationally most efficient, but generates annoying blocky zoomed images. The bilinear interpolation generates superfluous horizontal and vertical artifacts, and this is also true for the bi-cubic interpolation to a lesser extent. One can use DCT for image zooming, but again one may see the artifacts generated by the even reflection at the boundaries. Sinc (or band-limited) interpolation is theoretically ideal but its straightforward implementation does not work well due to the Gibbs phenomenon.

Another important application of PHLST is local feature computation. PHLST allows us to evaluate and compute various attributes (e.g., directional derivatives) at *any point* in the domain Ω_j even if we start from discrete samples. See Eqs. (7)–(10). We are currently investigating the interpolation of image values along a given *curve* as well as directional derivatives along such a curve, which is not easy using the conventional methods.

6.3. Relation to the other works

Retrospectively speaking, our work is related to many previous works done by other scientists. However, we did not find exactly the same strategy as ours in the other works. As early as 1938, Cornelius Lanczos [46] suggested that "denoising" and interpolation of digital signals sampled on an *equispaced* grid over a *finite interval* should be very nicely dealt with by trigonometric polynomials once the edge effect is taken care of. This was only an abstract given at the AMS conference. Somehow, a full version of the paper did not appear until 1952 [47]. He first used the line removal idea [46] corresponding to the 1D LLST in our case, and then proposed to remove a higher order polynomials [47,48]. As far as we know, Lanczos is one of the first scientists who recognized the importance of representing and interpolating data sampled at equispaced grid points using a combination of trigonometric polynomials and algebraic polynomials. He clearly understood that only using algebraic polynomials leads to the infamous Runge phenomenon, and only using trigonometric polynomial leads to the Gibbs phenomenon. Zygmund had a similar idea (i.e., removal of singularities) for different purposes in 1935 or earlier [49, Section 2.13]. See also [2, Section 2.2], [50, Chapter 4], [51, Chapter 2], and [48, Chapter 2]. The book of Kantrovich and V.I. Krylov [52] cites an early attempt of extending a function supported on $[0, 1]$ to $[-1, 1]$ smoothly and periodically (with period 2) by Maliev [53,54]. Smirnov [55] also cites the work of A.N. Krylov for speeding up the decay of Fourier coefficients of a compactly supported function using the line and polynomial removal.

In 1990, Madych and Nelson [56,57] introduced the so-called "polyharmonic cardinal splines," which uses the polyharmonic equations to interpolate the data given on the lattice $\mathbb{Z}^d$ in $\mathbb{R}^d$. Their main concern, however, is the interpolation, and they are not concerned with the residuals at all.

The "polysplines" proposed by Kounchev [58,59] are also related to our PHLST. In his case, though, he used a sequence of decreasing subdomains $\Omega = \Omega_0 \supset \Omega_1 \supset \cdots$ instead of the disjoint subdomains of our case. This led him to develop a new version of multidimensional wavelets. Again, he is not concerned with the residuals.

All of the above scientists except Lanczos only focused on the u component. As far as we know, Lanczos was the only one who seriously considered the residual v, but explored his idea neither for higher dimensions nor for multiscale setting.

Acknowledgments

This research was partially supported by the ONR grant N00014-00-1-0469 and the NSF grant DMS-0410406. We thank Professor Gregory Beylkin, University of Colorado at Boulder for fruitful discussions on the numerical issues of the Laplace equation solvers, Professor Grant Welland, University of Missouri at St. Louis for checking the proof of Theorem A.2, and Professor Raphy Coifman, Yale University for his warm encouragement.

Appendix A. Proof of Theorem 1

First we prove the following auxiliary theorems:

Theorem A.1. *Let $\mathbb{T}$ be a torus (i.e., $[0,1]$), and $f \in C^m(\mathbb{T})$ and periodic. Furthermore, let us assume that $f^{(m+1)}$ exists and in $BV[0,1]$. Then its Fourier coefficient $c_k = \hat{f}(k)$ decays as $O(|k|^{-m-2})$.*

Proof. We use the periodicity of f, i.e., $f^{(\ell)}(0) = f^{(\ell)}(1),\ \ell = 0, 1, \ldots, m$, and integration by parts.

$$\begin{aligned}
\hat{f}(k) &= \int_0^1 f(x)\mathrm{e}^{-2\pi \mathrm{i}kx}\,\mathrm{d}x = \frac{\mathrm{e}^{-2\pi \mathrm{i}kx}}{-2\pi \mathrm{i}k} f(x)\bigg|_0^1 + \frac{1}{2\pi \mathrm{i}k}\int_0^1 f'(x)\mathrm{e}^{-2\pi \mathrm{i}kx}\,\mathrm{d}x \\
&= \frac{\mathrm{e}^{-2\pi \mathrm{i}kx}}{-(2\pi \mathrm{i}k)^2} f'(x)\bigg|_0^1 + \frac{1}{(2\pi \mathrm{i}k)^2}\int_0^1 f''(x)\mathrm{e}^{-2\pi \mathrm{i}kx}\,\mathrm{d}x \\
&= \cdots \\
&= \frac{\mathrm{e}^{-2\pi \mathrm{i}kx}}{-(2\pi \mathrm{i}k)^{m+1}} f^{(m)}(x)\bigg|_0^1 + \frac{1}{(2\pi \mathrm{i}k)^{m+1}}\int_0^1 f^{(m+1)}(x)\mathrm{e}^{-2\pi \mathrm{i}kx}\,\mathrm{d}x \\
&= \frac{1}{(2\pi \mathrm{i}k)^{m+1}}\int_0^1 f^{(m+1)}(x)\mathrm{e}^{-2\pi \mathrm{i}kx}\,\mathrm{d}x.
\end{aligned}$$

By assumption, $f^{(m+1)} \in BV[0,1]$, so we can use the theorem of Taibleson [60] to get:

$$\left|\hat{f}(k)\right| \leqslant \frac{V(f^{(m+1)})}{(2\pi)^{m+1}|k|^{m+2}},$$

where $V(\cdot)$ is the total variation of the argument over $[0,1]$. This implies that $\hat{f}(k) = O(|k|^{-m-2})$. □

Theorem A.2. *Let $\mathbb{T}^d$ be a d-dimensional torus (i.e., $[0,1]^d$), and $f \in C^m(\mathbb{T}^d)$ and periodic. Furthermore, let us assume that $\partial_j^{m+1} f$ exists and in $BV[0,1]$, $j = 1,\ldots,d$. Then its Fourier coefficient $c_{\boldsymbol{k}} = \hat{f}(\boldsymbol{k})$ decays as $O(\|\boldsymbol{k}\|^{-m-2})$.*

Proof. We proceed essentially the same way as Körner [61, p. 409]. We consider each variable x_j in turn. Since f as a function of x_j (with all the other variables fixed) belongs to $C^m(\mathbb{T})$ and $\partial_j^{m+1} f \in BV[0,1]$, we can use Theorem A.1 as:

$$\left| \int_{\mathbb{T}} f(x_1,\ldots,x_j,\ldots,x_d) \mathrm{e}^{-2\pi \mathrm{i} k_j x_j}\,\mathrm{d}x_j \right| \leqslant \frac{C_j}{|k_j|^{m+2}}, \tag{A.1}$$

where $C_j > 0$ is a constant depending on j and k_j is a jth frequency index (nonzero integer). Then,

$$\begin{aligned}
\left|\hat{f}(\boldsymbol{k})\right| &= \left| \int_{\mathbb{T}} \cdots \int_{\mathbb{T}} f(x_1,\ldots,x_d) \mathrm{e}^{-2\pi \mathrm{i} \sum_j k_j x_j}\,\mathrm{d}x_1 \cdots \mathrm{d}x_d \right| \\
&\leqslant \int_{\mathbb{T}} \cdots \int_{\mathbb{T}} \left| \int_{\mathbb{T}} f(x_1,\ldots,x_d) \mathrm{e}^{-2\pi \mathrm{i} k_j x_j}\,\mathrm{d}x_j\, \mathrm{e}^{-2\pi \mathrm{i} \sum_{\ell \neq j} k_\ell x_\ell} \right| \mathrm{d}x_1 \cdots \mathrm{d}x_{j-1}\,\mathrm{d}x_{j+1} \cdots \mathrm{d}x_d \\
&\leqslant \int_{\mathbb{T}} \cdots \int_{\mathbb{T}} \frac{C_j}{|k_j|^{m+2}}\,\mathrm{d}x_1 \cdots \mathrm{d}x_{j-1}\,\mathrm{d}x_{j+1} \cdots \mathrm{d}x_d \\
&= \frac{C_j}{|k_j|^{m+2}}.
\end{aligned}$$

Therefore, we have the following estimate:

$$\left|\hat{f}(\boldsymbol{k})\right| \leqslant \frac{C_j}{|k_j|^{m+2}}, \quad j = 1,\ldots,d,\ k_j \neq 0. \tag{A.2}$$

Thus, if $\boldsymbol{k} \neq 0$, then

$$\begin{aligned}
\left|\hat{f}(\boldsymbol{k})\right| &\leqslant \min_{1\leqslant j\leqslant d} C_j |k_j|^{-m-2} \leqslant \left(\max_{1\leqslant j\leqslant d} C_j\right) \cdot \left(\min_{1\leqslant j\leqslant d} |k_j|^{-m-2}\right) = \left(\max_{1\leqslant j\leqslant d} C_j\right) \cdot \left(\max_{1\leqslant j\leqslant d} |k_j|\right)^{-m-2} \\
&\leqslant \left(\max_{1\leqslant j\leqslant d} C_j\right) \cdot \left(\|\boldsymbol{k}\|/\sqrt{d}\right)^{-m-2} = \frac{C}{\|\boldsymbol{k}\|^{m+2}},
\end{aligned}$$

where $C = \max_{1\leqslant j\leqslant d} C_j \cdot d^{1+m/2} > 0$. This implies the conclusion of the theorem. □

Now, we prove Theorem 1.

Proof. In this proof, for the notational simplicity, we use u, v, Ω instead of u_j, v_j, Ω_j, which will not generate any confusion. Since Ω is a rectangle in $\mathbb{R}^d$, it is easy to convert it to a unit cube $\mathbb{T}^d = [0,1]^d$ by rescaling and translation, which only changes the constants in the following argument. Therefore, we assume that $\Omega = \mathbb{T}^d$ below. Let us now consider the residual $v(\boldsymbol{x})$ over Ω. Let $\boldsymbol{x} = (x_1, \ldots, x_d) \in [0,1]^d$, and $\boldsymbol{\sigma} = (\sigma_1, \ldots, \sigma_d)$ be a d-dimensional vector whose entries consist of only 1 or -1. Now, the odd extension $\tilde{v}(\boldsymbol{x})$ of $v(\boldsymbol{x})$ to the extended cube $\tilde{\Omega} \triangleq [-1,1]^d$ can be defined as follows:

$$\tilde{v}(\sigma_1 \cdot x_1, \ldots, \sigma_d \cdot x_d) \triangleq \left(\prod_{k=1}^{d} \sigma_k \right) \cdot v(x_1, \ldots, x_d), \quad (x_1, \ldots, x_d) \in [0,1]^d.$$

The boundary conditions of $u(\boldsymbol{x})$ are:

$$u|_{\partial\Omega} = f|_{\partial\Omega}, \qquad \left.\frac{\partial^2 u}{\partial \nu^2}\right|_{\partial\Omega} = \left.\frac{\partial^2 f}{\partial \nu^2}\right|_{\partial\Omega}, \qquad \ldots, \qquad \left.\frac{\partial^{2m-2} u}{\partial \nu^{2m-2}}\right|_{\partial\Omega} = \left.\frac{\partial^{2m-2} f}{\partial \nu^{2m-2}}\right|_{\partial\Omega}.$$

Therefore, these imply the following in terms of $\tilde{v}$:

$$\tilde{v}|_{\partial\tilde{\Omega}} = 0, \tag{A.3}$$

$$\partial_j^{2k} \tilde{v}(x_1, \ldots, x_{j-1}, -1, x_{j+1}, \ldots, x_d) = \partial_j^{2k} \tilde{v}(x_1, \ldots, x_{j-1}, 1, x_{j+1}, \ldots, x_d) = 0, \tag{A.4}$$

$$\partial_j^{2k} \tilde{v}(x_1, \ldots, x_{j-1}, 0-, x_{j+1}, \ldots, x_d) = \partial_j^{2k} \tilde{v}(x_1, \ldots, x_{j-1}, 0+, x_{j+1}, \ldots, x_d) = 0, \tag{A.5}$$

$$\partial_j^{2k+1} \tilde{v}(x_1, \ldots, x_{j-1}, -1, x_{j+1}, \ldots, x_d) = \partial_j^{2k+1} \tilde{v}(x_1, \ldots, x_{j-1}, 1, x_{j+1}, \ldots, x_d), \tag{A.6}$$

$$\partial_j^{2k+1} \tilde{v}(x_1, \ldots, x_{j-1}, 0-, x_{j+1}, \ldots, x_d) = \partial_j^{2k+1} \tilde{v}(x_1, \ldots, x_{j-1}, 0+, x_{j+1}, \ldots, x_d), \tag{A.7}$$

where $j = 1, \ldots, d$ and $k = 0, \ldots, m-1$. Note that $k = 0$ in Eq. (A.4) means $\tilde{v}|_{\partial\tilde{\Omega}} = 0$, which is different from (A.3). Equations (A.3)–(A.7) imply that $\tilde{v} \in C^{2m-1}(\tilde{\Omega})$ and *periodic*. Therefore, we can invoke Theorem A.2 with m replaced by $2m-1$ so that we get:

$$\hat{f}(\boldsymbol{k}) = O\left(\|\boldsymbol{k}\|^{-2m-1}\right) \quad \text{for } \boldsymbol{k} \neq \boldsymbol{0}. \qquad \square$$

References

[1] G.H. Hardy, W.W. Rogosinski, Fourier Series, third ed., Cambridge Univ. Press, 1956, republished by Dover Publications, 1999.

[2] A. Zygmund, Trigonometric Series, third ed., Cambridge Mathematical Library/Cambridge Univ. Press, 2003, vols. I and II combined.

[3] M.A. Pinsky, Introduction to Fourier Analysis and Wavelets, Brooks/Cole, 2002.

[4] A. Cohen, I. Daubechies, P. Vial, Wavelets on the interval and fast wavelet transforms, Appl. Comput. Harmon. Anal. 1 (1) (1993) 54–81.

[5] B.K. Alpert, A class of bases in L^2 for the sparse representation of integral operators, SIAM J. Math. Anal. 24 (1) (1993) 246–262.

[6] R.R. Coifman, Y. Meyer, Remarques sur l'analyse de Fourier à fenêtre, C. R. Acad. Sci. Paris, Sér. I 312 (1991) 259–261.

[7] H.S. Malvar, The LOT: Transform coding without blocking effects, IEEE Trans. Acoust. Speech Signal Process. 37 (1989) 553–559.

[8] H.S. Malvar, Lapped transforms for efficient transform/subband coding, IEEE Trans. Acoust. Speech Signal Process. 38 (1990) 969–978.

[9] X. Fang, E. Séré, Adapted multiple folding local trigonometric transforms and wavelet packets, Appl. Comput. Harmon. Anal. 1 (1994) 169–179.

[10] L.F. Villemoes, Adapted bases of time–frequency local cosines, Appl. Comput. Harmon. Anal. 10 (2001) 139–162.
[11] H. Whitney, Analytic extensions of differentiable functions defined in closed sets, Trans. Amer. Math. Soc. 36 (1) (1934) 63–89.
[12] B. Larson, N. Saito, The continuous boundary local Fourier transform, in: A.F. Laine, M.A. Unser, A. Aldroubi (Eds.), Wavelets IX, in: Proc. SPIE, vol. 4478, 2001, pp. 415–426.
[13] B. Larson, The continuous boundary local trigonometric transform, Ph.D. thesis, Department of Mathematics, University of California, Davis, 2002.
[14] M.V. Wickerhauser, Smooth localized orthonormal bases, C. R. Acad. Sci. Paris, Sér. I 316 (1993) 423–427.
[15] M.V. Wickerhauser, Adapted Wavelet Analysis from Theory to Software, A K Peters, Wellesley, MA, 1994, with diskette.
[16] G. Wahba, Spline Models for Observational Data, CBMS-NSF Regional Conference Series in Applied Mathematics, vol. 59, SIAM, Philadelphia, 1990.
[17] Y. Meyer, Oscillating Patterns in Image Processing and Nonlinear Evolution Equations, Univ. Lecture Ser., vol. 22, AMS, Providence, RI, 2001.
[18] S. Jaffard, Y. Meyer, R.D. Ryan, Wavelets: Tools for Science & Technology, SIAM, Philadelphia, 2001.
[19] A. Averbuch, M. Israeli, L. Vozovoi, A fast Poisson solver of arbitrary order accuracy in rectangular regions, SIAM J. Sci. Comput. 19 (3) (1998) 933–952.
[20] E. Braverman, M. Israeli, A. Averbuch, L. Vozovoi, A fast 3D Poisson solver of arbitrary order accuracy, J. Comput. Phys. 144 (1998) 109–136.
[21] W.L. Briggs, V.E. Henson, The DFT: An Owner's Manual for the Discrete Fourier Transform, SIAM, Philadelphia, 1995.
[22] A. Iserles, A First Course in the Numerical Analysis of Differential Equations, Cambridge Texts in Applied Mathematics, Cambridge Univ. Press, New York, 1996.
[23] G. Strang, The discrete cosine transform, SIAM Rev. 41 (1) (1999) 135–147.
[24] R.A. DeVore, Nonlinear approximation, in: Acta Numerica, Cambridge Univ. Press, 1998, pp. 51–150.
[25] I. Daubechies, Orthonormal bases of compactly supported wavelets. II. Variations on a theme, SIAM J. Math. Anal. 24 (2) (1993) 499–519.
[26] I. Daubechies, Ten Lectures on Wavelets, CBMS-NSF Regional Conference Series in Applied Mathematics, vol. 61, SIAM, Philadelphia, 1992.
[27] B. Bénichou, N. Saito, Sparsity vs. statistical independence in adaptive signal representations: A case study of the spike process, in: G.V. Welland (Ed.), Beyond Wavelets, in: Stud. Comput. Math., vol. 10, Academic Press, San Diego, CA, 2003, pp. 225–257, Ch. 9.
[28] N. Saito, The generalized spike process, sparsity, and statistical independence, in: D. Rockmore, J.D. Healy (Eds.), Modern Signal Processing, in: MSRI Publications, vol. 46, Cambridge Univ. Press, 2004, pp. 317–340.
[29] Z. Wang, A.C. Bovik, H.R. Sheikh, E.P. Simoncelli, Image quality assessment: From error measurement to structural similarity, IEEE Trans. Image Process. 13 (4) (2004) 600–613.
[30] W.B. Pennebaker, J.L. Mitchell, JPEG Still Image Data Compression Standard, Van Nostrand Reinhold, New York, 1993.
[31] G.K. Wallace, The JPEG still picture compression standard, IEEE Trans. Consumer Electron. 38 (1) (1992) xviii–xxxiv.
[32] R.R. Coifman, M.V. Wickerhauser, Entropy-based algorithms for best basis selection, IEEE Trans. Inform. Theory 38 (2) (1992) 713–719.
[33] J. Rissanen, Stochastic Complexity in Statistical Inquiry, World Scientific, Singapore, 1989.
[34] M.H. Hansen, B. Yu, Model selection and the principle of minimum description length, J. Amer. Statist. Assoc. 96 (454) (2001) 746–774.
[35] Y.G. Leclerc, Constructing simple stable descriptions for image partitioning, Intern. J. Computer Vision 3 (1989) 73–102.
[36] N. Saito, Simultaneous noise suppression and signal compression using a library of orthonormal bases and the minimum description length criterion, in: E. Foufoula-Georgiou, P. Kumar (Eds.), Wavelets in Geophysics, Academic Press, San Diego, CA, 1994, pp. 299–324, Ch. XI.
[37] S.G. Chang, B. Yu, M. Vetterli, Adaptive wavelet thresholding for image denoising and compression, IEEE Trans. Image Process. 9 (9) (2000) 1532–1546.
[38] M. Hansen, B. Yu, Wavelet thresholding via MDL: Simultaneous denoising and compression, IEEE Trans. Inform. Theory 46 (5) (2000) 1778–1788.
[39] E.Y. Lam, J.W. Goodman, A mathematical analysis of the DCT coefficient distributions for images, IEEE Trans. Image Process. 9 (10) (2000) 1661–1666.
[40] R.A. DeVore, Wavelets and approximation, Presented at the SPIE Conference on Wavelets X, August 2003.

[41] R.A. DeVore, V.N. Temlyakov, Nonlinear approximation by trigonometric sums, J. Fourier Anal. Appl. 2 (1) (1995) 29–48.
[42] F.G. Meyer, R.R. Coifman, Brushlets: A tool for directional image analysis and image compression, Appl. Comput. Harmon. Anal. 4 (1997) 147–187.
[43] G.B. Folland, Introduction to Partial Differential Equations, second ed., Princeton Univ. Press, 1995.
[44] K. Yamatani, N. Saito, Improvement of DCT-based compression algorithms using Poisson's equation, Technical report, Department of Mathematics, University of California, Davis, 2005, in preparation.
[45] N. Smith, The higher dimensional extension of the polyharmonic local trigonometric transforms, Ph.D. thesis, Department of Mathematics, University of California, Davis, 2005, in preparation.
[46] C. Lanczos, A simple interpolation method for the representation of rugged curves, Abstract of contributed paper given at the November Meeting of the AMS in Cleveland, OH, November 25–26, 1938.
[47] C. Lanczos, Smoothing of noisy data by trigonometric truncation, in: National Bureau of Standards Report, No. 1582, 1952, pp. 1–16.
[48] C. Lanczos, Discourse on Fourier Series, Hafner, New York, 1966.
[49] A. Zygmund, Trigonometrical Series, Chelsea, 1952.
[50] C. Lanczos, Applied Analysis, Prentice–Hall, Englewood Cliffs, NJ, 1956, republished by Dover Publications, 1988.
[51] C. Lanczos, Linear Differential Operators, D. Van Nostrand, New York, 1961, republished by Dover Publications, 1997.
[52] L.V. Kantrovich, V.I. Krylov, Approximate Methods of Higher Analysis, Interscience, New York, 1958.
[53] A.S. Maliev, Fourier series of heightened convergence for functions defined in a given interval, Izv. AN SSSR OMEN 10 (1932) 1437–1450.
[54] A.S. Maliev, On the expansion in Fourier series of heightened convergence of functions defined in a given interval, Izv. AN SSSR OMEN 8 (1933) 1113–1120 (in Russian).
[55] V.I. Smirnov, A Course of Higher Mathematics, vol. II, Pergamon Press, New York, 1964, translated by D.E. Brown.
[56] W.R. Madych, S.A. Nelson, Polyharmonic cardinal splines, J. Approx. Theory 60 (2) (1990) 141–156.
[57] W.R. Madych, S.A. Nelson, Polyharmonic cardinal splines: A minimization property, J. Approx. Theory 63 (3) (1990) 303–320.
[58] O.I. Kounchev, Minimizing the Laplacian of a function squared with prescribed values on interior boundaries—Theory of polysplines, Trans. Amer. Math. Soc. 350 (5) (1998) 2105–2128.
[59] O. Kounchev, Multivariate Polysplines: Applications to Numerical and Wavelet Analysis, Academic Press, San Diego, CA, 2001.
[60] M. Taibleson, Fourier coefficients of functions of bounded variation, Proc. Amer. Math. Soc. 18 (4) (1967) 766.
[61] T.W. Körner, Fourier Analysis, Cambridge Univ. Press, 1988.

APPENDIX SHIRANI01

screenshot-catalog.libraries.psu.edu-2023.12.05-15_44_41
https://catalog.libraries.psu.edu/catalog/1181068/marc_view
05.12.2023

MARC View

LEADER 07877nas a22009611a 4500				
001 1181068				
003 SIRSI				
005 20151215050216.0				
008 830531c19839999nyumr 0 0eng d				
010				a| 83643067 z| sn82005410
019				a| MARS
022	0			a| 0733-8716
035				a| LIAS1351817
035				a| (OCoLC)9450566
040				d| UtOrBLW
245	0	0	a|	IEEE journal on selected areas in communications : b| a publication of the IEEE Communications Society.
246	3	9	a|	IEEE journal on selected areas in communications
246	3	0	a|	Selected areas in communications
264		1	a|	New York, N.Y. : b| Institute of Electrical and Electronics Engineers, c| [1983-]
264		4	c|	©1983-
300			a|	volumes : b| illustrations ; c| 28 cm
310			a|	Monthly, b| 2005-
321			a|	Frequency varies, b| 1983-2004
336			a|	text b| txt 2| rdacontent
337			a|	unmediated b| n 2| rdamedia
338			a|	volume b| nc 2| rdacarrier
362	0		a|	Vol. SAC-1, no. 1 (Jan. 1983)- v.SAC-5, no. 9 (1987) ; Vol. 6, no. 1 (Jan. 1988)-
710	2		a|	Institute of Electrical and Electronics Engineers.
710	2		a|	IEEE Communications Society.
533			a|	Microform. b| [New York, N.Y.? c| IEEE], d| 19__? e| microfiches ; 11 x 15 cm.
949			a|	Microfiche w| ASIS c| 1 i| 1181068-1001 d| 3/19/2001 l| MICROS-HB m| HARRISBURG r| Y s| Y t| MICROFORM u| 4/13/2001
949			a|	TK5101.A1I16 v.SAC-1 1983 w| LCPER c| 1 i| 000018892062 d| 3/19/2001 e| 3/19/2001 l| ACAD-BLDG m| UP-ANNEX r| Y s| Y t| PERIODICAL u| 4/13/2001 z| 862
949			a|	TK5101.A1I16 v.SAC-3 no.4-6 1985 w| LCPER c| 1 i| 000045496486 l| ACAD-BLDG m| UP-ANNEX r| Y s| Y t| PERIODICAL u| 2/12/2002 z| 862
949			a|	TK5101.A1I16 v.SAC-2 1984 w| LCPER c| 1 i| 000060038159 l| ACAD-BLDG m| UP-ANNEX r| Y s| Y t| PERIODICAL u| 10/3/2007 z| 862
949			a|	TK5101.A1I16 v.SAC-3 no.1-3 1985 w| LCPER c| 1 i| 000060038166 l| ACAD-BLDG m| UP-ANNEX r| Y s| Y t| PERIODICAL u| 10/3/2007 z| 862
949			a|	TK5101.A1I16 v.SAC-4 no.1-5 1986 w| LCPER c| 1 i| 000060038067 l| ACAD-BLDG m| UP-ANNEX r| Y s| Y t| PERIODICAL u| 10/3/2007 z| 865
949			a|	TK5101.A1I16 v.SAC-4 no.6-9 1986 w| LCPER c| 1 i| 000060038074 l| ACAD-BLDG m| UP-ANNEX r| Y s| Y t| PERIODICAL u| 10/3/2007 z| 865
949			a|	TK5101.A1I16 v.SAC-5 no.1-4 1987 w| LCPER c| 1 i| 000060037954 l| ACAD-BLDG m| UP-ANNEX r| Y s| Y t| PERIODICAL u| 10/3/2007 z| 865
949			a|	TK5101.A1I16 v.SAC-5 no.5-9 1987 w| LCPER c| 1 i| 000060037961 l| ACAD-BLDG m| UP-ANNEX r| Y s| Y t| PERIODICAL u| 10/3/2007 z| 865
949			a|	TK5101.A1I16 v.SAC-6 no.1-5 1988 w| LCPER c| 1 i| 000060037978 l| ACAD-BLDG m| UP-ANNEX r| Y s| Y t| PERIODICAL u| 10/3/2007 z| 865
949			a|	TK5101.A1I16 v.6 no.6-9 1988 w| LCPER c| 1 i| 000060037985 l| ACAD-BLDG m| UP-ANNEX r| Y s| Y t| PERIODICAL u| 10/3/2007 z| 865
949			a|	TK5101.A1I16 v.7 no.1-5 1989 w| LCPER c| 1 i| 000060037893 l| ACAD-BLDG m| UP-ANNEX r| Y s| Y t| PERIODICAL u| 10/3/2007 z| 865
949			a|	TK5101.A1I16 v.7 no.6-9 1989 w| LCPER c| 1 i| 000060037800 l| ACAD-BLDG m| UP-ANNEX r| Y s| Y t| PERIODICAL u| 10/3/2007 z| 865
949			a|	TK5101.A1I16 v.8 Jan-Apr 1990 w| LCPER c| 1 i| 000018894073 l| CATO-2 m| UP-ANNEX r| Y s| Y t| PERIODICAL u| 3/5/2003 z| 7769
949			a|	TK5101.A1I16 v.8 May-Aug 1990 w| LCPER c| 1 i| 000018894080 l| CATO-2 m| UP-ANNEX r| Y s| Y t| PERIODICAL u| 3/5/2003 z| 7769

949 a| TK5101.A1I16 v.8 Sept-Dec 1990 w| LCPER c| 1 i| 000018894097 l| CATO-2 m| UP-ANNEX r| Y s| Y t| PERIODICAL u| 3/5/2003 z| 7769

949 a| TK5101.A1I16 v.9 Jan-Apr 1991 w| LCPER c| 1 i| 000018894103 l| CATO-2 m| UP-ANNEX r| Y s| Y t| PERIODICAL u| 3/5/2003 z| 7769

949 a| TK5101.A1I16 v.9 May-Aug 1991 w| LCPER c| 1 i| 000018894110 l| CATO-2 m| UP-ANNEX r| Y s| Y t| PERIODICAL u| 3/5/2003 z| 7769

949 a| TK5101.A1I16 v.9 Sept-Dec 1991 w| LCPER c| 1 i| 000018894127 l| CATO-2 m| UP-ANNEX r| Y s| Y t| PERIODICAL u| 3/5/2003 z| 7769

949 a| TK5101.A1I16 v.10 Jan-June 1992 w| LCPER c| 1 i| 000018894134 l| CATO-2 m| UP-ANNEX r| Y s| Y t| PERIODICAL u| 3/5/2003 z| 7769

949 a| TK5101.A1I16 v.10 Aug-Dec 1992 w| LCPER c| 1 i| 000018894141 l| CATO-2 m| UP-ANNEX r| Y s| Y t| PERIODICAL u| 3/5/2003 z| 7769

949 a| TK5101.A1I16 v.11 Jan-June 1993 w| LCPER c| 1 i| 000018894158 d| 10/11/2006 l| CATO-2 m| UP-ANNEX q| 1 r| Y s| Y t| PERIODICAL u| 3/5/2003 z| 7769

949 a| TK5101.A1I16 v.11 Aug-Dec 1993 w| LCPER c| 1 i| 000018894165 d| 10/11/2006 l| CATO-2 m| UP-ANNEX q| 1 r| Y s| Y t| PERIODICAL u| 3/5/2003 z| 7769

949 a| TK5101.A1I16 v.12 Jan-May 1994 w| LCPER c| 1 i| 000018894172 l| CATO-2 m| UP-ANNEX r| Y s| Y t| PERIODICAL u| 3/5/2003 z| 7769

949 a| TK5101.A1I16 v.12 June-Dec 1994 w| LCPER c| 1 i| 000018894189 l| CATO-2 m| UP-ANNEX r| Y s| Y t| PERIODICAL u| 3/5/2003 z| 7769

949 a| TK5101.A1I16 v.13 Jan-June 1995 w| LCPER c| 1 i| 000018894196 l| CATO-2 m| UP-ANNEX r| Y s| Y t| PERIODICAL u| 3/5/2003 z| 7769

949 a| TK5101.A1I16 v.13 Aug-Dec 1995 w| LCPER c| 1 i| 000018894202 d| 9/18/2008 l| CATO-2 m| UP-ANNEX q| 1 r| Y s| Y t| PERIODICAL u| 3/5/2003 z| 7769

949 a| TK5101.A1I16 v.14 Jan-June 1996 w| LCPER c| 1 i| 000018894219 l| CATO-2 m| UP-ANNEX r| Y s| Y t| PERIODICAL u| 3/5/2003 z| 7769

949 a| TK5101.A1I16 v.14 July-Dec 1996 w| LCPER c| 1 i| 000018894226 l| CATO-2 m| UP-ANNEX r| Y s| Y t| PERIODICAL u| 3/5/2003 z| 7769

949 a| TK5101.A1I16 v.15 Jan-June 1997 w| LCPER c| 1 i| 000018894233 l| CATO-2 m| UP-ANNEX r| Y s| Y t| PERIODICAL u| 3/5/2003 z| 7769

949 a| TK5101.A1I16 v.15 July-Dec 1997 w| LCPER c| 1 i| 000018894240 l| CATO-2 m| UP-ANNEX r| Y s| Y t| PERIODICAL u| 3/5/2003 z| 7769

949 a| TK5101.A1I16 v.16 Feb-June 1998 w| LCPER c| 1 i| 000018894257 l| CATO-2 m| UP-ANNEX r| Y s| Y t| PERIODICAL u| 3/5/2003 z| 7769

949 a| TK5101.A1I16 v.16 Aug-Dec 1998 w| LCPER c| 1 i| 000018894264 l| CATO-2 m| UP-ANNEX r| Y s| Y t| PERIODICAL u| 3/5/2003 z| 7769

949 a| TK5101.A1I16 v.17 Jan-June 1999 w| LCPER c| 1 i| 000018894271 l| CATO-2 m| UP-ANNEX r| Y s| Y t| PERIODICAL u| 3/5/2003 z| 7769

949 a| TK5101.A1I16 v.17 July-Dec 1999 w| LCPER c| 1 i| 000018894288 l| CATO-2 m| UP-ANNEX r| Y s| Y t| PERIODICAL u| 3/5/2003 z| 7769

949 a| TK5101.A1I16 v.18 Jan-June 2000 w| LCPER c| 1 i| 000018894295 d| 7/11/2003 l| CATO-2 m| UP-ANNEX q| 1 r| Y s| Y t| PERIODICAL u| 3/5/2003 z| 7769

949 a| TK5101.A1I16 v.18 July-Sept.2000 w| LCPER c| 1 i| 000047609952 l| CATO-2 m| UP-ANNEX r| Y s| Y t| PERIODICAL u| 11/1/2001 z| 7769

949 a| TK5101.A1I16 v.18 Oct.-Dec.2000 w| LCPER c| 1 i| 000047609808 l| CATO-2 m| UP-ANNEX r| Y s| Y t| PERIODICAL u| 11/1/2001 z| 7769

949 a| TK5101.A1I16 v.19 Jan-Mar 2001 w| LCPER c| 1 i| 000048255431 l| CATO-2 m| UP-ANNEX r| Y s| Y t| PERIODICAL u| 11/28/2001 z| 7769

949 a| TK5101.A1I16 v.19 Apr-June 2001 w| LCPER c| 1 i| 000048255424 l| CATO-2 m| UP-ANNEX r| Y s| Y t| PERIODICAL u| 11/28/2001 z| 7769

949 a| TK5101.A1I16 v.19 July-Sept 2001 w| LCPER c| 1 i| 000048424660 l| CATO-2 m| UP-ANNEX r| Y s| Y t| PERIODICAL u| 11/4/2002 z| 7769

949 a| TK5101.A1I16 v.20 Jan-June 2002 w| LCPER c| 1 i| 000051870089 d| 7/7/2004 l| CATO-2 m| UP-ANNEX q| 1 r| Y s| Y t| PERIODICAL u| 5/2/2003 z| 7769

949 a| TK5101.A1I16 v.20 Aug-Dec 2002 w| LCPER c| 1 i| 000051870157 l| CATO-2 m| UP-ANNEX r| Y s| Y t| PERIODICAL u| 5/2/2003 z| 7769

949 a| TK5101.A1I16 v.21 Jan-June 2003 w| LCPER c| 1 i| 000052812422 l| CATO-2 m| UP-ANNEX r| Y s| Y t| PERIODICAL u| 3/17/2004 z| 7769

949 a| TK5101.A1I16 v.21 Aug-Dec 2003 w| LCPER c| 1 i| 000052812415 l| CATO-2 m| UP-ANNEX r| Y s| Y t| PERIODICAL u| 3/17/2004 z| 7769

949 a| TK5101.A1I16 v.22 Jan-June 2004 w| LCPER c| 1 i| 000054847187 l| CATO-2 m| UP-ANNEX r| Y s| Y t| PERIODICAL u| 4/8/2005 z| 7769

949 a| TK5101.A1I16 v.22 Aug-Dec 2004 w| LCPER c| 1 i| 000054847194 l| CATO-2 m| UP-ANNEX r| Y s| Y t| PERIODICAL u| 4/7/2005 z| 7769

949 a| TK5101.A1I16 v.23 Jan-Apr 2005 w| LCPER c| 1 i| 000054976375 l| CATO-2 m| UP-ANNEX r| Y s| Y t| PERIODICAL u| 4/18/2006 z| 7769

949 a| TK5101.A1I16 v.23 May-Aug 2005 w| LCPER c| 1 i| 000054976368 l| CATO-2 m| UP-ANNEX r| Y s| Y t| PERIODICAL u| 4/18/2006 z| 7769

949 a| TK5101.A1I16 v.23 Sept-Dec 2005 w| LCPER c| 1 i| 000054976351 l| CATO-2 m| UP-ANNEX r| Y s| Y t| PERIODICAL u| 4/18/2006

			z| 7769
949			a| TK5101.A1I16 v.24 Jan-Apr 2006 w| LCPER c| 1 i| 000055217415 l| CATO-2 m| UP-ANNEX r| Y s| Y t| PERIODICAL u| 6/12/2007 z| 7769
949			a| TK5101.A1I16 v.24 May-Aug 2006 w| LCPER c| 1 i| 000055217293 l| CATO-2 m| UP-ANNEX r| Y s| Y t| PERIODICAL u| 6/12/2007 z| 7769
949			a| TK5101.A1I16 v.24 Sept-Dec 2006 w| LCPER c| 1 i| 000055217422 l| CATO-2 m| UP-ANNEX r| Y s| Y t| PERIODICAL u| 6/12/2007 z| 7769
852	0	1	a| PSt b| UP-ANNEX c| ANNEX h| TK5101.A1 i| I16
866		0 8	0 a| v.SAC-1(1983)-v.SAC-6:no.5(1988), v.6:no.6(1988)-v.15(1997), v.16:Feb.(1998)-v.24(2006)
852	8		a| PSt b| HARRISBURG c| MICROS-HB h| Microfiche
866		0 8	0 a| v.1 1983-v.17 1999

PennState

Copyright @2019 The Pennsylvania State University. All rights reserved. Except where otherwise noted, this work is subject to a Creative Commons Attribution 4.0 license. Details and exceptions.

Legal Statements | PSU Hotlines

PENN STATE UNIVERSITY LIBRARIES

Libraries Home (814) 865-6368
Libraries Intranet (Staff Only)
Accessibility Help
Website Feedback
Policies and Guidelines
Staff Directory

screenshot-catalog.libraries.psu.edu-2023.12.05-15_43_54
https://catalog.libraries.psu.edu/catalog/1181068
05.12.2023

IEEE journal on selected areas in communications : a publication of the IEEE Communications Society

Additional Titles:	IEEE journal on selected areas in communications and Selected areas in communications
Published:	New York, N.Y. : Institute of Electrical and Electronics Engineers, [1983-]
Copyright Date:	©1983-
Physical Description:	volumes : illustrations ; 28 cm
Additional Creators:	Institute of Electrical and Electronics Engineers and IEEE Communications Society

Availability

Browse Nearby on Shelf I Want It

Penn State Harrisburg (1 item)

Call number	Material	Location
Harrisburg - Microforms - 2nd Floor - In-Library Use: Holdings Summary v.1 1983-v.17 1999		
Microfiche	Microfilm, Microfiche, etc.	Harrisburg - Microforms - 2nd Floor - In-Library Use

Library Storage (52 items)

Call number	Material	Location
Annexed Material: Holdings Summary v.SAC-1(1983)-v.SAC-6:no.5(1988), v.6:no.6(1988)-v.15(1997), v.16:Feb.(1998)-v.24(2006)		
TK5101.A1I16 v.6 no.6-9 1988	Bound Journal	Annexed Material
TK5101.A1I16 v.7 no.1-5 1989	Bound Journal	Annexed Material
TK5101.A1I16 v.7 no.6-9 1989	Bound Journal	Annexed Material
TK5101.A1I16 v.8 Jan-Apr 1990	Bound Journal	Annexed Material
TK5101.A1I16 v.8 May-Aug 1990	Bound Journal	Annexed Material
TK5101.A1I16 v.8 Sept-Dec 1990	Bound Journal	Annexed Material
TK5101.A1I16 v.9 Jan-Apr 1991	Bound Journal	Annexed Material
TK5101.A1I16 v.9 May-Aug 1991	Bound Journal	Annexed Material
TK5101.A1I16 v.9 Sept-Dec 1991	Bound Journal	Annexed Material
TK5101.A1I16 v.10 Aug-Dec 1992	Bound Journal	Annexed Material
TK5101.A1I16 v.10 Jan-June 1992	Bound Journal	Annexed Material
TK5101.A1I16 v.11 Aug-Dec 1993	Bound Journal	Annexed Material
TK5101.A1I16 v.11 Jan-June 1993	Bound Journal	Annexed Material
TK5101.A1I16 v.12 Jan-May 1994	Bound Journal	Annexed Material
TK5101.A1I16 v.12 June-Dec 1994	Bound Journal	Annexed Material
TK5101.A1I16 v.13 Aug-Dec 1995	Bound Journal	Annexed Material
TK5101.A1I16 v.13 Jan-June 1995	Bound Journal	Annexed Material
TK5101.A1I16 v.14 Jan-June 1996	Bound Journal	Annexed Material
TK5101.A1I16 v.14 July-Dec 1996	Bound Journal	Annexed Material
TK5101.A1I16 v.15 Jan-June 1997	Bound Journal	Annexed Material
TK5101.A1I16 v.15 July-Dec 1997	Bound Journal	Annexed Material

TK5101.A1I16 v.16 Aug-Dec 1998	Bound Journal	Annexed Material
TK5101.A1I16 v.16 Feb-June 1998	Bound Journal	Annexed Material
TK5101.A1I16 v.17 Jan-June 1999	Bound Journal	Annexed Material
TK5101.A1I16 v.17 July-Dec 1999	Bound Journal	Annexed Material
TK5101.A1I16 v.18 Jan-June 2000	Bound Journal	Checked out
TK5101.A1I16 v.18 July-Sept.2000	Bound Journal	Annexed Material
TK5101.A1I16 v.18 Oct.-Dec.2000	Bound Journal	Annexed Material
TK5101.A1I16 v.19 Apr-June 2001	Bound Journal	Annexed Material
TK5101.A1I16 v.19 Jan-Mar 2001	Bound Journal	Annexed Material
TK5101.A1I16 v.19 July-Sept 2001	Bound Journal	Annexed Material
TK5101.A1I16 v.20 Aug-Dec 2002	Bound Journal	Annexed Material
TK5101.A1I16 v.20 Jan-June 2002	Bound Journal	Annexed Material
TK5101.A1I16 v.21 Aug-Dec 2003	Bound Journal	Annexed Material
TK5101.A1I16 v.21 Jan-June 2003	Bound Journal	Annexed Material
TK5101.A1I16 v.22 Aug-Dec 2004	Bound Journal	Annexed Material
TK5101.A1I16 v.22 Jan-June 2004	Bound Journal	Annexed Material
TK5101.A1I16 v.23 Jan-Apr 2005	Bound Journal	Annexed Material
TK5101.A1I16 v.23 May-Aug 2005	Bound Journal	Annexed Material
TK5101.A1I16 v.23 Sept-Dec 2005	Bound Journal	Annexed Material
TK5101.A1I16 v.24 Jan-Apr 2006	Bound Journal	Annexed Material
TK5101.A1I16 v.24 May-Aug 2006	Bound Journal	Annexed Material
TK5101.A1I16 v.24 Sept-Dec 2006	Bound Journal	Annexed Material
TK5101.A1I16 v.SAC-1 1983	Bound Journal	Annexed Material
TK5101.A1I16 v.SAC-2 1984	Bound Journal	Annexed Material
TK5101.A1I16 v.SAC-3 no.1-3 1985	Bound Journal	Annexed Material
TK5101.A1I16 v.SAC-3 no.4-6 1985	Bound Journal	Annexed Material
TK5101.A1I16 v.SAC-4 no.1-5 1986	Bound Journal	Annexed Material
TK5101.A1I16 v.SAC-4 no.6-9 1986	Bound Journal	Annexed Material
TK5101.A1I16 v.SAC-5 no.1-4 1987	Bound Journal	Annexed Material
TK5101.A1I16 v.SAC-5 no.5-9 1987	Bound Journal	Annexed Material
TK5101.A1I16 v.SAC-6 no.1-5 1988	Bound Journal	Annexed Material

Dates of Publication and/or Sequential Designation:
Vol. SAC-1, no. 1 (Jan. 1983)- v.SAC-5, no. 9 (1987) ; Vol. 6, no. 1 (Jan. 1988)-

ISSN:
0733-8716

Publication Frequency:
Monthly, 2005-
Frequency varies, 1983-2004

Reproduction Note:
Microform. [New York, N.Y.? IEEE], 19__? microfiches ; 11 x 15 cm.

View MARC record | catkey: 1181068

PennState

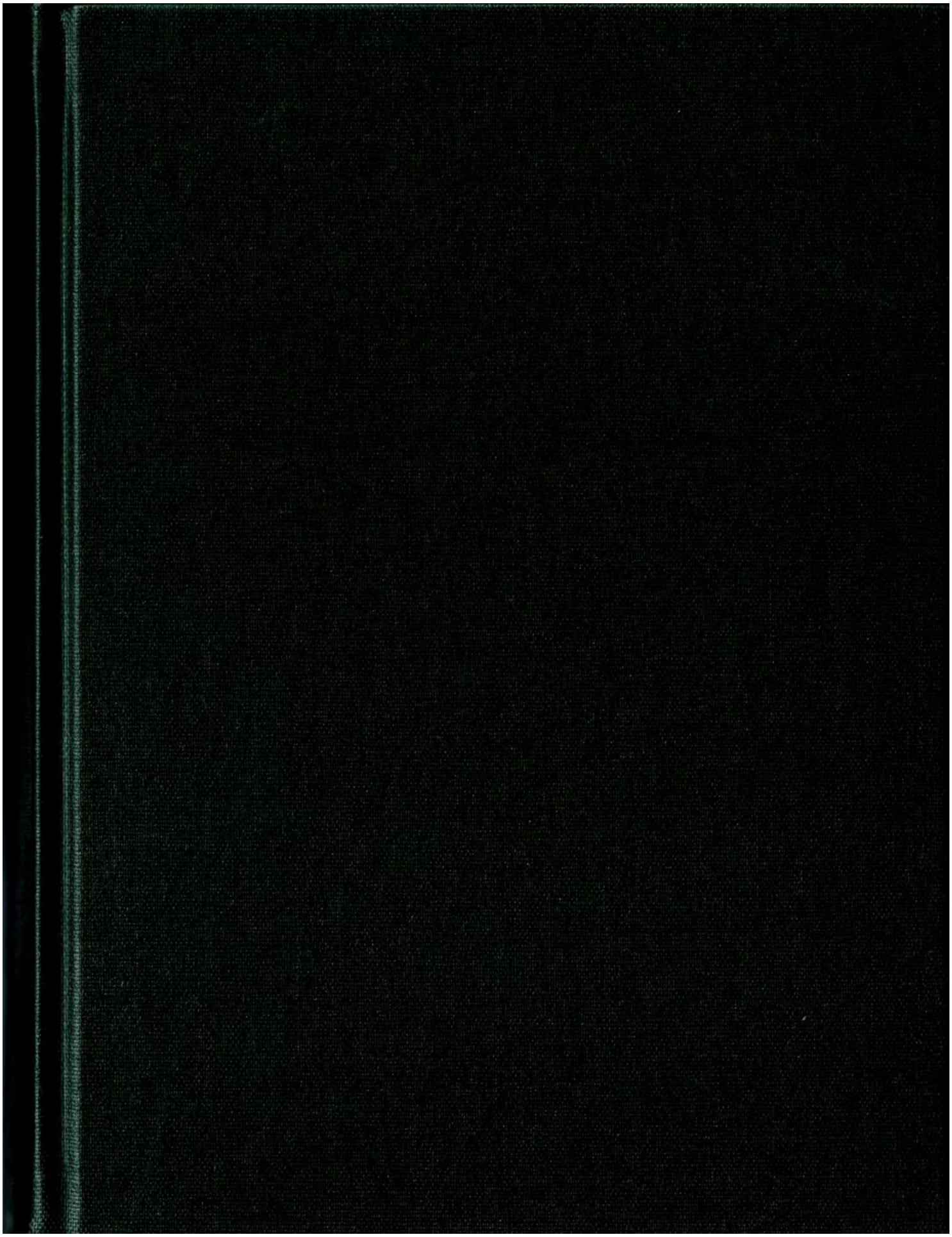
Copyright @2019 The Pennsylvania State University. All rights reserved. Except where otherwise noted, this work is subject to a Creative Commons Attribution 4.0 license. Details and exceptions.

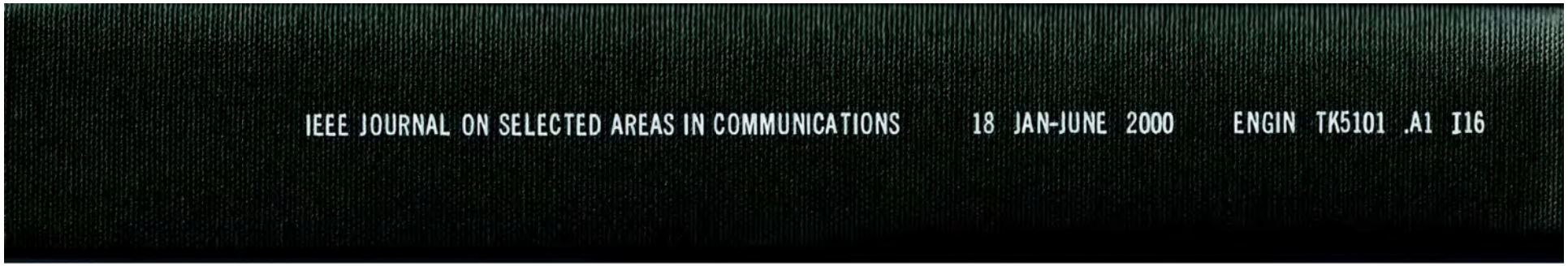
Legal Statements | PSU Hotlines

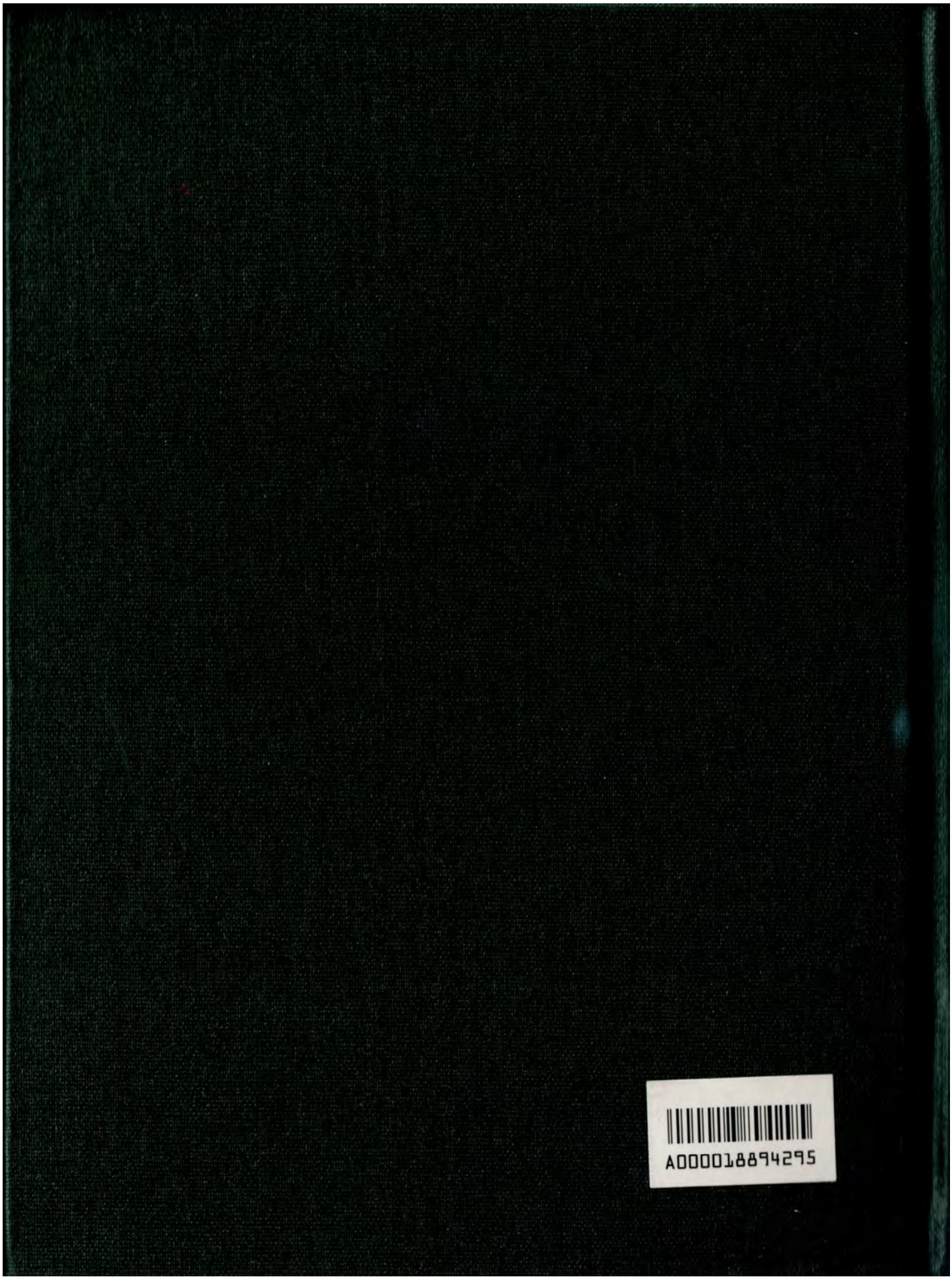
PENN STATE UNIVERSITY LIBRARIES

Libraries Home (814) 865-6368
Libraries Intranet (Staff Only)
Accessibility Help
Website Feedback
Policies and Guidelines
Staff Directory

APPENDIX SHIRANI02




IEEE JOURNAL ON SELECTED AREAS IN COMMUNICATIONS 18 JAN-JUNE 2000 ENGIN TK5101 .A1 I16
126


A000018894295

ENGINEERING LIBRARY

SHELVED IN
BOUND
PERIODICAL
COLLECTION

Engin

IEEE JOURNAL ON

SELECTED AREAS IN COMMUNICATIONS

A PUBLICATION OF THE IEEE COMMUNICATIONS SOCIETY



RECEIVED JUN 10 2000 PENNSYLVANIA STATE UNIVERSITY LIBRARIES

JUNE 2000 VOLUME 18 NUMBER 6 ISACEM (ISSN 0733–8716)

ERROR-RESILIENT IMAGE AND VIDEO TRANSMISSION

Guest Editors—C. W. Chen, P. Cosman, N. Kingsbury, J. Liang, and J. W. Modestino

Guest Editorial ..... *C. W. Chen, P. Cosman, N. Kingsbury, J. Liang, and J. W. Modestino* 809

PAPERS

Unequal Error Protection of SPIHT Encoded Image Bit Streams ..... *A. A. Alatan, M. Zhao, and A. N. Akansu* 814
Unequal Loss Protection: Graceful Degradation of Image Quality over Packet Erasure Channels Through Forward Error Correction ..... *A. E. Mohr, E. A. Riskin, and R. E. Ladner* 819
A Vector Set Partitioning Noisy Channel Image Coder with Unequal Error Protection ..... *D. Mukherjee and S. K. Mitra* 829
Power Minimization for Delivering Integrated Multimedia Services over Digital Subscriber Line ..... *H. Zheng and K. J. R. Liu* 841
Progressive Transmission of Images over Memoryless Noisy Channels ..... *V. Chande and N. Farvardin* 850
Arithmetic Coding-Based Continuous Error Detection for Efficient ARQ-Based Image Transmission ..... *J. Chou and K. Ramchandran* 861
Turbo Codes for Image Transmission—A Joint Channel and Source Decoding Approach ..... *Z. Peng, Y.-F. Huang, and D. J. Costello, Jr.* 868
Combined Source-Channel Coding Schemes for Video Transmission over an Additive White Gaussian Noise Channel ..... *M. Bystrom and J. W. Modestino* 880
A Wavelet Domain Diversity Method for Transmission of Images over Wireless Channels ..... *L. C. Ramac and P. K. Varshney* 891
Error-Resilient Coding in JPEG-2000 and MPEG-4 ..... *I. Moccagatta, S. Soudagar, J. Liang, and H. Chen* 899
Permuted Smoothed Descriptions and Refinement Coding for Images ..... *J. Ridge, F. W. Ware, and J. D. Gibson* 915
Robust Image Transmission Using Resynchronizing Variable-Length Codes and Error Concealment ..... *S. S. Hemami* 927
Image Coding with Robust Channel-Optimized Trellis-Coded Quantization ..... *T.-T. Lam, G. P. Abousleman, and L. J. Karam* 940

(Contents Continued on Back Cover)

(Contents Continued from Front Cover)

Optimal Mode Selection and Synchronization for Robust Video Communications over Error-Prone Networks ..... *G. Côté, S. Shirani, and F. Kossentini* 952
Video Coding with Optimal Inter/Intra-Mode Switching for Packet Loss Resilience ..... *R. Zhang, S. L. Regunathan, and K. Rose* 966
An End-to-End Approach for Optimal Mode Selection in Internet Video Communication: Theory and Application ..... *D. Wu, Y. T. Hou, B. Li, W. Zhu, Y.-Q. Zhang, and H. J. Chao* 977
Efficient Video Transmission over Correlated Nakagami Fading Channels for IS-95 CDMA Systems ..... *N. H. L. Chan and P. T. Mathiopoulos* 996
Analysis of Video Transmission over Lossy Channels ..... *K. Stuhlmüller, N. Färber, M. Link, and B. Girod* 1012
Error Recovery for Interactive Video Transmission over the Internet ..... *I. Rhee and S. R. Joshi* 1033
Error-Resilient Video Transmission Using Long-Term Memory Motion-Compensated Prediction ..... *T. Wiegand, N. Färber, K. Stuhlmüller, and B. Girod* 1050
Error-Resilient Transcoding for Video over Wireless Channels ..... *G. de los Reyes, A. R. Reibman, S.-F. Chang, and J. C.-I. Chuang* 1063
Loss-Resilient ATM Protocol Architecture for MPEG-2 Video Communications ..... *P. Cuenca, L. Orozco-Barbosa, F. J. Quiles, and A. Garrido* 1075
MPEG-4 Image Transmission Using MAP Source-Controlled Channel Decoding ..... *R. E. Van Dyck* 1087
Zerotree Pattern Coding of Motion Picture Residues for Error-Resilient Transmission of Video Sequences ..... *J. A. Robinson and Y. Shu* 1099
DCT Information Recovery of Erroneous Image Blocks by a Neural Predictor ..... *F. G. B. De Natale, C. Perra, and G. Vernazza* 1111
A Concealment Method for Video Communications in an Error-Prone Environment ..... *S. Shirani, F. Kossentini, and R. Ward* 1122
Error Concealment in MPEG Video Streams over ATM Networks ..... *P. Salama, N. B. Shroff, and E. J. Delp* 1129

Upcoming Issues of the IEEE JOURNAL ON SELECTED AREAS IN COMMUNICATIONS

Topic	Date of Call*
Analysis and Synthesis of MAC Protocols	March 1999
Wideband CDMA	April 1999
Protocols and Architectures for Next Generation Optical WDM Networks	April 1999
Quality of Service (QoS) in the Internet	June 1999
Signal Processing for High Density Storage Channels	September 1999
Active and Programmable Networks	November 1999
The Turbo Principle: From Theory to Practice	December 1999
IEEE J-SAC: Wireless Communications Series	Ongoing

*Issue of J-SAC in which the Call for Papers first appears.

A Concealment Method for Video Communications in an Error-Prone Environment

Shahram Shirani, *Member, IEEE*, Faouzi Kossentini, *Senior Member, IEEE*, and Rabab Ward, *Fellow, IEEE*

***Abstract*—In this paper, we propose a two-stage error-concealment method for block-based compressed video which was transmitted in an error-prone environment. In the first stage, we obtain initial estimates of the missing blocks. If the motion vectors associated with the missing blocks are available, motion compensation is used to provide good estimates. Otherwise, a novel algorithm which preserves image continuity is used to estimate the blocks. In the second stage, a maximum *a posteriori* (MAP) estimator, which employs an adaptive Markov random field (MRF) as the image *a priori* model, is used to improve the video reconstruction quality. The adaptive model enables the estimation to incorporate information embedded not only in the immediate neighborhood pixels but also in a wider neighborhood into the reconstruction procedure without increasing the order of the MRF model. The proposed concealment method achieves very good computation–performance tradeoffs, as demonstrated via experimental results.**

***Index Terms*—Error concealment, image reconstruction, Markov random fields.**

I. Introduction

DIGITAL image and video signals require very high bit rates, thus, compression of such signals before their transmission is necessary. Communication channels are not error free and, consequently, the encoded bit streams are vulnerable to transmission errors—usually causing loss of blocks of data and/or loss of synchronization. Despite the various methods that have been proposed to combat or localize the effects of channel errors, the quality of a decoded video sequence may degrade significantly because of the residual errors. Error concealment intends to conceal the effects of such errors by exploiting redundancies in the video signal and limitations of the human visual system, without requiring additional information.

Temporal concealment methods are usually used for error concealment in inter-coded frames. Data of an inter-coded block are composed of the motion vector and the DCT coefficients of the prediction error. If the motion vectors are received without errors, the missing blocks are set to their corresponding motion compensated blocks. Since in many of the video compression algorithms (e.g., H.263) the coded motion vectors and the DCT coefficients are interleaved, the loss of data of a block usually results in the loss of both the motion vectors and the DCT coefficients.[1] Therefore, most of the proposed temporal concealment methods first estimate the motion vector associated with a missing block using the motion vectors of adjacent blocks [1], [2]. The estimated motion vector is then used to find a block in the previous frame which yields the restoration of the missing block. One problem associated with these methods is that if the adjacent blocks are coded in a nonpredictive way (e.g., intra-coded), there would not be any data available to estimate the missing motion vectors. Thus, ad hoc assumptions for estimating the missing motion vector should be made, and the results may be unreliable. Moreover, if the missing block lies on the boundary of two objects moving in opposite directions, such methods will perform quite poorly.

Spatial error-concealment methods restore the missing blocks using the information in the current frame. In [3], to restore the missing data, a measure of variations (e.g., gradient or Laplacian) between adjacent pixels is minimized. The underlying smoothness assumption of this method limits its ability in restoring image details. In [4], each pixel in a damaged block is interpolated from the corresponding pixels in its four neighboring blocks such that the total squared border error is minimized. In [5] and [6], the missing information is interpolated utilizing spatially correlated edge information from a large local neighborhood. Note that although these edge-based methods are generally more accurate than other approaches, they are computationally more intensive. In [7], a computationally simple, spatial directional interpolation scheme has been proposed. The two nearest surrounding layers of pixels of a missing block are converted into a binary pattern to reveal the local geometrical structure. Then, the missing pixels are interpolated in a way to preserve the local geometrical structures. In the statistical error concealment methods, for example the one proposed in [8], it is assumed that the pixel values in an image or video signal are realizations of an underlying statistical model (e.g., MRF model). The statistical approaches of spatial error concealment are expected to outperform the deterministic ones, as they provide a systematic way for incorporating the *a priori* information about the video signal in the restoration procedure.

Previous spatial error-concealment methods employing the MRF model usually yield blurry images with a significant loss of detail in the high frequency or edge portions of the image. This is due to 1) the type of the MRF selected as the image model, and 2) the fact that the amount of information that is

Manuscript received May 4, 1999; revised November 30, 1999. This work was supported by MDSI, BC ASI, and NSERC.

The authors are with the Department of Electrical and Computer Engineering, University of British Columbia, Vancouver, BC, V6T 1Z4, Canada.

Publisher Item Identifier S 0733-8716(00)04337-7.

[1]Recognizing the need to improve the concealment capabilities, in the new generation of video compression standards (e.g., MPEG 4, H.263++), the motion information is separated from other information through partitioning of the coded data.

0733–8716/00$10.00 © 2000 IEEE

used in the reconstruction process is often restricted to a single-pixel wide region around the erroneous area. Incorporating more pixels in order to enhance restoration of edges and high-frequency parts would usually require a higher order MRF model. However, this is computationally expensive, as the complexity grows exponentially with the order of the MRF model.

In this paper, we propose a two-stage error-concealment method for compressed video. In the first stage, if applicable, we use the information in the previous frame to obtain initial estimates of the missing blocks. If the motion vectors of the missing blocks are available, motion compensation is used to provide the estimates. Otherwise, an algorithm which preserves image continuity is employed to compute the initial estimates. In the second stage, a MAP estimator is used for refinement of the initial estimates. The MAP estimator employs an adaptive MRF as the image *a priori* model. The proposed adaptive MRF takes into account the local image characteristics embedded not only in the immediate neighborhood pixels of the damaged area but also in a wider neighborhood without a dramatic increase in computational complexity. Our concealment method improves on the existing statistical methods in that it yields good reconstruction performance regardless of the content of the missing blocks.

To make the compressed data more error resilient, most of the standard-compliant video compression systems partitioned a video frame into Groups of Blocks (GOB's) or "slices," which are coded independently. Therefore, the output bit stream usually consists of segments separated with markers, where each segment corresponds to the coded data of the blocks in a GOB or a slice. When channel errors occur, the decoder usually discards the erroneous data between two markers surrounding the erroneous data, effectively discarding the GOB or the slice. Then, loss of data of a slice does not affect the rest of the compressed video sequence. In our work, it is assumed that the frames of the coded video sequence are partitioned into GOB's or slices and, thus, the missing data belong to blocks of a GOB or a slice. Moreover, it is assumed that the decoder knows the locations of the missing blocks. This information (e.g., the checksum information) can be obtained from the network or it can be inferred, for example, by detecting the semantic or syntactic violations as a result of errors [9].

The rest of this paper is organized as follows. In Section II, MAP estimation of missing data is briefly reviewed. Section III presents the proposed error concealment method. Section IV discusses the computational complexity of the proposed method. Sections V and VI present our experimental results and conclusions, respectively.

II. MAP Estimation of Missing Data

Let the corrupted image be represented by the vector $\boldsymbol{Y}$, while the decompressed image without errors can be represented by $\boldsymbol{X}$. Using MAP estimation, the decompressed image estimate is given by

$$\hat{\boldsymbol{X}} = \arg\max_{\boldsymbol{X}} \log \Pr(\boldsymbol{X} \mid \boldsymbol{Y}).$$

Using the Bayes' rule we, obtain

$$\begin{aligned}\hat{\boldsymbol{X}} &= \arg\max_{\boldsymbol{X}} \left\{ \log \frac{\Pr(\boldsymbol{Y} \mid \boldsymbol{X}) \Pr(\boldsymbol{X})}{\Pr(\boldsymbol{Y})} \right\} \\ &= \arg\max_{\boldsymbol{X}} \{\log \Pr(\boldsymbol{Y} \mid \boldsymbol{X}) + \log \Pr(\boldsymbol{X})\} \end{aligned} \tag{1}$$

where the term $\log \Pr(\boldsymbol{Y})$ has been dropped because it is independent of $\boldsymbol{X}$. The corrupted image can be expressed as $\boldsymbol{Y} = \mathcal{T}\boldsymbol{X}$, where $\mathcal{T}$ is the transform that converts the decompressed image $\boldsymbol{X}$ into the corrupted one $\boldsymbol{Y}$.[2] The conditional probability of the corrupted image can be then written as follows:

$$\Pr(\boldsymbol{Y} \mid \boldsymbol{X}) = \begin{cases} 1: & \boldsymbol{Y} = \mathcal{T}\boldsymbol{x} \\ 0: & \boldsymbol{Y} \neq \mathcal{T}\boldsymbol{x}. \end{cases} \tag{2}$$

Substituting (2) in (1), the MAP estimation becomes

$$\hat{\boldsymbol{X}} = \arg\min_{\boldsymbol{X} \in \mathcal{S}} \{-\log \Pr(\boldsymbol{X})\} \tag{3}$$

where $\mathcal{S} = \{\boldsymbol{z}: \boldsymbol{Y} = \mathcal{T}\boldsymbol{z}\}$.

For image *a priori* model $(\Pr(\boldsymbol{X}))$, we use the MRF. According to the Hammersley–Clifford theorem, every MRF should have a Gibbs distribution [10] in the following form:

$$\Pr(\boldsymbol{X} = x) = \frac{1}{Z} \exp\left\{ -\sum_{c \in C} V_c(x) \right\} \tag{4}$$

where Z is a normalizing constant, $V_c(\cdot)$ is called a potential function and is a function of a local group of pixels c called clique, and C denotes the set of all cliques throughout the image. The potential function characterizes the relationship between a group of pixels by assigning larger costs to configurations of pixels which are less likely to occur. The choice of the potential function impacts substantially the performance of the image model. The function $\sum_{c \in C} V_c(x)$ should be convex in order to have an easily obtainable global minimum. Otherwise, local minima will be present, and the function must then be minimized via a computationally expensive technique such as simulated annealing. Commonly, the potential functions are selected to be of the form

$$\sum_{c \in C} V_c(x) = \sum_{c \in C} \rho\left(\boldsymbol{d}_{\boldsymbol{c}}^{\boldsymbol{t}} \boldsymbol{x}\right) \tag{5}$$

where $\boldsymbol{d}_{\boldsymbol{c}}$ is a coefficient vector, $\boldsymbol{x}$ is the vector of pixels in the clique c, and $\rho(\cdot)$ is the cost function. The convexity property of the cost function insures that the $\sum_{c \in C} V_c(x)$ remains convex. The coefficients $\boldsymbol{d}_{\boldsymbol{c}}$ are usually selected such that $\boldsymbol{d}_{\boldsymbol{c}}^{\boldsymbol{t}} \boldsymbol{x}$ provides an approximation of the first or second derivative of the image at each pixel. For the special case of $\rho(x) = x^2$, the model is called a Gauss–Markov random field (GMRF).

III. Proposed Method

As mentioned earlier, our method consists of two stages. The purpose of the first stage of our method is to obtain an initial estimate of the missing block using information from the previous frame. If the missing block has been intra-coded, the initial estimate is set to zero. If the missing block has been inter-coded, and its motion vector is received correctly (e.g., because the encoded

[2]See [8] for a more detailed discussion of the transform.

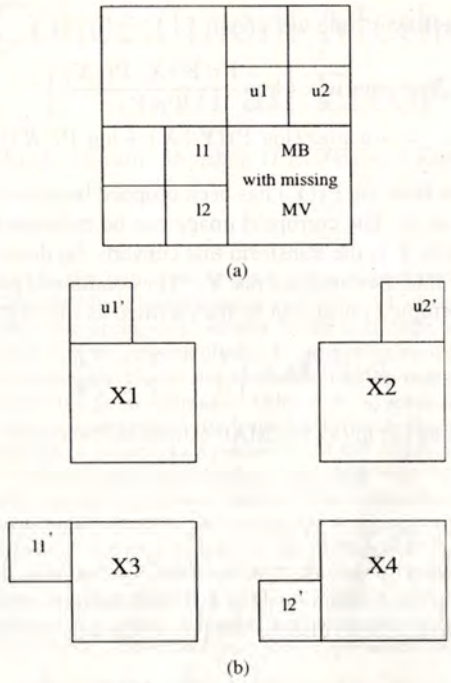


Fig. 1. (a) The four subblocks, (b) their corresponding subblocks in the previous frame, and the blocks connected to them.

data have been partitioned), then the estimate is set to the corresponding motion compensation block. When the motion vector is not available, we find an estimate of the missing block such that image continuity inside the block and across its boundaries is preserved [11]. To do this, subblocks adjacent to the missing block, i.e., $u1, u2, l1$, and $l2$ in Fig. 1(a), are considered. First, for each of these subblocks, a corresponding subblock in the previous frame is determined. The corresponding subblock is found by searching a small area around the point corresponding to the center of each of the subblocks $u1, u2, l1, l2$ in the previous frame. The sum of absolute differences is used as the measure of similarity. The four subblocks $u1, u2, l1, l2$ and their corresponding subblocks $u1', u2', l1', l2'$ in the previous frame are shown in Fig. 1(a) and (b). For example, $u1'$ is the subblock corresponding to $u1$. Then, four blocks, namely $\boldsymbol{X1}, \boldsymbol{X2}, \boldsymbol{X3}$, and $\boldsymbol{X4}$, which are connected to $u1', u2', l1'$, and $l2'$ (respectively), are determined. To obtain an initial estimate of the missing block that smoothly connects to the rest of the image, a block from the above four blocks that minimizes the squared sums of border errors, between the estimated block and its adjacent above and left blocks, is selected. Thus,

$$\hat{\boldsymbol{X}} = \arg \min_{\boldsymbol{X1},\boldsymbol{X2},\boldsymbol{X3},\boldsymbol{X4}} \epsilon^2$$

where

$$\epsilon^2 = \epsilon_T^2 + \epsilon_L^2. \tag{6}$$

Each of the border errors ϵ_T and ϵ_L is defined in terms of pixels by

$$\epsilon_T^2 = \|(\hat{\boldsymbol{x}}_t - \boldsymbol{p}_{\mathrm{Tb}})\|^2 \quad \text{and} \quad \epsilon_L^2 = \|(\hat{\boldsymbol{x}}_l - \boldsymbol{p}_{\mathrm{Lr}})\|^2$$

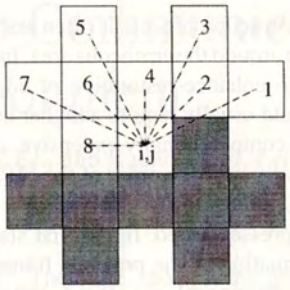


Fig. 2. A pixel, its clique c, and the eight directions. The complement of the clique c' is the dark area.

where the vector $\boldsymbol{p}_{\mathrm{Tb}}$ consists of the bottom line pixels of the block to the top of the missing block, and $\boldsymbol{p}_{\mathrm{Lr}}$ consists of the right column pixels of the block to the left of missing block. The vectors $\hat{\boldsymbol{x}}_t$ and $\hat{\boldsymbol{x}}_l$ are those elements of the estimated block $\hat{\boldsymbol{X}}$ that correspond to the pixels in its top row and left column, respectively. To ensure the online applicability (e.g., concealment while decoding the blocks in raster scan), only subblocks to the left and above the missing block are used. If the condition of online concealment is relaxed, the same method can be extended to include the subblocks of the blocks to the right and below of the missing block.

The estimation of motion of the subblocks has a high computational overhead which can possibly introduce unacceptable requirements on decoder. The computational overhead can be reduced if the search for displacement of each of the subblocks is restricted to a set of candidate motion vectors. This is a decoder option and can be used to trade performance against computational complexity. The set consists of the motion vector of the block corresponding to the missing block in the previous frame, the motion vectors of available neighboring blocks, the median of the motion vectors of available neighboring blocks, the average of the motion vectors of available neighboring blocks, and the zero motion vector [2].

In the second stage of our proposed error-concealment method, the information around each missing block is used to refine the initial estimate. This stage is based on a MAP estimator. We consider a GMRF model with an eight-pixel clique around each pixel as the image *a priori* model (see Fig. 2). The reason for selecting an eight-pixel clique in the manner shown in Fig. 2 will become clear later. The potential function of (5) is selected as

$$\sum_{c \in C} V_c(x) = \sum_i \sum_j \sum_{(k,l) \in c} w_{i,j \to k,l}\, \rho(x_{i,j} - x_{k,l}) \tag{7}$$

where c is the clique, $w_{i,j \to k,l}$ is the weight assigned to the difference between the values of the pixel in position (i, j) and the pixel in its clique at position (k, l) and $\rho(x) = x^2$.

Combining the MAP estimator of (3) with the image model [(4) and (7)], the restoration of missing data eventuates in the following minimization problem:

$$\hat{\boldsymbol{X}} = \min_{x_{i,j}} \sum_{i,j \in \mathcal{M}} \sum_{k,l \in c} w_{i,j \to k,l}\, \rho(x_{i,j} - x_{k,l}) \tag{8}$$

where $\mathcal{M}$ is the set of all missing pixels in the frame. Since $\rho(x) = x^2$ is a convex function, the above minimization problem yields a unique global solution. In fact, the estimated value of a pixel is given by

$$\hat{x}_{i,j} = \sum_{(k,l)\in c\cup c'} w_{i,j\to k,l} \quad x_{k,l} \Big/ \sum_{(k,l)\in c\cup c'} w_{i,j\to k,l} \qquad (9)$$

where c is the clique and c' is its complement shown in Fig. 2.

In our adaptive MRF model, the weight corresponding to the difference between a pixel and one of the pixels in its clique [$w_{i,j\to k,l}$ in (9)] is selected adaptively, based on the likelihood of an edge in the direction of the subject pair of pixels. The rationale behind this selection is to weigh more the difference between the pixels in that direction which will cause the values of the pixels in that direction to get closer to each other. The likelihood of edges in each of the eight directions is computed using blocks around the missing block. In this way, the available information in a larger area is exploited without increasing the order of the MRF model (which increases dramatically the computational complexity). To determine the likelihood of edges in each of the eight directions, edges in the blocks surrounding the missing block whose directions imply that they pass through the missing block are determined. That is, we first obtain

$$g_x = x_{i+1,j-1} - x_{i-1,j-1} + 2x_{i+1,j} - 2x_{i-1,j} + x_{i+1,j+1} - x_{i-1,j+1}$$

and

$$g_y = x_{i-1,j+1} - x_{i-1,j-1} + 2x_{i,j+1} - 2x_{i,j-1} + x_{i+1,j+1} - x_{i+1,j-1}$$

for every pixel in the blocks to the left, right, top, and bottom of the missing block. The magnitude and angular direction of the edge at pixel (i,j) are

$$G = \sqrt{g_x^2 + g_y^2} \quad \text{and} \quad \theta = \arctan\left(\frac{g_y}{g_x}\right)$$

where θ determines if the edge at pixel (i,j) passes through the missing block. Since there are eight pixels in the clique, the value of θ is rounded to one of the eight directions equally spaced in the range from 0° to 180°. There is a counter c_m $(m = 1,2,\ldots,8)$ for each of the eight directions. If the extension of an edge at pixel (i,j) belonging to one of the neighboring blocks passes through the missing area, the counter for that particular direction is incremented by the amount of G. Since the employed edge detector is sensitive to the image noise, the values of c_ms, $m = 1,\ldots,8$ are compared to a threshold. If any of them is less than the threshold, it is set to zero.

There are eight pixels in the clique of each pixel, and eight directions for the detected edges. Each pixel in the clique of a pixel corresponds to a direction. In our proposed method, $w_{i,j\to k,l}$ is selected based on the edge counter of the direction corresponding to (i,j) and (k,l), i.e.,

$$w_{i,j\to k,l} = \beta c_m \qquad (10)$$

where β is a constant and c_m is the counter corresponding to direction m, and direction m corresponds to the direction formed by (i,j) and (k,l). Finally, the second stage of the proposed error-concealment method can be summarized as follows. 1) Determine the edges in the neighboring blocks and assign them to eight equally spaced directions. Compute the counter for each direction. 2) Use (10) to find a set of weights for each missing block. 3) Use (9) to obtain an estimate of each missing pixel employing the weights obtained in the previous step. 4) Iteratively reestimate the missing pixels using (9) until convergence. Note that since the cost function is convex, convergence is guaranteed.

For intra-coded blocks, the missing pixel values are initially set to zero and then the MAP estimator, using the adaptive MRF and the data of the neighboring blocks, is applied. For missing inter-coded blocks, an initial estimate are obtained using information from the previous frame. Estimates of the prediction errors are found using the adaptive MRF model along with the prediction error signals of the neighboring blocks. The estimated values are then added to the initial estimates. Since the prediction error signal consists mostly of high-frequency components, the MAP estimation stage (i.e., the second stage) will improve the video reconstruction quality, especially around the edges.

IV. Computational Complexity

The numbers provided below for computational complexity correspond to a block and subblock of sizes 16 × 16 and 8 × 8, respectively. The computational load of the first stage of the proposed method consists of those computations required in 1) estimating the motion, and 2) computing the error of (6). For motion estimation, we used a spiral search method using an area of 16 × 16. This requires approximately 197 000 operations. If the search for the displacement of each of the subblocks is restricted to the set of candidate motion vectors explained in Section III, the required number of operation will reduce to 6100. The number of operations required to find the total error of (6) for four blocks is approximately 380.

For the second stage, the computational load consists of those computations required in adapting the weights of the MRF model, which are approximately 18 400 operations for a missing block, assuming four available neighboring blocks. The estimation of missing pixels using (9) is an iterative procedure which, for each iteration, requires approximately 30 operations for each missing pixel, or 16 × 16 × 30 operations for each missing block. On average, 80 iterations are required for the algorithm to converge for a block.

Clearly, the computational load of our error-concealment method is quite reasonable. Our simulation experiments confirm that the run time of our method is indeed acceptable. In fact, real-time decoding (e.g., 10 frames/s for QCIF video sequences) is still possible on a Pentium 300 MHz PC.

V. Experimental Results

Although the method proposed in this paper is general and can be applied to any block-based video compression method, H.263 is used as our video coding framework. QCIF (176 × 144) video sequences at a temporal resolution of 10 frames/s are

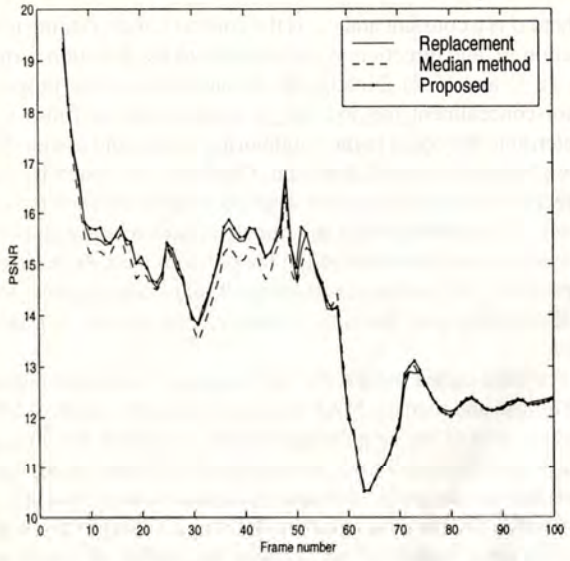


Fig. 3. PSNR values for image sequence Foreman with 10% GOB missing for different concealment methods.

coded at 64 kbps and then decoded in the presence of slice/GOB errors. The size of the blocks is 16×16, that of the subblock is 8×8.

To simulate the channel errors, the following tasks are performed. Coded video information is first grouped into packets, where each video packet consists of the coded data of a GOB or a slice. The video packets are then multiplexed with audio information according to the H.223 standard. We used an H.223 multiplexing simulator which receives video packets, simulates audio traffic, applies errors to the multiplexed bit stream according to an error pattern stored in a file, and outputs the packets [12]. The error pattern that we employed corresponds to a mobile channel [13]. Burst errors will most likely not corrupt two consecutive video packet, since audio packets are inserted between them. The erroneous bit stream is decoded such that the effect of errors will appear as missing slices/GOB's.

For inter-coded blocks, our error concealment consists of obtaining an initial estimate of the missing block using information from the previous frame, and finding an estimate of the prediction error using the adaptive MRF model. We compare the performance of the above method with two other methods: 1) a replacement method, where a missing block is replaced with the same block in the previous frame; and 2) a median method, where the motion vector of a missing block is set to the median of motion vectors of blocks to the left, above and above-right of it, and the estimated motion vector is used to obtain a motion compensation block which serves as the concealment of the missing block. Here, we consider only the case where a GOB is placed in each of the video packets. Shown in Fig. 3 are the concealment PSNR values for the three methods mentioned above for the video sequence Foreman with a 10% packet (GOB) loss rate. As can be seen, for video sequences with a large amount of motion like Foreman, the performance of the proposed method and the median method are close to each other, and both are better than the replacement method. Although the performance



Fig. 4. An inter-coded frame of the sequence Foreman concealed by the (a) replacement, (b) median, and (c) proposed methods.

of the above methods is comparable in terms of PSNR, the video sequences obtained using the proposed method are more visually appealing than the ones obtained using the other two methods. Fig. 4(a), (b), and (c) shows the reconstructed video frame (inter-coded) of the video sequence Foreman. As can be seen in the images, the replacement method does not generate good results, especially around the nose area. Moreover, the concealment result of the proposed method is clearly better than that of the other two methods.

For intra-coded blocks, we compare the performance of our method (which consists of estimating the missing block using the adaptive MRF model) to that of four other efficient methods: 1) a MAP estimator using a nonadaptive GMRF as the *a priori* model where each missing pixel is basically set to the average of the pixels around it, 2) a suboptimal version of the MAP estimator where a missing pixel is set to the median of pixels around it [8], 3) the deterministic method proposed in [4], and 4) the deterministic method proposed in [3]. Although there are other deterministic methods that are likely to outperform the above two methods, for example, the ones proposed in [6] and [7], we restrict our comparison to the above two deterministic methods. In fact, a direct comparison of our method, which is statistical, to deterministic methods is difficult because of different design approaches. Our main aim here is to compare our method to previously proposed statistical methods.

In this experiment, we employ different video sequences and different packetization schemes. In the first set of simulation experiments, we assign a slice which consists of one block, to a packet. Fig. 5(a) shows a frame of the image sequence Foreman encoded and decoded using an H.263 compliant coder. Fig. 5(b)–(g), shows (respectively) the same frame: 1) missing approximately 20% of the packets (blocks), 2) reconstructed using the nonadaptive GMRF model, 3) using the suboptimal MRF model, 4) using the method proposed in [4], 5) using the method proposed in [3], and 6) using our proposed adaptive MRF error concealment method. Clearly, our proposed method performs best in reconstruction quality, particularly in retrieving the edges and in the areas of the frame that correspond to adjacent missing blocks.

In the next set of simulation experiments, we assign the coded data of a GOB, which consists of 11 blocks, to each of the video packets. Fig. 6(a) shows a frame of the video sequence Foreman with two missing packets (GOB's), at approximately 18% loss rate. Fig. 6(b) and (c) shows the error- concealment result obtained using the nonadaptive GMRF model and suboptimal MRF models, respectively. Fig. 6(d) and (e) shows the result obtained using the methods proposed in [4] and [3], respectively. Fig. 6(f) shows the result obtained using our adaptive

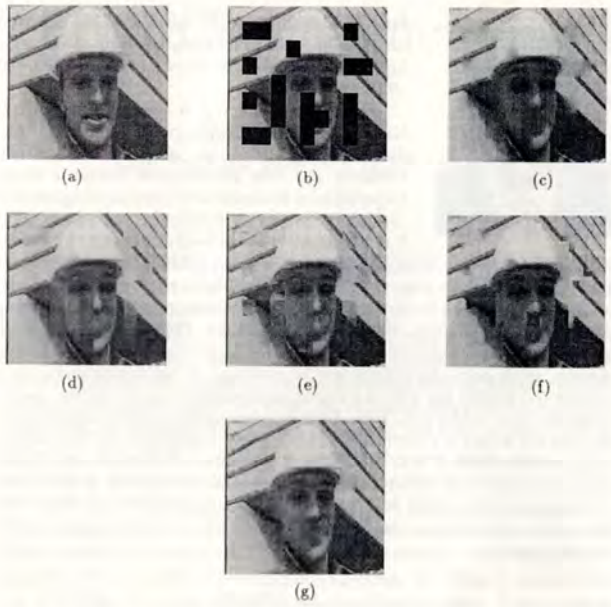


Fig. 5. A frame from the video sequence Foreman: (a) original; (b) missing blocks; reconstructed using (c) a nonadaptive GMRF model; (d) a suboptimal MRF model; (e) the method proposed in [4]; (f) the method proposed in [3]; and (g) our adaptive MRF model.

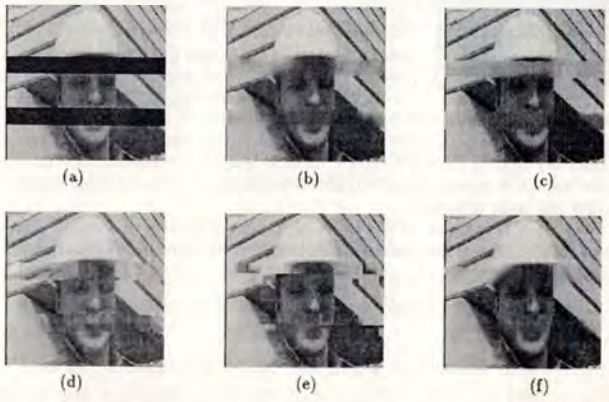


Fig. 6. A frame from the video sequence Foreman: (a) with missing GOB's, reconstructed using (b) a nonadaptive GMRF model; (c) a suboptimal MRF model; (d) the method proposed in [4]; (e) the method proposed in [3]; and (f) our adaptive MRF model.

MRF model. By comparing the figures, the superior performance of our method becomes obvious. This performance advantage is demonstrated in the blocks that contain edges. For a quantitative evaluation, Table I provides the PSNR values of the above concealment methods (for both packetization cases) for the video sequence Foreman. The table demonstrates that our method outperforms the other methods by at least 2 dB.

Finally, we compare the computational complexity of our method in terms of required number of additions and multiplications to the methods proposed in [4] and [3]. The total number of additions and multiplications required for restoring a 16 × 16 block are approximately 4500 and 20 000 using the method proposed in [4] and our method, respectively. The method proposed in [3] requires approximately 650 000 additions and multiplications to restore a 16 × 16 block. Therefore, the number of computations of our method is 4.4:1 larger than that of [4] and 1:0.03 less than those of [3]. However, our method outperforms [4] substantially in terms of the quality of the reconstructed images. This can be seen in Figs. 5 and 6. This quality improvement justifies, in most applications, the additional computational complexity.

TABLE I
PSNR (dB) COMPARISON OF DIFFERENT METHODS FOR THE VIDEO SEQUENCE FOREMAN

Method	No loss	20% Block loss	GOB missing
GMRF	32.1	26.3	25.3
Suboptimal MRF	32.1	25.4	23.1
Method proposed in [4]	32.1	24.3	23.8
Method proposed in [3]	32.1	25.2	24.1
Adaptive MRF	32.1	28.6	27.2

VI. CONCLUSION

This paper introduces a new method of error concealment for block-based coded video communications over error-prone channels. The proposed method employs an adaptive MRF as the image *a priori* model in a MAP estimation paradigm. The adaptation enables the estimation procedure to incorporate more information without increasing the order of the MRF. The proposed concealment method is able to restore missing blocks located in smooth and low-frequency areas, as well as in high-frequency and edge portions of a video frame. Our concealment method achieves very good computation–performance tradeoffs, and outperforms previously proposed MRF-based concealment methods.

ACKNOWLEDGMENT

The authors would like to thank the anonymous reviewers for their insightful comments and constructive suggestions. The authors would also like to gratefully acknowledge the help and support provided by G. Cote, their colleague in the Signal Processing and Multimedia Group at the University of British Columbia.

REFERENCES

[1] M. Ghanbari and V. Seferidis, "Cell loss concealment in ATM video codecs," *IEEE Trans. Circuit System Video Technol.*, vol. 3, pp. 238–247, June 1993.
[2] W. M. Lam, A. R. Reibman, and B. Liu, "Recovery of lost or erroneously received motion vectors," in *Proc. Int. Conf. Acoust., Speech, Signal Processing*, vol. V, 1993, pp. 417–420.
[3] Y. Wang, Q. F. Zhu, and L. Shaw, "Maximally smooth image recovery in transform coding," *IEEE Trans. Commun.*, vol. 41, pp. 1544–1551, Oct. 1993.
[4] S. S. Hemami and T. H. Y. Meng, "Transform coded image reconstruction exploiting interblock correlations," *IEEE Trans. Image Processing*, vol. 4, pp. 1023–1027, July 1995.
[5] H. Sun and W. Kwok, "Concealment of damaged block transform coded images using projection onto convex sets," *IEEE Trans. Image Processing*, vol. 4, pp. 470–477, Apr. 1995.
[6] W. Kwok and H. Sun, "Multi-directional interpolation for spatial error concealment," *IEEE Trans. Consumer Electron.*, vol. 39, pp. 455–460, Aug. 1993.
[7] W. Zeng and B. Liu, "Geometric-structure-based error concealment with novel applications in block-based low-bit-rate coding," *IEEE Trans. Circuits Syst. Video Technol.*, vol. 9, pp. 648–665, June 1999.

[8] P. Salama, N. Shroff, E. J. Coyle, and E. J. Delp, "Error concealment in encoded video streams," in *Signal Recovery Techniques for Image and Video Compression and Transmission*, N. P. Galatsanos and A. K. Katsaggelos, Eds. Boston, MA: Kluwer Academic, 1998.

[9] R. Talluri, "Error resilient video coding in the MPEG-4 standard," *IEEE Commun. Mag.*, vol. 26, pp. 112–119, June 1998.

[10] S. Geman and D. Geman, "Stochastic relaxation, Gibbs distribution, and the Bayesian restoration of images," *IEEE Trans. Pattern Anal. Machine Intell.*, vol. 11, pp. 689–691, 1984.

[11] S. Shirani, F. Kossentini, and R. Ward, "Reconstruction of motion vector missing macroblocks in H.263 encoded video transmission over lossy networks," in *Proc. Int. Conf. Image Processing*, vol. III, Oct. 1998, pp. 487–491.

[12] G. Sullivan, "A Simple Video Packet Mux Simulator Program for Video Streams in H.263/M Using AL3 Mux of H.223 Annex B," ITU-T Study Group 15, Video Coding Expert Group, Doc. Q15-F-16, Nov. 1996.

[13] Ericsson Sweden, "WCDMA Error Patterns at 64 kb/s," ITU-T Study Group 16, Multimedia Terminals and Systems Expert Group, Cannes, France, June 1998.



Shahram Shirani (S'88–M'89) received the B.Sc. degree in electrical engineering from Esfahan University of Technology, Esfahan, Iran, in 1989 and the M.Sc. degree in biomedical engineering from Amirkabir University of Technology, Tehran, Iran in 1994. Currently, he is pursuing the Ph.D. degree in the Department of Electrical and Computer Engineering, University of British Columbia, Vancouver, B.C., Canada.

From 1994 to 1996, he was with the Department of Electrical Engineering, University of Tehran. His research interests include image and video compression, video communications, signal processing and ultrasonic imaging.



Faouzi Kossentini (S'89–M'89–SM'98) received the B.S., M.S., and Ph.D. degrees from the Georgia Institute of Technology, Atlanta, in 1989, 1990, and 1994, respectively.

During 1995, he was a Research Scientist at Nichols Research Corporation, Huntsville, AL. Since January 1996, he has been an Assistant Professor and then an Associate Professor in the Department of Electrical and Computer Engineering, University of British Columbia, vancouver, B.C., Canada, where he is involved in research in the areas of signal processing, communications, and multimedia. He has coauthored more than 100 journal papers, conference papers, book chapters and patents.

Dr. Kossentini has been active as a Voting Member, and recently as head of delegation, of the Canadian delegate to ISO/IEC JTC1/SC29, which is responsible for the standardization of coded representation of audiovisual, multimedia, and hypermedia information. In particular, he has participated in most current JBIG/JPEG and MPEG-4 standardization activities. He has also participated in most current ITU-T low bit rate video coding standardization activities. He has served as a technical area coordinator and member of the technical program committee of ICIP-1997, and as a Member of the technical program committee of ISCAS-1999. He is also the Vice General Chairman of ICIP-2000. Dr. Kossentini is currently an Associate Editor for the IEEE TRANSACTIONS ON IMAGE PROCESSING. He is also an Associate Editor for the IEEE TRANSACTIONS ON MULTIMEDIA.



Rabab Ward (F'98) received the B.Sc. degree in electrical engineering from University of Cairo, Egypt, in 1966 and the M.Sc. and the Ph.D. in electrical and computer engineering from University of California, Berkeley, in 1969 and 1972, respectively.

She is a Professor in the Electrical and Computer Engineering Department, University of British Columbia, Vancouver, B.C., Canada, and is the Director of the Center for Integrated Computer Systems Research there. Her research interests are mainly in the areas of signal processing and image processing. She has made contributions in the areas of signal detection, image encoding, compression, recognition, restoration and enhancement, and their applications to infant cry signals, cable TV, HDTV, medical images, and astronomical images. She holds five patents related to cable television picture monitoring, measurement and noise reduction.

Dr. Ward is a fellow of the EIC and the Royal Society of Canada. She is currently serving as the General Chair of ICIP'2000 to be held in Vancouver.

Wert
Bookbinding
Grantville, PA
JULY-DEC 2000
"We're Quality Bound"

APPENDIX STOCKHAMMER01

screenshot-catalog.libraries.psu.edu-2023.12.18-12_34_43
https://catalog.libraries.psu.edu/catalog/1397806
18.12.2023

MARC View

LEADER 04464nas a22007211a 4500			
001 1397806			
003 SIRSI			
005 20151215012754.0			
008 910515c19919999xx qu 0 0eng d			
010			a| 91642188 z| sn90001281
019			a| MARS
022	0		a| 1051-8215
030			a| ITCTEM
032			a| 006329 b| USPS
035			a| LIAS1562226
035			a| (CStRLIN)MDJGAEF1049-S
035			a| (OCoLC)24382124
040			d| UtOrBLW
050	0	0	a| TK6630.A1 b| I37
245	0	0	a| IEEE transactions on circuits and systems for video technology.
246	3	0	a| Circuits and systems for video technology
264		1	a| New York, NY : b| Institute of Electrical and Electronics Engineers, c| [1991-]
264		4	c| ©1991-
300			a| volumes : b| illustrations ; c| 28 cm
310			a| Quarterly.
336			a| text b| txt 2| rdacontent
337			a| unmediated b| n 2| rdamedia
338			a| volume b| nc 2| rdacarrier
362	0		a| Vol. 1, no. 1 (Mar. 1991)-
500			a| Title from cover.
550			a| "A publication of the Circuits and Systems Society.
650		0	a| High definition television v| Periodicals.
650		0	a| Digital television v| Periodicals.
650		0	a| Image processing x| Digital techniques v| Periodicals.
650		0	a| Resolution (Optics) v| Periodicals.
710	2		a| IEEE Circuits and Systems Society.
710	2		a| Institute of Electrical and Electronics Engineers. t| IEEE Xplore.
533			a| Microfiche. b| [New York, N.Y.? c| IEEE], e| microfiches ; 11 x 15 cm.
949			a| Microfilm w| ASIS c| 1 i| 1397806-1001 d| 11/7/2000 l| MICROS-HB m| HARRISBURG r| Y s| Y t| MICROFORM u| 4/13/2001
949			a| TK6679.I33 v.1 1991 w| LCPER c| 1 i| 000051829223 l| CATO-2 m| UP-ANNEX r| Y s| Y t| PERIODICAL u| 4/2/2003 z| 7757
949			a| TK6679.I33 v.2 1992 w| LCPER c| 1 i| 000051829230 l| CATO-2 m| UP-ANNEX r| Y s| Y t| PERIODICAL u| 4/2/2003 z| 7757
949			a| TK6679.I33 v.3 1993 w| LCPER c| 1 i| 000051829247 l| CATO-2 m| UP-ANNEX r| Y s| Y t| PERIODICAL u| 4/2/2003 z| 7757

949			a| TK6679.I33 v.4 1994 w| LCPER c| 1 i| 000051829254 l| CATO-2 m| UP-ANNEX r| Y s| Y t| PERIODICAL u| 4/2/2003 z| 7757
949			a| TK6679.I33 v.5-6 1995-1996 w| LCPER c| 1 i| 000051829261 d| 10/13/2023 e| 10/13/2023 k| CHECKEDOUT l| CATO-2 m| UP-ANNEX n| 1 r| M s| Y t| PERIODICAL u| 4/2/2003 z| 7757
949			a| TK6679.I33 v.7 1997 w| LCPER c| 1 i| 000051829278 l| CATO-2 m| UP-ANNEX r| Y s| Y t| PERIODICAL u| 4/2/2003 z| 7757
949			a| TK6679.I33 v.8 1998 w| LCPER c| 1 i| 000051829285 l| CATO-2 m| UP-ANNEX r| Y s| Y t| PERIODICAL u| 4/2/2003 z| 7757
949			a| TK6679.I33 v.9 1999 w| LCPER c| 1 i| 000051829292 l| CATO-2 m| UP-ANNEX r| Y s| Y t| PERIODICAL u| 4/2/2003 z| 7757
949			a| TK6679.I33 v.10 no.1-4 2000 w| LCPER c| 1 i| 000048234948 d| 11/7/2000 l| CATO-2 m| UP-ANNEX r| Y s| Y t| PERIODICAL u| 4/13/2001 z| 7757
949			a| TK6679.I33 v.10 no.5-8 2000 w| LCPER c| 1 i| 000048234931 l| CATO-2 m| UP-ANNEX r| Y s| Y t| PERIODICAL u| 10/2/2001 z| 7757
949			a| TK6679.I33 v.11 no.1-6 2001 w| LCPER c| 1 i| 000048427524 l| CATO-2 m| UP-ANNEX r| Y s| Y t| PERIODICAL u| 11/5/2002 z| 7757
949			a| TK6679.I33 v.11 no.7-12 2001 w| LCPER c| 1 i| 000048427517 l| CATO-2 m| UP-ANNEX r| Y s| Y t| PERIODICAL u| 11/5/2002 z| 7757
949			a| TK6679.I33 v.12 no.1-6 2002 w| LCPER c| 1 i| 000052496431 l| CATO-2 m| UP-ANNEX r| Y s| Y t| PERIODICAL u| 6/16/2003 z| 7757
949			a| TK6679.I33 v.12 no.7-12 2002 w| LCPER c| 1 i| 000052496424 l| CATO-2 m| UP-ANNEX r| Y s| Y t| PERIODICAL u| 6/16/2003 z| 7757
949			a| TK6679.I33 v.13 no.1-6 2003 w| LCPER c| 1 i| 000052816321 l| CATO-2 m| UP-ANNEX r| Y s| Y t| PERIODICAL u| 4/1/2004 z| 7757
949			a| TK6679.I33 v.13 no.7-12 2003 w| LCPER c| 1 i| 000052816314 l| CATO-2 m| UP-ANNEX r| Y s| Y t| PERIODICAL u| 4/1/2004 z| 7757
949			a| TK6679.I33 v.14 no.1-4 2004 w| LCPER c| 1 i| 000055002318 l| CATO-2 m| UP-ANNEX r| Y s| Y t| PERIODICAL u| 6/15/2005 z| 7757
949			a| TK6679.I33 v.14 no.5-8 2004 w| LCPER c| 1 i| 000055013178 l| CATO-2 m| UP-ANNEX r| Y s| Y t| PERIODICAL u| 6/15/2005 z| 7757
949			a| TK6679.I33 v.14 no.9-12 2004 w| LCPER c| 1 i| 000055002301 l| CATO-2 m| UP-ANNEX r| Y s| Y t| PERIODICAL u| 6/15/2005 z| 7757
949			a| TK6679.I33 v.15 no.1-4 2005 w| LCPER c| 1 i| 000055120340 l| CATO-2 m| UP-ANNEX r| Y s| Y t| PERIODICAL u| 6/8/2006 z| 7757
949			a| TK6679.I33 v.15 no.5-8 2005 w| LCPER c| 1 i| 000055120609 l| CATO-2 m| UP-ANNEX r| Y s| Y t| PERIODICAL u| 6/8/2006 z| 7757
949			a| TK6679.I33 v.15 no.9-12 2005 w| LCPER c| 1 i| 000055120333 l| CATO-2 m| UP-ANNEX r| Y s| Y t| PERIODICAL u| 6/8/2006 z| 7757
949			a| TK6679.I33 v.16 no.1-6 2006 w| LC c| 1 i| 000061732261 l| CATO-2 m| UP-ANNEX r| Y s| Y t| PERIODICAL u| 9/18/2007 z| 7757
949			a| TK6679.I33 v.16 no.7-12 2006 w| LC c| 1 i| 000061732278 l| CATO-2 m| UP-ANNEX r| Y s| Y t| PERIODICAL u| 9/18/2007 z| 7757
852	0	1	a| PSt b| UP-ANNEX c| ANNEX h| TK6679 i| .I33
866		0	8| 0 a| v.1(1991)-v.16(2006)
852	8		a| PSt b| HARRISBURG c| MICROS-HB h| Microfiche
866		0	8| 0 a| v.1(1991)-v.9(1999)

PennState

Copyright @2019 The Pennsylvania State University. All rights reserved. Except where otherwise noted, this work is subject to a Creative Commons Attribution 4.0 license. Details and exceptions.

Legal Statements | PSU Hotlines

PENN STATE UNIVERSITY LIBRARIES

Libraries Home (814) 865-6368
Libraries Intranet (Staff Only)
Accessibility Help
Website Feedback
Policies and Guidelines
Staff Directory

screenshot-catalog.libraries.psu.edu-2023.12.18-12_34_43
https://catalog.libraries.psu.edu/catalog/1397806
18.12.2023

IEEE transactions on circuits and systems for video technology

Additional Titles:	Circuits and systems for video technology
Published:	New York, NY : Institute of Electrical and Electronics Engineers, [1991-]
Copyright Date:	©1991-
Physical Description:	volumes : illustrations ; 28 cm
Additional Creators:	IEEE Circuits and Systems Society and Institute of Electrical and Electronics Engineers

Availability

Browse Nearby on Shelf I Want It

Penn State Harrisburg (1 item)

Call number	Material	Location
Harrisburg - Microforms - 2nd Floor - In-Library Use: Holdings Summary v.1(1991)-v.9(1999)		
Microfilm	Microfilm, Microfiche, etc.	Harrisburg - Microforms - 2nd Floor - In-Library Use

Library Storage (24 items)

Call number	Material	Location
Annexed Material: Holdings Summary v.1(1991)-v.16(2006)		
TK6679.I33 v.1 1991	Bound Journal	Annexed Material
TK6679.I33 v.2 1992	Bound Journal	Annexed Material
TK6679.I33 v.3 1993	Bound Journal	Annexed Material
TK6679.I33 v.4 1994	Bound Journal	Annexed Material
TK6679.I33 v.5-6 1995-1996	Bound Journal	Annexed Material
TK6679.I33 v.7 1997	Bound Journal	Annexed Material
TK6679.I33 v.8 1998	Bound Journal	Annexed Material
TK6679.I33 v.9 1999	Bound Journal	Annexed Material
TK6679.I33 v.10 no.1-4 2000	Bound Journal	Annexed Material
TK6679.I33 v.10 no.5-8 2000	Bound Journal	Annexed Material
TK6679.I33 v.11 no.1-6 2001	Bound Journal	Annexed Material

TK6679.I33 v.11 no.7-12 2001	Bound Journal	Annexed Material
TK6679.I33 v.12 no.1-6 2002	Bound Journal	Annexed Material
TK6679.I33 v.12 no.7-12 2002	Bound Journal	Annexed Material
TK6679.I33 v.13 no.1-6 2003	Bound Journal	Checked out
TK6679.I33 v.13 no.7-12 2003	Bound Journal	Checked out
TK6679.I33 v.14 no.1-4 2004	Bound Journal	Annexed Material
TK6679.I33 v.14 no.5-8 2004	Bound Journal	Annexed Material
TK6679.I33 v.14 no.9-12 2004	Bound Journal	Annexed Material
TK6679.I33 v.15 no.1-4 2005	Bound Journal	Annexed Material
TK6679.I33 v.15 no.5-8 2005	Bound Journal	Annexed Material
TK6679.I33 v.15 no.9-12 2005	Bound Journal	Annexed Material
TK6679.I33 v.16 no.1-6 2006	Bound Journal	Annexed Material
TK6679.I33 v.16 no.7-12 2006	Bound Journal	Annexed Material

Dates of Publication and/or Sequential Designation:
Vol. 1, no. 1 (Mar. 1991)-

Subject(s):
High definition television—Periodicals
Digital television—Periodicals
Image processing—Digital techniques—Periodicals
Resolution (Optics)—Periodicals

ISSN:
1051-8215

Publication Frequency:
Quarterly.

Note:
Title from cover.

Reproduction Note:
Microfiche. [New York, N.Y.? IEEE], microfiches ; 11 x 15 cm.

Issuing Body:
"A publication of the Circuits and Systems Society.

View MARC record | catkey: 1397806

PennState

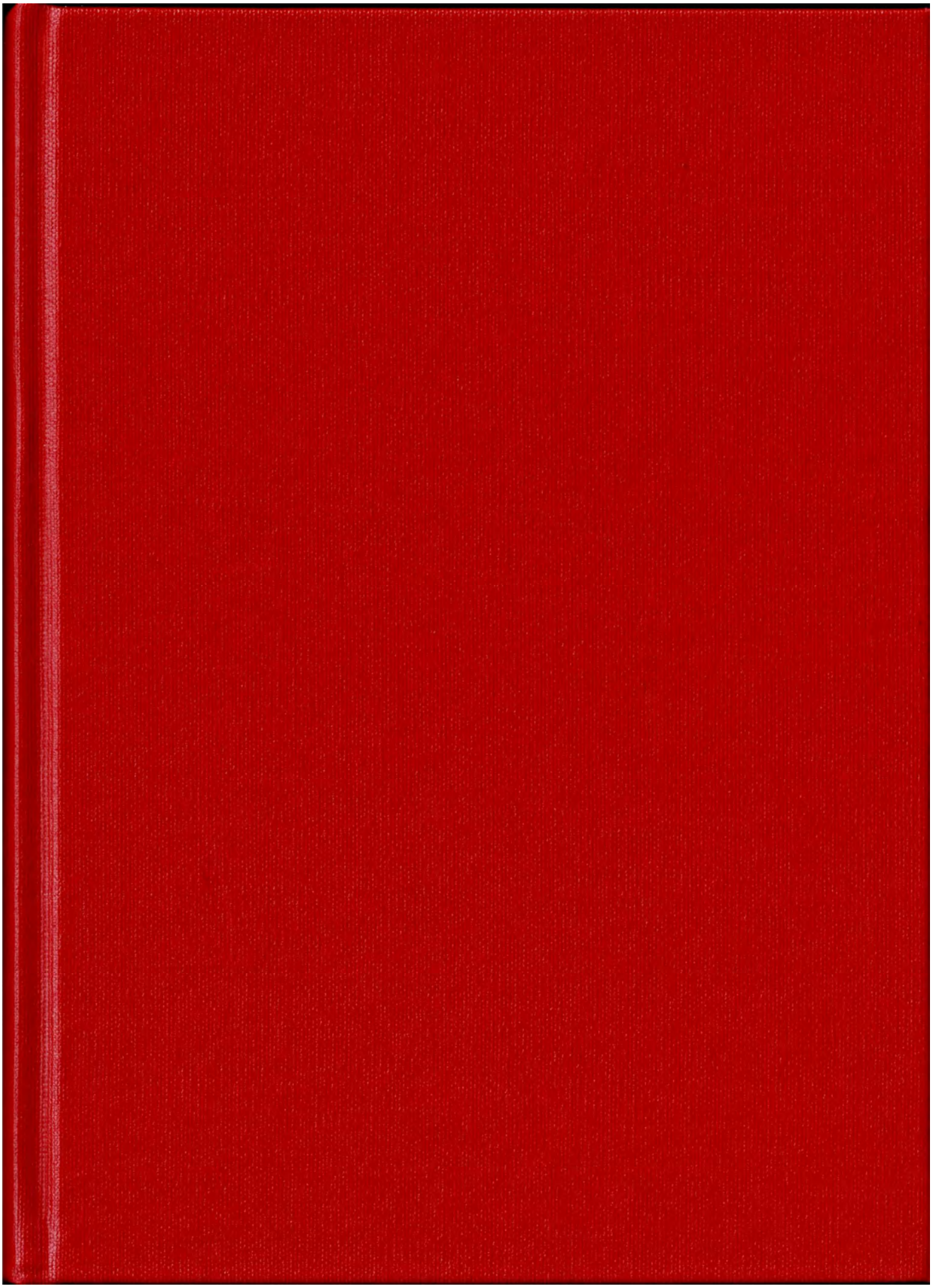
Copyright @2019 The Pennsylvania State University. All rights reserved. Except where otherwise noted, this work is subject to a Creative Commons Attribution 4.0 license. Details and exceptions.

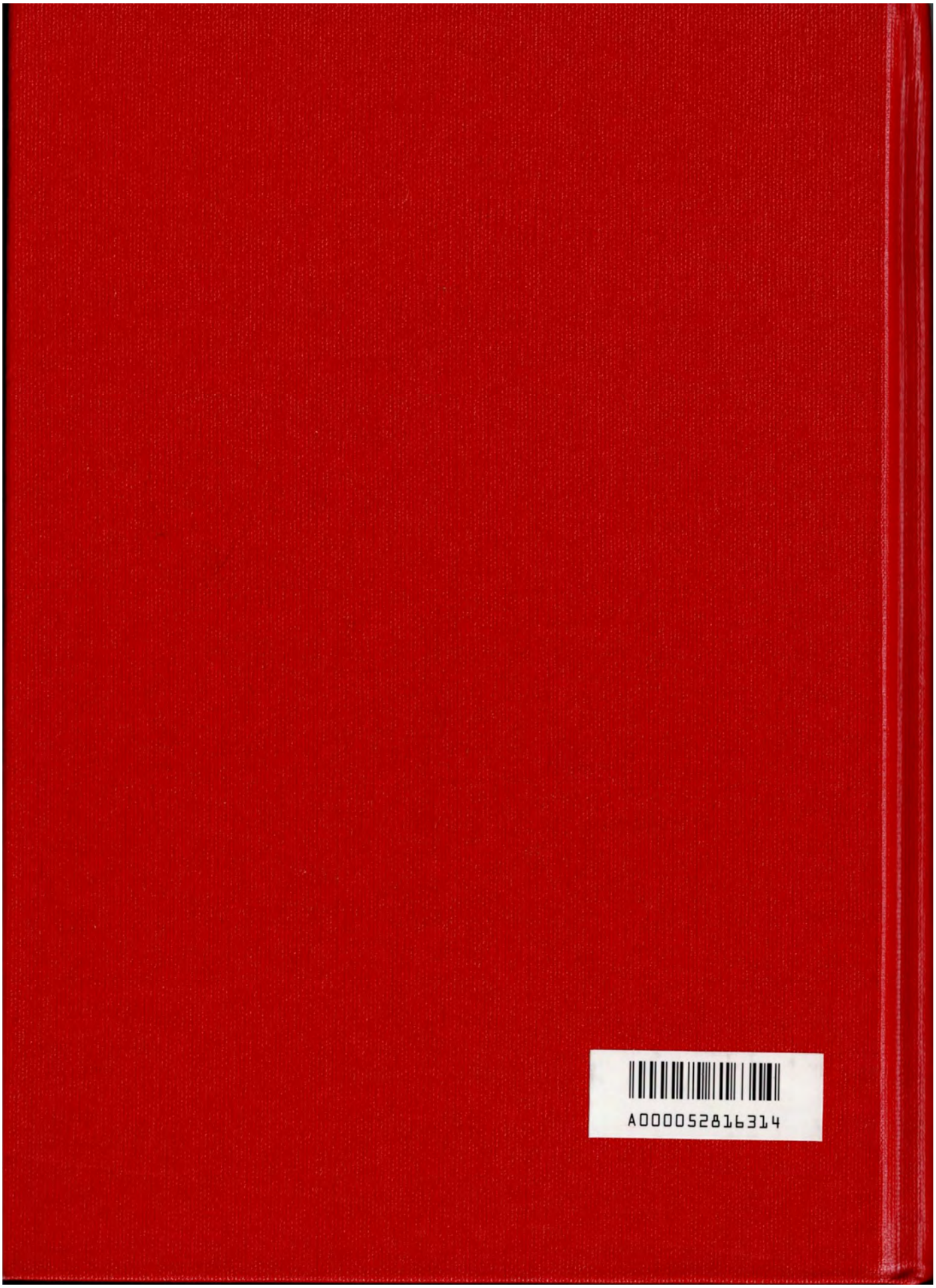
Legal Statements | PSU Hotlines

PENN STATE UNIVERSITY LIBRARIES

Libraries Home (814) 865-6368
Libraries Intranet (Staff Only)
Accessibility Help
Website Feedback
Policies and Guidelines
Staff Directory

APPENDIX STOCKHAMMER02




A000052816314

SHELVED IN
BOUND
PERIODICAL
COLLECTION

ENGINEERING LIBRARY

Engin

IEEE TRANSACTIONS ON

CIRCUITS AND SYSTEMS FOR VIDEO TECHNOLOGY

A PUBLICATION OF THE IEEE CIRCUITS AND SYSTEMS SOCIETY

WWW.IEEE-CAS.ORG



RECEIVED AUG 6

JULY 2003 VOLUME 13 NUMBER 7 ITCTEM (ISSN 1051-8215)

SPECIAL ISSUE ON THE H.264/AVC VIDEO CODING STANDARD

GUEST EDITORIAL

Introduction to the Special Issue on the H.264/AVC Video Coding Standard . . . *A. Luthra, G. J. Sullivan, and T. Wiegand* 557

PAPERS

Overview of the H.264/AVC Video Coding Standard . . . . . *T. Wiegand, G. J. Sullivan, G. Bjøntegaard, and A. Luthra* 560
Motion- and Aliasing-Compensated Prediction for Hybrid Video Coding . . . . . *T. Wedi and H. G. Musmann* 577
Generalized B Pictures and the Draft H.264/AVC Video-Compression Standard . . . . . *M. Flierl and B. Girod* 587
Low-Complexity Transform and Quantization in H.264/AVC . . . . . *H. S. Malvar, A. Hallapuro, M. Karczewicz, and L. Kerofsky* 598
Variable Block-Size Transforms for H.264/AVC . . . . . *M. Wien* 604
Adaptive Deblocking Filter . . . . . *P. List, A. Joch, J. Lainema, G. Bjøntegaard, and M. Karczewicz* 614
Context-Based Adaptive Binary Arithmetic Coding in the H.264/AVC Video Compression Standard . . . . . *D. Marpe, H. Schwarz, and T. Wiegand* 620
The SP- and SI-Frames Design for H.264/AVC . . . . . *M. Karczewicz and R. Kurceren* 637
H.264/AVC Over IP . . . . . *S. Wenger* 645
H.264/AVC in Wireless Environments . . . . . *T. Stockhammer, M. M. Hannuksela, and T. Wiegand* 657
A Generalized Hypothetical Reference Decoder for H.264/AVC . . . *J. Ribas-Corbera, P. A. Chou, and S. L. Regunathan* 674
Rate-Constrained Coder Control and Comparison of Video Coding Standards . . . . . *T. Wiegand, H. Schwarz, A. Joch, F. Kossentini, and G. J. Sullivan* 688
H.264/AVC Baseline Profile Decoder Complexity Analysis . . . . . *M. Horowitz, A. Joch, F. Kossentini, and A. Hallapuro* 704
Complexity of Optimized H.26L Video Decoder Implementation . . . *V. Lappalainen, A. Hallapuro, and T. D. Hämäläinen* 717

COMMENTS AND CORRECTIONS

Corrections to "Genetic Algorithm Optimization of Multidimensional Grayscale Soft Morphological Filters With Applications in Film Archive Restoration . . . . . *M. S. Hamid, N. R. Harvey, and S. Marshall* 726

CALLS FOR PAPERS

ISCAS 2004 727
Special Issue on Integrated Multimedia Platforms 728

IEEE CIRCUITS AND SYSTEMS SOCIETY

The Circuits and Systems Society is an association of IEEE members with professional interest in the field of circuits and systems theory. All members of the IEEE are eligible for membership in the Society and will receive this TRANSACTIONS upon payment of the annual Society membership fee of $12.00, plus an annual subscription fee of $18.00. For information on joining, write to the IEEE at the address below. *Member copies of Transactions/Journals are for personal use only.*

IEEE TRANSACTIONS ON CIRCUITS AND SYSTEMS FOR VIDEO TECHNOLOGY

Editor-in-Chief
THOMAS SIKORA
Inst. for Telecommunications
Communication Systems Dept.
Technical Univ. Berlin
Sekr. EN-1, Einsteinufer 17
10587 Berlin, Germany
Phone: +1 49 30 314 25799
Fax: +1 49 30 314 22514
E-mail: sikora@nue.tu-berlin.de
http://www.nue.tu-berlin.de

Past Editor-in-Chief
WEIPING LI
WebCast Technologies, Inc.
1153 Bordeaux Dr., Ste. 205
Sunnyvale, CA 94089
Phone: +1 408 541 4150
Fax: +1 408 745 0249
E-mail: li@webcasttech.com

Associate Editors

ISHFAQ AHMAD
Dept. Comput. Sci. & Eng.
Univ. Texas at Arlington
248 D/E Nedderman Hall
416 Yates St., Box 19015
Arlington, TX 76019-0015
iahmad@cse.uta.edu

KIYOHARU AIZAWA
Dept. Elect. Eng.
Univ. Tokyo
7-3-1 Hongo, Bunkyo-ku
Tokyo 113 Japan
aizawa@ee.t.u-tokyo.ac.jp

OSAMA K. AL-SHAYKH
PacketVideo Technologies
10350 Science Ctr. Dr., Ste. 140
San Diego, CA 92121
osama@packetvideo.com

JOHN F. ARNOLD
Schl. Elect. Eng.
Univ. College, UNSW
Australian Defence Force Academy
Canberra ACT 2600, Australia
j.arnold@adfa.edu.au

RAJARATHNAM CHANDRAMOULI
Dept. Elect. Comput. Eng.
207 Burchard Building
Stevens Inst. Technol.
Hoboken, NJ 07030
rchandr1@stevens-tech.edu

CHANG WEN CHEN
Dept. Elect. Comput. Eng.
Florida Inst. of Technol.
Melbourne, FL 32091
cchen@fit.edu

LIANG-GEE CHEN
Dept. Elect. Eng.
National Taiwan Univ.
Taipei, Taiwan 10764 R.O.C.
lgchen@cc.ee.ntu.edu.tw

SHERMAN CHEN
Broadband Systems Engineering
Broadcom Corp.
16215 Alton Parkway
P.O. Box 57013
Irvine, CA 92619-7013
schen@broadcom.com

LEONARDO CHIARIGLIONE
Multimedia & Video Services
CSELT
Via G. Reiss Romoli, 274
Torino I-10148 Italy
leonardo.chiariglione@cselt.it

HAMID GHARAVI
NIST
U.S. Dept. Commerce
100 Bureau Dr., Stop 8920
Gaithersburg, MD 20899-8920
gharavi@antd.nist.gov

JENQ-NENG HWANG
Dept. Elect. Eng.
Univ. Washington
Seattle, WA 98195
hwang@ee.washington.edu

EBROUL IZQUIERDO
Elect. Eng. Dept.
Queen Mary, Univ. of London
London E1 4NS, UK
ebroul.izquierdo@elec.qmul.ac.uk

ROB KOENEN
InterTrust Technologies Corp.
4750 Pattrick Henry Dr.
Santa Clara, CA 95054
rob.koenen@ieee.org

ALEX KOT
Schl. Elect. Electron. Eng.
Nanyang Technol. Univ.
S1, Nanyang Ave.
Singapore 639798
eackot@ntu.edu.sg

S. Y. KUNG
Dept. Elect. Eng.
Princeton Univ.
Princeton, NJ 08544
kung@princeton.edu

MURAT KUNT
Dept. Elect. Eng.
Swiss Federal Inst. Technol.
Lausanne CH-1015 Switzerland
kunt@epfl.ch

ROSA LANCINI
CEFRIEL
Via Fucini, 2
Milano 20133 Italy
rosa@cefriel.it

SANG UK LEE
School Elect. Eng.
Seoul National Univ.
Kwanak, P.O. Box 34
Seoul 151-742 Korea
sanguk@sting.snu.ac.kr

JENS-RAINER OHM
Inst. Commun. Eng.
Aachen Univ. Technol.
Melatener Str. 23
Aachen D-52072, Germany
ohm@ient.rwth-aachen.de

LEVENT ONURAL
Elect. & Electron. Eng. Dept.
Bilkent Univ.
TR-06533 Ankara, Turkey
l.onural@ieee.org

SETHURAMAN PANCHANATHAN
Dept. Comput. Sci. Eng.
Arizona State Univ.
Tempe, AZ 85287-5406
panch@asu.edu

FERNANDO PEREIRA
Dept. Elect. Comput. Eng.
Instituto Superior Tecnico
Av. Rovisco Pais
Lisboa Codex 1096 Portugal
fp@lx.it.pt

ERIC PETAJAN
face2face animation, inc.
2 Kent Place Blvd.
Summit, NJ 07901
eric@f2f-inc.com

ATUL PURI
Apple Computer
2 Infinite Loops
MS 302-3KS
Cupertino, CA 95014
apuri@apple.com
apuri@ieee.org

HARRY SHUM
Microsoft Research Asia
3/F Beijing Sigma Center
Beijing 100080, China
hshum@microsoft.com

ROBERT L. STEVENSON
Dept. Elect. Eng.
Univ. Notre Dame
Notre Dame, IN 46556
Stevenson.1@nd.edu

MICHAEL G. STRINTZIS
Elect. Comput. Eng. Dept.
Univ. Thessaloniki
Thessaloniki 540 06 Greece
strintzi@eng.auth.gr

HUIFANG SUN
Mitsubishi Electric Research Labs
558 Central Ave.
New Providence, NJ 07974
hsun@merl.com

ALI TABATABAI
Sony Electronics
3300 Zanker Rd., MD SJ2C4
San Jose CA 95134
ali.tabatabai@am.sony.com

QI TIAN
Kent Ridge Digital Labs
21 Heng Mui Keng Terrace
Singapore 119613
tian@lit.org.sg

KOU-HU TZOU
Divio, Inc.
441 DeGuigne Drive
Sunnyvale, CA 94085
ktzou@divio.com

HIROSHI WATANABE
Visual Commun. Lab. 922A
NTT Human Interface Labs.
1-1 Hikarinooka
Yokosuka 239 Japan
hiroshi@giti.waseda.ac.jp

ZIXIANG XIONG
Dept. Elect. Eng.
Texas A&M Univ.
College Station, TX 77843
zx@lena.tamu.edu

THE INSTITUTE OF ELECTRICAL AND ELECTRONICS ENGINEERS, INC.

Officers

MICHAEL S. ADLER, *President*
ARTHUR W. WINSTON, *President-Elect*
LEVENT ONURAL, *Secretary*
PEDRO A. RAY, *Treasurer*
RAYMOND D. FINDLAY, *Past President*
JAMES M. TIEN, *Vice President, Educational Activities*
MICHAEL R. LIGHTNER, *Vice President, Publication Services and Products*
W. CLEON ANDERSON, *Vice President, Regional Activities*
GERALD H. PETERSON, *President, IEEE Standards Association*
LEAH H. JAMIESON, *Vice President, Technical Activities*
JAMES V. LEONARD, *President, IEEE-USA*
CARY Y. YANG, *Director, Division I—Circuits and Devices*

Executive Staff

DANIEL J. SENESE, *Executive Director*
DONALD CURTIS, *Human Resources*
ANTHONY DURNIAK, *Publications Activities*
JUDITH GORMAN, *Standards Activities*
CECELIA JANKOWSKI, *Regional Activities*
BARBARA COBURN STOLER, *Educational Activities*
MATTHEW LOEB, *Corporate Strategy & Communications*
RICHARD D. SCHWARTZ, *Business Administration*
W. THOMAS SUTTLE, *IEEE-USA*
MARY WARD-CALLAN, *Technical Activities*
JOHN WITSKEN, *Information Technology*

IEEE Periodicals
Transactions/Journals Department
Staff Director: FRAN ZAPPULLA
Editorial Director: DAWN MELLEY *Production Director*: ROBERT SMREK
Managing Editor: MONA MITTRA *Senior Editor*: JILL A. SINAY

IEEE TRANSACTIONS ON CIRCUITS AND SYSTEMS FOR VIDEO TECHNOLOGY (ISSN 1051-8215) is published monthly by the Institute of Electrical and Electronics Engineers, Inc. Responsibility for the contents rests upon the authors and not upon the IEEE, the Society/Council, or its members. **IEEE Corporate Office:** 3 Park Avenue, 17th Floor, New York, NY 10016-5997. **IEEE Operations Center:** 445 Hoes Lane, P.O. Box 1331, Piscataway, NJ 08855-1331. **NJ Telephone:** +1 732 981 0060. **Price/Publication Information:** Individual copies: IEEE Members $10.00 (first copy only), nonmembers $20.00 per copy. (Note: Add $4.00 postage and handling charge to any order from $1.00 to $50.00, including prepaid orders.) Member and nonmember subscription prices available upon request. Available in microfiche and microfilm.

Copyright and Reprint Permissions: Abstracting is permitted with credit to the source. Libraries are permitted to photocopy for private use of patrons, provided the per-copy fee indicated in the code at the bottom of the first page is paid through the Copyright Clearance Center, 222 Rosewood Drive, Danvers, MA 01923. For all other copying, reprint, or republication permission, write to Copyrights and Permissions Department, IEEE Publications Administration, 445 Hoes Lane, P.O. Box 1331, Piscataway, NJ 08855-1331. Copyright © 2003 by The Institute of Electrical and Electronics Engineers, Inc. All rights reserved.

Periodicals Postage Paid at New York, NY and at additional mailing offices. **Postmaster:** Send address changes to IEEE TRANSACTIONS ON CIRCUITS AND SYSTEMS FOR VIDEO TECHNOLOGY, IEEE, 445 Hoes Lane, P.O. Box 1331, Piscataway, NJ 08855-1331. GST Registration No. 125634188. Printed in U.S.A.

Introduction to the Special Issue on the H.264/AVC Video Coding Standard

OVER THE LAST one and a half decades, digital video and audio compression technologies have fundamentally changed the way we create, communicate, and consume audio-visual information. They have not only transformed existing applications and services like the distribution of entertainment video to the home but also spawned brand new industries and services like video-conferencing, direct-to-home satellite distribution, digital video recording, video-on-demand services, high-definition TV, video on mobile devices, streaming video, etc.

Since the early 1990s, when the technology was in its infancy, international video coding standards such as H.261, MPEG-1, MPEG-2/H.262, H.263, and MPEG-4 (Part 2) have been powerful engines behind the commercial success of digital video compression. They have played pivotal roles in establishing the technology via providing interoperability among products developed by different manufacturers and at the same time allowing flexibility for ingenuity in optimizing and molding the technology to fit a given application and making the cost-performance tradeoffs well suited to particular requirements. They have provided much needed assurance to the content creators that their content will run everywhere and that they do not have to create and manage multiple copies of the same content to match the products of different manufacturers. They have permitted the economy of scale to allow steep reduction in cost for masses to be able to afford the technology. They have nurtured open interactions among experts from different companies to spurt exponential growth in innovation to keep pace with the implementation technology and the needs of the applications.

The subject of this Special Issue is the newest entry in the line of international video coding standards, referred to formally as ITU-T Recommendation H.264 and ISO/IEC MPEG-4 (Part 10) Advanced Video Coding (or referred to in short as H.264/AVC). H.264/AVC is the powerful and state-of-the-art video compression standard recently developed by the ITU-T/ISO/IEC Joint Video Team (JVT) consisting of experts from ITU-T's Video Coding Experts Group (VCEG) and ISO/IEC's Moving Picture Experts Group (MPEG). As has been the case with past video coding standards, its design represents a delicate balance between coding gain, implementation complexity, and costs based on state of VLSI (ASICs and Microprocessors) design technology. It has brought the coding algorithm technology in synch with the VLSI technology that is available today or will be available in near future. Some algorithmic features that could not be considered in the past due to implementation complexity could now be accepted. New techniques developed since the time of the prior designs could be incorporated. Some features that provided some increase in coding gain but were too expensive to implement were not included. In the process, the H.264/AVC design emerged with an improvement in coding efficiency typically by a factor of two over MPEG-2—the most widely used video coding standard today—while keeping the cost within the acceptable range. Similar quality gains were shown relative to other prior designs for a very broad range of applications. Above all, this project has proven that the predictions of the demise of video compression algorithm innovations were little premature and that they are continuing to flourish vigorously.

This Special Issue opens with an overview paper about the H.264/AVC standard by Wiegand *et al.* As the title suggests, it provides a concise description of the most important tools used in the standard.

We then dive deeper into the algorithm. We start with two papers on inter-picture prediction and processing. Wedi and Musmann provide good insight into the workings of fractional-sample motion-compensated prediction in their paper "Motion and Aliasing Compensated Prediction for Hybrid Video Coding". Flierl and Girod describe how and why B-pictures work and some ways the B picture concept has been extended in H.264/AVC in their paper "Generalized B Pictures and the Draft H.264/AVC Video Compression Standard".

The next two papers focus on the transforms used and considered in the standardization process. The first of these, "Low-Complexity Transform and Quantization in H.264/AVC" by Malvar *et al.*, describes the integer DCT-like transform and quantization scaling methods adopted in the standard. This transform was designed with particular attention paid to the fact that real-number-based transform specification causes mismatches between encoders and decoders, and can be expensive to implement in products that do not have high end microprocessor or ASIC. The second paper, "Variable Block Size Transforms for H.264/AVC" by Wien, describes the effort spent by JVT on adapting the transform size to the motion estimation block size. This technology was considered to be very interesting but not fully mature or sufficiently clearly beneficial to coding efficiency, and a bit too difficult to implement for inclusion in the standard at this stage.

Deblocking filtering has been one of the centers of great discussions among the experts and has divided the video compression community for a long time. In H.264/AVC, years of past experience in this field have culminated into the development of a new and powerful design. In their paper "Adaptive Deblocking Filter" List *et al.* explain how the filter adapts itself based on the quantization parameter, different compression modes, and motion in a scene to be able to differentiate compression artifacts from the content of the scene. The result has been a filter design that has reasonable implementation complexity and provides a substantial benefit to both subjective and objective video quality.

Digital Object Identifier 10.1109/TCSVT.2003.815169

1051-8215/03$17.00 © 2003 IEEE

H.264/AVC in Wireless Environments

Thomas Stockhammer, Miska M. Hannuksela, and Thomas Wiegand

***Abstract*—Video transmission in wireless environments is a challenging task calling for high-compression efficiency as well as a network friendly design. Both have been major goals of the H.264/AVC standardization effort addressing "conversational" (i.e., video telephony) and "nonconversational" (i.e., storage, broadcast, or streaming) applications. The video compression performance of the H.264/AVC video coding layer typically provides a significant improvement. The network-friendly design goal of H.264/AVC is addressed via the network abstraction layer that has been developed to transport the coded video data over any existing and future networks including wireless systems. The main objective of this paper is to provide an overview over the tools which are likely to be used in wireless environments and discusses the most challenging application, wireless conversational services in greater detail. Appropriate justifications for the application of different tools based on experimental results are presented.**

***Index Terms*—Error concealment, error-resilient video coding, H.264/AVC, multiple reference frames, rate-distortion optimization, video coding standards, wireless video transmission.**

I. Introduction

SINCE 1997, the ITU-T's Video Coding Experts Group (VCEG) has been working on a new video coding standard with the internal denomination H.26L. In late 2001, the Moving Picture Expert Group (MPEG) and VCEG decided to work together as a Joint Video Team (JVT), and to create a single technical design called H.264/AVC for a forthcoming ITU-T Recommendation H.264/AVC and for a new part of the MPEG-4 standard called AVC [1][1], [2]. Since the meeting in November 2002, the technical specification is frozen and the standard text and software have been finalized. The primary goals of H.264/AVC are *improved coding efficiency* and *improved network adaptation*. The syntax of H.264/AVC typically permits a significant reduction in bit rate [3] compared to all previous standards such as ITU-T Rec. H.263 [4] and ISO/IEC JTC 1 MPEG-4 [5] at the same quality level.

The demand for fast and location-independent access to multimedia services offered on today's Internet is steadily increasing. Hence, most current and future cellular networks, like GSM-GPRS, UMTS, or CDMA-2000, contain a variety of packet-oriented transmission modes allowing transport of practically any type of IP-based traffic to and from mobile terminals, thus providing users with a simple and flexible transport interface. The third generation partnership project (3GPP) has selected several multimedia codecs for the inclusion into its multimedia specifications [6]. To provide basic video service in the first release of the 3G wireless systems, the well-established and almost identical baseline H.263 and the MPEG-4 visual simple profile have been integrated. The choice was based on the manageable complexity of the encoding and decoding process, as well as on the maturity and simplicity of the design.

However, due to the likely business models in emerging wireless systems in which the end-user's costs are proportional to the transmitted data volume and also due to limited resources bandwidth and transmission power, compression efficiency is the main target for wireless video and multimedia applications. This makes H.264/AVC coding an attractive candidate for all wireless applications including multimedia messaging services (MMS), packet-switched streaming services (PSS), and conversational applications. However, to allow transmission in different environments, not only is coding efficiency relevant, but also seamless and easy integration of the coded video into all current and possible future protocol and multiplex architectures. In addition, for conversational applications the video codec's support of enhanced error-resilience features is of major importance. This has also been taken into account in the standardization of this codec.

This paper is structured as follows. Section II introduces applications and transmission characteristics for wireless video applications. The transport of H.264/AVC video is briefly discussed and common test conditions for mobile video transmission are presented. Section III provides an overview over the H.264/AVC video coding standard from the perspective of wireless video applications. We categorize features according to their applicability in different video services. Section IV discusses the most challenging application in terms of delay constraints and error resilience, namely wireless conversational applications. A system description and problem formulation is followed by providing several alternatives on the system design using H.264/AVC as well as the combination of several modes. Section V provides experimental results for selected system concepts based on the common test conditions.

II. Video in Mobile Networks

A. Overview: Applications and Constraints

Video transmission for mobile terminals is likely to be a major application in emerging 3G systems and may be a key factor in their success. The video-capable display on mobile devices paves the road to several new applications. Three

Manuscript received April 9, 2002; revised May 10, 2003.

T. Stockhammer is with the Institute for Communications Engineering (LNT), Munich University of Technology (TUM), 80290 Munich, Germany (e-mail: stockhammer@ei.tum.de).

M. M. Hannuksela is with the Nokia Corporation, 33721 Tampere, Finland (e-mail: miska.hannuksela@nokia.com).

T. Wiegand is with the Fraunhofer-Institute for Telecommunications—Heinrich-Hertz-Institute Einsteinufer 37, 10587 Berlin, Germany (e-mail: wiegand@hhi.de).

Digital Object Identifier 10.1109/TCSVT.2003.815167

[1]All referenced standard documents can be accessed via anonymous ftp at ftp://standard.pictel.com/video_site, ftp://ftp.imtc-files.org/jvt-experts, ftp://ftp.ietf.org/, or ftp://www.3gpp.org/Specs/archive.

1051-8215/03$17.00 © 2003 IEEE

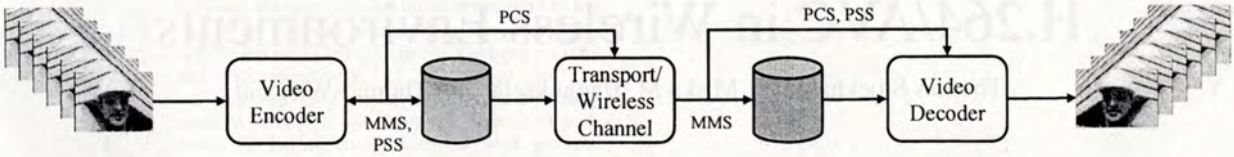


Fig. 1. Wireless video application MMS, PSS, and PCS: differentiation by real-time or offline processing for encoding, transmission, and decoding.

major service categories were identified in the H.264/AVC standardization process [7].

1) Circuit-switched [8] and packet-switched conversational services (PCS) [9] for video telephony and conferencing.
2) Live or pre-recorded video packet-switched streaming services (PSS) [10].
3) Video in multimedia messaging services (MMS) [11].

Although new services such as multimedia broadcast/multicast services (MBMS) [12] are planned for future releases of wireless networks, we restrict ourselves to single receiver applications. Mobile devices are hand-held and constrained in processing power and storage capacity. Therefore, a mobile video codec design must minimize terminal complexity while remaining consistent with the efficiency and robustness goals of the design. As complexity issues are discussed elsewhere in this issue [13], [14], we restrict ourselves to transmission constraints and properties.

The transmission requirements for the three identified applications can be distinguished with respect to requested data rate, the maximum allowed end-to-end delay, and the maximum delay jitter. This results in different system architectures for each of these applications. A simplified illustration is provided in Fig. 1. As MMS does not include any real-time constraints, encoding, transport, and decoding are completely separated. The recorded video signal is offline encoded and locally stored. The transmission is started using the stored signal at any time. The decoding process at the receiver is in general not started until the completion of the download. In PSS applications, the user typically requests pre-coded sequences, which are stored at a server. Whereas encoding and transmission are separated, decoding and display is started during transmission to minimize the initial delay and memory usage in mobile devices. Finally, in conversational services, the end-to-end delay has to be minimized to avoid any perceptual disturbances and to maintain synchronicity of audio and video. Therefore, encoding, transmission and decoding is performed simultaneously in real-time and, moreover, in both directions. These different ancillary conditions permit and require different strategies in encoding, transport, decoding, as well as in the underlying network and control architecture.

In general, the available bandwidth and therefore the bit-rate over the radio link are limited and the costs for a user are expected to be proportional to the reserved bit rate or the number of transmitted bits over the radio link. Thus, low bit rates are likely to be typical, and *compression efficiency* is the main requirement for a video coding standard to be successful in a mobile environment. This makes H.264/AVC a prime candidate for the use in wireless systems, because of its superior compression efficiency [3].

In addition, the mobile environment is characterized by harsh transmission conditions in terms of attenuation, shadowing, fading, and multi-user interference, which result in time- and location-varying channel conditions. The frequency of the channel variations highly depends on the environment, the user topology, the velocity of the mobile user, and the carrier frequency of the signal. For sufficiently long code words averaging over channel statistics is possible and transmission strategies can be used that are based on the long-term averages of fading states and the ergodic behavior of the channel. Many highly sophisticated radio link features such as broadband access, diversity techniques, space-time coding, multiple antenna systems, fast power control, interleaving, and forward error correction (FEC) by Turbo codes are used in 3G systems to reduce variations in channel conditions. However, only for fast-moving users and relatively large tolerated maximum delay can these advanced techniques provide a negligible bit error and radio block loss rate. Usually, some amount of residual errors has to be tolerated for low-delay applications due to the nonergodic behavior of the channel and the imperfectness of the applied signal processing. Therefore, in addition to high compression efficiency and reasonable complexity, a video coding standard to be applicable for conversational services in wireless environments has to be error resilient.

In addition, it is worth noting at this point that new directions in the design of wireless systems do not necessarily attempt to minimize the error rates in the system, but to maximize the throughput. This is especially appealing for services with relaxed delay constraints such as PSS and MMS. The nonergodic behavior of the channel is exploited such that in case of good channel states significantly higher data rate is supported than in bad channel states. In addition, reliable link layer protocols with persistent Automatic Repeat reQuest (ARQ) are usually used to guarantee error-free delivery. For example, in the high-speed downlink packet access (HSDPA) concept [15] ARQ, adaptive modulation schemes, and multiuser scheduling taking into account the channel states are combined to significantly enhance the throughput in wireless systems.

3G wireless transmission stacks usually consist of two different bearer types, dedicated and shared channels. Whereas in dedicated channels one user gets assigned a fixed data rate for the entire transmission interval, shared channels allow a dynamic bit-rate allocation similar to ATM or GSM GPRS. HSDPA will be an extension of the shared channel concept on the air interface. Except for MMS all streaming and conversational applications are assumed to use dedicated channels in the initial phase of 3G wireless systems due to their almost constant bit-rate behavior. In modern system designs, an application can request one of many different quality-of-service (QoS) classes. QoS classes contain parameters like a maximum error rate,

TABLE I
QoS SERVICE CLASSES IN PACKET RADIO SYSTEMS [15]

Traffic Class	Fundamental Characteristics	Typical Examples
Conversational	Preserve time relation between information entities of the stream Conversational pattern (stringent and low delay)	Voice and video telephony, Video conferencing
Streaming	Preserve time relation (variation) between information entities of the stream	Streaming multimedia (video, audio, etc.)
Interactive	Request response pattern, Preserve data integrity	Web browsing, network games
Background	Destination is not expecting the data within a certain time Preserve data integrity	Background download of e-mails, files, etc.

maximum delay, and a guaranteed maximum data rate. Furthermore, according to [16], applications are usually divided into different service classes: conversational, streaming, interactive, and background traffic. Characteristics and typical examples are shown in Table I.

B. Transport of H.264/AVC Video in Wireless Systems

According to Fig. 2, H.264/AVC distinguishes between two different conceptual layers, the video coding layer (VCL) and the network abstraction layer (NAL). Both the VCL and the NAL are part of the H.264/AVC standard. The VCL specifies an efficient representation for the coded video signal. The NAL of H.264/AVC defines the interface between the video codec itself and the outside world. It operates on NAL units which give support for the packet-based approach of most existing networks. At the NAL decoder interface, it is assumed that the NAL units are delivered in decoding order and that packets are either received correctly, are lost, or an error flag in the NAL unit header can be raised if the payload contains bit errors. The latter feature is not part of the standard as the flag can be used for different purposes. However, it provides a way to signal an error indication through the entire network. Additionally, interface specifications are required for different transport protocols that will be specified by the responsible standardization bodies. The exact transport and encapsulation of NAL units for different transport systems, such as H.320 [17], MPEG-2 Systems [18], and RTP/IP [19], are also outside the scope of the H.264/AVC standardization. The NAL decoder interface is normatively defined in the standard, whereas the interface between the VCL and the NAL is conceptual and helps in describing and separating the tasks of the VCL and the NAL.

For real-time video services over 3G mobile networks, two protocol stacks are of major interest. 3GPP has specified a multimedia telephony service for circuit-switched channels [8] based on ITU-T Recommendation H.324M. For IP-based packet-switched communication, 3GPP has chosen to use SIP and SDP for call control [20] and RTP for media transport [9]. In other words, the IP-based protocol stack as presented in [21] will be used in packet-switched 3G mobile services. While the H.324 and the RTP/UDP/IP stacks have different roots and a completely different switching philosophy, the loss and delay effects on the media data when transmitting over wireless dedicated channels are very similar.

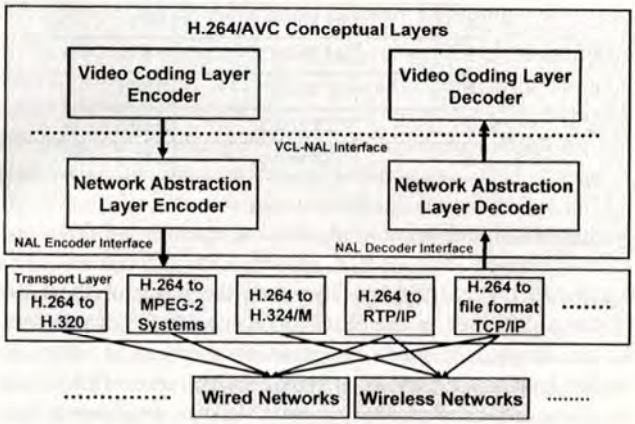


Fig. 2. H.264/AVC standard in transport environment.

H.324 [22] was primarily established by the ITU-T for low-bit-rate circuit-switched modem links and error prone extensions for mobile circuit switched low-bit-rate conversational services have been added. H.324M officially known as ITU-T Rec. H.324 Annex C, allows transmission over low, moderate, and high bit-error rate circuit switched links. 3GPP adopted H.324M including an error robust extension of the multiplexing protocol H.223 known as H.223 Annex B as the protocol used for circuit-switched video communication. This multiplexing protocol includes two layers: an error-resilient packet-based multiplex layer and an adaptation layer featuring common error detection capabilities, such as sequence numbering and cyclic redundancy checks (CRSs). Therefore, it is very similar to the RTP/UDP/IP stack (see [21]).

For packet-switched services, 3GPP/3GPP2 agreed on an IP-based stack. Fig. 3 shows a typical packetization of a NAL unit encapsulated in RTP/UDP/IP [19] through the 3GPP2 user plane protocol stack. After robust header compression (RoHC) [23] this IP/UDP/RTP packet is encapsulated into one packet data convergence protocol/point-to-point protocol (PDCP/PPP) packet that becomes a radio link control (RLC)-service data unit (SDU). The RLC protocol can operate in three modes: 1) transparent; 2) unacknowledged; and 3) acknowledged mode [26]. The RLC protocol provides segmentation and retransmission services for both users and control data. The transparent and unacknowledged mode RLC entities are defined to be

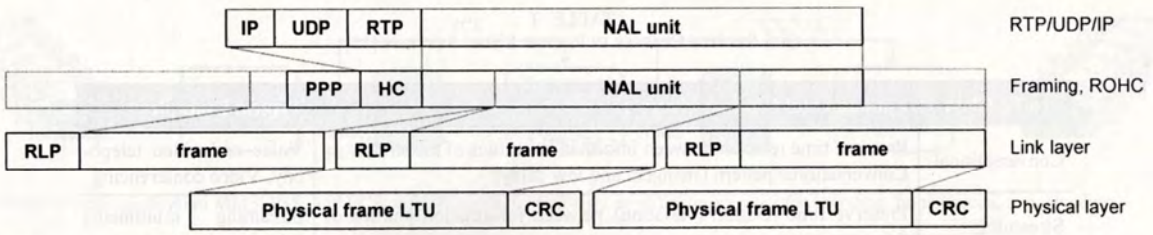


Fig. 3. Packetization through 3GPP2 user plane protocol stack.

TABLE II
BIT-ERROR PATTERNS

No.	Bit rate	Length	BER	Mobile Speed	Application
1	64 kbit/s	60 s	9.3e-3	3 km/h	Streaming
2	64 kbit/s	60 s	2.9e-3	3 km/h	Streaming
3	64 kbit/s	180 s	5.1e-4	3 km/h	Conversational
4	64 kbit/s	180 s	1.7e-4	50km/h	Conversational
5	128 kbit/s	180 s	5.0e-4	3 km/h	Conversational
6	128 kbit/s	180 s	2.0e-4	50km/h	Conversational

unidirectional and acknowledged mode entities are described as bi-directional. For all RLC modes, CRC error detection is performed on the physical layer and the result of the CRC check is delivered to the RLC together with the actual data. In the transparent mode no protocol overhead is added to higher layer data. Erroneous protocol data units (PDUs) can be discarded or marked erroneous. In the unacknowledged mode, no retransmission protocol is in use and data delivery is not guaranteed. Received erroneous data is either marked or discarded depending on the configuration. In the acknowledged mode, an automatic repeat request mechanism is used for backward error correction.

As video packets are of varying length by nature, the length of RLC-SDU's varies as well. If an RLC-SDU is larger than an RLC-PDU, the SDU is segmented into several PDUs. In the used, unacknowledged, and acknowledged modes, the flow of variable-size RLC-SDUs is continuous to avoid padding of bits as necessary for the transparent mode. In unacknowledged mode, if any of the RLC-PDUs containing data from a certain RLC-SDU have not been received correctly, the RLC-SDU is typically discarded. In acknowledged mode, the RLC/radio link protocol (RLP) layer can perform re-transmissions.

Additionally, both protocol stacks H.324 and RTP/IP/UDP use reliable setup and control protocols, H.245 and SIP, respectively. Hence, it can be assumed that a small amount of control information can be transported out-of-band in a reliable way. The resulting properties of real-time low-delay video transmission are therefore very similar in both cases. Packets are transmitted over underlying transports protocols and channels, which provide framing, encapsulation, error detection, and reliable setup. We focus hereafter on the RTP/IP-based transmission over wireless channels [21].

C. Common Test Conditions for Wireless Video

In the H.264/AVC standardization process, the importance of mobile video transmission has been recognized by adopting appropriate common test conditions for 3G mobile transmission for circuit switched conversational services based on H.324M [24] and for packet-switched conversational and streaming services [25]. These test conditions permit the selection of appropriate coding features, testing and evaluating error-resilience features, as well as meaningful anchor results. In this paper, we focus on the IP-based test conditions. The common test conditions define six test-case combinations for packet-switched conversational services as well as packet-switched streaming services over 3G mobile networks. Additionally, the test conditions include simplified offline 3GPP/3GPP2 simulation software, programming interfaces and evaluation criteria. Radio channel conditions are simulated with bit-error patterns, which were generated from simulated mobile radio channel conditions. The bit-error patterns are captured above the physical layer and below the RLC/RLP layer and, therefore, they are used as the physical layer simulation in practice. The properties bit rate, length, bit-error rate, and the mobile speed of the bit-error patterns are presented in Table II.

The bit errors in the files are statistically dependent, as channel coding and decoding included in 3G systems produces burst errors. This has been taken into account by evaluating the bit-error pattern files in the following. Patterns 1 and 2 are mostly suited to be used in video streaming applications, where RLP/RLC layer re-transmissions can correct many of the frame losses. The applied channel-coding scheme is a Turbo code scheme and power control targeting throughput maximization rather than error minimization. Patterns 1 and 2 are unrealistic for conversational service, as an acceptable quality cannot be achieved with such high error rates without retransmissions.

Patterns 3–6 are meant to simulate a more reliable, lower error-rate bearer that is required in conversational applications. Assuming a random byte starting position within the file the packet error probability $p_e(r)$ depending of the length of the packet r in bytes can be determined. These error probabilities $p_e(r)$ for all bit-error patterns are shown in Fig. 4. It is obvious

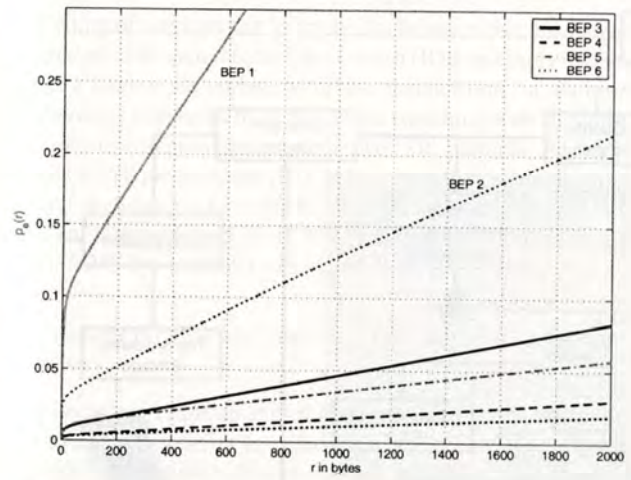


Fig. 4. Packet-loss probability $p_e(r)$ over packet length r in bytes for bit-error patterns according to [25].

that the error rate increases significantly with increasing packet length. For bit-error patterns (BEP1 and 2), the loss rates are not acceptable as already short packets, e.g., 500 bytes, have loss probabilities up to 25%. The high error rates require retransmission on the link layer.

The patterns useful for conversational services provide very decent error characteristics for reasonable packet lengths. The loss probability for reasonable packet sizes up to 1000 bytes is below 5%. This means that typical fixed Internet packet loss probabilities (compare [21]) are not exceeded. Note that with higher speed (50 km/h), the channel tends to be "more ergodic" than in case of the walking user (3 km/h). Therefore, the error rates are usually higher for slowly moving users than for fast-moving users.

During the standardization process, it was agreed in the very beginning that the standard should include error-resilience features for IP-based wired and wireless transmission. Usually two kinds of errors are present in today's transmission systems: bit inversion errors or packet losses. However, all relevant multiplexing protocols like H.223 and UDP/IP and almost all underlying mobile systems include packet loss and bit-error detection capabilities applying sequence numbering and block check sequences, respectively. Therefore, it can be assumed that a vast majority of erroneous transmission packets can be detected. Moreover, even if packets were detected to contain bit errors, decoding could be attempted. Some research has been conducted in this area and, in a few scenarios, gains have been reported for still image transmission [27]. However, in the standardization of H.264/AVC for the development of the reference software, bit-erroneous packets have been considered as being discarded by the receiver for the following reasons.

1) Processing of bit-erroneous packets is likely to be possible in a receiving mobile device only, as gateways and receivers having fixed network connection typically drop erroneous packets.
2) Joint source-channel decoding, such as trellis-based decoding of variable-length codes or iterative source and channel decoding might be applied. However, these techniques have not yet shown significant improvements for video decoding.
3) The decoding based on lost packets serves as a lower bound on the performance in bit-error-prone environments and, therefore, provides a valid benchmark of the performance of H.264/AVC in error-prone environment.
4) Finally, handling of bit errors generally complicates the implementation of decoder software significantly. As the test model software for H.264 was developed for multiple purposes, only simple but meaningful network interfaces have been integrated.

III. H.264/AVC—An Efficient and Flexible Video Coding Toolbox

A. *Compression Efficiency and Encoder Flexibility*

The features for compression efficiency are discussed elsewhere in this issue, we will only briefly present the key features of the standard, for more details we refer to [2]. Although the design of the H.264/AVC codec basically follows the hybrid design (motion compensation with lossy coding of residual signal) of prior video coding standards such as MPEG-2, H.263, and MPEG-4, it contains many new features that enable it to achieve a significant improvement in terms of compression efficiency. This is the main reason why H.264/AVC will be very attractive for use in wireless environments with the costly resource bit rate. The main features for significantly increased coding efficiency are multiframe motion-compensated prediction, adaptive block size for motion compensation, generalized B-pictures concepts, quartel-pel motion accuracy, intra coding utilizing prediction in the spatial domain, in-loop deblocking filters, and efficient entropy-coding methods.

The normative part of a video coding standard in general only consists of the appropriate definition of the order and semantics of the syntax elements and the decoding of error-free bit streams. This allows a significant flexibility at the encoder, which can, on the one hand, be exploited for pure compression efficiency, and on the other hand, several included features in the standard can be selected by the encoder for other purposes such as error resilience, random access, etc. A typical encoder with the main encoding options is shown in Fig. 5.

The encoding options relevant for wireless transmission are highlighted. The recorded video data is preprocessed by appropriate spatial and temporal preprocessing such that the data rates and displays in a wireless environment are well-matched. For the quantization of transform coefficients, H.264 coding uses scalar quantization. The quantizers are arranged in a way that there is an increase of approximately 12.5% from one quantization parameter (QP) to the next. The quantized transform coefficients are converted into coding symbols and all syntax elements of a macroblock (MB) including the coding symbols are conveyed by entropy coding methods. A MB can always be coded in one of several intra modes with and without prediction, as well as various efficient inter modes. Each motion-compensated mode corresponds to a specific partition of the MB into fixed-size blocks used for motion description, and up to 16 motion vectors may be transmitted for a MB. In addition, for each MB, a different reference frame can be selected. Finally, a NAL

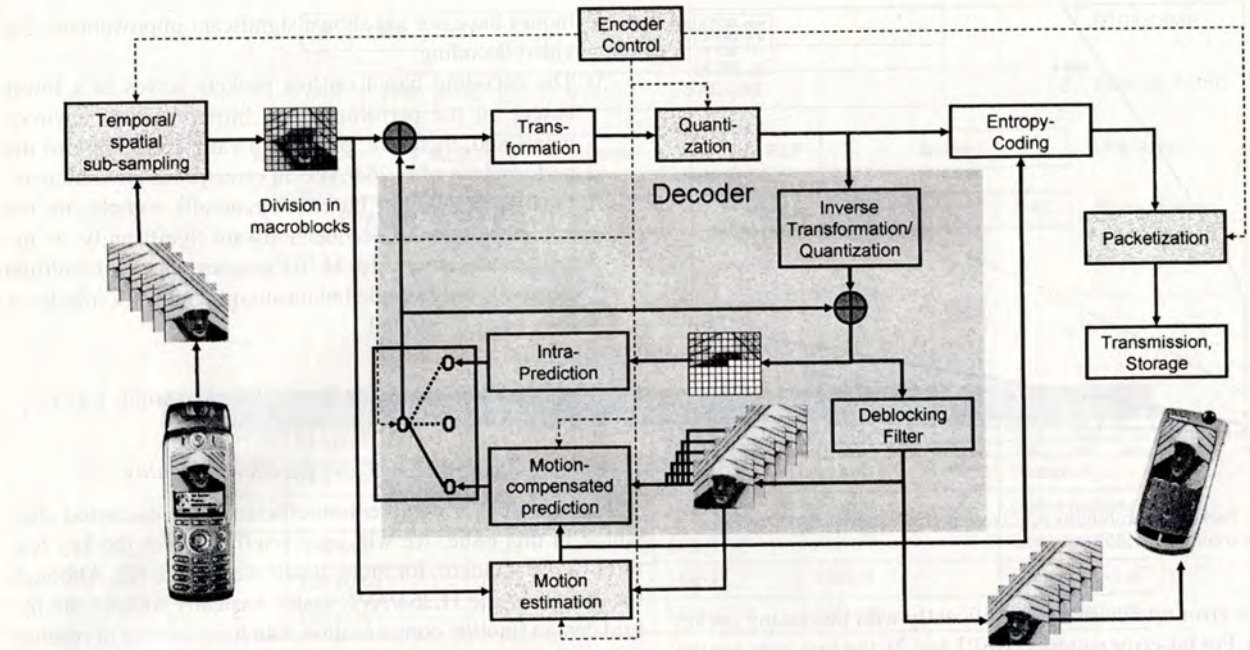


Fig. 5. H.264/AVC encoder realization with coding options.

unit in single-slice mode consists of the coded MBs of an entire frame or a subset of frame. More details on the packetization as well as on the appropriate selection of the presented different modes are discussed in Section IV.

B. Features for Multimedia Messaging and Wireless Packet-Based Streaming

In addition to pure compression efficiency features, additional tools for different purposes have been included in H.264/AVC. We will highlight those features with application to wireless video transmission. Because of the strict separation of encoding, transmission, and decoding, the main issue for MMS is compression efficiency. Other helpful features include the insertion of regular intra frames with instantaneous decoder refresh (IDR) for random access and fast forward. The rate control is typically applied such that video quality is almost constant over the sequence, regardless of the scene complexity except for constraints from the hypothetical reference decoder (HRD) [28]. If time, memory capabilities, and battery power permit, even several encoding passes for optimized rate-distortion (R-D) performance would be possible. On the link layer, reliable transmission strategies as known for data transmission such as file download are used.

Due to on-line transmission and decoding, streaming applications involve more technical challenges than MMS. Usually, pre-encoded data is requested by the user, which inherently does not allow an adaptation to the transmission conditions such as bit rate or error rate in the encoding process. However, the receiver usually buffers the received data and starts play-back after a few seconds. Once starting playback, a continuous presentation of the sequence should be guaranteed. As wireless channels usually show ergodic behavior within a window of a few seconds, reliable transmission schemes can be applied on the link layer, especially when the channel is known at the transmitter or retransmissions for erroneous link layer packets can be used as for example in the acknowledged mode. Slow variance due to distance, shadowing, or varying multiuser topology in the supported cell with renewed resource allocation transform the wireless channel in a slowly varying variable-bit-rate channel. With an appropriate setting of the initial delay and receiver buffer a certain quality of service can be guaranteed [28].

Furthermore, general channel-adaptive streaming technologies, which allow reacting to variable bit-rate channels, have gained significant interest recently. According to [30], these techniques can be grouped into three different categories. Firstly, *adaptive media playout* [31] is a new technique that allows a streaming media client, without the involvement of the server, to control the rate at which data is consumed by the playout process. Therefore, the probability of decoder buffer underflows and overflows can be reduced, but still noticeable artifacts in the displayed video occur. A second technology for a streaming media system is proposed, which makes decisions that govern how to allocate transmission resources among packets. Recent work [32] provides a flexible framework to allow *R-D optimized packet scheduling*. Finally, it is shown that this R-D-optimized transmission can be supported, if media streams are pre-encoded with appropriate packet dependencies, possibly adapted to the channel (*channel-adaptive packet dependency control*) [33].

The latter techniques are supported by H.264/AVC by various means. As the streaming server is in general aware of the current channel bit rate, the transmitter can decide to send one of several pre-encoded versions of the same content taking into account the expected channel behavior. If the channel rate fluctuates only in a small range, frame dropping of nonreference frames might be sufficient resulting in well-known temporal scalability.

Switching of versions can be applied at I-frames that are also indicated as instantaneous decoder refresh (IDR) pictures to compensate large scale variations of the channel rate. In addition, H.264/AVC supports efficient version switching with the introduction of synchronization-predictive (SP) pictures. For more details on SP pictures, see [35]. Note that quality scalable video coding methods such as MPEG-4 fine-grain scalability (FGS) [34] are not supported by H.264/AVC and such extensions of H.264/AVC are currently not planned.

C. Features for Wireless Conversational Services—Error Resilience

A necessary requirement for conversational services is a low end-to-end delay being less that 250 ms. This delay constraint has two main impacts on the video transmitted over wireless bearer services with constant bit rate. Firstly, features have to be provided which allow adapting the bit-rate such that over a short window a constant bit-rate can be maintained. In addition, usually only temporally backward references in motion compensation are used in conversational applications, since prediction from future frames would introduce additional delay. Secondly, within the round-trip time of the communication, the channel usually shows nonergodic behavior and transmission errors cannot be avoided. Whereas the first issue can be solved by adapting the QP appropriately, the second issue requires error-resiliency tools in the video codec itself. More exactly, an error-resilient video coding standard suitable for conversational wireless services has to provide features to combat two problems: on the one hand, it is necessary to minimize the visual effect of errors within one frame. On the other hand, as errors cannot be avoided, the well-known problem of spatio-temporal error propagation in hybrid video coding has to be limited. We will present all error-resilience features included in the H.264/AVC standard and provide further details on the exact application in Section IV.

Packet loss probability and the visual degradation from packet losses can be reduced by introducing slice-structured coding. A slice is a sequence of MBs and provides spatially distinct resynchronization points within the video data for a single frame. No intra-frame prediction takes place across slice boundaries. With that, packet loss probability can be reduced if slices and, therefore, transmission packets are relatively small, since the probability of a bit-error hitting a short packet is generally lower than for large packets (see, e.g., Fig. 4). Moreover, short packets reduce the amount of lost information and, hence, the error is limited and error concealment methods can be applied successfully. However, the loss of intra-frame prediction and the increased overhead associated with decreasing slice sizes adversely affect coding performance and requires additional overhead per slice. Especially for mobile transmission, where the packet size clearly affects loss probability, a careful selection of the packet size is necessary. H.264/AVC specifies several enhanced concepts to reduce the artifacts caused by packet losses within one frame. Slices can be grouped by the use of aggregation packets into one packet and, therefore, concepts such as group-of-block (GOB) and *slice interleaving* [37], [38] are possible. This does not reduce the coding overhead in the VCL, but the costly RTP overhead of up to 40 bytes per packet can be avoided.

A more advanced and generalized concept is provided by a feature that has been called by the proponents *flexible MB ordering* (FMO) [39]. FMO permits the specification of different patterns for the mapping of MBs to slices including checkerboard-like patterns, sub-pictures within a picture (e.g., splitting a CIF picture into four QCIF pictures), or a dispersed mapping of MBs to slices. FMO is especially powerful in conjunction with appropriate error concealment when the samples of a missing slice are surrounded by many samples of correctly decoded slices. For more details on FMO, see [21].

Another error-resilience feature in H.264/AVC is *data partitioning*, which can also reduce visual artifacts resulting from packet losses, especially if prioritization or unequal error protection is provided by the network. For more details on the data-partitioning mode, we refer to [21]. In general, any kind of *forward error protection* (FEC) in combination with interleaving for packet lossy channels can be applied. A simple solution is provided by RFC2733 [40], more advanced schemes have been evaluated in many papers, e.g., [41], [42]. However, in the following, we do not consider FEC schemes in the transport layer as this requires a reasonable number of packets per codeword.

Despite all these techniques, packet losses and resulting reference frame mismatches between encoder and decoder are usually not avoidable. Then, the effects of spatio-temporal error propagation are, in general, severe. The impairment caused by transmission errors decays over time to some extent. However, the leakage in standardized video decoders, such as H.264/AVC, is not very strong, and quick recovery can only be achieved when image regions are encoded in intra mode, i.e., without reference to a previously coded frame. Completely intra-coded frames are usually not inserted in real-time and conversational video applications as the instantaneous bit rate and the resulting delay is increased significantly. Instead, H.264/AVC allows encoding of single MBs for regions that cannot be predicted efficiently as it is also known from other standards. In H.264/AVC, the efficient intra prediction can be constrained to intra MBs only to avoid error propagation from inter-coded MBs to refreshing intra-coded MBs. Another feature in H.264/AVC is the possibility to select the reference frame from the multiframe buffer. Both features have mainly been introduced for improved coding efficiency, but they can efficiently be used to limit the error propagation. Conservative approaches transmit a number of intra-coded MBs anticipating transmission errors. In this situation, the selection of intra-coded MBs can be done either randomly or preferably in a certain update pattern. For details and early work on this subject, see [43]–[45]. Multiple reference frames can also be used to limit the error propagation, for example in *video redundancy coding* schemes (see, e.g., [46]). In addition, a method known from H.263 under the acronym *redundant slices* will be supported in JVT coding. This will allow sending the same slice predicted from different reference frames which provides the decoder the possibility to predict this slice from error-free reference areas. Finally, multiple reference frames can be successfully combined with a feedback channel, which will be discussed in detail among others in Section IV.

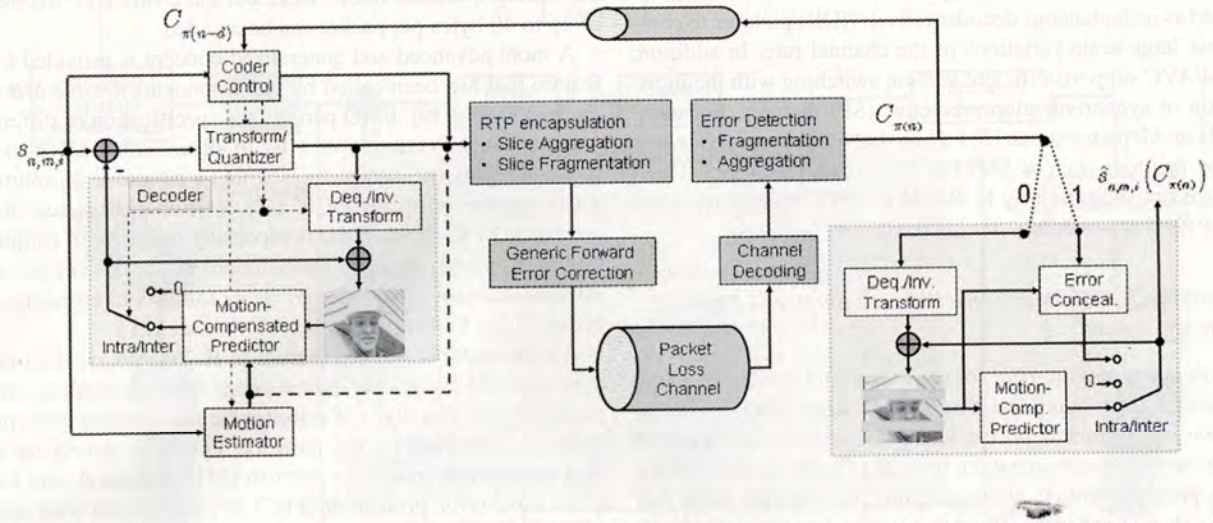


Fig. 6. H.264/AVC in IP-based packet-lossy environment with RTP encapsulation, generic forward error correction, delayed feedback information, and error concealment.

IV. Using H.264/AVC in Wireless Conversational Services

A. Problem Formulation and System Setup

The various error-resilience tools as described in the previous section provide a significant amount of freedom and flexibility for the implementation of H.264/AVC in wireless conversational services. A main criterion for the performance of the system is the appropriate selection of one or several of the mentioned tools together with the exact parameters, e.g., the position and number of intra MBs.

We will discuss in the following channel behavior and error concealment by formalizing the notation for sample representation. The investigated video transmission system is shown in Fig. 6. H.264/AVC video encoding is based on a sequential encoding of frames denoted with the index $n = 1, \ldots, N$ with N being the total number of frames to be encoded. In most existing video coding standards including H.264/AVC, within each frame video encoding is typically based on sequential encoding of MBs (except for FMO) denoted by index $m = 1, \ldots, M$, where M specifies the total number of MBs in one frame and depends on the spatial resolution of the video sequence. The encoding process creates slices by grouping a certain number of MBs. Picture number n and start MB address m_j are binary coded in the slice header. The coded representation of a slice is the payload of a NAL unit. The RTP payload specification specifies simple encapsulation of NAL units. In addition, several NAL units can be combined into one aggregation packet or one NAL unit can be fragmented into several transport packets [19], [21].

For notational convenience, let us define the number of transmission packets to transmit all frames up to n as $\pi(n)$. With that, we can define the packet loss or channel behavior c as a binary sequence $\{0,1\}^{\pi(n)}$ indicating whether a slice is lost (indicated by 1) or correctly received (indicated by 0). Obviously, if a NAL unit with the encapsulated slice is lost, all MBs contained by this slice are lost. It can be assumed that the decoder is aware of any lost packet as discussed previously. The channel-loss sequence is random and, therefore, we denote it as $C_{\pi(n)}$, where the statistics are in general unknown to the encoder. According to Fig. 6, in addition to the forward link it possible that a low-bit-rate reliable back-channel from the decoder to the encoder is available which allows reporting a d-frame delayed version $C_{\pi(n-d)}$ of the observed channel behavior at the decoder to the encoder. In RTP/IP environments, this is usually based on RTCP messages, and in wireless environments, internal protocols might be used.

The decoder processes the received sequence of packets. Whereas correctly received packets are decoded as usual for the lost packet, an error-concealment algorithm has to be invoked. The reconstructed sample $s_{n,m,i}$ at position i in MB m and frame n depends on the channel behavior and on the decoder error concealment. In inter-coding mode, i.e., when motion-compensated prediction (MCP) is utilized, the loss of information in one frame has a considerable impact on the quality of the following frames, if the concealed image content is referenced for MCP. Because errors remain visible for a longer period of time, the resulting artifacts are particularly annoying. Therefore, due to the motion-compensation process and the resulting error propagation, the reconstructed image depends not only on the lost packets for the current frame, but in general on the entire channel-loss sequence $C_{\pi(n)}$. We denote this dependency by $\hat{s}_{n,m,i}(o, C_{\pi(n)})$

In the following, we will discuss appropriate extensions of the encoder, the decoder, and the transmission environment, which are either necessary or at least beneficial to enhance the quality of the transmitted video.

B. Decoder Extensions—Loss Detection and Error Concealment

The H.264 standard defines how a decoder reacts to an error-free bit stream. In addition, a decoder implementation has also to deal with transmission errors. As we discussed earlier, it is assumed that bit errors are detected by the lower layer

entities and any remaining transmission error results in a packet loss. Therefore, we address the reaction of the decoder to slice losses. Two major issues are important for an error-resilient decoder: a robust video decoder has to detect transmission errors, and appropriate concealment on detected errors has to be applied. In this section, we present how the H.264 test model decoder meets the goal of error resiliency.

The error detection capabilities of the test model decoder are based on two assumptions about the error detection operation of the underlying system. First, bit-erroneous slices are discarded prior to passing the slices to the test model decoder. Second, received data is buffered in a way that the correct decoding order is recovered. In other words, the test model decoder expects noncorrupted slices in a correct decoding order. Temporal and spatial localization of lost packets is left to the decoder. In particular, the decoder has to detect if an entire picture or one or more slices of a picture were lost. Losses of entire pictures are detected using frame numbers associated with each frame and carried in slice headers. A frame number n is incremented by one for each coded and transmitted frame that is further used for motion compensation. These frames are herein referred to as reference frames. For disposable nonreference pictures, such as conventional B-pictures, the frame number is incremented relative to the value in the most recent reference frame that precedes the disposable picture in the bit-stream order.

The decoder generates a slice structure for each received single slice packet and forwards it to the VCL decoder which maintains a state machine that keeps track of the expected frame number n_e. Moreover, the decoder maintains a loss indication for each MB within the current picture. At the beginning of a new picture, the binary map is reset to indicate that all MBs were lost. If the frame number n of the next slice to be decoded equals n_e, the decoder decodes the slice and updates the binary map. If n is greater than n_e, it is deduced that all the received slices of the previous picture have been decoded. Then, the binary map is investigated, and if the picture is not fully covered by correctly decoded MBs, a slice loss is inferred and losses are concealed as presented in the following. Moreover, if n is greater than $n_e + 1$, the decoder infers a loss of pictures and inserts concealed pictures to the reference picture buffer as if the lost pictures were decoded. The concealment is accomplished by copying the previous decoded picture. Finally, the decoder resets the binary map and decodes the next slice of the next picture.

Error concealment is a nonnormative feature in the H.264 test model. The target for the selected error concealment is to provide a basic level of error resiliency for the decoder. Any error-robust coding scheme proposed for H.264 should be compared against the H.264 test model equipped with the selected error concealment algorithms. Two well-known concealment algorithms, weighted pixel value averaging for intra pictures [47] and boundary-matching-based motion vector recovery for inter pictures [48], were tailored for H.264 as summarized below and described in details in [49] and [50].

Weighted pixel value averaging operates as follows. If a MB has not been received, it is concealed from the pixel values of spatially adjacent MBs. If a lost MB has at least two correctly decoded neighboring MBs, only these neighbors are used in the concealment process. Otherwise, previously concealed neighboring MBs take part in the process, too. Each pixel value in a MB to be concealed is formed as a weighted sum of the closest boundary pixels of the selected adjacent MBs. The weight associated with each boundary pixel is relative to the inverse distance between the pixel to be concealed and the boundary pixel. The performance of the intra concealment method is shown in Fig. 7



Fig. 7. Intra frame error concealment.

In the motion vector recovery algorithm, the motion activity of the correctly received slices of the current picture is investigated first. If the average length of a motion vector component is smaller than a pre-defined threshold (currently 1/4 pixels), all the lost slices are copied from co-located positions in the reference frame. Otherwise, motion-compensated error concealment is used, and the motion vectors of the lost MBs are predicted as described in the following paragraphs. The image is scanned MB-column-wise from left and right edges to the center of the image. Consecutive lost MBs in a column are concealed starting from top and bottom of the lost area toward to center of the area. This processing order is used to ensure that lost MBs at the center of an image are concealed using as many neighboring concealed MBs as possible.

Each 8×8 luminance block of a MB to be concealed is handled separately. If a block has spatially adjacent blocks whose motion vectors are correctly received, these motion vectors and their reference pictures are used to obtain a candidate prediction block. If all the motion vectors in the adjacent blocks are lost, neighboring concealed motion vectors are used similarly. In addition, the spatially co-located block from the previous frame is always one of the candidates. The candidate prediction block whose boundary matching error is the smallest is chosen. The boundary matching error is defined as the sum of the pixel-wise absolute differences of the adjacent luminance pixels in the concealed block and its decoded or concealed neighbor blocks. The lost prediction error block is not concealed. The performance of the inter-frame concealment is shown in Fig. 8.

C. Encoder Extensions

Let us now consider algorithms and rules for the appropriate selection of different encoding parameters according to the presentation in Fig. 5 for wireless conversational services. First, the rate control has to guarantee that the delay jitter is as small as possible. A good choice is to adapt for each frame to obtain almost constant encoding, but keep the QP within one frame constant. In the case that the highest QP cannot achieve the required bit rate, frame dropping is introduced; otherwise, the frame rate

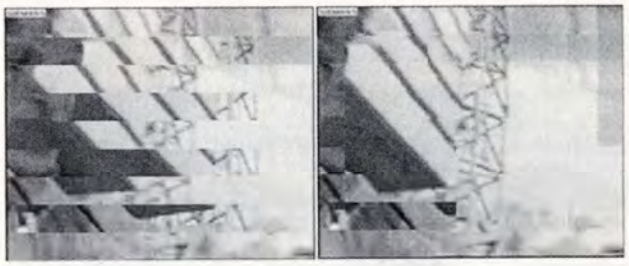


Fig. 8. Inter-frame error concealment.

is kept constant. Obviously, this results in varying quality depending of the complexity of the scene. Low-motion scenes with little complexity have higher quality than for example frames at the beginning of a sequence or at a scene cut.

As discussed in Section III, H.264/AVC provides a large flexibility on the selection of appropriate coding modes. The concept of selecting appropriate coding options in optimized encoder designs for many video coding standards is based on R-D optimization algorithms [51],[52]. The two cost terms "rate" and "distortion" are linearly combined and the mode is selected such that the total cost is minimized. This can be formalized by defining the set of selectable coding options for one MB as $\mathcal{O}$. Assuming the introduced distortion when encoding with a certain mode o as $D(o)$ and the corresponding rate as $R(o)$, the rate-constrained mode decision selects the coding option o^* such that the Lagrangian cost functional is minimized, i.e.,

$$o^* = \arg\min_{o\in\mathcal{O}}(D(o) + \lambda R(o)) \tag{1}$$

with λ being the Lagrange parameter for appropriate weighting of rate and distortion. In the H.264/AVC test model, the Lagrangian mode selection is used for motion vector search as well as MB mode and reference frame selection. Then, for the distortion $D(o)$, the sum of squared sample differences (SSD) or the sum of absolute sample difference (SAD) are used, and for the rate $R(o)$, the number of bits for the encoding is used. The selection of the Lagrange parameter depends on the selected QPs (for details, see [53]). In addition, the mode selection might be extended by selecting the appropriate QP for each MB, as the QP can be changed at least in small ranges for each MB. This is not considered in the following.

As discussed in Section III-C, the tools for increased error resilience, in particular those to limit error propagation, do not significantly differ from those used for compression efficiency. Features like multiframe prediction or intra MB coding are not exclusively error-resilience tools. They are also used to increase coding efficiency in error-free environments providing a trade-off that is left to the encoder. This also means that bad decisions at the encoder can lead to poor results in coding efficiency or error resiliency or both. Therefore, the selection of the coding mode according to (1) is modified taking into account the influence of the random lossy channel. In the case of error-prone transmission, the distortion in (1) is replaced with the expected decoder distortion when encoding with mode o. Assuming that the encoder can access information about the channel statistics $C_{\pi(n)}$, the encoder can get an estimate of the expected decoder distortion $D_{n,m}(o, C_{\pi(n)})$ when encoding MB m in frame n at the decoder by the expected distortion as

$$D_{n,m}\left(o, C_{\pi(n)}\right) = \sum_{i=1}^{I} E_{C_{\pi(n)}}\left|s_{n,m,i} - \hat{s}_{n,m,i}\left(o, C_{\pi(n)}\right)\right|^2 \tag{2}$$

where the expectation is over the random process characterizing the channel $C_{\pi(n)}$. With the expected distortion measure, the mode selection for lossy channels is identical to that in (1) except for modified distortion term according to (2). However, the same parameter λ [54] and the same set of possible coding options $\mathcal{O}$ are used.

This leaves the problem of computing the expected decoder distortion at the encoder which depends on the coding mode o, the channel statistics $C_{\pi(n)}$, and the applied error concealment in the decoder. The estimate of the expected sample distortion in packet loss environment has been addressed in several publications. For example, in [58], [55], or [56], methods to estimate the distortion introduced due the transmission errors and the resulting drift are presented. A similar approach has recently been proposed within the H.264/AVC standardization process which attempts to measure the drift noise between encoder and decoder [57]. In suboptimal approaches [55]–[57], the quantization noise and the distortion introduced by the transmission errors are linearly combined. The encoder keeps track of an estimated sample distortion and, therefore, requires additional complexity in encoder, which is dependent on the actual method chosen.

The most recognized out of these methods, called recursive optimal per-sample estimate (ROPE) algorithm [58], provides an estimation by keeping track of the first- and second-order moment of $\hat{s}_{n,m,i}, E\left\{\hat{s}_{n,m,i}(o, C_{\pi(n)})\right\}$, and $E\left\{\hat{s}^2_{n,m,i}(o, C_{\pi(n)})\right\}$, respectively. For H.263-like encoding ROPE can provide an exact estimate of the expected decoder distortion. As two moments for each sample have to be tracked in the encoder, the added complexity of ROPE is approximately twice the complexity of the decoder. However, the extension of the ROPE algorithm to H.264/AVC is not straightforward. The in-loop deblocking filter, the fractional sample motion accuracy, the complex intra prediction and the advanced error concealment require taking into account the expectation of products of samples at different positions to obtain an accurate estimation which makes the ROPE either infeasible or inaccurate in this case.

Therefore, a powerful yet complex method has been introduced into the H.264/AVC test model to estimate the expected decoder distortion [54]. Let us assume that we have K copies of the random variable channel behavior at the encoder, denoted as $C_{\pi(n)}(k)$. Additionally, assume that the set of random variables $C_{\pi(n)}(k), k = 1, \cdots, K$ are *identically* and *independently* distributed (*i.i.d.*). Then, as $K \to \infty$, it follows by the strong law of large numbers that

$$\frac{1}{K}\sum_{k=1}^{K}\left|s_{n,m,i} - \hat{s}_{n,m,i}\left(C_{\pi(n)}(k)\right)\right|^2 = E_{C_{\pi(n)}}\left|s_{n,m,i} - \hat{s}_{n,m,i}\left(C_{\pi(n)}\right)\right|^2 \tag{3}$$

holds with probability 1. An interpretation of the left-hand side leads to a simple solution of the previously stated problem to estimate the expected sample distortion. In the encoder, K copies of the random variable channel behavior and the decoder are operated. The reconstruction of the sample value depends on the channel behavior $C_{\pi(n)}(k)$ and the decoder including error concealment. The K copies of channel and decoder pairs in the encoder operate independently. Therefore, the expected distortion at the decoder can be estimated accurately in the encoder if K is chosen large enough. However, the added complexity in the encoder is obviously at least K times the decoder complexity. For details on the implementation as well as comparison of suboptimal modes based on ROPE, we refer to [54].

It was later demonstrated in [59] and [60] that a technique known as isolated regions, which combines periodical intra MB coding and limitation of inter prediction, can provide competitive simulation results compared to the error-robust MB mode selection of H.264 test model, and the best simulation results were obtained when the two MB mode-selection algorithms were combined.

The packet size is usually upper bounded by a MTU size of the underlying network. However, if bit errors cause entire packet losses, it might be an advantage to reduce the packet size. Conservative approaches limit the packet or (in our simulation environment) slice size to a fixed number of MBs, e.g., a line of MBs is transmitted in one packet. However, this makes especially important image parts very susceptible to packet losses as for example suddenly appearing objects need intra coding or high motion areas require an extensive motion vector rate. A more suitable, but still conservative, approach is the introduction of slice boundaries such that slices have almost the same length in number of bytes. This makes all packets similarly susceptible to bit errors. This method has been proven to work quite well already for MPEG-4 and can also be applied with the flexible encoding framework of H.264/AVC.

D. Exploiting Feedback in H.264/AVC

Multiple reference frames used in error-prone environment can most successfully be combined with a feedback channel. Due to the bidirectional nature of conversational applications, it is common that the encoder has knowledge of the experienced channel at the decoder, usually with a small delay. In our framework this can be expressed by the knowledge of a d-frame delayed version of the random channel $C_{\pi(n-d)}$ at the encoder. This characteristic can be conveyed from the decoder to the encoder by acknowledging correctly received slices (ACK), sending a not-acknowledge message (NAK) for missing slices or both types of messages. In general, it can be assumed that the reverse channel is error-free and the overhead is negligible. In common data transmission applications, the lost packets would obviously be re-transmitted. However, in a low-delay environment, this is not feasible, but the observed channel characteristic are still useful at the encoder even if the erroneous frame has already been decoded and concealed. The support of these techniques is out of the focus of the standardization of H.264, and a full support of the presented concepts might not be possible with current transport and control protocols. However, it seems worth to mention and discuss these concepts in here in detail as it shows the flexibility of H.264 as well as it provides motivation for inclusion of feedback in system designs.

In previous standards and transport environments similar approaches have already been discussed, usually limited by the reduced syntax capabilities of the video standard. A simple yet powerful approach suitable for video codecs using just one reference frame such as MPEG-2, H.261, or H.263 version 1 has been introduced in [61] and [62] under the name *error tracking*. When receiving a NAK on parts of frame $n-d$ or the entire frame $n-d$, the encoder attempts to track the error to obtain an estimate of the quality of frame $n-1$, which serves as reference for frame n. Appropriate actions after having tracked the error are for example presented in [56], and [61]–[64]. Note that with this concept, error propagation in frame n is only removed if frames $n-d+1,\ldots,n-1$ have been received at the decoder without any error.

A technique addressing the problem of continuing error propagation has been introduced, among others, in [65]–[67] under the acronym *NEWPRED*. Based on these early nonstandard compliant solutions in H.263 Annex N [68], a reference picture selection (RPS) for each GOB is specified such that the NEWPRED technique can be applied. RPS can be operated in two different modes. In the negative acknowledgment mode (NAM), the encoder only alters its operation in the case of reception of a NAK. Then, the encoder attempts to use an intact reference frame for the erroneous GOBs. To completely eliminate error propagation, this mode has to be combined with independent segment decoding (ISD) according to Annex R of H.263 [68]. In the positive acknowledgment mode (PAM), the encoder is only allowed to reference confirmed GOBs. If no GOBs are available to be referenced, intra coding has to be applied. NEWPRED allows to completely eliminate error propagation in frame n, even if additional errors have occurred in frames $n-d+1,\ldots,n-1$.

The flexibility provided in H.263 Annex U [68] and especially H.264/AVC to select the MB mode and reference frames on MB or subMB basis allows incorporating NEWPRED in a straightforward manner [56]. Therefore, let us define three different states of transmitted packets at the encoder: ACK, NAK, and outstanding acknowledgment (OAK). Then, based on the exploitation of these messages in the encoder, we discuss three modes which can elegantly be integrated into the R-D optimized mode selection according to (1).

1) Feedback Mode 1: Restricting Reference Areas to ACK: In this case, the reference area is restricted to frames or slices which have been acknowledged. This can be formalized in the context of (1) by applying the encoding distortion $D(o)$ in (1), but altering the accessible coding options $\mathcal{O}$ such that only acknowledged areas can be used for reference. In addition, if no reference area is available, or if no satisfying match is found in the allowed area, intra coding is applied. Although in the presentation of a single frame an error might be visible, error propagation and reference frame mismatch between encoder can be completely avoided independent of the error concealment applied at the decoder if correctly decoded samples are not altered. However, in the used test model JM1.7, the deblocking filter operation in the motion-compensation

loop is applied over slice boundaries, which restricts the area to be referenced significantly, or a complete removal of encoder and decoder mismatch is not possible. Although the influence of this mismatch is, in general, negligible, in the final design of H.264/AVC the deblocking filter can adaptively be switched on and off at slice boundaries to allow mismatch-free operation.

2) Feedback Mode 2: Referencing ACK and Error Concealed NAK: In this case, the reference area is again restricted; however, in addition to acknowledged areas, also the areas which the decoder signaled as lost can be referenced. Therefore, the reference frames in the encoders multi-frame frame buffer are updated with reception of each ACK and NAK by applying the identical error concealment as the decoder applies. This is obviously very critical, as the error concealment is—for good reasons—nonnormative in common video coding standards including H.264/AVC. Only if the encoder is aware of the decoder's error concealment by any external means, this mode can provide benefits compared to feedback mode 1. In the context of the mode decision in (1), we have again a restricted set of coding modes $\mathcal{O}$ and, in addition, the encoding distortion is replaced by the deterministic decoder distortion.

3) Feedback Mode 3: Unrestricted Reference Areas With Expected Distortion Updating: In [56] and [58], techniques have been proposed which allow combining the error-resilient MB mode selection with feedback information. In this case, the expected decoder distortion computation is altered such that, for all packets $1, \ldots, \pi(n-d)$, the channel is deterministic at the encoder, and the expected distortion is computed for the packets with status OAK. In our case, packets containing MBs in frames $\pi(n-d)+1, \ldots, \pi(n)$ are random. The set of selectable coding options $\mathcal{O}$ is not altered compared to pure coding efficiency mode selection. This method is especially beneficial compared to mode 1 and 2, if the feedback is significantly delayed. In the case of the multiple decoder approach, this can be integrated by applying feedback mode 2 not only to the reference frames, but also to all decoders in the encoder. In combination with ROPE, however, the complexity of this method increases since the moments of the previous d frames have to be re-tracked [58].

V. Selected Simulation Results for Different System Concepts

A. Simulation Conditions and Evaluation Criteria

In the following, we will present simulation results based on the test conditions that show the influence of the selection of different error-resilience features for the quality of the decoded images. For all following tests the H.264/AVC test model software version JM1.7 is used. Note that in the final standard [1], the zig-zag scanning and run-length coding is replaced by context-adaptive variable length codes (CVLC). All UVLCs are replaced by CVLC, which are adapted to the statistics of different syntax elements. In addition, quantizer values have been shifted. However, all changes from JM1.7 to the final standard are of little relevance to the presented results and conclusions in this paper.

The reported PSNR is the arithmetic mean over the decoded luminance PSNR over all frames of the encoded sequence and over 100 transmission and decoding runs. The 100 starting positions for the error patterns have been selected such that they are almost equally distributed over the error pattern. For all comparable results, the same starting positions and, therefore, the same channel statistics have been applied. In addition, we present results for the cumulative distribution of the decoded luminance PSNR for each frame, i.e., the likelihood that the PSNR of the frames of the sequence is smaller than the value on the x axis. This shows the variance in the decoded quality. It is assumed that the high-level syntax parameters have been transmitted in advance and out-of-band applying a reliable setup protocol. The NAL overhead, the RTP/UDP/IP overhead after RoHC, and the link layer overhead is taken into account in the bit-rate constraints according to [25].

For the following simulations, we concentrate on test case 5 from [25], which includes the QCIF test sequence "Foreman" (30 Hz, 300 frames) at a constant frame rate of 7.5 Hz at bit-error pattern 3 according to Table II, i.e., a mobile user at 3 km/h and maximum bit-rate 64 kbit/s. This is the most critical case in terms of error probability, additional test results will be made available online[2]. For the following tests, entropy coding based on the UVLC and only one reference frame has been applied, if not stated otherwise. The encoded sequences are I-P-P-P... sequences; B-pictures are excluded due to the unacceptable delay involved in the encoding process. Note that due to the repeated decoding of an encoded file, every 75th frame is an I-frame, i.e., an I-frame occurs every 10 s. Constrained intra has been used to avoid error propagation from inter MBs to intra MBs. For all encoding runs, R-D optimized mode selection and motion vector selection according to (1) have been used. The distortion $D(o)$ and the set of coding modes $\mathcal{O}$ is appropriately selected according to the applied features. In the case of using the expected decoder distortion, the number of decoders operated in the encoder has been fixed to $K = 100$. Unless stated otherwise, the error concealment in the decoder is based on the advanced error concealment as presented in Section IV-B, whereas the multiple decoders in the encoder always apply previous frame concealment. This reduces encoding complexity significantly and results only in negligible performance losses for the investigated cases.

B. Low-Delay Rate Control

Version JM1.7 of the H.264/AVC test model encoder which is used in the experiments does not include a rate control to achieve a constant bit rate for wireless conversational services. Moreover, the rate control introduced in later versions of H.264/AVC test model encoder is not suitable for constant rate encoding. For this reason we have added a rate control which provides an almost constant bit-rate encoding for each frame by adapting the QP for each frame appropriately. Therefore, before we investigate the error-resilience features in H.264/AVC, we will first focus on the effect of bit-rate control that is necessary for constant bit-rate conversational applications. Fig. 9 shows the cumulative distribution of the encoding PSNR for the applied rate control and a fixed QP such that both encoded files result in the

[2]For additional simulation results, we refer to http://www.lnt.ei.tum.de/~stockhammer.

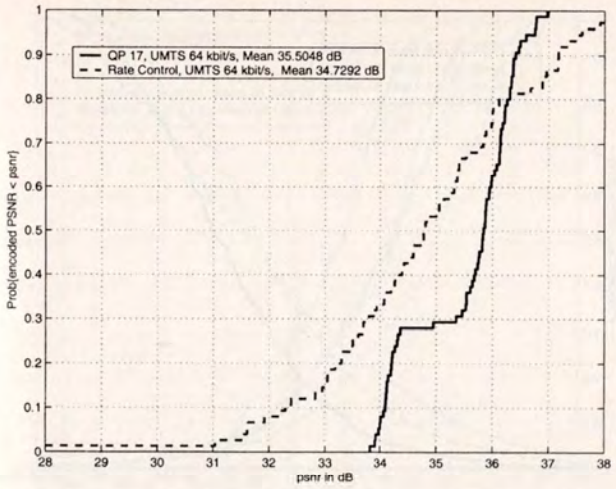


Fig. 9. Cumulative distribution of encoding luminance PSNR for each frame for constant QP 17 and constant bit rate such that rate constraint of 64 kbit/s for UMTS is fulfilled.

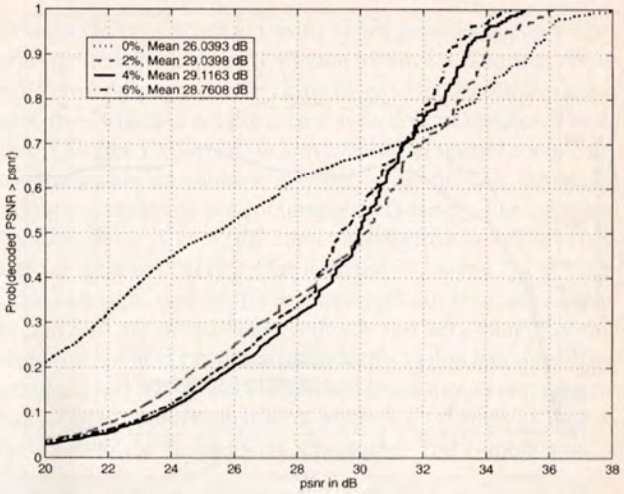


Fig. 10. Cumulative distribution of decoded PSNR for different NAL unit erasure rates for the estimation of the expected distortion in the encoder.

same total bit-rate, and, additionally the file can be transmitted over the 64 kbit/s link including NAL unit, packet, and link layer overhead. However, the fixed QP results in an extremely varying data rate and, therefore, the introduced delay jitter is not acceptable. In the encoding process, no error-resilience tools have been used, i.e., one frame is encapsulated into one NAL unit, for $D(o)$ the encoding distortion is applied, and the set of coding modes $\mathcal{O}$ is unrestricted.

The average PSNR for the rate control is about 0.8 dB below the PSNR for the fixed QP. In addition, the probability for low encoded PSNR is significantly higher as for complex scenes the QP has to be adapted appropriately. Therefore, it can be seen that the rate control necessary for conversational applications involves an inherent decrease in quality if the average PSNR is the measure of interest.

C. $R - E\{D\}$-Optimized MB Mode Selection

In this section we investigate the performance of the system in case that the channel statistics are taken into account into the selection of the coding options in the encoder. For this purpose we replace the encoding distortion $D(o)$ in (1) by the expected decoder distortion assuming a channel producing independent packet losses with probability p. As we use the mapping of one frame to one transport packet and apply the strict rate control producing almost a constant number of bytes for each encoded frame, the size of each frame results in roughly 1000 bytes. The corresponding loss rate for packets of this size for bit-error pattern 3 is approximately 4%–5% according to Fig. 4. Fig. 10 shows the cumulative distribution of decoded PSNR for different NAL unit erasure rates $p = \{0, 0.02, 0.04, 0.06\}$ for the estimation of the expected distortion in the encoder. Looking at the results for the average PSNR, it can be seen that the introduction of loss-aware R-D optimization ($p > 0$) increases the decoded quality significantly compared to the results with pure encoding distortion ($p = 0$). The average PSNR increases by at least 3 dB when compared to the to pure R-D optimization. The advantage of $R-E\{D\}$ optimization is even more evident when looking at the cumulative distribution of the different strategies. Whereas in the case of no error resilience, the probability of bad frames (frames below 22 dB) is at an unacceptable ratio of about 30%, for loss-aware coding, this is reduced significantly to less than 8%. It is also obvious that if the expected error rate matches the experienced error rate on the channel, the performance is optimal (see $p = 4\%$). However, it can also be seen that a mismatch in the expected error rate in the encoder does not have significant influence. The performance of $p = 2\%$ and $p = 6\%$ is only slightly inferior to the matching expected error rate. Therefore, a rough estimation of the expected decoder distortion at the encoder seems to be good enough for a good mode selection. Note the significant loss in average PSNR for wireless transmission compared to the error-free transmission according to Fig. 9 of more than 5 dB.

D. Slices and Error Concealment

The introduction of slices in the encoding has two beneficial aspects when transmitting over wireless channels, but adversely affects the coding efficiency due to increased packet overhead and reduced prediction within one frame, as e.g., motion vector prediction and spatial intra prediction is not allowed over slice boundaries. The two positive effects with the introduction of slices are the reduced error probability of shorter packets (see Fig. 4) and, the re-synchronization possibility within one frame. The latter technique allows restarting the decoding process at each slice and, in addition, it allows applying advanced error concealment as for example presented in Section IV-B. However, for packet-lossy transmission over the Internet, the introduction of slices does not, in general, provide gains in the decoded quality [69] as long as the slice size is below the MTU size, as the loss of a packet is then independent of its length. This is different for wireless transmission: Fig. 11 shows the average decoded PSNR for different number of packets per frame N_p and MB mode decision with encoding distortion. The experimental conditions are similar to the above section otherwise. For a given number of packets per frame, the size of each packet is selected such that the packets roughly have the same number of bytes. This makes their susceptibility to bit errors almost identical.

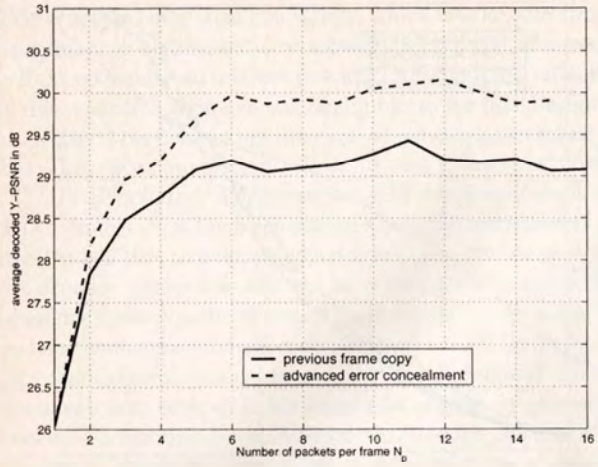


Fig. 11. Average decoded PSNR for different number of packets per frame and different error-concealment schemes; mode selection with encoding distortion.

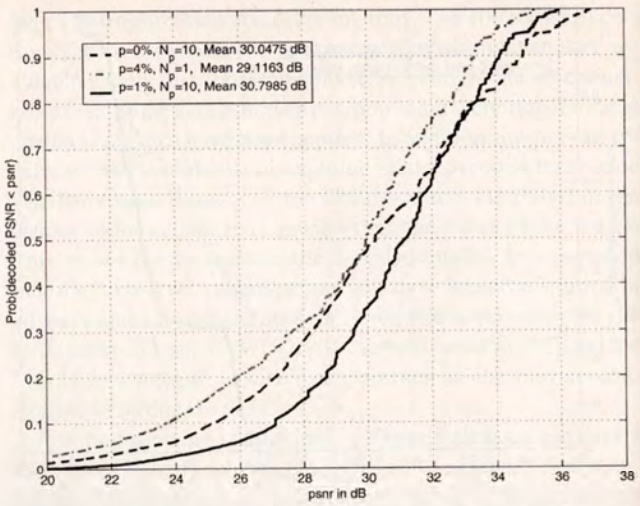


Fig. 12. Cumulative distribution of decoded PSNR for different error-resilience strategies: $R - E\{D\}$-optimized intra updates with and without slice structuring and delay $d = 2$ for different assumed loss probabilities p.

The average decoded PSNR is shown for previous frame copy error concealment and advanced error concealment according to Section IV-B. The benefit of introducing slice structuring in the encoding process is obvious from the results. Compared to the "one frame—one packet" mode indicated by $N_p = 1$ the introduction of shorter packets increases the decoded quality significantly for both error concealment methods. For about $N_p = 6$, the curve flattens out and decreases again for higher $N_p > 12$ due to increasing packet overhead and the reduced compression efficiency. Although a clear maximum cannot be determined, for the wireless environment according to our test conditions, a reasonable number of packets per frame is about 10. The resulting packet size in this case is in the range of 100 bytes. However, note that for the simulations, RoHC was applied, which reduces the typical IP/UDP/RTP overhead from 40 bytes to about 3 bytes and, therefore, the packetization overhead is less significant. The benefits of the advanced error concealment are also obvious from Fig. 11. As can be seen, the gains for advanced error concealment increase with increasing number of packets, as better concealment is possible due to increased number of neighboring MBs in case of losing a single slice.

For the experiments in Fig. 11, no explicit means to reduce the error propagation have been used. However, we can obviously combine the MB mode selection based on the expected decoder distortion with the slice structured coding. As indicated, the loss rate for decreased packet size decreases compared to the single packet for one frame. The loss rate can be estimated by dividing the approximated number of bytes for each frame, roughly 1000 bytes, by the number of packets. The loss probability can then again be estimated with Fig. 4 using the resulting average packet length. The combination of slice-structured coding and adaptive intra MB updates has been investigated and a comparison with the best cases of the previous two system designs is provided in Fig. 12 based on the cumulative distribution of the decoded PSNR. For the slice-structured coding with encoding distortion ($p = 0\%$) the number of packets is selected as $N_p = 10$. For the expected decoder distortion without slice-structuring ($N_p = 1$), the adapted loss-rate $p = 4\%$ is chosen. Finally, for the combination of slice-structured coding and channel-adaptive intra updates, the number of packets per frame is selected as $N_p = 10$ and, therefore, the appropriate loss probability to compute the expected decoder distortion according to Fig. 4 is about $p = 1\%$.

The average decoded PSNR indicates that an optimized combination of both error-resilience schemes outperforms each of the presented error-resilience schemes significantly. The result that slice-structured coding is superior to intra updates cannot be generalized for all sequences. The repeated I-frame insertion and the camera pan in the test sequence "Foreman" results in a significant amount of intra information, even if only the encoding distortion is chosen in the mode selection. This might change for different or longer sequences with less intra information. From the cumulative distribution, it can be observed that the probability for bad frames below 22 dB in PSNR is almost vanishing for the combined mode. The presented results indicate that slices in combination with advanced error concealment significantly outperform the single packet for one frame approach. However, the loss compared to error-free transmission is still about 4 dB in average PSNR.

From the results, it can be conjectured that for wireless transmission as investigated in this case, other approaches, which reduce the artifacts within one frame, might provide additional benefits. This includes concepts such as FMO, slice interleaving, or even generic forward-error correction in combination with a NAL unit fragmentation scheme as recently introduced in the draft RTP payload specification for H.264/AVC [19]. Also, data partitioning with appropriate unequal error protection might enhance the quality of the decoded video. In addition, it is conjectured from the results that a better adaptation of the link layer error protection scheme with appropriate interleaving could increase the overall system performance. These features are currently investigated and are subject of future work.

E. Exploiting Feedback in Video Encoding

Finally, we investigate a system which exploits multiple reference frames and network feedback. We restrict our simula-

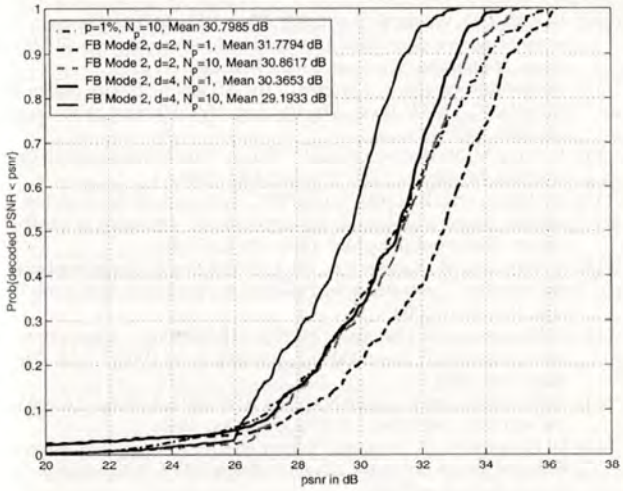


Fig. 13. Cumulative distribution of decoded PSNR for different error-resilience strategies: R-D-optimized intra updates with slice structuring, and feedback mode 2 with and without slice structuring for delay $d = 2$ and $d = 4$.

tion results to feedback mode 2 according to the presentation in Section IV-D with advanced error concealment. There are two reasons for this. On the one hand, the deblocking and mismatch problem present for JM1.7 can be avoided. On the other hand, it has been shown previously that feedback mode 1 and feedback mode 2 result in almost identical performance [70]. Therefore, we chose feedback mode 2 due to the simpler implementation, at least in our simulation environment. Feedback mode 3 is excluded as, on the one hand, the complexity of this mode is rather high and, on the other hand, as we operate with low feedback delays, the expected benefits are only marginal. In contrast to the previous simulations, we use five reference frames for the feedback mode. Fig. 13 shows the cumulative distribution of decoded PSNR for different error-resilience strategies: R-D-optimized intra updates with slice structuring, as well as feedback mode 2 with and without slice structuring for delay $d = 2$ and $d = 4$ frames, which corresponds to a round-trip time of about 250 and 500 ms, respectively.

Let us focus on the delay $d = 2$ case first. The results indicate that the optimized intra mode with slice structuring and MB mode selection with expected decoder distortion and feedback mode 2 perform very similar based on the cumulative distribution and the average decoded PSNR. The feedback mode might still be beneficial in this case as the complex estimation of the decoder distortion is not necessary for the feedback case. However, much more interesting is the case with feedback and no slice structuring. In contrast to the case without feedback (see Fig. 12), the renouncement of slice-structured coding provides a significantly higher average decoded PSNR. Initially, this is obviously surprising, as packet loss rate is still much lower when several slices are used and also the visual effects for a decoded frame when losing a single slice should be lower than in case of losing an entire frame. The first effect can indeed be observed from the cumulative distribution. The probability of bad frames (PSNR below 22 dB) is higher for $N_p = 1$ than for $N_p = 10$. However, in the case of no errors, the increased coding efficiency when not using slices provides many frames with significantly higher PSNR than for slice structuring. As we avoid error propagation, the correctly received frames are really error-free, which is not the case if we use intra updates. Therefore, if feedback information is available and several completely lost frames are tolerable, it is better to use no slice structured coding than harming the compression efficiency. For increased feedback delay $d = 4$, the curves are shifted to the left compared to feedback delay 2. However, the $d = 4$ and $N_p = 1$ performs almost as well as the best case without feedback. Therefore, in the case of available feedback, this very simple system without considering expected decoder distortion and slice structuring and just relying on multiple reference frames outperforms many highly sophisticated error-resilience schemes as long as the delay of the feedback is reasonable. The combination of these methods according to feedback mode 3 is currently investigated and should allow adaptively selecting the best methods, however, with significantly increased encoding complexity.

VI. Conclusions

H.264/AVC promises some significant advances of the state-of-the-art of standardized video coding in mobile applications. In addition to excellent coding efficiency, the design of H.264/AVC also takes into account network adaptation providing large flexibility for its use in wireless applications. The tools provided in H.264/AVC for error resilience do not necessarily differ from the compression efficiency features such as intra MBs or multiple reference frames. However, in the case of error-prone transmission, the selection methods have to be changed by using the expected decoder distortion or by restricting the set of accessible coding options. In experimental results based on common test conditions, it has been shown that in case without any feedback, several slices in combination with channel-adaptive R-D optimized mode selection is a promising approach. In this case, further investigation with advanced error-resilience tools such as flexible MB ordering, data partitioning, and generic forward error correction, might provide benefits. However, in the case of available feedback, the application of multiple reference frames to exclude error propagation without slice structuring provides excellent results.

Acknowledgment

The authors would like to thank T. Oelbaum, D. Kontopodis, Y.-K. Wang, V. Varsa, and A. Hourunranta for implementing and testing parts of the algorithms, V. Varsa and G. Liebl for providing the test conditions and software simulator, S. Wenger, N. Färber, K. Stuhlmüller, E. Steinbach, and B. Girod for useful discussions, and JVT for the collaborative work and the technically outstanding discussions and contributions.

References

[1] "Final committee draft: Editor's proposed revisions," in *Joint Video Team (JVT) of ISO/IEC MPEG and ITU-T VCEG*, T. Wiegand, Ed., Feb. 2003, JVT-F100.

[2] T. Wiegand, G. J. Sullivan, G. Bjøntegaard, and A. Luthra, "Overview of the H.264/AVC video coding standard," *IEEE Trans. Circuits Syst. Video Technol.*, vol. 13, pp. 560–576, July 2003.

[3] T. Wiegand, H. Schwarz, A. Joch, F. Kossentini, and G. J. Sullivan, "Rate-constrained coder control and comparison of video coding standards," *IEEE Trans. Circuits Syst. Video Technol.*, vol. 13, pp. 688–703, July 2003.
[4] "Video Coding for Low Bitrate Communication, Version 1," ITU-T, ITU-T Recommendation H.263, 1995.
[5] "Coding of Audio-Visual Objects—Part 2: Visual," ISO/IEC JTC1, ISO/IEC 14 496-2 (MPEG-4 visual version 1), 1999.
[6] "Multimedia Messaging Service (MMS); Media Formats and Codecs," 3GPP Technical Specification 3GPP TR 26.140.
[7] S. Wenger, M. Hannuksela, and T. Stockhammer, "Identified H.26L Applications," ITU-T SG 16, Doc. VCEG-L34, Eibsee, Germany, 2001.
[8] "Codec for Circuit Switched Multimedia Telephony Service; General Description," 3GPP Technical Specification 3GPP TR 26.110.
[9] "Packet Switched Conversational Multimedia Applications; Default Codecs," 3GPP Technical Specification 3GPP TR 26.235.
[10] "Transparent End-to-End Packet Switched Streaming Service (PSS); RTP Usage Model," 3GPP Technical Specification 3GPP TR 26.937.
[11] "Multimedia Messaging Service (MMS); Media Formats and Codecs," 3GPP Technical Specification 3GPP TR 26.140.
[12] "Multimedia Broadcast/Multicast Services," 3GPP Technical Specification 3GPP TR 29.846.
[13] M. Horowitz, A. Joch, F. Kossentini, and A. Hallapuro, "H.264/AVC decoder complexity analysis," *IEEE Trans. Circuits Syst. Video Technol.*, vol. 13, pp. 704–716, July 2003.
[14] V. Lappalainen, A. Hallapuro, and T. D. Hämäläinen, "Complexity of optimized H.264/AVC video decoder implementation," *IEEE Trans. Circuits Syst. Video Technol.*, vol. 13, pp. 717–725, July 2003.
[15] "High Speed Downlink Packet Access (HSDPA); Overall UTRAN Description," 3GPP Technical Specification 3GPP TR 25.855.
[16] H. Holma and A. Toskala, Eds., *WCDMA for UMTS: Radio Access For Third Generation Mobile Communications*. New York: Wiley, 2000.
[17] *Narrow-Band Visual Telephone Systems and Terminal Equipment, Rev. 4*, ITU-T Recommendation H.320, 1999.
[18] "Generic Coding of Moving Pictures and Associated Audio Information," ISO/IEC International Standard 13 818, 1994.
[19] S. Wenger, T. Stockhammer, and M. M. Hannuksela, "RTP payload format for H.264 video," in *Internet Draft, Work in Progress*, Mar. 2003, Draft-wenger-avt-rtp-h264-01.txt.
[20] "3rd GPP; Technical Specification Group Core Network; IP Multimedia Call Control Protocol Based on SIP and SDP," 3GPP Technical Specification 3GPP TS 24.229.
[21] S. Wenger, "H.264/AVC over IP," *IEEE Trans. Circuits Syst. Video Technol.*, vol. 13, pp. 645–656, July 2003.
[22] D. Lindberg, "The H.324 multimedia communication standard," *IEEE Commun. Mag.*, vol. 34, pp. 46–51, Dec. 1996.
[23] H. Hannu, L.-E. Jonsson, R. Hakenberg, T. Koren, K. Le, Z. Liu, A. Martensson, A. Miyazaki, K. Svanbro, T. Wiebke, T. Yoshimura, and H. Zheng, "RObust header compression (ROHC): Framework and four profiles: RTP, UDP, ESP, and uncompressed," in RFC 3095, July 2001.
[24] "Common conditions for video performance evaluation in H.324/M error-prone systems, VCEG (SG16/Q15)," in Ninth Meeting, Redbank, NJ, Oct. 1999, ITU-T Q15-I-60.
[25] G. Roth, R. Sjöberg, G. Liebl, T. Stockhammer, V. Varsa, and M. Karczewicz, "Common Test Conditions for RTP/IP Over 3GPP/3GPP2,", Austin, TX, ITU-T SG16 Doc. VCEG-M77, 2001.
[26] "Radio Link Control (RLC) Protocol Specification," 3GPP Technical Specification 3GPP TS 25.322.
[27] S. S. Hemami, "Robust image transmission using resynchronizing variable-length codes and error concealment," *IEEE J. Select. Areas Commun.*, vol. 18, pp. 927–939, June 2000.
[28] J. Ribas-Corbera, P. A. Chou, and S. Regunathan, "A generalized hypothetical reference decoder for H.264/AVC," *IEEE Trans. Circuits Syst. Video Technol.*, vol. 13, pp. 674–687, July 2003.
[29] H. Jenkac, T. Stockhammer, and G. Kuhn, "Streaming media in variable bit-rate environments," presented at the Packet Video Workshop, Nantes, France, Apr..
[30] B. Girod, M. Kalman, Y. J. Liang, and R. Zhang, "Advances in video channel-adaptive streaming," in ICIP 2002, Rochester, NY, Sept. 2002.
[31] E. G. Steinbach, N. Färber, and B. Girod, "Adaptive play-out for law latency video streaming," presented at the ICIP 2001, Thessaloniki, Greece, Oct. 2001.
[32] P. A. Chou and Z. Miao, "Rate-distortion optimized streaming of packetized media," *IEEE Trans. Multimedia*, submitted for publication.
[33] Y. J. Liang and B. Girod, "Rate-distortion optimized low—Latency video streaming using channel-adaptive bitstream assembly," presented at the ICME2002, Lausanne, Switzerland, Aug. 2002.
[34] H. Radha, M. van der Schaar, and Y. Chen, "The MPEG-4 fine-grained scalable video coding method for multimedia streaming over IP," *IEEE Trans. Multimedia*, vol. 3, pp. 53–68, Mar. 2001.
[35] M. Karczewicz and R. Kurçeren, "The SP and SI frames design for H.264/AVC," *IEEE Trans. Circuits Syst. Video Technol.*, vol. 13, pp. 637–644, July 2003.
[36] V. Varsa, M. M. Hannuksela, and Y. Wang, "Non-Normative Error Concealment Algorithms," ITU-T VCEG-N62, 2001.
[37] S. Wenger and G. Cotê, "Using RFC 2429 and H.263+ at low to medium bit-rates for low-latency applications," presented at the Proc. Packet Video Workshop, New York, NY, Apr. 1999.
[38] V. Varsa and M. Karczewicz, "Slice interleaving in compressed video packetization," presented at the Packet Video Workshop 2000, Forte Village, Italy, May 2000.
[39] S. Wenger and M. Horowitz, "Flexible MB ordering—A new error resilience tool for IP-based video," presented at the IWDC 2002, Capri, Italy, Sept. 2002.
[40] J. Rosenberg and H. Schulzrine, "An RTP payload format for generic forward error correction," in RFC 2733, Dec. 1999.
[41] G. Carle and E. W. Biersack, "Survey of error recovery techniques for IP-based audio-visual multicast applications," *IEEE Network Mag.*, vol. 11, pp. 2–14, Nov. 1997.
[42] U. Horn, K. Stuhlmüller, M. Link, and B. Girod, "Robust internet video transmission based on scalable coding and unequal error protection," *IEEE Trans. Image Processing*, vol. 15, pp. 77–94, Sept. 1999.
[43] Q. F. Zhu and L. Kerofsky, "Joint source coding, transport processing, and error concealment for H.323-based packet video," *Proc. SPIE VCIP*, vol. 3653, pp. 52–62, Jan. 1999.
[44] P. Haskell and D. Messerschmitt, "Resynchronization of motion-compensated video affected by ATM cell loss," *Proc. IEEE ICASSP*, vol. 3, pp. 545–548, 1992.
[45] J. Liao and J. Villasenor, "Adaptive intra update for video coding over noisy channels," *Proc. ICIP*, vol. 3, pp. 763–766, Oct. 1996.
[46] S. Wenger, G. Knorr, J. Ott, and F. Kossentini, "Error resilience support in H.263+," *IEEE Trans. Circuits Syst. Video Technol.*, vol. 8, pp. 867–877, Nov. 1998.
[47] P. Salama, N. B. Shroff, and E. J. Delp, "Error concealment in encoded video," in *Image Recovery Techniques for Image Compression Applications*. Norwell, MA: Kluwer, 1998.
[48] W. M. Lam, A. R. Reibman, and B. Liu, "Recovery of lost or erroneously received motion vectors," in *Proc. ICASSP*, vol. 5, Mar. 1993, pp. 417–420.
[49] V. Varsa, M. M. Hannuksela, and Y.-K. Wang, "Non-Normative Error Concealment Algorithms," ITU-T VCEG-N62, 2001.
[50] Y.-K. Wang, M. M. Hannuksela, V. Varsa, A. Hourunranta, and M. Gabbouj, "The error concealment feature in the H.26L test model," in *Proc. ICIP*, vol. 2. Sept. 2002, pp. 729–732.
[51] T. Wiegand, M. Lightstone, D. Mukherjee, T. G. Campbell, and S. K. Mitra, "Rate-distortion optimized mode selection for very low bit rate video coding and the emerging H.263 standard," *IEEE Trans. Circuits Syst. Video Technol.*, vol. 6, pp. 182–190, Apr. 1996.
[52] G. J. Sullivan and T. Wiegand, "Rate-distortion optimization for video compression," *IEEE Signal Processing Mag.*, vol. 15, pp. 74–90, Nov. 1998.
[53] T. Wiegand and B. Girod, "Lagrangian multiplier selection in hybrid video coder control," presented at the Proc. ICIP 2001, Oct. 2001.
[54] T. Stockhammer, D. Kontopodis, and T. Wiegand, "Rate-distortion optimization for H.26L video coding in packet loss environment," presented at the Packet Video Workshop 2002, Pittsburgh, PA, Apr. 2002.
[55] G. Cote, S. Shirani, and F. Kossentini, "Optimal mode selection and synchronization for robust video communications over error-prone networks," *IEEE J. Select. Areas Commun.*, vol. 18, pp. 952–965, Dec. 2000.
[56] T. Wiegand, N. Färber, K. Stuhlmüller, and B. Girod, "Error-resilient video transmission using long-term memory motion-compensated prediction," *IEEE J. Select. Areas Commun.*, vol. 18, pp. 1050—1050-, Dec. 2000.
[57] C. W. Kim, D. W. Kang, and I. S. Kwang, "High-complexity mode decision for error prone environment," in JVT-C101, May 2002.
[58] R. Zhang, S. L. Regunathan, and K. Rose, "Video coding with optimal inter/intra-mode switching for packet loss resilience," *IEEE J. Select. Areas Commun.*, vol. 18, pp. 966–976, 2000.
[59] Y.-K. Wang and M. M. Hannuksela, "Error-robust video coding using isolated regions," in JVT-C073, May 2002.
[60] Y.-K. Wang, M. M. Hannuksela, and M. Gabbouj, "Error-robust inter/intra mode selection using isolated regions," in Proc. Int. Packet Video Workshop 2003, Nantes, France, Apr. 2003.

[61] E. Steinbach, N. Färber, and B. Girod, "Standard compatible extension of H.263 for robust video transmission in mobile environments," *IEEE Trans. Circuits Syst. Video Technol.*, vol. 7, pp. 872–881, Dec. 1997.
[62] B. Girod and N. Färber, "Feedback-based error control for mobile video transmission," *Proc. IEEE*, vol. 97, pp. 1707–1723, Oct. 1999.
[63] W. Wada, "Selective recovery of video packet losses using error concealment," *IEEE J. Select. Areas Commun.*, vol. 7, pp. 807–814, June 1989.
[64] Y. Wang and Q. Zhu, "Error control and concealment for video communication: A review," *Proc. IEEE*, vol. 86, pp. 974–997, May 1998.
[65] T. Nakai and Y. Tomita, "Core Experiments on Feedback Channel Operation for H.263+," ITU-T SG15 LBC96-308, 1996.
[66] S. Fukunaga, T. Nakai, and H. Inoue, "Error resilient video coding by dynamic replacing of reference pictures," in *Proc. IEEE GLOBECOM*, vol. 3, Nov. 1996, pp. 1503–1508.
[67] Y. Tomita, T. Kimura, and T. Ichikawa, "Error resilient modified inter-frame coding system for limited reference picture memories," presented at the Picture Coding Symposium, Berlin, Germany, Sept. 1997.
[68] "Video Coding for Low Bit-Rate Communication, Version 1," ITU-T Recommendation H.263, 1995.
[69] T. Stockhammer, T. Wiegand, T. Oelbaum, and F. Obermeier, "Video coding and transport layer techniques for H.264-based transmission over packet-lossy networks," presented at the ICIP, Barcelona, Spain, Sept. 2003.
[70] T. Stockhammer and S. Wenger, "Standard-compliant enhancement of JVT coded video for transmission over fixed and wireless IP," presented at the IWDC 2002, Capri, Italy, Sept. 2002.



Thomas Stockhammer received the Diplom.-Ing. degree in electrical engineering in 1996 from the Munich University of Technology (TUM), Munich, Germany, where he is currently working toward the Dr.-Ing. degree in the area of source and video transmission over mobile and packet-lossy channels.

In 1996, he visited Rensselear Polytechnic Institute (RPI), Troy, NY to perform his diploma thesis in the area of combined source channel coding for video and coding theory. There he began research in video transmission and combined source and channel coding. In 2000, he was Visiting Researcher in the Information Coding Laboratory, University of San Diego at California (UCSD). Since then, he has published several conference and journal papers and holds several patents. He regularly participates and contributes to different standardization activities, e.g., ITU-T H.324, H.264, ISO/IEC MPEG, JVT, and IETF. He acts as a member of several technical program committees, as Reviewer for different journals, and as an Evaluator for the European Commission. His research interests include joint source and channel coding, video transmission, system design, rate-distortion optimization, information theory, and mobile communications.



Miska M. Hannuksela received the M.S. degree in engineering from Tampere University of Technology, Tampere, Finland, in 1997.

He is currently a Research Manager in the Visual Communications Laboratory, Nokia Research Center, Tampere, Finland. From 1996 to 1999, he was a Research Engineer with Nokia Research Center in the area of mobile video communications. From 2000 to 2003, he was a Project Team Leader and a specialist in various mobile multimedia research and product projects in Nokia Mobile Phones. He has been an active participant in the ITU-T Video Coding Experts Group since 1999 and in the Joint Video Team of ITU-T and ISO/IEC since its foundation in 2001. He has co-authored more than 80 technical contributions to these standardization groups. His research interests include video error resilience, scalable video coding, and video communication systems.



Thomas Wiegand received the Dr.-Ing. degree from the University of Erlangen-Nuremberg, Erlangen-Nuremberg, Germany, in 2000 and the Dipl.-Ing. degree in electrical engineering from the Technical University of Hamburg-Harburg, Hamburg-Harburg, Germany, in 1995.

He is the Head of the Image Communication Group in the Image Processing Department, Fraunhofer–Institute for Telecommunications – Heinrich Hertz Institute (HHI), Berlin, Germany. During 1997 to 1998, he was a Visiting Researcher at Stanford University, Stanford, CA, and served as a Consultant to 8x8, Inc., Santa Clara, CA. From 1993 to 1994, he was a Visiting Researcher at Kobe University, Kobe, Japan. In 1995, he was a Visiting Scholar at the University of California at Santa Barbara, where he began his research on video compression and transmission. Since then, he has published several conference and journal papers on the subject and has contributed successfully to the ITU-T Video Coding Experts Group (ITU-T SG16 Q.6—VCEG)/ISO/IEC Moving Pictures Experts Group (ISO/IEC JTC1/SC29/WG11—MPEG)/Joint Video Team (JVT) standardization efforts and holds various international patents in this field. He has been appointed as the Associated Rapporteur of the ITU-T VCEG (October 2000), the Associated Rapporteur/Co-Chair of the JVT that has been created by ITU-T VCEG and ISO/IEC MPEG for finalization of the H.264/AVC video coding standard (December 2001), and the Editor of the H.264/AVC video coding standard (February 2002).


Wert
Bookbinding
Grantville, PA
JAN-JUNE 2004
"We're Quality Bound"

APPENDIX WADA01

screenshot-catalog.libraries.psu.edu-2023.12.18-12_41_23
https://catalog.libraries.psu.edu/catalog/1181068
18.12.2023

MARC View

LEADER 07877nas a22009611a 4500			
001 1181068			
003 SIRSI			
005 20151215050216.0			
008 830531c19839999nyumr 0 0eng d			
010			a| 83643067 z| sn82005410
019			a| MARS
022	0		a| 0733-8716
035			a| LIAS1351817
035			a| (OCoLC)9450566
040			d| UtOrBLW
245	0	0	a| IEEE journal on selected areas in communications : b| a publication of the IEEE Communications Society.
246	3	9	a| IEEE journal on selected areas in communications
246	3	0	a| Selected areas in communications
264		1	a| New York, N.Y. : b| Institute of Electrical and Electronics Engineers, c| [1983-]
264		4	c| ©1983-
300			a| volumes : b| illustrations ; c| 28 cm
310			a| Monthly, b| 2005-
321			a| Frequency varies, b| 1983-2004
336			a| text b| txt 2| rdacontent
337			a| unmediated b| n 2| rdamedia
338			a| volume b| nc 2| rdacarrier
362	0		a| Vol. SAC-1, no. 1 (Jan. 1983)- v.SAC-5, no. 9 (1987) ; Vol. 6, no. 1 (Jan. 1988)-
710	2		a| Institute of Electrical and Electronics Engineers.
710	2		a| IEEE Communications Society.
533			a| Microform. b| [New York, N.Y.? c| IEEE], d| 19__? e| microfiches ; 11 x 15 cm.
949			a| Microfiche w| ASIS c| 1 i| 1181068-1001 d| 3/19/2001 l| MICROS-HB m| HARRISBURG r| Y s| Y t| MICROFORM u| 4/13/2001
949			a| TK5101.A1I16 v.SAC-1 1983 w| LCPER c| 1 i| 000018892062 d| 3/19/2001 e| 3/19/2001 l| ACAD-BLDG m| UP-ANNEX r| Y s| Y t| PERIODICAL u| 4/13/2001 z| 862
949			a| TK5101.A1I16 v.SAC-3 no.4-6 1985 w| LCPER c| 1 i| 000045496486 l| ACAD-BLDG m| UP-ANNEX r| Y s| Y t| PERIODICAL u| 2/12/2002 z| 862
949			a| TK5101.A1I16 v.SAC-2 1984 w| LCPER c| 1 i| 000060038159 l| ACAD-BLDG m| UP-ANNEX r| Y s| Y t| PERIODICAL u| 10/3/2007 z| 862
949			a| TK5101.A1I16 v.SAC-3 no.1-3 1985 w| LCPER c| 1 i| 000060038166 l| ACAD-BLDG m| UP-ANNEX r| Y s| Y t| PERIODICAL u| 10/3/2007 z| 862
949			a| TK5101.A1I16 v.SAC-4 no.1-5 1986 w| LCPER c| 1 i| 000060038067 l| ACAD-BLDG m| UP-ANNEX r| Y s| Y t| PERIODICAL u| 10/3/2007 z| 865
949			a| TK5101.A1I16 v.SAC-4 no.6-9 1986 w| LCPER c| 1 i| 000060038074 l| ACAD-BLDG m| UP-ANNEX r| Y s| Y t| PERIODICAL u| 10/3/2007 z| 865
949			a| TK5101.A1I16 v.SAC-5 no.1-4 1987 w| LCPER c| 1 i| 000060037954 l| ACAD-BLDG m| UP-ANNEX r| Y s| Y t| PERIODICAL u| 10/3/2007 z| 865

949	a| TK5101.A1I16 v.SAC-5 no.5-9 1987 w| LCPER c| 1 i| 000060037961 l| ACAD-BLDG m| UP-ANNEX r| Y s| Y t| PERIODICAL u| 10/3/2007 z| 865
949	a| TK5101.A1I16 v.SAC-6 no.1-5 1988 w| LCPER c| 1 i| 000060037978 l| ACAD-BLDG m| UP-ANNEX r| Y s| Y t| PERIODICAL u| 10/3/2007 z| 865
949	a| TK5101.A1I16 v.6 no.6-9 1988 w| LCPER c| 1 i| 000060037985 l| ACAD-BLDG m| UP-ANNEX r| Y s| Y t| PERIODICAL u| 10/3/2007 z| 865
949	a| TK5101.A1I16 v.7 no.1-5 1989 w| LCPER c| 1 i| 000060037893 l| ACAD-BLDG m| UP-ANNEX r| Y s| Y t| PERIODICAL u| 10/3/2007 z| 865
949	a| TK5101.A1I16 v.7 no.6-9 1989 w| LCPER c| 1 i| 000060037800 l| ACAD-BLDG m| UP-ANNEX r| Y s| Y t| PERIODICAL u| 10/3/2007 z| 865
949	a| TK5101.A1I16 v.8 Jan-Apr 1990 w| LCPER c| 1 i| 000018894073 l| CATO-2 m| UP-ANNEX r| Y s| Y t| PERIODICAL u| 3/5/2003 z| 7769
949	a| TK5101.A1I16 v.8 May-Aug 1990 w| LCPER c| 1 i| 000018894080 l| CATO-2 m| UP-ANNEX r| Y s| Y t| PERIODICAL u| 3/5/2003 z| 7769
949	a| TK5101.A1I16 v.8 Sept-Dec 1990 w| LCPER c| 1 i| 000018894097 l| CATO-2 m| UP-ANNEX r| Y s| Y t| PERIODICAL u| 3/5/2003 z| 7769
949	a| TK5101.A1I16 v.9 Jan-Apr 1991 w| LCPER c| 1 i| 000018894103 l| CATO-2 m| UP-ANNEX r| Y s| Y t| PERIODICAL u| 3/5/2003 z| 7769
949	a| TK5101.A1I16 v.9 May-Aug 1991 w| LCPER c| 1 i| 000018894110 l| CATO-2 m| UP-ANNEX r| Y s| Y t| PERIODICAL u| 3/5/2003 z| 7769
949	a| TK5101.A1I16 v.9 Sept-Dec 1991 w| LCPER c| 1 i| 000018894127 l| CATO-2 m| UP-ANNEX r| Y s| Y t| PERIODICAL u| 3/5/2003 z| 7769
949	a| TK5101.A1I16 v.10 Jan-June 1992 w| LCPER c| 1 i| 000018894134 l| CATO-2 m| UP-ANNEX r| Y s| Y t| PERIODICAL u| 3/5/2003 z| 7769
949	a| TK5101.A1I16 v.10 Aug-Dec 1992 w| LCPER c| 1 i| 000018894141 l| CATO-2 m| UP-ANNEX r| Y s| Y t| PERIODICAL u| 3/5/2003 z| 7769
949	a| TK5101.A1I16 v.11 Jan-June 1993 w| LCPER c| 1 i| 000018894158 d| 10/11/2006 l| CATO-2 m| UP-ANNEX q| 1 r| Y s| Y t| PERIODICAL u| 3/5/2003 z| 7769
949	a| TK5101.A1I16 v.11 Aug-Dec 1993 w| LCPER c| 1 i| 000018894165 d| 10/11/2006 l| CATO-2 m| UP-ANNEX q| 1 r| Y s| Y t| PERIODICAL u| 3/5/2003 z| 7769
949	a| TK5101.A1I16 v.12 Jan-May 1994 w| LCPER c| 1 i| 000018894172 l| CATO-2 m| UP-ANNEX r| Y s| Y t| PERIODICAL u| 3/5/2003 z| 7769
949	a| TK5101.A1I16 v.12 June-Dec 1994 w| LCPER c| 1 i| 000018894189 l| CATO-2 m| UP-ANNEX r| Y s| Y t| PERIODICAL u| 3/5/2003 z| 7769
949	a| TK5101.A1I16 v.13 Jan-June 1995 w| LCPER c| 1 i| 000018894196 l| CATO-2 m| UP-ANNEX r| Y s| Y t| PERIODICAL u| 3/5/2003 z| 7769
949	a| TK5101.A1I16 v.13 Aug-Dec 1995 w| LCPER c| 1 i| 000018894202 d| 9/18/2008 l| CATO-2 m| UP-ANNEX q| 1 r| Y s| Y t| PERIODICAL u| 3/5/2003 z| 7769
949	a| TK5101.A1I16 v.14 Jan-June 1996 w| LCPER c| 1 i| 000018894219 l| CATO-2 m| UP-ANNEX r| Y s| Y t| PERIODICAL u| 3/5/2003 z| 7769
949	a| TK5101.A1I16 v.14 July-Dec 1996 w| LCPER c| 1 i| 000018894226 l| CATO-2 m| UP-ANNEX r| Y s| Y t| PERIODICAL u| 3/5/2003 z| 7769
949	a| TK5101.A1I16 v.15 Jan-June 1997 w| LCPER c| 1 i| 000018894233 l| CATO-2 m| UP-ANNEX r| Y s| Y t| PERIODICAL u| 3/5/2003 z| 7769
949	a| TK5101.A1I16 v.15 July-Dec 1997 w| LCPER c| 1 i| 000018894240 l| CATO-2 m| UP-ANNEX r| Y s| Y t| PERIODICAL u| 3/5/2003 z| 7769
949	a| TK5101.A1I16 v.16 Feb-June 1998 w| LCPER c| 1 i| 000018894257 l| CATO-2 m| UP-ANNEX r| Y s| Y t| PERIODICAL u| 3/5/2003 z| 7769
949	a| TK5101.A1I16 v.16 Aug-Dec 1998 w| LCPER c| 1 i| 000018894264 l| CATO-2 m| UP-ANNEX r| Y s| Y t| PERIODICAL u| 3/5/2003 z| 7769
949	a| TK5101.A1I16 v.17 Jan-June 1999 w| LCPER c| 1 i| 000018894271 l| CATO-2 m| UP-ANNEX r| Y s| Y t| PERIODICAL u| 3/5/2003 z| 7769
949	a| TK5101.A1I16 v.17 July-Dec 1999 w| LCPER c| 1 i| 000018894288 l| CATO-2 m| UP-ANNEX r| Y s| Y t| PERIODICAL u| 3/5/2003 z| 7769
949	a| TK5101.A1I16 v.18 Jan-June 2000 w| LCPER c| 1 i| 000018894295 d| 7/11/2003 l| CATO-2 m| UP-ANNEX q| 1 r| Y s| Y t| PERIODICAL u| 3/5/2003 z| 7769

949			a| TK5101.A1I16 v.18 July-Sept.2000 w| LCPER c| 1 i| 000047609952 l| CATO-2 m| UP-ANNEX r| Y s| Y t| PERIODICAL u| 11/1/2001 z| 7769
949			a| TK5101.A1I16 v.18 Oct.-Dec.2000 w| LCPER c| 1 i| 000047609808 l| CATO-2 m| UP-ANNEX r| Y s| Y t| PERIODICAL u| 11/1/2001 z| 7769
949			a| TK5101.A1I16 v.19 Jan-Mar 2001 w| LCPER c| 1 i| 000048255431 l| CATO-2 m| UP-ANNEX r| Y s| Y t| PERIODICAL u| 11/28/2001 z| 7769
949			a| TK5101.A1I16 v.19 Apr-June 2001 w| LCPER c| 1 i| 000048255424 l| CATO-2 m| UP-ANNEX r| Y s| Y t| PERIODICAL u| 11/28/2001 z| 7769
949			a| TK5101.A1I16 v.19 July-Sept 2001 w| LCPER c| 1 i| 000048424660 l| CATO-2 m| UP-ANNEX r| Y s| Y t| PERIODICAL u| 11/4/2002 z| 7769
949			a| TK5101.A1I16 v.20 Jan-June 2002 w| LCPER c| 1 i| 000051870089 d| 7/7/2004 l| CATO-2 m| UP-ANNEX q| 1 r| Y s| Y t| PERIODICAL u| 5/2/2003 z| 7769
949			a| TK5101.A1I16 v.20 Aug-Dec 2002 w| LCPER c| 1 i| 000051870157 l| CATO-2 m| UP-ANNEX r| Y s| Y t| PERIODICAL u| 5/2/2003 z| 7769
949			a| TK5101.A1I16 v.21 Jan-June 2003 w| LCPER c| 1 i| 000052812422 l| CATO-2 m| UP-ANNEX r| Y s| Y t| PERIODICAL u| 3/17/2004 z| 7769
949			a| TK5101.A1I16 v.21 Aug-Dec 2003 w| LCPER c| 1 i| 000052812415 l| CATO-2 m| UP-ANNEX r| Y s| Y t| PERIODICAL u| 3/17/2004 z| 7769
949			a| TK5101.A1I16 v.22 Jan-June 2004 w| LCPER c| 1 i| 000054847187 l| CATO-2 m| UP-ANNEX r| Y s| Y t| PERIODICAL u| 4/8/2005 z| 7769
949			a| TK5101.A1I16 v.22 Aug-Dec 2004 w| LCPER c| 1 i| 000054847194 l| CATO-2 m| UP-ANNEX r| Y s| Y t| PERIODICAL u| 4/7/2005 z| 7769
949			a| TK5101.A1I16 v.23 Jan-Apr 2005 w| LCPER c| 1 i| 000054976375 l| CATO-2 m| UP-ANNEX r| Y s| Y t| PERIODICAL u| 4/18/2006 z| 7769
949			a| TK5101.A1I16 v.23 May-Aug 2005 w| LCPER c| 1 i| 000054976368 l| CATO-2 m| UP-ANNEX r| Y s| Y t| PERIODICAL u| 4/18/2006 z| 7769
949			a| TK5101.A1I16 v.23 Sept-Dec 2005 w| LCPER c| 1 i| 000054976351 l| CATO-2 m| UP-ANNEX r| Y s| Y t| PERIODICAL u| 4/18/2006 z| 7769
949			a| TK5101.A1I16 v.24 Jan-Apr 2006 w| LCPER c| 1 i| 000055217415 l| CATO-2 m| UP-ANNEX r| Y s| Y t| PERIODICAL u| 6/12/2007 z| 7769
949			a| TK5101.A1I16 v.24 May-Aug 2006 w| LCPER c| 1 i| 000055217293 l| CATO-2 m| UP-ANNEX r| Y s| Y t| PERIODICAL u| 6/12/2007 z| 7769
949			a| TK5101.A1I16 v.24 Sept-Dec 2006 w| LCPER c| 1 i| 000055217422 l| CATO-2 m| UP-ANNEX r| Y s| Y t| PERIODICAL u| 6/12/2007 z| 7769
852	0	1	a| PSt b| UP-ANNEX c| ANNEX h| TK5101.A1 i| I16
866		0	8| 0 a| v.SAC-1(1983)-v.SAC-6:no.5(1988), v.6:no.6(1988)-v.15(1997), v.16:Feb.(1998)-v.24(2006)
852	8		a| PSt b| HARRISBURG c| MICROS-HB h| Microfiche
866		0	8| 0 a| v.1 1983-v.17 1999

PennState

Copyright @2019 The Pennsylvania State University. All rights reserved. Except where otherwise noted, this work is subject to a Creative Commons Attribution 4.0 license. Details and exceptions.

Legal Statements | PSU Hotlines

PENN STATE UNIVERSITY LIBRARIES

Libraries Home (814) 865-6368
Libraries Intranet (Staff Only)
Accessibility Help
Website Feedback
Policies and Guidelines
Staff Directory

screenshot-catalog.libraries.psu.edu-2023.12.18-12_41_23
https://catalog.libraries.psu.edu/catalog/1181068
18.12.2023

IEEE journal on selected areas in communications : a publication of the IEEE Communications Society

Additional Titles:	IEEE journal on selected areas in communications and Selected areas in communications
Published:	New York, N.Y. : Institute of Electrical and Electronics Engineers, [1983-]
Copyright Date:	©1983-
Physical Description:	volumes : illustrations ; 28 cm
Additional Creators:	Institute of Electrical and Electronics Engineers and IEEE Communications Society

Availability

Browse Nearby on Shelf I Want It

Penn State Harrisburg (1 item)

Call number	Material	Location
Harrisburg - Microforms - 2nd Floor - In-Library Use: Holdings Summary v.1 1983-v.17 1999		
Microfiche	Microfilm, Microfiche, etc.	Harrisburg - Microforms - 2nd Floor - In-Library Use

Library Storage (52 items)

Call number	Material	Location
Annexed Material: Holdings Summary v.SAC-1(1983)-v.SAC-6:no.5(1988), v.6:no.6(1988)-v.15(1997), v.16:Feb.(1998)-v.24(2006)		
TK5101.A1I16 v.6 no.6-9 1988	Bound Journal	Annexed Material
TK5101.A1I16 v.7 no.1-5 1989	Bound Journal	Checked out
TK5101.A1I16 v.7 no.6-9 1989	Bound Journal	Checked out
TK5101.A1I16 v.8 Jan-Apr 1990	Bound Journal	Annexed Material
TK5101.A1I16 v.8 May-Aug 1990	Bound Journal	Annexed Material
TK5101.A1I16 v.8 Sept-Dec 1990	Bound Journal	Annexed Material
TK5101.A1I16 v.9 Jan-Apr 1991	Bound Journal	Annexed Material
TK5101.A1I16 v.9 May-Aug 1991	Bound Journal	Annexed Material
TK5101.A1I16 v.9 Sept-Dec 1991	Bound Journal	Annexed Material

TK5101.A1I16 v.10 Aug-Dec 1992	Bound Journal	Annexed Material
TK5101.A1I16 v.10 Jan-June 1992	Bound Journal	Annexed Material
TK5101.A1I16 v.11 Aug-Dec 1993	Bound Journal	Annexed Material
TK5101.A1I16 v.11 Jan-June 1993	Bound Journal	Annexed Material
TK5101.A1I16 v.12 Jan-May 1994	Bound Journal	Annexed Material
TK5101.A1I16 v.12 June-Dec 1994	Bound Journal	Annexed Material
TK5101.A1I16 v.13 Aug-Dec 1995	Bound Journal	Annexed Material
TK5101.A1I16 v.13 Jan-June 1995	Bound Journal	Annexed Material
TK5101.A1I16 v.14 Jan-June 1996	Bound Journal	Annexed Material
TK5101.A1I16 v.14 July-Dec 1996	Bound Journal	Annexed Material
TK5101.A1I16 v.15 Jan-June 1997	Bound Journal	Annexed Material
TK5101.A1I16 v.15 July-Dec 1997	Bound Journal	Annexed Material
TK5101.A1I16 v.16 Aug-Dec 1998	Bound Journal	Annexed Material
TK5101.A1I16 v.16 Feb-June 1998	Bound Journal	Annexed Material
TK5101.A1I16 v.17 Jan-June 1999	Bound Journal	Annexed Material
TK5101.A1I16 v.17 July-Dec 1999	Bound Journal	Annexed Material
TK5101.A1I16 v.18 Jan-June 2000	Bound Journal	Being transferred between libraries
TK5101.A1I16 v.18 July-Sept.2000	Bound Journal	Annexed Material
TK5101.A1I16 v.18 Oct.-Dec.2000	Bound Journal	Annexed Material
TK5101.A1I16 v.19 Apr-June 2001	Bound Journal	Annexed Material
TK5101.A1I16 v.19 Jan-Mar 2001	Bound Journal	Annexed Material
TK5101.A1I16 v.19 July-Sept 2001	Bound Journal	Annexed Material
TK5101.A1I16 v.20 Aug-Dec 2002	Bound Journal	Annexed Material
TK5101.A1I16 v.20 Jan-June 2002	Bound Journal	Annexed Material
TK5101.A1I16 v.21 Aug-Dec 2003	Bound Journal	Annexed Material
TK5101.A1I16 v.21 Jan-June 2003	Bound Journal	Annexed Material
TK5101.A1I16 v.22 Aug-Dec 2004	Bound Journal	Annexed Material
TK5101.A1I16 v.22 Jan-June 2004	Bound Journal	Annexed Material
TK5101.A1I16 v.23 Jan-Apr 2005	Bound Journal	Annexed Material
TK5101.A1I16 v.23 May-Aug 2005	Bound Journal	Annexed Material
TK5101.A1I16 v.23 Sept-Dec 2005	Bound Journal	Annexed Material
TK5101.A1I16 v.24 Jan-Apr 2006	Bound Journal	Annexed Material
TK5101.A1I16 v.24 May-Aug 2006	Bound Journal	Annexed Material
TK5101.A1I16 v.24 Sept-Dec 2006	Bound Journal	Annexed Material
TK5101.A1I16 v.SAC-1 1983	Bound Journal	Annexed Material
TK5101.A1I16 v.SAC-2 1984	Bound Journal	Annexed Material
TK5101.A1I16 v.SAC-3 no.1-3 1985	Bound Journal	Annexed Material
TK5101.A1I16 v.SAC-3 no.4-6 1985	Bound Journal	Annexed Material
TK5101.A1I16 v.SAC-4 no.1-5 1986	Bound Journal	Annexed Material
TK5101.A1I16 v.SAC-4 no.6-9 1986	Bound Journal	Annexed Material

TK5101.A1I16 v.SAC-5 no.1-4 1987	Bound Journal	Annexed Material
TK5101.A1I16 v.SAC-5 no.5-9 1987	Bound Journal	Annexed Material
TK5101.A1I16 v.SAC-6 no.1-5 1988	Bound Journal	Annexed Material

Dates of Publication and/or Sequential Designation:
Vol. SAC-1, no. 1 (Jan. 1983)- v.SAC-5, no. 9 (1987) ; Vol. 6, no. 1 (Jan. 1988)-

ISSN:
0733-8716

Publication Frequency:
Monthly, 2005-
Frequency varies, 1983-2004

Reproduction Note:
Microform. [New York, N.Y.? IEEE], 19__? microfiches ; 11 x 15 cm.

View MARC record | catkey: 1181068

PennState

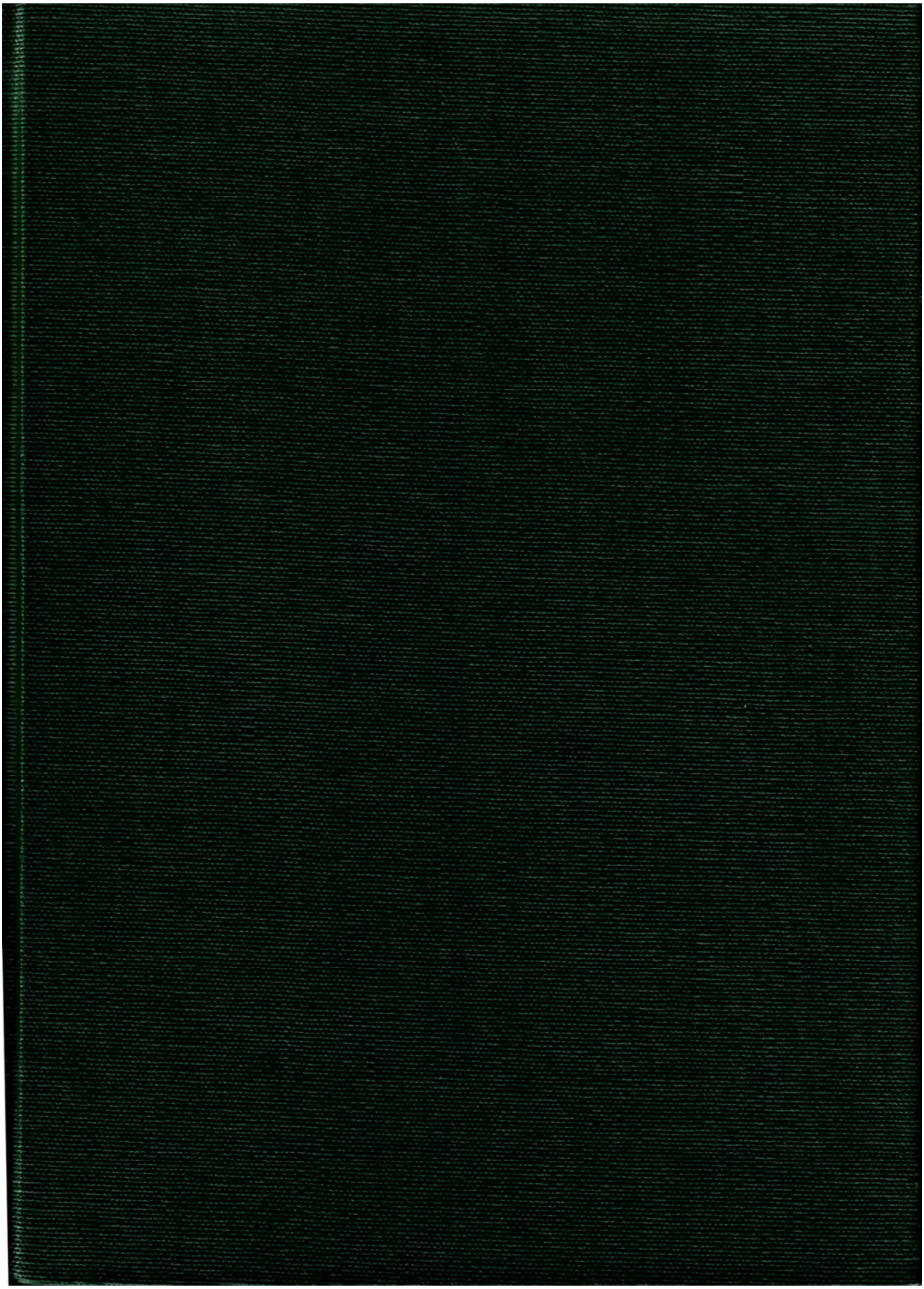
Copyright @2019 The Pennsylvania State University. All rights reserved. Except where otherwise noted, this work is subject to a Creative Commons Attribution 4.0 license. Details and exceptions.

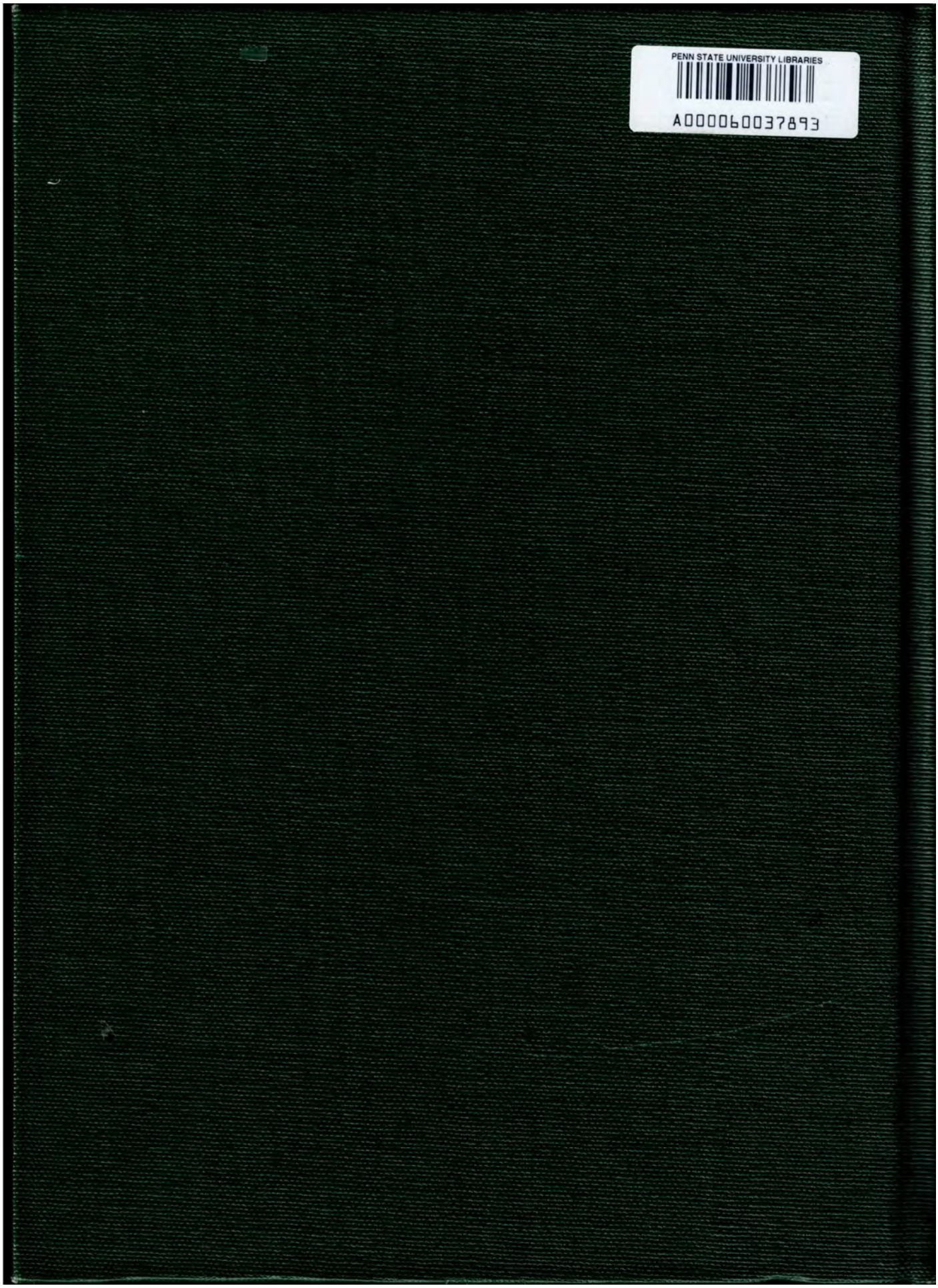
Legal Statements | PSU Hotlines

PENN STATE UNIVERSITY LIBRARIES

Libraries Home (814) 865-6368
Libraries Intranet (Staff Only)
Accessibility Help
Website Feedback
Policies and Guidelines
Staff Directory

APPENDIX WADA02




PENN STATE UNIVERSITY LIBRARIES
A000060037893

Engin

RECEIVED
JUN 2 6
PENNSYLVANIA STATE
UNIVERSITY LIBRARIES

IEEE JOURNAL ON

SELECTED AREAS IN COMMUNICATIONS

JUNE 1989 VOLUME 7 NUMBER 5 (ISSN 0733-8716)

A PUBLICATION OF THE IEEE COMMUNICATIONS SOCIETY

I-11

JUN 1989
RECEIVED
Engineering
Library

PACKET SPEECH AND VIDEO

Guest Editors—L. Turner, T. Aoyama, D. Pearson, D. Anastassiou, and T. Minami

Guest Editorial ..... *L. Turner, T. Aoyama, D. Pearson, D. Anastassiou, and T. Minami* 629

PAPERS

Dynamic Priority Protocols for Packet Voice ..... *T. M. Chen, J. Walrand, and D. G. Messerschmitt* 632
Priority Discarding of Speech in Integrated Packet Networks ..... *D. W. Petr, L. A. DaSilva, Jr., and V. S. Frost* 644
Comparative Performance of Voice/Data Local Area Networks ..... *T. A. Gonsalves and F. A. Tobagi* 657
An Integrated Services Token-Controlled Ring Network ..... *P.-C. Wong and T.-S. P. Yum* 670
A Compatible Fixed-Frame ISDN Gateway for Broadband Metropolitian Area Networks ..... *T. D. Todd and P. A. Lopinski* 680
Error Control Techniques for Integrated Services Packet Networks ..... *M. J. Miller* 690
Implementation Mechanisms for Packet Switched Voice Conferencing ..... *C. Ziegler, G. Weiss, and E. Friedman* 698
Missing Packet Recovery Techniques for Low-Bit-Rate Coded Speech ..... *J. Suzuki and M. Taka* 707
End-to-End Performance Models for Variable Bit Rate Voice Over Tandem Links in Packet Networks ..... *S. Dravida and K. Sriram* 718
Queueing Analysis of Delay Constrained Voice Traffic in a Packet Switching System ..... *C. Yuan and J. A. Silvester* 729
Packet Video and Its Integration into the Network Architecture ..... *G. Karlsson and M. Vetterli* 739
Basic Characteristics of Variable Rate Video Coding in ATM Environment ..... *M. Nomura, T. Fujii, and N. Ohta* 752
A Variable Rate Video Codec for Asynchronous Transfer Mode Networks ..... *W. Verbiest and L. Pinnoo* 761
Two-Layer Coding of Video Signals for VBR Networks ..... *M. Ghanbari* 771
Packet Communication Protocol for Image Services on a High-Speed Multimedia LAN ..... *H. Shimizu, M. Mera, and H. Tani* 782
Fixed Distortion Subband Coding of Images for Packet-Switched Networks ..... *J. C. Darragh and R. L. Baker* 789
Variable Bit-Rate Coding of Video Signals for ATM Networks ..... *F. Kishino, K. Manabe, Y. Hayashi, and H. Yasuda* 801
Selective Recovery of Video Packet Loss Using Error Concealment ..... *M. Wada* 807
Shared Access Packet Transmission Systems for Compressed Digital Video ..... *K. Joseph, D. Raychaudhuri, and J. Zdepski* 815
Statistics of Video Signals for Viewphone-Type Pictures ..... *H. S. Chin, J. W. Goodge, R. Griffiths, and D. J. Parish* 826
Generation Interval Distribution Characteristics of Packetized Variable Rate Video Coding Data Streams in an ATM Network ..... *R. Kishimoto, Y. Ogata, and F. Inumaru* 833
Packetized Radiographic Image Transfers over Local Area Networks for Diagnosis and Conferencing ..... *R. Kositpaiboon, P. Tsingotjidis, L. O. Barbosa, and N. D. Georganas* 842
Encoding Facsimilie Images for Packet-Switched Networks ..... *C. Chamzas and D. L. Duttweiler* 857
Models for Packet Switching of Variable-Bit-Rate Video Sources ..... *P. Sen, B. Maglaris, N.-E. Rikli, and D. Anastassiou* 865

CALL FOR PAPERS

Computer-Aided Modeling, Analysis, and Design of Communication Networks 870
Communications Software 871
Microelectronics and Photonics in Communications 872

IEEE COMMUNICATIONS SOCIETY

The field of interest of the IEEE Communications Society consists of all telecommunications including telephone, telegraphy, facsimile, and point-to-point television, by electromagnetic propagation including radio; wire; aerial, underground, coaxial, and submarine cables; waveguides, communication satellites, and lasers; in marine, aeronautical, space, and fixed station services; repeaters, radio relaying, signal storage, and regeneration; telecommunication error detection and correction; multiplexing and carrier techniques; communication switching systems; data communications; and communication theory.

In addition to the above, this JOURNAL or the IEEE TRANSACTIONS ON COMMUNICATIONS contains papers pertaining to analog and digital signal processing and modulation, audio and video encoding techniques, the theory and design of transmitters, receivers, and repeaters for communications via optical and sonic media, the design and analysis of computer communication systems, and the development of communication software. Contributions of theory enhancing the understanding of communication systems and techniques are included, as are discussions of the social implications of the development of communication technology. All members of the IEEE are eligible for membership in the Society upon payment of the annual Society membership fee of $12.00. Members may receive this JOURNAL or the IEEE TRANSACTIONS ON COMMUNICATIONS upon payment of an additional $10.00 ($22.00 total), or both publications upon payment of an additional $20.00 ($32.00 total). For information on joining, write to the IEEE at the address below.

IEEE COMMUNICATIONS SOCIETY
JOURNAL Editorial Board 1989

S. D. PERSONICK, *Director of Publications*
Bellcore, Rm. NVC-2Z463A
Box 7020
331 Newman Springs Rd.
Red Bank, NJ 07701

W. H. TRANTER, *Editor-in-Chief*
Dep. Elec. Eng.
Ur...
R...

SUE L. MCDONALD, *Assistant Editor*
Bellcore, Rm. 2P-293
445 South Street
Morristown, NJ 07960-1910

N. K. CHEUNG
Bellcore, Rm. 3Z-219
331 Newman Springs Rd.
Red Bank, NJ 07701

W. D. SINCOSKIE
Bellcore, Rm. 2Q-286
445 South Street
Morristown, NJ 07960-1910

M. KAWASHIMA
Fujitsu Limited
6-1, Marunouchi 1-chome
Chiyoda-ku
Tokyo 100, Japan

R. YATSUBOSHI
Fujitsu Labs.
1015 Kamikodnaka Nakahara-ku
Kawasaki 211, Japan

PENNSTATE
1855
UNIVERSITY
LIBRARIES

THE INSTITUTE OF ELECTRICAL AND ELECTRONICS ENGINEERS, INC.
Officers

EMERSON W. PUGH, *President*
CARLETON A. BAYLESS, *President-Elect*
GEORGE F. ABBOTT, *Executive Vice President*
HUGO RÜCHARDT, *Secretary*
WALLACE S. READ, *Treasurer*
HARRY W. MERGLER, *Vice President, Educational Activities*
EDWARD C. BERTNOLLI, *Vice President, Professional Activities*
TIMOTHY N. TRICK, *Vice President, Publication Activities*
MICHAEL J. WHITELAW, *Vice President, Regional Activities*
H. TROY NAGLE, JR., *Vice President, Technical Activities*
RALPH W. WYNDRUM, JR., *Director, Division III—Communications Technology Division*

Headquarters Staff
ERIC HERZ, *Executive Director and General Manager*

THOMAS W. BARTLETT, *Controller*
DONALD CHRISTIANSEN, *Editor, IEEE Spectrum*
IRVING ENGELSON, *Staff Director, Technical Activities*
LEO FANNING, *Staff Director, Professional Activities*
ANDREW G. SALEM, *Staff Director, Standards*
DAVID L. STAIGER, *Staff Director, Publishing Services*
RUDOLF A. STAMPFL, *Staff Director, Educational Activities*
CHARLES F. STEWART, JR., *Staff Director, Administration*
DONALD L. SUPPERS, *Staff Director, Field Services*
THOMAS C. WHITE, *Staff Director, Public Information*

Publications Department
Publications Managers: ANN H. BURGMEYER, GAIL S. FERENC, CAROLYNE TAMNEY
Associate Editor: DONNA INCORVAIA

IEEE JOURNAL ON SELECTED AREAS IN COMMUNICATIONS is published nine times a year in January, February, April, May, June, August, September, October, and December by The Institute of Electrical and Electronics Engineers, Inc. Responsibility for the contents rests upon the authors and not upon the IEEE, the Society/Council, or its members. **IEEE Headquarters:** 345 East 47 Street, New York, NY 10017. **NY Telephone:** 212-705 + extension: Information -7900; General Manager -7910; Controller -7748; Public Information -7867; Publishing Services -7560; Spectrum -7556; Standards -7960; Technical Activities -7890. **Telecopiers:** NY (Headquarters) 212-752-4929, NY (Publications/Standards) 212-682-6005; **NY Telex:** 236-411 (international messages only). **IEEE Service Center** (for orders, subscriptions, address changes, Educational Activities, Region/Section/Student Services): 445 Hoes Lane, P.O. Box 1331, Piscataway, NJ 08855-1331. **NJ Telephone:** 201-981-0060. **IEEE Washington Office** (for U.S. professional activities): 1111 19th Street, NW, Suite 608, Washington, DC 20036. **Washington Telephone:** 202-785-0017. **Price/Publication Information:** Individual copies: IEEE members $10.00 (first copy only), nonmembers $20.00 per copy. (Note: Add $4.00 postage and handling charge to any order from $1.00 to $50.00, including prepaid orders.) Member and nonmember subscription prices available on request. Available in microfiche and microfilm. **Copyright and Reprint Permissions:** Abstracting is permitted with credit to the source. Libraries are permitted to photocopy beyond the limits of the U.S. Copyright Law for private use of patrons: 1) those post-1977 articles that carry a code at the bottom of the first page, provided the per-copy fee indicated in the code is paid through the Copyright Clearance Center, 29 Congress Street, Salem, MA 01970; 2) pre-1978 articles without fee. Instructors are permitted to photocopy isolated articles for noncommercial classroom use without fee. For all other copying, reprint, or republication permission, write to Copyrights and Permissions Department, IEEE Publishing Services, 345 East 47th Street, New York, NY 10017. Copyright © 1989 by The Institute of Electrical and Electronics Engineers, Inc. All rights reserved. Second-class postage paid at New York, NY, and at additional mailing offices. **Postmaster:** Send address changes to IEEE JOURNAL ON SELECTED AREAS IN COMMUNICATIONS, IEEE, 445 Hoes Lane, P.O. Box 1331, Piscataway, NJ 08855-1331.

Selective Recovery of Video Packet Loss Using Error Concealment

MASAHIRO WADA

Abstract—**A new efficient recovery method using error concealment is proposed for video packet loss in fast packet switching networks. In the packet switching network, packet loss is unavoidable and a correction method is required for video packet transmission which takes characteristics of video signals and video coding into account. In the method, the receiver detects the damaged picture area caused by packet loss from the structured picture data received, makes error concealments, notifies the transmitter, and continues decoding. The transmitter, having received the notice, calculates the affected picture area in the local-decoded picture and continues encoding without using this affected area. In this selective recovery method, video signals are not stopped even if a long propagation delay exists, no additional information is transmitted, and conventional coding algorithms can be applied. Also, the proposed method is suitable for multipoint communication. The relation tables of picture block propagation required at the transmitter consist of small amounts of bits. Simulation results show the affected picture area is localized for a considerable time, and concealed picture quality is sufficient.**

I. Introduction

FAST packet switching is considered the major candidate for building broadband ISDN [1] where video communications will be a main service. Fast packet switching can efficiently handle variable bit rate signals, and is suitable for bit-rate-reduced video signals [2].

Since fast packet switching achieves high utilization efficiency of circuits by statistical multiplexing, unavoidable packet loss occurs which causes serious errors in low-bit-rate video transmission where interframe coding is adopted. A method is therefore required for video packet transmission which recovers packet loss efficiently [3]. Unlike data communication, video communication is usually interactive and real-time critical; therefore, conventional retrieval protocol like HDLC is inapplicable when propagation delay exists.

This paper proposes a packet loss recovery method for low-bit-rate video transmission in the packet switching network which uses error concealment and selective correction. The method has higher efficiency than a conventional demand refresh which forces the encoding mode of a whole frame into intraframe. It also allows free-running of video signals, transmits no additional information for error recovery, and is applicable to conventional coding algorithms. Futhermore, the proposed method is suitable for multipoint communication.

Manuscript received August 11, 1988; revised November 1, 1988.

The author is with KDD Kamihukuoka Research and Development Laboratories, Kamifukuoka-shi, Saitama-ken 356, Japan.

IEEE Log Number 8927585.

In the following sections, Section II describes some requirements which restrict coding structures, Section III explains the selective recovery method, Section IV discusses transmission data structure, and Section V gives some simulation results which show the method is effective.

II. Restrictions on Coding

The proposed method requires the following restrictions on coding. These conditions seem adequate for the recent coding algorithms used for low-bit-rate video communications.

1) Localization of coded signals: Coding is carried out independently in one frame by each picture area called a picture block. Loss of some picture blocks does not affect other blocks in the same frame, i.e., decoding of the frame can be continued after loss of picture blocks.

2) Localization of packetized signals: Picture blocks are packed into one or several packets in a structured manner and the influence of packet loss is limited to one or several packets, i.e., the received bit streams are decodable after a packet loss.

For restriction 1), most picture coding algorithms currently used for low and medium bit rates are adopting interframe/intrablock adaptive prediction based on pixel blocks [4], [6], and this trend will increase due to progress in the study of orthogonal transforms such as DCT and vector quantization [7]. Frame-by-frame propagation of packet loss influence basically depends on the range of motion compensation adopted.

Restriction 2) can easily be realized under the condition that restriction 1) is guaranteed. Details of the packing structure of coded data will be described in Section IV.

With these restrictions, the damage of packet loss is localized within a certain area of the picture frame.

III. Selective Recovery Method

A. Basic Procedure at the Receiver

In this method, a receiver terminal operates according to the following procedures.

1) Packet loss is detected by a network or the receiver terminal. In the latter case a sequential number will be added to each packet.

2) Damaged picture block(s) is (are) specified by calculating the received data structure.

3) Notice of packet loss with the address(es) of damaged picture block(s) is sent back to the transmitter.

0733-8716/89/0600-0807$01.00 © 1989 IEEE

4) Error concealment is carried out over damaged picture block(s). For example, error concealment can be done by replacing the damaged picture block(s) with the block(s) in the previous frame.

5) Decoding is continued.

Calculation of damaged picture block(s) depends on the transmitted data structure and is discussed in Section IV.

B. Basic Procedure at the Transmitter

There are two possible procedures at the transmitter as follows.

Method A:

1) Notice of packet loss is received with the address(es) of damaged picture block(s).

2) The affected picture area in local-decoded frames is calculated from the point of the damaged block(s) up to the currently encoded frame as shown in Fig. 1.

3) Encoding is continued without using the affected picture area.

Method B:

1) Notice of packet loss is received with the address(es) of damaged picture block(s).

2) The same error concealment as is performed at the receiver is carried out in the local-decoded frame stored, as shown in Fig. 2.

3) Local decoding is reexecuted from the point of the concealed block(s) up to the currently encoded block using the transmitted data stored so that the local-decoded picture at the transmitter becomes the same as the decoded picture at the receiver, as shown in Fig. 3, where local-decoded picture data stored in memory and concealing data give the initial value for decoding.

4) Encoding is normally continued throughout the above sequence.

In Method A, the amount of calculation is small, only the propagation tree of the affected picture blocks is required to be stored for a depth Td (Td is the response delay, i.e., equals the propagation delay of the transmission link plus the operation delay of packet loss detection), multipoint communication is possible, and overhead due to coding efficiency deterioration will be small when the affected picture area is localized. Moreover, as encoding without using the affected picture area does not necessarily mean intrablock coding, the coding efficiency deterioration itself will also be small.

In Method B, the encoding operation is not interrupted, the local-decoding process for recovery can run concurrently, and efficiency loss of encoding will be negligible. However, local-decoded pictures and transmitted data have to be stored for the above-mentioned depth Td at the transmitter, and multipoint communication is difficult.

From these comparisons, here we choose Method A, but due to its high efficiency and absence of effect on coding operation, Method B is still attractive when Td is small (in extreme cases, when the concealed picture area does not yet affect the encoding, it is required only to replace the corresponding area in a local-decoded frame by concealing data).

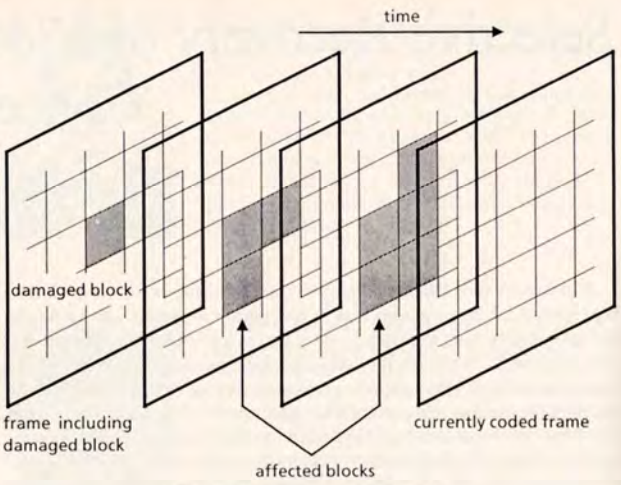


Fig. 1. Illustration of Method A.

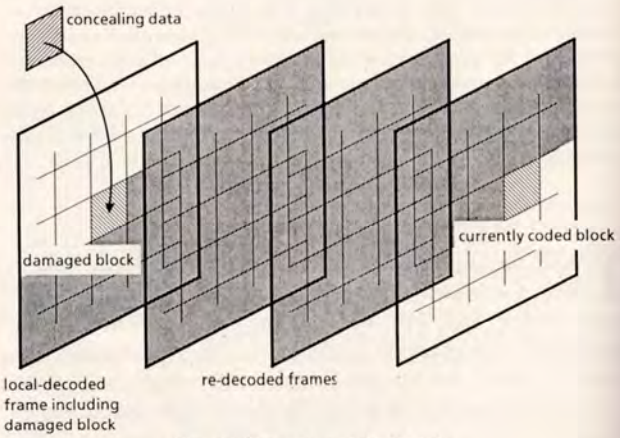


Fig. 2. Illustration of Method B.

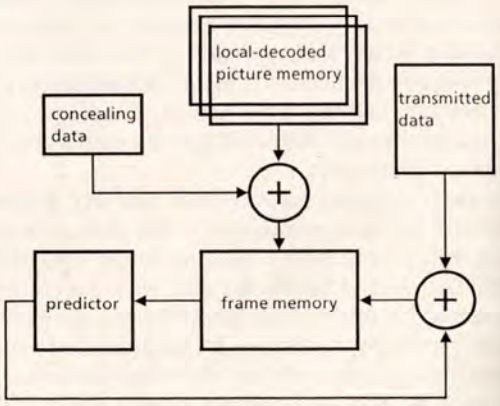


Fig. 3. Redecoding algorithm of Method B.

C. Propagation Tree

A propagation tree is used at the transmitter to specify the affected area in the local-decoded pictures. Fig. 4 shows an example of the tree where one block is damaged in frame i and three, four, and five blocks are affected in frame $i+1$, $i+2$, and $i+3$, respectively.

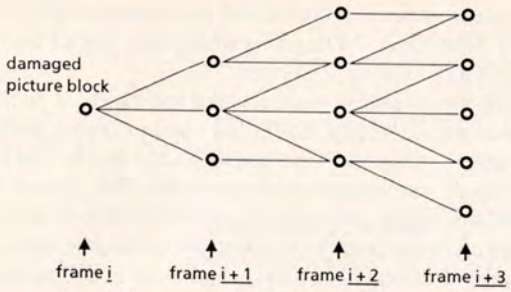


Fig. 4. An example of block propagation tree.

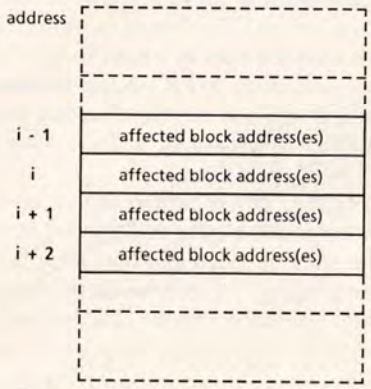


Fig. 5. Structure of block relation table.

In order to calculate the tree, relation tables shown in Fig. 5 are made for each frame simultaneously in the encoding operation. Each address of the table corresponds to the picture block address in the frame, and contains the address(es) of block(s) which used (a) pixel(s) in the addressed block for encoding.

One address may contain several blocks, and the maximum number is basically determined by the range of motion compensation adopted. The total number of blocks contained in a table, however, is at most four times as much as the number of blocks in one frame when an orthogonal block lattice is used.

When packet loss is notified, the table for the frame having the corresponding picture area is first searched by the informed address(es) of damaged block(s), and the address(es) of the affected block(s) is (are) selected. This procedure is repeated, and the propagation tree is thereby constructed.

IV. Transmitted Data Structure

A. Premises

In a fast packet switching network, transmitted signals are divided into smaller units named cells and then multiplexed [1]. The cell bit length is usually fixed for stable synchronization, although a variable length cell is more efficient. Here, therefore, the cell length is assumed fixed. On the other hand, a coded picture block has a variable bit length, and therefore efficient packing of each picture block has to be considered in this case. Here, we present an example of the transmitted data structure which satisfies the requirements mentioned in Section II.

In order to simplify the discussion, the following premises are made.

1) When conditional replenishment is adopted, nothing is transmitted on nonreplenished picture blocks. This is effective for increasing coding efficiency.

2) Packet loss is detected by the network or terminal by procedures outside the scope of this paper.

3) Coded data are sequentially decodable. Unique words are not used for efficiency.

These premises lay few constraints on coding algorithms.

B. Data Structure [5]

Two cases have to be considered, i.e., that the bit length of a picture block is shorter than a packet length, and that it is longer.

Fig. 6 shows the transmitted data structure. When a picture block length is shorter than a packet length, one packet can contain several blocks as is shown in Fig. 6(a), but a picture block is prevented from spreading over two packets. The first block in a packet has an absolute address (AA) for localization of packet loss influence, while (an)other block(s) in the same packet has(ve) a relative address (RA) for addressing efficiency. Valid information in a packet is terminated by an end-of-information code (EOI). This code can be used to reduce the packaging delay when the block bit length remains small.

When a picture block length is longer than a packet length, one picture block is divided into several packets as is shown in Fig. 6(b), where an absolute address (AA) is attached at the head of the block information in the first packet while a continuation flag is attached at the same area in other packet(s). It may be prevented from including the next picture block in the last packet in order to limit packet loss influence.

In this data structure, tradeoff between packaging efficiency and error resilience should be considered. If error resilience is considerable, one packet should contain a smaller number of blocks. Picture block size should also be determined from this point.

C. Operation of the Receiver

Based on the transmission data structure mentioned above, the receiver terminal operates according to the state transition diagram shown in Fig. 7. In the figure, three normal states and two temporary states exist.

"Idle" means no packet is under processing, and when a packet is received with a correct sequential number (event CPR), it transfers to a "decoding" state with absolute block address and an incrementing packet sequence number. The picture block information in the received packet is then decoded.

In this state, if decoding of one block is terminated (event EOB), the received block address is renewed and it transfers to "next address check." If decoding of one

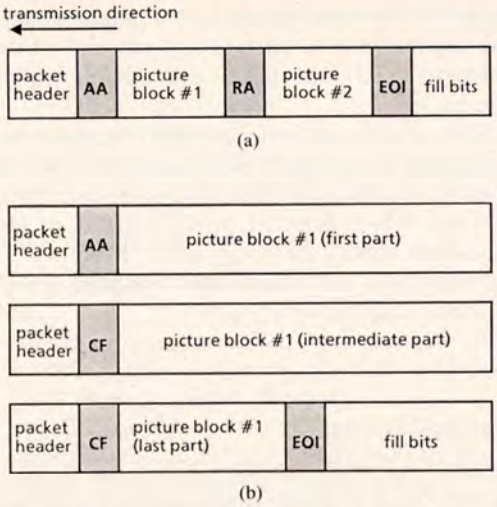
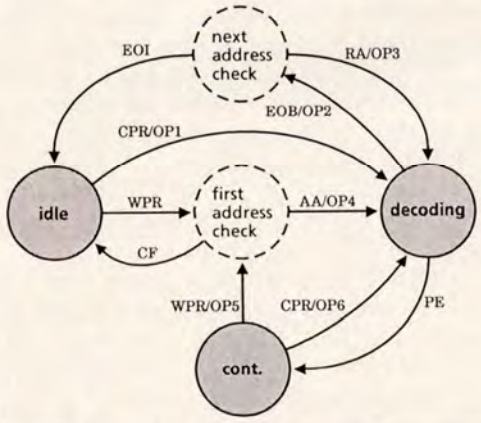


Fig. 6. Structure of data packing. (a) Picture block length < packet length. (b) Picture block length > packet length.



trigger events	
CPR	correct packet reception
WPR	wrong packet reception
EOB	end of block
EOI	end of information
AA	absolute address
RA	relative address
PE	packet end
CF	continuation flag

operations	
OP1	get absolute block address increment packet sequence number
OP2	renew received block address
OP3	get relative block address
OP4	error concealment notice of damaged picture block(s) reset packet sequence number get absolute block address
OP5	discard stored information
OP6	increment packet sequence number

Fig. 7. State transition diagram for packet receiving.

packet is finished before EOB (event PE), a state transition occurs to "cont."

In the temporary state "next address check," an address field after the processed block is examined and if a relative address is detected (event RA), decoding of the next block in the same packet restarts. In case that EOI code is detected (event EOI), it transfers back to the "idle" state.

In the "cont." state, when the next packet is received with a correct sequential number (event CPR), the packet sequence number is incremented and a state transition occurs to "decoding." Decoding of the next part of the same picture block is then continued.

When a packet loss has occurred and the next packet is received with a wrong sequential number (event WPR) in the "idle" state, the first address field in the packet is checked. If an absolute address is detected (event AA), this means synchronization of picture blocks is resumed, and error concealment over damaged picture block(s), notification of damaged block(s), and reset of the packet sequence number are carried out. After these operations, the state transfers to "decoding," and decoding of the picture block with the absolute address starts. If a continuation flag is detected (event CF), however, no operation takes place and the state remains in "idle."

When the same event WPR occurs in state "cont.," some of the information of the decoded picture block stored in memory is discarded, and the same procedures follow.

Damaged picture blocks which the receiver estimates may contain noncoded blocks which have not been transmitted. If the error concealment operation is the same as that of the noncoding, the overheads of the transmission and transmitter operation required for recovery can be reduced.

V. Simulation and Discussion

This section evaluates the proposed recovery method by simulation experiments using three kinds of video signals from videoconferencing/videophone sequences, "Salesman," "Miss America," and "Claire," which are used for CCITT standardization. Picture frame size is 352 pels × 288 lines, each pel consists of Y, R–Y, B–Y, each having 8 bits, and the frame rate is 10 frames/s. The coding algorithm used here is based on motion-compensated interframe prediction and discrete cosine transform (DCT) with conditional replenishment [4]. Motion compensation range reaches ±7 pels/frame in both directions, and the picture block size is 16 pels × 16 lines (i.e., 396 blocks/frame). The step size of the quantizer is fixed, and the SN ratio of the coded picture becomes stable. The relation between the step size and SN ratio depends on used pictures. Table I shows characteristics of coding results averaged for 32 frames.

A. Characteristics of Propagation Tree

In the proposed method, the influence of damaged picture block(s) is propagated through consecutive frames, so the speed at which this influence spreads greatly affects the coding efficiency, because these affected picture blocks cannot be used for encoding. Fig. 8 shows the number of affected blocks in subsequent frames after loss of one picture block. These results are averages of coded (replenished) picture blocks for 16 frames. The number of affected blocks increases moderately, and the rate of increase falls as the frame depth advances.

Differences of slopes can be explained by the ratio of motion-compensated (MC) blocks among all coded

TABLE I
CHARACTERISTICS OF CODING RESULTS

sequence name	Salesman			Miss America			Claire		
quantizer step size (×1/256)	8	12	16	8	12	16	8	12	16
luminance SN ratio (dB)	38.8	36.3	34.6	41.3	40.0	39.0	43.6	41.6	40.0
coded blocks/all blocks ratio	0.98	0.82	0.65	0.97	0.67	0.53	0.53	0.37	0.32
MC blocks/all blocks ratio	0.22	0.17	0.14	0.33	0.32	0.29	0.11	0.11	0.12
MC blocks/coded blocks ratio	0.22	0.21	0.21	0.34	0.48	0.54	0.21	0.30	0.37
coded bitrate (kbit/s)	665	333	200	378	182	102	204	122	86

MC : motion-compensated
coded : replenished

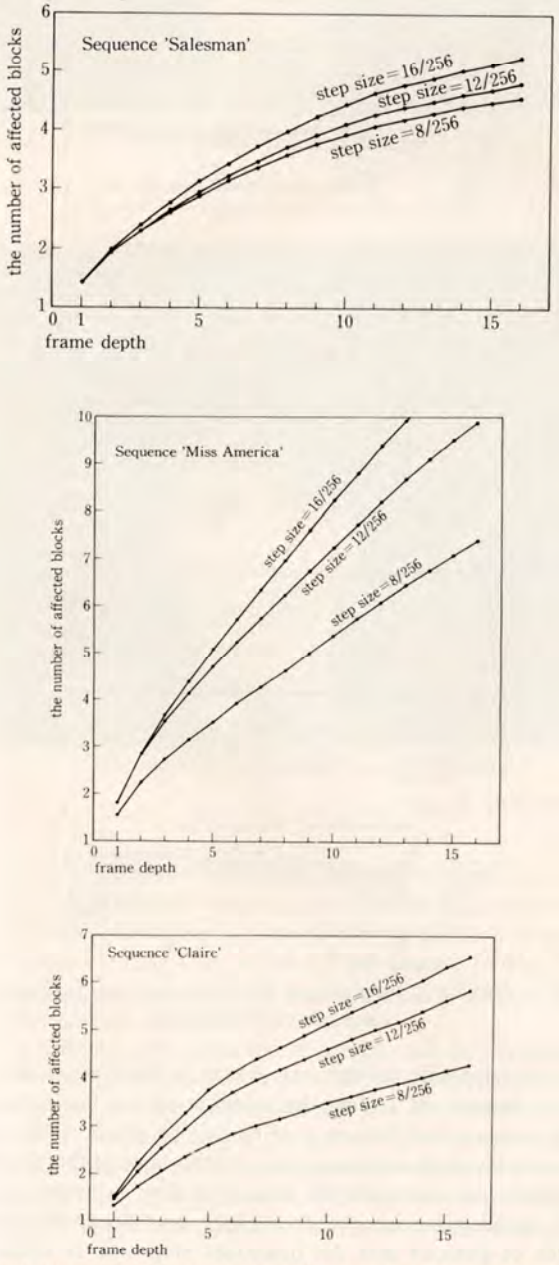


Fig. 8. The number of affected blocks after loss of one picture block.

blocks, i.e., if this ratio is high, the number of blocks which is used for encoding one block becomes high. For the "Miss America" and "Claire" sequences, as is shown in Table I, this MC/coded ratio also increases as the step size of the quantizer increases because the number of MC blocks does not vary greatly, while the percentage of coded blocks decreases. The slopes of the graphs therefore increase according to the step size. On the other hand, this MC/coded ratio does not vary for the "Salesman" sequence, and therefore the slopes of the graphs for this sequence are not very different.

The reason that the number of affected blocks does not increase exponentially is that the picture blocks in the next frame which are affected by the neighboring picture blocks in the previous frame overlap to some extent. Actually, the number of affected blocks is limited to 10 per 396 after 13 frames (1.3 s) even for the most severe case.

As is described in Section IV, one packet can contain several picture blocks, so a loss of consecutive picture blocks may occur. Fig. 9 shows the number of affected blocks in subsequent frames after loss of consecutive picture blocks. These results are averages of coded (replenished) picture blocks for 24 frames, and the quantizer step size is fixed to 12/256 (this means pel values range from 0 to 255 and the step size for coefficients in the transformed domain is fixed to 12). The slopes of the graphs vary very little for a different initial number of blocks, and all graphs are in a parallel shift relation. The ratio of increase per initial block is almost constant in the same sequence, and it varies from 1 to 2 among sequences. The reason why there is no exponential increase is the same as above.

These experimental results and considerations show the proposed method is efficient even if the response delay is long or one packet contains several blocks.

Table II shows the required overhead for error recovery by the proposed method and conventional demand refresh method, i.e., the ratio of bit increase per normally coded bits when error recovery is carried out in the fourth frame after packet loss. These values are averages for all coded (replenished) picture blocks in the frame where packet loss occurs. In the proposed method, a simple coding mode decision algorithm is adopted where blocks which are normally interframe coded using affected picture blocks

TABLE II
REQUIRED OVERHEAD RATIO FOR ERROR RECOVERY

sequence name	Salesman			Miss America			Claire		
quantizer step size (×1/256)	8	12	16	8	12	16	8	12	16
proposed method (1block lost)	0.01	0.01	0.02	0.01	0.03	0.05	0.04	0.08	0.10
proposed method (2 block lost)	0.01	0.02	0.02	0.02	0.04	0.07	0.06	0.11	0.15
conventional demand refresh	1.35	1.93	2.50	0.97	1.83	3.00	2.69	3.98	4.87

Error recovery is carried out in the 4th frame after packet loss

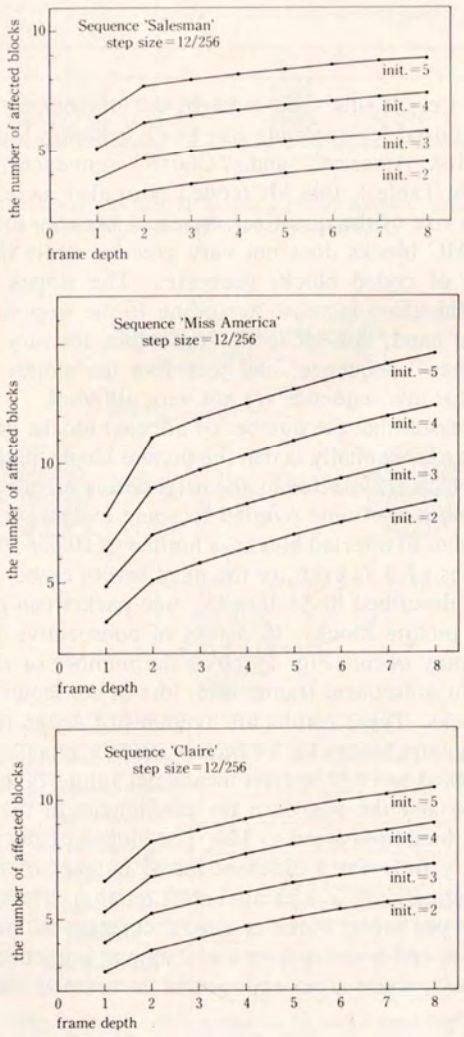


Fig. 9. The number of affected blocks after loss of consecutive picture blocks.

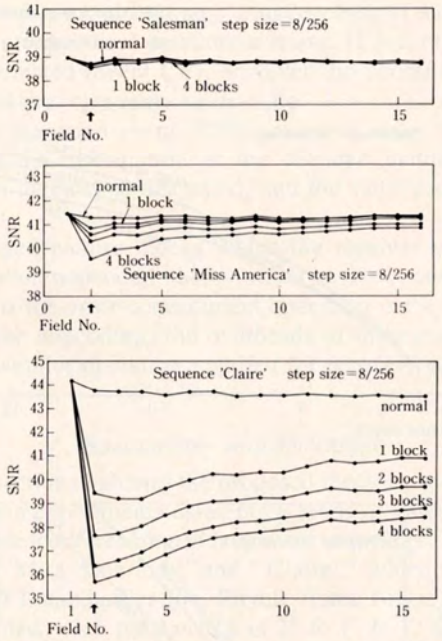


Fig. 10. SNR of decoded pictures after error concealment in the second frame.

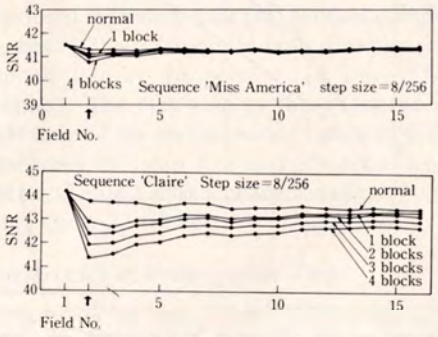


Fig. 11. SNR of decoded pictures after motion-compensated error concealment in the second frame.

are intrablock coded. The ratio of bit increase by the proposed method remains very low. It should be noted that this overhead is only required for one frame where error recovery coding is performed.

B. Picture Quality

Decoded pictures remain erroneous for several frames after error concealment has been made, and picture quality in this period therefore decides the validity of the method. Picture quality by error concealment, however, greatly depends on the area where a block loss occurs. For example, if a block loss occurs on the background, the influence on picture quality will be small, while if it occurs on the face of a person, it will damage the picture.

Here, we examined the picture quality deterioration in the worst case, i.e., when a block loss occurred on the eyes of persons and the quantizer step size is small as described later. Fig. 10 shows the SNR of decoded pictures after error concealment in the second frame. Blocks

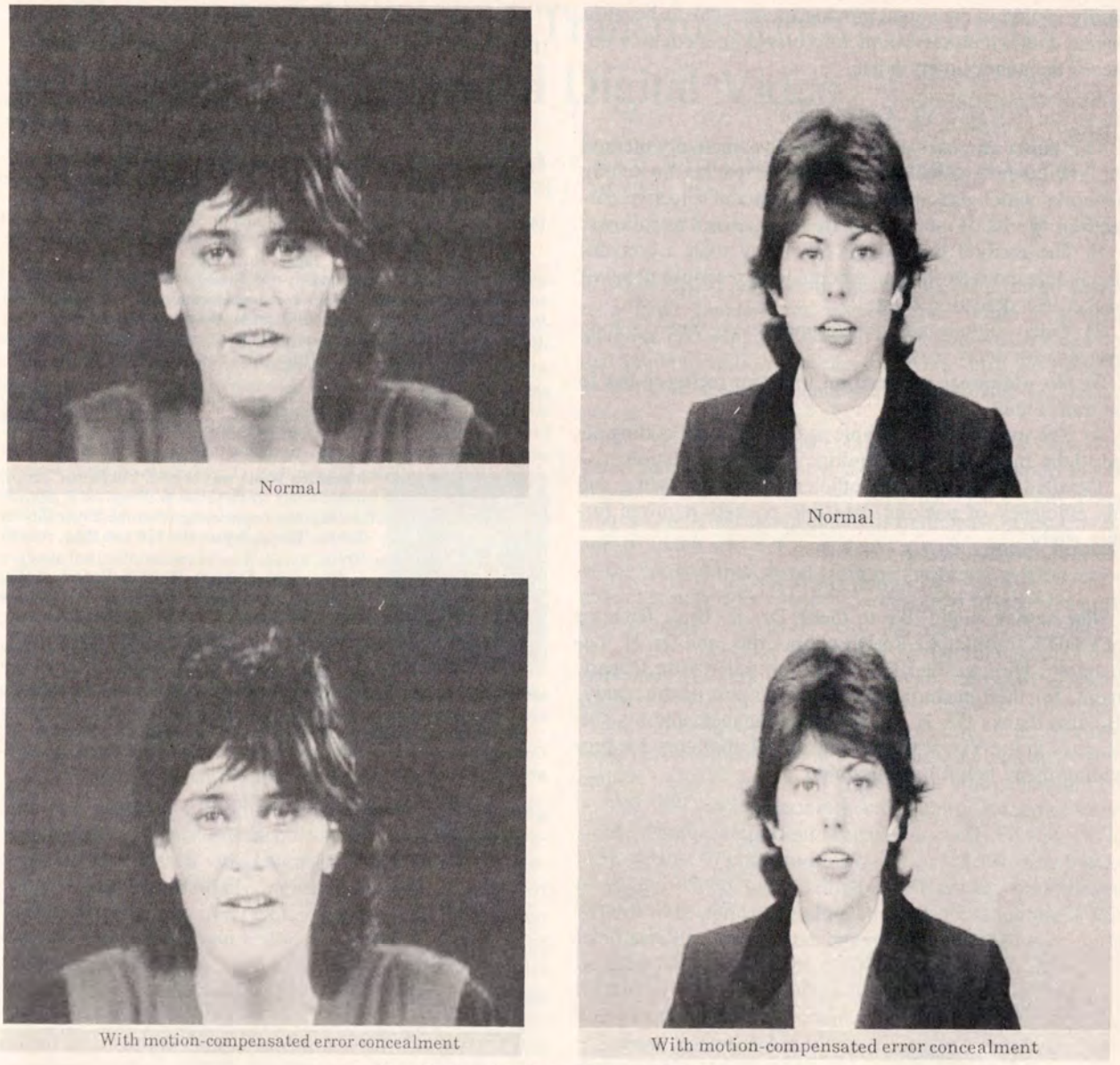


Fig. 12. Decoded picture of the second frame.

in the previous frame were used for concealment and the number of concealed blocks is 1 to 4. SNR falls initially, but after several frames it grows better rather than worse. This means coding data which refresh picture blocks decrease mismatch between the local-decoded picture of the encoder and the picture of the decoder.

The difference between the sequences can be explained as follows. If the ratio of coded blocks is high, the concealed area is frequently refreshed and the mismatch is alleviated. Furthermore, if the normal SNR of the coded picture is low, the influence of concealment itself will be small. This can also explain the fact that the drop of SNR caused by block loss decreases as the quantizer step size grows.

The results of subjective estimation indicated that the picture quality achieved by the concealment method mentioned above was sufficient for the "Salesman" and "Miss America" sequences, but some block noise could be noticed for the "Claire" sequence which has very high SNR.

In order to reduce the deterioration of SNR and increase the picture quality, motion compensation is effective for error concealment. Fig. 11 shows the SNR of decoded pictures after motion-compensated error concealment in the second frame. Blocks in the previous frame shifted by the average motion vectors of neighboring blocks of the concealed area were used for concealment. The SNR is greatly improved by motion compensation.

Fig. 12 shows the normally decoded pictures and pictures of the frames where a picture block around the eyes is lost and concealed with motion compensation. Slight block noise can be seen in the frame, but this noise is

hardly visible in the actual moving image. This is because coding data which refresh picture blocks immediately decrease the concealment noise.

VI. Conclusion

This paper proposes a new packet loss recovery method for low-bit-rate video transmission in packet switching networks which uses error concealment and selective correction. Merits of the method are summarized as follows.

1) The method has higher efficiency than a conventional demand refresh even when a long response delay of packet loss detection exists.

2) Video signals are not stopped even when a long propagation delay exists.

3) No additional information for error recovery has to be transmitted.

4) The method is applicable to conventional coding algorithms and suitable for multipoint communication.

Detailed analysis of the efficiency loss of coding and the efficiency of packing data into packets requires further study.

Acknowledgment

The author would like to thank Dr. K. Ono, Director of KDD Kamifukuoka R&D Laboratories, and Dr. H. Yamamoto, Director of KDD R&D Administration Department, for their encouragement and support of this study. He also thanks Dr. H. Murakami, Manager, and his colleagues in the Visual Communication Laboratory for providing many helpful discussions.

References

[1] P. Gonet, "Fast packet approach to integrated broadband networks," *Comput. Commun.*, vol. 9, Dec. 1986.

[2] B. Maglaris, D. Anastassiou, P. Sen, G. Karlsson, and J. D. Robbins, "Performance models of statistical multiplexing in packet video communications," *IEEE Trans. Commun.*, vol. COM-36, pp. 834–844, July 1988.

[3] F. Kishino and H. Yasuda, "Video packet coding for multiple video sources," in *Proc. IEEE COMSOC Int. Workshop Future Prospects Burst/Packetized Multimedia Commun.*, Nov. 1987, Ohsaka, Japan.

[4] S. Okubo, R. Nicol, B. Haskell, and S. Sabri, "Progress of CCITT standardization on n × 384 kbit/s video codec," in *Proc. GLOBECOM '87*, vol. 1, Tokyo, Japan, Nov. 1987, pp. 36–39.

[5] M. Wada and H. Yamaguchi, "Multimedia transmission method for 64 kbit/s integrated visual telecommunication" *Trans. IEICE*, vol. J70-B, pp. 451–460, Apr. 1987 (in Japanese).

[6] S. Ericsson, "Fixed and adaptive prediction for hybrid predictive/transform coding," *IEEE Trans. Commun.*, vol. COM-33, pp. 1291–1302, Dec. 1985.

[7] N. Nasrabadi and R. King, "Image coding using vector quantization: A review," *IEEE Trans. Commun.*, vol. COM-36, pp. 957–971, Aug. 1988.



Masahiro Wada was born in Yokohama, Japan, in 1956. He received the B.S. and M.S. degrees in electrical engineering from the University of Tokyo, Tokyo, Japan, in 1979 and 1981, respectively.

He joined Kokusai Denshin Denwa (KDD) Company, Ltd., Tokyo, Japan, in 1981 and has been at the Research and Development Laboratories since 1983, where he has been engaged in research on the coding and communication systems of video signals. His current interests are the development and standardization of a videophone system, and study of packet video communication for the ATM network.

Mr. Wada is a member of the Institute of Electronics, Information, and Communications Engineers of Japan and the Institute of Television Engineers of Japan.


WERT
BOOKBINDING
Grantville, Pa.
NOV DEC 1989